A DIRECT APPROACH TO COMPUTER MODELLING OF FLUIDS

by

John Geoffrey Liam Aston

A Thesis Submitted for the Degree of Doctor of Philosophy

Faculty of Engineering

UNIVERSITY OF LONDON

July 1990

Department of Mechanical Engineering
University College London
Torrington Place
LONDON WC1E 7JE

ABSTRACT

Conventional approaches to Computational Fluid Dynamics (CFD) are highly mathematical in content and presentation, and physical interpretation of the algorithms can often be obscure. This is believed to inhibit advances in the CFD field and the importance of such advances for Naval Architecture, as a particular application, is discussed. As a possible alternative to conventional methods, a "direct" approach to computer modelling of fluids is proposed where all the algorithms involved are "physically transparent" in that they avoid intermediate mathematical interpretations. Rules for the development of such a model are formulated, and a programming strategy, which advocates modularising the algorithms to reflect the cause and effect mechanisms in real fluids, is outlined. The principles of the direct modelling approach are demonstrated in the development of a computer program for 2-dimensional, incompressible, inviscid flows. The technique requires that the total pressure in a flow is decomposed into two principal components, the temporal pressure and the convective pressure, associated respectively with the temporal and convective accelerations of the fluid. The model incorporates a numerically "explicit" pressure spreading algorithm for determining the temporal pressure and acceleration responses to external disturbances. The actual compressibility of the "incompressible" fluid is modelled via the bulk modulus. Convective pressure is synthesised as flow develops by accounting for the small spatial variations in the fluid's density associated with the temporal pressure field. Simple internal flows, and the acceleration of bodies at or near a free-surface, have been modelled successfully. Flows with a finite free-surface distortion or system geometry change will require the incorporation of grid re-generation algorithms for the spatial discretisation. Routes for future developments, including viscous modelling, are discussed. Apart from potential advantages for CFD, the direct approach should benefit general fluid dynamics education since the concepts involved promote a better understanding of fluid behaviour.

TABLE OF CONTENTS

LIST OF FIGURES

CHAPTER 1

CHAPTER 2

CHAPTER 3

CHAPTER 4

CHAPTER 5

CHAPTER 6

Dedicated to my mother and father.

ACKNOWLEDGMENTS

I would like to thank my supervisor, Professor B.R. Clayton, and my colleagues Professor R.K. Burcher and Dr. W.H. Barclay at UCL for all the encouragement, help and advice they gave me.

This work was, in part, funded by the Admiralty Research Establishment (Haslar) under MOD Contract 2047/138/ARE(H) and I am grateful to Mr. B. Bowden at Haslar for his support.

FOREWORD

This thesis has been structured to reflect, as far as possible, the chronological sequence of the developments that were made in this research into a direct approach to computer modelling of fluids. Certainly the contents of chapters 3, 4, and 5, which cover the actual "hands-on" computer work, reasonably fitted this scheme. However, some of the content of chapters 1 and 2, which examine the background of conventional techniques and current research in Computational Fluid Dynamics, was actually synthesised during the course of the whole project. This more gradual assimilation of work in the field than the layout of the early chapters might suggest was quite deliberate; for it was considered to be dangerous to get embroiled in the details of conventional treatments too early as it can be very easy to get trapped along conventional lines of thought. As it was impossible to present this background study exactly "as it happened", it was considered expedient, and indeed believed to be more instructive, to present this part of the work as the foundation for the developments that were actually made. As a result, however, certain considerations within the development work may seem curious in the light of the background as presented, but this will be pointed out in the text.

Much of the development of the flow modelling algorithms relied upon the graphical output of flow characteristics from the evolving computer program as feedback. Also, the author preferred to use diagrams as far as possible, rather than excessive text, to describe modelling concepts and algorithms. For these reasons chapters 4 and 5 contain rather more figures than could be managably interspersed with the text while keeping the text readable and it was, therefore, considered better to group the figures together at the end of each of these chapters. For consistency throughout the thesis this layout was adopted for all the chapters and the author hopes that this is not too irritating to the reader.

Although the project involved the development of a computer program, no listing of that program is provided here. Instead, those diagrams which describe the models devised and tested in the program refer to the actual computer variable names that were used in order to illustrate how the algorithms can be coded. For this reason a description of the program variables is included in the Notation section.

The section numbering scheme adopted does not include the chapter number. This is because of the level of sub-sectioning that was required and the author's personal dislike of more than three digits to designate the lowest numbered level of sectioning. For this reason each chapter may have, for example, a section 3.2. If, simply, "section 3.2" is

referred to within the text then this will relate to section 3.2 of the current chapter. Alternatively, reference to section 3.2 of another chapter will include the chapter number as, say, "chapter 4, section 3.2".

Finally, the nature of the work carried out meant that most of the references to be cited were of a review nature covering a variety of topics in fluid dynamics, CFD, and specific applications. In order that the reader may follow up any particular area with ease, the references are grouped together under thirteen separate and numbered headings and are labelled alphabetically within each group. Within the text a reference to [2b], then, refers to the specific volume labelled (b) in reference grouping 2. A reference to [5] on the other hand, without an alphabetic designation, refers generally to all the literature covered in reference grouping 5.

NOTATION

ANALYTICAL VARIABLES

Symbol	Meaning(s)
A	Radius of inner cylinder in fluid annulus problem OR Face area of control volume
a_p, a_j	Discretisation coefficients
B	Radius of outer cylinder in fluid annulus problem
b	Discretisation coefficient
C_μ, C_1, C_2	Empirical coefficients associated with k-ε model of turbulence
c	Speed of sound
D	Diameter of cylinder
e_{ij}	Generalised strain
e_{xx}, e_{yy}, e_{zz}, e_{xy},...	Strain components
e_v	Volumetric strain
F	Volume flow rate
g	Acceleration due to gravity
h	Head of fluid
K	Bulk Modulus of fluid
k	Turbulent kinetic energy of fluid
n	Unit vector normal to a surface
p	Pressure
Q	Volume flow rate OR General scalar quantity
q_r, q_θ	Radial and tangential velocity components
q	Fluid velocity vector
R	Gas constant
Re	Reynolds Number

r	Radial position in radial coordinates
s_j	Position on jth panel (Panel Method)
S_ϕ	Source term in generalised equation for fluid flow
T	Temperature
t	Time
U	Speed of a body
u	Fluid velocity component in x-direction (Cartesian Notation)
u_1, u_2, u_3	Fluid velocity components (Suffix Notation:- 1=x; 2=y; 3=z)
u_e	Velocity at the edge of a boundary layer
V	Volume of control volume
v	Fluid velocity component in y-direction (Cartesian Notation)
w	Fluid velocity component in z-direction (Cartesian Notation)
X	Body force in x-direction (Cartesian Notation)
X_1, X_2, X_3	Body force components (Suffix Notation:- 1=x; 2=y; 3=z)
x	Displacement in x-direction (Cartesian Notation)
x_1, x_2, x_3	Displacement components (Suffix Notation:- 1=x; 2=y; 3=z)
Y	Body force in y-direction (Cartesian Notation)
y	Displacement in y-direction (Cartesian Notation)
Z	Body force in z-direction (Cartesian Notation)
z	Displacement in z-direction (Cartesian Notation)

Greek Symbol Meaning(s)

δ	Boundary layer thickness
δ_{ij}	Kronecker delta $\delta_{ij} = \begin{cases} 0 \text{ for } i \neq j \\ 1 \text{ for } i = j \end{cases}$
$\delta x, \delta y, \delta z$	Spacial discretisation intervals in coordinate directions
δt	Temporal discretisation interval or "timestep"

ε	Rate of dissipation of turbulent kinetic energy
ε_{ij}	Generalised rate of strain
ε_{xx}, ε_{yy}, ε_{zz}, ε_{xy},...	Rate of strain components
ε_v	Rate of volumetric strain
ϕ	Flow potential OR Principal variable in generalised form of governing equations of motion for viscous fluids
Γ_ϕ	Exchange coefficient in generalised form of governing equations of motion for viscous fluids
γ	Ratio of inner to outer cylinder radii in fluid annulus problem
η	Free-surface displacement
μ	(Dynamic) viscosity
μ_t	Turbulent (or eddy) viscosity
μ_{eff}	Effective viscosity ($= \mu + \mu_t$)
ν	Kinematic viscosity
θ	Angular displacement in radial coordinates
ρ	Density of fluid
σ_j	Strength of source panel j (Source density)
σ_{xx}, σ_{yy}, σ_{zz}	Direct stress components
σ_m	Mean of direct stress components
σ_k, σ_ε	Empirical coefficients in k-ε model of turbulence
τ_{ij}	Generalised shear stress
τ_{xy}, τ_{yx}, τ_{zx}, τ_{zy},...	Shear stress components

Subscript	Meaning(s)
C	Convective value
N, S, E, W, NW, NE, SE, SW	Compass designations for nodes adjacent to node P in simple 2-dimensional representation of node neighbours
n, s, e, w	Compass designations for values on faces of control volumes (in the Finite Volume Method) in simple 2-dimensional representation
i, j, k	Repeated term designation in Suffix Notation:- Terms containing i include the leading equation suffix 1, 2, or 3 only. Terms containing j should be repeated for j = 1, 2, 3. Terms containing k refer to the sum of the given term for k = 1, 2, 3.
m	Mean value
max	Maximum value
P	Relating to node point P
T	Temporal value
xx, yy, zz, xy,...	Tensor notation
v	Volumetric

Superscripts	Meaning(s)
M	Iteration counter
n	New time level
o	Old time level
$\bar{}$ (overbar)	Time averaged value
' (prime)	Fluctuation from the mean value

PROGRAM VARIABLES

Variable or Array	Description
AREA (MNOEDG)	Array of edge areas
BULKMOD	Bulk Modulus
BODY_VEL (2)	Body velocity vector array

CENTRD (MNOREG,2)	Array of region centroid coordinates
COEDGE (MNOEDG,2,2)	Array of edge coordinates
CUM_EXCHANGE	Cumulative exchange (in convective pressure calculation)
DINC (MNOEDG)	Array of *virtual* flow displacement increments across edges
DT	Sub-timestep in temporal pressure algorithm
DENSIT	Fluid density
DIST_N_R	Distance between the centroid of a region and the centroid of an adjacent (neighbouring) region
DIST_C_E	Distance between the centroid of a region and the intersection on the common edge with a neighbouring region of a line joining the centroids of the two regions
EFF_AREA	Effective area of a partial edge or an edge between subdivision levels
EFF_VOLUME	Effective volume of a partial region or a region on subdivision border
EDGE_PRESS (MNOEDG)	Array of total (average) pressure levels at edges
EDGE_PRESS_T (MNOEDG)	Array of average temporal pressure levels at edges
EDGE_PRESS_C (MNOEDG)	Array of average convective pressure levels at edges
FLOW (MNOEDG)	Array of volume flow rates across edges
FG_ACC (MNOEDG)	Array of fluid normal accelerations at edges
FG_VEL (MNOEDG)	Array of fluid normal velocities at edges
FG_DISP (MNOEDG)	Array of fluid normal displacements at edges
FIELD_VEL (2)	Velocity components of acceleration field
FRACTION_DIFF	Fractional difference in SQF values calculated between sub-timesteps. (Used for termination test.)
GRAVITATION	Acceleration due to gravity
GROWTH	Growth factor
IEDG	Current edge number
IREG	Current region number
IDN	Current neighbouring region number
IDEDGE (MNOREG,10)	Array of edges associated with each region

IDNEIG (MNOREG, 10)	Array of neighbouring regions for each region
IDREG (MNOEDG,2)	Array of regions associated with each edge
MNOEDG	Maximum number of edges that the program can accommodate. (Maximum dimension of arrays containing edge information.)
MNOREG	Maximum number of regions that the program can accommodate. (Maximum dimension of arrays containing region information.)
MAX_FRACTION_DIFF	Maximum fractional difference. (See FRACTION_DIFF.)
NOEDG	Actual number of edges in discretised system
NOREG	Actual number of regions in discretised system
NTYPE (MNOEDG)	Array of edge type numbers
OLD_VEL	Old velocity value
PRESS (MNOREG)	Array of total (average) pressure in each region
PRESS_T (MNOREG)	Array of average temporal pressure in each region
PRESS_C (MNOREG)	Array of average convective pressure in each region
PRESSINC	Pressure increment
PRESS_GRAD	Pressure gradient
ROTATION (MNOREG)	Array of averaged ROTATION in each region
REG_VEL(MNOREG,2)	Array of average flow velocity in each region
REG_ACC(MNOREG,2)	Array of average flow acceleration in each region
REL_VEL (MNOEDG,2)	Array of relative velocities between the fluid and the acceleration field at each edge
REL_VEL_OLD (MNOEDG,2)	Previous values of REL_VEL
RFACT	Relaxation factor
RLIMIT	Relaxation limit
SQF (MNOREG)	Array of squeeze factors for each region
SQFINTEG (MNOREG)	Array of integrated squeeze factors for each region
S_DINC_AREA	Sum of the products of DINC times AREA for all the edges of a region
S_DINC_A_IN	Sum of the products of DINC times AREA for the edges where flow passes into a region

S_DINC_A_OUT	Sum of the products of DINC times AREA for the edges where flow passes out of a region
SQFREF	Reference level of squeeze factor
TAREA	Total area for outflow from a region
TINC	Main timestep
TVOLRED	Total volume reduction
VOLUME (MNOREG)	Array of region volumes
VEL (MNOREG,2)	Array of averaged region velocities
VISVEL (MNOREG,2)	Array of averaged region viscous velocity increments
V_DV_DS	Convective acceleration
VOL_REG_LEVEL (8)	Nominal volumes of regions on each of the 8 discretisation levels

CHAPTER 1

MOTIVATION AND DIRECTION

1. INTRODUCTION

There are three broad categories of research effort in engineering. These are:-

(i) *Speculative Research:-* To look for unexplained phenomena and/or to identify inadequacies in contemporary systems.

(ii) *Systematic Research:-* Recognition of an inadequacy of performance of some system and a quest for its improvement.

(iii) *Investigative Research:-* Awareness of an unexplained phenomenon and a quest to understand it.

Any given research study will likely contain a combination of such elements and in order to present a complete picture of the work it is helpful to trace these within the overall project. This research study concerns the development of a "direct" approach to computer modelling of fluids, having recognised certain deficiencies of conventional approaches in the field of Computational Fluid Dynamics (CFD). The work falls predominantly into category (ii) and this systematic research, along with some necessary investigative research elements, forms the more tangible effort which is presented within the later chapters of this thesis. This first chapter covers the less tangible effort that was involved in deciding upon this research topic. It will be seen that the motivation may be attributed to a combination of some "speculative research" (on a quite different topic) plus a general exposure to the field of Naval Architecture, an engineering discipline where advances in fluid modelling, which really hold the key to significant progress and innovation in ship design, are embarrassingly slow.

2. RESEARCH ORIGINS

The author began his principal research effort on the topic of "Unsteady Flow in Marine Propellers". This was speculative in nature where particular interest was directed towards the generation of vertical and lateral forces and moments when such devices operate in oblique inflow. If such parasitic loading turned out to be significant with certain propeller designs and/or operating conditions, then this could have had interesting consequential implications for propeller damping effects with ship motions or, indeed, roll excitation influences in certain wave conditions.

The speculative nature of the research meant that the level of funding was low. This demanded that experimental work be carried out in a low-cost air system, where 7 inch diameter propeller models were to be tested in an open-jet wind tunnel. The experiments carried out, however, were inconclusive due to measurement difficulties with the apparatus used. Vibration in the testing rig largely obscured the small force signals of interest from the load transducers and meant that no distinctive trends could be observed.

These propeller experiments were performed alongside studies into the possibilities of analytically or numerically modelling the physical system along conventional lines. It was here that the first sense of unease was experienced with the techniques of Computational Fluid Dynamics. Lifting Surface Theory (see [9b,9c,9d]), the most common numerical technique used for propeller design and performance analysis, used modelling concepts so far removed from physical reality that it stifled any encouragement to proceed with a development of such an approach for oblique flow considerations. Indeed, the highly mathematical nature of <u>all</u> the conventional CFD techniques strongly suggested that there had to be an easier way to model the behaviour of a fluid using a digital computer.

In addition to this study of marine propellers the author was involved with the teaching of Naval Architecture and investigations into the use of computers in ship design. The teaching involvements indicated how desperately developments in Naval Architecture depend upon advances in CFD. This topic is addressed further in section 3 where it supports the *justification* for switching the principal direction of research towards CFD. The study of the use of computing in ship design, on the other hand, had much more fundamental impact on the *philosophy* of the new line of research. It revealed how, unwittingly, the power of computers could be misused in engineering design work and how the full potential of digital computing can so easily be overlooked by traditional thinking.

A particular area of interest in ship design procedures was the assessment of adequacy of hydrostatic stability. Two levels of effort can be identified in such a process. First, the fundamental calculation of stability information for a given design in a given operating condition; and second, the organisation and presentation of the results of such calculations to illustrate the comparative merits of different hull options. On examination of conventional approaches used in computer-aided ship design (CASD), each of these aspects provided evidence of the poor usage of the power of present-day computers.

Considering the first aspect, almost every computer code for calculating the stability characteristics of ships was based on a "volume integral" approach similar in logic to the

hand calculations which had to be used before the days of computers. Only as recently as 1985 was it recognised that a surface pressure integration approach offered a much more flexible and versatile tool [13b]. With hindsight it is easy to see why: the surface pressure integration approach directly models the physics of the problem. What is so instructive about this example is that nobody appeared to consider this much more obvious calculation procedure for so long, possibly due to the constraints of traditional lines of thought.

Considering the second aspect, the procedures used for assessing the stability of hull forms in the early design stages were found to be seriously flawed. The lack of detail on relevant design parameters in the early "design cycle" estimates of stability means that the selection of a hull form is made, not on the basis of a full assessment process, but rather on *predictions* of stability based on initial stability characteristics. These characteristics, in turn, may have been derived from empirical/historical formulae. Selection of viable designs is then made by comparing the predicted characteristics with historical trends of such data for vessels that were found to be adequately stable in the past. Two obvious dangers are associated with this approach. The first is that if a nearly finalised design is found to be deficient in stability in some respect, this will necessitate either substantial re-design or a compromise in the the vessel's allowable loading conditions. The second is that such reliance on historical data unduly restricts the degree of innovation in the hull form and layout of new designs. As a result of these observations, and some lateral thinking on the difficulties of the ship stability problem, a procedure for a more *comprehensive* assessment of the stability characteristics of hull form proposals in early design stages was developed. The procedure was made possible with the widespread availability of hull form generation CASD programs which in turn made it possible to derive all the hydrostatic data relevant to the stability assessment process which were dependent only on the geometries of the hull options: these data could then be presented in such a way as to indicate and compare the scope of the stability characteristics of proposed hull forms. The scheme is reported in [13a] and the work provided a lesson of being wary of traditional procedures in engineering, and being open to possibly quite radical alternatives.

The experience of such computer applications in ship design helped to qualify the "unease" that was experienced with conventional CFD techniques when considering analytical possibilities for the marine propeller problem. It seemed that a single observation could be made to explain the discomfort with those approaches, and this was that all of the computer models seemed to be either wholly, or in part, models of *mathematical models* of a fluid rather than direct models of the fluid itself. Such a distinction was important because it was believed that too much emphasis on the mathematical interpretation and manipulation of flow equations could actually inhibit the understanding of fluid behavioural mechanisms. Also, the need to become involved with fairly complex

mathematics in order to understand CFD software and its limitations is very off-putting for most design engineers; this could explain, at least in part, why CFD application and development have been relatively slow to advance. It seemed possible that the techniques in CFD could represent yet another example in engineering where the reaction to the advent of the digital computer was, perhaps, too short-sighted and unimaginative, thereby stifling subsequent development in the field. For here a machine was provided allowing numerical techniques (which were known about for a long time before the arrival of the computer but were too extensive to apply by hand) to be developed and used to solve the mathematical equations describing fluid motion; perhaps too little consideration was given to the new possibilities for analysis afforded by the power of digital computing. And so, it was with a belief in the importance of the concepts being formed that the author decided to redirect his research investigations towards the development of a more "direct" computer model for fluid behaviour where all mathematical interpretations and distractions would be avoided. If such a model could be developed it could have radical effects, not only in Naval Architecture, but in all fluids-related disciplines.

3. THE NEED FOR COMPUTER MODELLING OF FLUIDS IN NAVAL ARCHITECTURE

Before continuing with a discussion of the specifics of the approaches and the current capabilities of CFD it is useful first to demonstrate more emphatically the *need* for CFD in engineering applications and to identify what engineers should view as the ideal capabilities of such techniques. An examination of the process of designing a ship is most suited to this task since it represents, probably, the most demanding engineering design problem where fluid motions are involved.

The ship design process is illustrated in figure 1.1. Neglecting the economic survey and mission analysis components, it starts, generally, with a specification of the payload (cargo in a merchant ship and weapons in a warship) and a previously acquired knowledge of the mass and volume of the machinery, equipment, stores and personnel, etc, that are required to support this. The design problem, then, is essentially one of finding the best hull and superstructure combination to contain all of these items. The choice of this "best" hull form must be based on prediction of the performance of the vessel in certain key areas: STABILITY, CONTROLLABILITY, SEAKEEPING, and POWERING, with a view towards ensuring adequate *STRENGTH* in the structure, a certain amount of *STYLE* in the overall aesthetic appearance of the form and, of course, the inevitable constraints on *COST*. The reason why *predictions* have to be made of the dynamic performance is because the scale of, and the demand for, the product makes it impractical and

uneconomical to build and test prototypes. This creates constraints within ship design which are far more restricting than in most other engineering endeavours.

Before the advent of the digital computer the only tools at the disposal of the naval architect to make the necessary dynamic performance predictions were:-

- Physical Modelling
- Past Experience / Historical Databases
- Certain Mechanical Calculation Devices

Mechanical calculation devices, although helpful to the Naval Architect in fairly simple numerical calculations, were still relatively slow to use and not suited to the vast set of calculations required in most ship dynamics problems. To avoid these calculations it was necessary to utilise what has been referred to as the ultimate analogue computer for fluid modelling - namely, the ship towing tank. However, such physical model testing was always a time-consuming and expensive activity and therefore was never suited to the process of comparative testing for option selection as needed in the early stages of design. The role of model testing, then, was mainly one of *design validation*, being carried out at a fairly late stage of the design process, with designers "keeping their fingers crossed" that the test results would match their predictions made by the only other means at their disposal - estimates based essentially on past experience. This ultimate reliance on historical data meant that that ship forms were very slow to evolve. New ships, therefore, looked very much like the designs that were reasonably successful in the past since the financial penalties of attempting to be innovative were too severe.

Since the advent of digital computing the situation has not changed as dramatically as one might have hoped or expected. There is still much reliance on historical data in contemporary ship design procedures for reasons that will be explained further in section 4. For the present purposes, the situation that existed before computers were available suffices to define the ultimate goal for computational fluid modelling in Naval Architecture as follows. Computational fluid modelling is required to provide full ship performance data significantly more quickly and more cheaply than tank testing in order to make the comparative testing of alternative hull geometries feasible and cost effective in early design. Furthermore, the computer model must be equally sensitive to the subtlest of design changes as the real system is known to be. If this goal could be achieved then hydrodynamic design in Naval Architecture would be freed from the constraints and compromises imposed by current reliance on historical data.

4. CURRENT CAPABILITIES OF CFD

The degree to which the ultimate goal of CFD for naval architecture (as described in section 3) has been realised is sobering. As Morgan and Lin [3f] point out, most solutions of practical application to ship design are those derived from linear theories where viscosity is neglected. It will be many years before the Navier-Stokes equations can be modelled on a computer at the ship's scale Reynolds Number to yield the detail necessary for reliable estimates of the most basic and crucial performance characteristic - resistance.

Admittedly, the ship problem is particularly demanding, not only because of the Reynolds number scale of turbulence detail involved, but also because of the presence of the air/water interface and the complications of free-surface distortions. One might naturally think, then, that much greater advances would have been made in CFD applied in other branches of engineering. This is true to a certain extent, but rather because there are greater numbers of researchers interested in non-marine pursuits; Reynolds number limitations still apply, and the reliability of all the developed techniques is still questionable. Many items of literature on CFD, and particularly those related to a commercial software product, may give the impression of a capability far greater than that merited. According to Boris [3d], "Today CFD methods can simulate flow either in complex geometry with simple physics or with complex physics in relatively simple geometry, but they cannot do both."

So what *can* CFD techniques presently achieve? It is perhaps indicative of the current state-of-the-art that it is easier to answer this question by describing what CFD presently cannot do. For apart from the known inability to achieve adequate discretisation levels in realistic flows of practical interest, even in much simpler systems which are more in line with the capabilities of current computer hardware, the *reliability* of current algorithms is disappointing. It is probably true that you can model anything you like using present CFD techniques, but it is necessary to be very cautious of the degree of faith you place in the answers. This is an important point because much available software will produce an impressive mass of detail on any flow problem you care to specify, and it is a quirk of the computer age that users of any software (sometimes even if they have written it themselves) often tend to believe what the computer tells them without question.

A very realistic picture of the current capabilities and limitations in CFD is provided by Spalding [3g] who sets out typical "goals" and "stepping stones" for researchers in CFD to aim for within the next decade. The "goals" cited are examples of prediction capabilities which have not yet been achieved but which, when realised, would represent significant advances in CFD. The "stepping stones" are lesser prediction tasks which must

be accomplished on the way to realising the grander goals. Spalding suggests goals and stepping stones for three principal flow types; *External Flow*, *Internal Flow (Without Chemical Reaction)*, and *Internal Flow (With Chemical Reaction)*. For the present purpose it will suffice to outline those he describes for the External Flow category which are most akin to naval architecture requirements. Three of the goals described are quoted as follows:

"**Goal (a)** *Predictions of the aerodynamic characteristics of air-borne vehicles, whether conventional aircraft, helicopters, VTOL machines or airships.*

Attainment of this goal, to the extent of enabling wind-tunnel testing to be used mainly for CFD-model validation, involves the abilities to:-

- predict economically the partly-turbulent flow-field around the vehicle, with allowance for recirculation zones, ground effects, compressibility and engine-airframe interaction;

- predict with sufficient accuracy the transition to turbulence in the boundary layer;

- predict with sufficient accuracy the conditions for and the location of boundary layer breakaway on smooth or rough curved three-dimensional boundaries.

Goal (b) *As for Goal (a), but applied to ground vehicles, with special attention to the complexities of geometry afforded by wheels, window recesses, wing mirrors, etc.*

Attainment of this goal necessitates the creation of computational grids which are finely spaced where geometric details are intricate, but coarsely spaced elsewhere.

Goal (c) *Prediction of the flow fields around and downstream of buildings and other man-made structures, with attention to the distribution of pollutants from chimneys, and allowance for the effects of gusts and of non-uniformities of nearby terrain.*

Attainment of this goal requires capabilities which are similar to those involved in (a) and (b), but with less emphasis on boundary layers and more on recirculation zones and wakes. The large sizes of the objects in question (e.g. 'skyscrapers'), and the modest velocities of flow, render allowance for gravitational effects important, which is one reason for the inability of wind-tunnel tests to provide all the necessary information."

Spalding's "Stepping Stone 1" for external flow gives an even clearer indication of what cannot yet be modelled reliably:-

"**Stepping Stone 1 (SS1)** *Predictions of the steady flow (if it indeed exists!) over and around a cylindrical shell supported (never mind how) with its axis at right angles to a nearby plane surface. The diameter of the cylinder is D; the height of its lower edge is l from the plane, and that of its upper edge is u. The flow is to be predicted for various Reynolds numbers, and for various values of l/D and u/D.*

This stepping-stone task is relevant to the first three external-flow goals; but it has the advantage of possessing a rather simple geometry. One may reasonably ask, if this flow cannot be reasonably-well predicted, what hope is there of predicting

> flows around aircraft, automobiles and buildings? It therefore may serve as a useful test of ability and a challenge to the improvement of the methods."

That this comparatively simple flow (see figure 1.2) cannot yet be reliably predicted indicates that the field of CFD is a long way from being able to accurately model the flow around a ship's hull in its various performance modes.

Before leaving this section it is only fair to be more positive about what CFD *can* achieve in Naval Architecture. So far the impression created has been bleak, mainly because the "bread and butter" ship performance characteristics of resistance and propulsion are a long way from being reliably predicted using CFD techniques. Nevertheless, advances have been made towards predicting the various performance characteristics by attacking the sub-elements of the problems in a manner reflecting the traditional approach to prediction. For example, in Resistance and Propulsion (see [12c,12d] for background), where the traditional approach is to consider the components of skin friction, form drag, wave resistance, propeller thrust, and propeller-hull interaction separately, advances have been made in predictions of the wave resistance component [7c,7h] and propeller performance [9d] using CFD techniques. In the seakeeping area, although the overall system of a moving ship interacting with a moving sea cannot be modelled directly using CFD, the problem can be tackled by treating the ship as a rigid body and subjecting it to a wave loading "input". The wave loading and the inherent added mass and damping characteristics of the hull required for such an approach can be computed using inviscid CFD techniques, usually in the form of strip-theory approaches (see [12b] and [12f] for background).

The main successes in ship performance prediction involve flows where viscosity generally has a second order influence; and it is fair to say that if a computational tool is available that takes viscosity into account in some way then it will always give better results when the extent of viscous action is small. It is for this reason that progress in even the sub-elements of the prediction of transverse stability of ship motions (one of the most crucial considerations in ship design) has been very slow; for here the action of viscosity rather than the generation of surface waves dominates the roll damping characteristics of the hull. Consequently, regulatory assessment of the safety of a ship against capsize is likely to remain based on simplified interpretation of hydrostatics for some time. (See [12c] for details of the principles and [13g] for details of current research effort.)

As a final point in this section, it should be noted that the actual usage of CFD in ship design certainly does not reflect the current capabilities, however far these may be from the ideal. Morgan and Lin [3f] describe "the natural conservatism of ship designers" as an excuse for the somewhat slow impact of CFD on Naval Architecture; this is probably a

"nice way" of putting it. Ship design procedures have not really changed since the arrival of the computer. The basic approach is the same. Most of the computer tools available tend to be used in the detailed development stages, essentially for validation of the design in a way similar to the use of physical model testing, whilst the crucial early hull form selection process is still based on the historical data approach. There are now sufficient computing capabilities to make more rational design decisions in the early phases of the ship design process; the example of the assessment of hydrostatic stability has already been described in section 2 and potential exists also in all of the other performance areas. Indeed the current potential of computing in Naval Architecture makes it possible to rationalise the whole methodology of ship design, and exciting ideas in this area may be followed up in [13c].

5. RESEARCH DIRECTIONS IN CFD

There is already a vast literature in Computational Fluid Dynamics, even though the subject is relatively young. Useful reviews of the conventional approaches in the field may be found in [3], with an eye particularly towards the future given in [3a,3d].

The techniques described by the author as "conventional" are those that have been around for some time and are used to some extent in industry, rather than being the subject of pure research. The categorisation of these conventional approaches is shown in figure 1.3, ranging from the obvious space discretisation techniques such as the finite difference method, to the less physically tangible techniques of panel and boundary-integral methods and the almost abstract concepts of spectral methods. Within each category there are considerable ranges of sub-techniques and subtleties, the discussion and arguments over which form the bulk of the literature. All of these techniques are simply different ways of treating different discretisations of the partial differential equations which govern the flow in order to obtain solutions for particular flow systems. The overall strategy, the discretisation processes, the solution procedures, and the *presentation* of all these, tend to be highly mathematical and more detail of these techniques will be presented in chapter 2.

Most contemporary research in CFD is involved with improving these conventional approaches in order to obtain finer, faster and more reliable simulations of fluid flow. Spalding [3g] has set sample goals for modelling capability within the next decade (some of which have been described in section 4). He also pinpoints the specific areas requiring improvement, particularly concerning versatile grid generation techniques, low numerical diffusion formulations, and the exploitation of the relatively new "vectorised" and "parallel processing" computer architectures that are being offered by more computer

manufacturers. There is clearly a distinctive interdisciplinary nature to the efforts in mainstream CFD research such that significant advances could be made by a numerical analyst or a computer scientist, just as easily as by a fluid dynamicist.

Section 2 has presented the origins, motivation and theme of this particular work, the nature of which places it out of the mainstream research effort in CFD, and it was encouraging to discover that the need to investigate such "alternative" approaches was recognised. Aref [3a], for example, describes and encourages mainstream research on conventional approaches as "a noble endeavour" as it will remain the most convincing way of producing flow solutions for the "foreseeable future". He points out, however, that it "does lack an inherent quality of originality" and reminds us that the computer is capable of so many other things.

In order to be able to classify any contribution of this thesis to the field of CFD it is useful to categorise the possible areas of new developments generally. Innovative ideas in CFD can occur (and have occurred) on three distinct levels; the REPRESENTATION LEVEL, the ALGORITHMIC LEVEL, and the IMPLEMENTATION LEVEL. The representation level concerns the way in which the fluid is conceptually modelled; the algorithmic level concerns the "solution procedure"; and the implementation level concerns the matching of the algorithm to the computer architecture. (For illustration, these levels distinguished for conventional approaches are shown in figure 1.4.) Any innovative piece of research may include aspects from more than one level. For example, a new representation would likely be associated with different algorithms which in turn would have scope for novel implementation. On the other hand, developments in algorithms and implementation could take place individually.

Representations

Novel representations are easy to distinguish in the field. Examples are the cellular-automata models [5] and the particle models [6] for fluid flow. Each of these concepts strives to represent the molecular structure of fluids and therefore departs from the continuum model adopted in all conventional approaches. The principles of the two models are illustrated in figures 1.5 and 1.6. Whereas the cellular-automata representation uses a very simple logic to model only "collisions" between particles (i.e. very strong interactions) and the consequences of such collisions, particle models consider explicitly forces between all the near neighbours in the system. Particle models use simplified force laws for computational expediency, but obviously to a much lesser degree than the simple logic based force model of cellular-automata which sacrifice physical veracity for computational simplicity.

A justification for pursuing such representations of fluids may be obtained from recognising a certain redundancy of effort in the conventional continuum representation. Fluids, of course, are known to be comprised of molecules which essentially form a finite number of degrees of freedom. When adopting a continuum representation to get smooth and continuous distributions of flow properties, the number of degrees of freedom is effectively increased to infinity. Numerical solution of continuum equations, however, then demands that the continuous distributions be discretised in some way to get a manageable number of degrees of freedom. Proponents of cellular-automata and particle modelling argue that rather than discretising a set of continuum equations of motion, it is more sensible to use instead simplified versions of the underlying deterministic Newton's Laws for molecules and to statistically average the particle attributes to obtain the macroscopic fluid variables of interest.

In principle the ideas of cellular-automata and particle modelling are sound. In practice, however, the number of particles required to reduce the statistical fluctuations of flow properties to an acceptable level in even small volumes of modelled fluid is unacceptably large. And so, although these techniques have been described as "novel", cellular-automata have been around for about ten years whilst particle modelling may be traced back almost thirty years [6a,6b]. The delay of their establishment in CFD is due to their computational demand being too great for contemporary computing power and capacity.

Implementations

Novel implementations, too, are simple to identify in CFD. They are represented by significant departures from the standard sequential approach to processing of conventional computers. Such departures are:-

- Use of Vector Registers and Arithmetic Pipelines. In an arithmetic pipeline the individual processes associated with repeated calculations are carried out simultaneously. These include the fetching of data from memory, the several stages of each arithmetic operation, the storage of the computed results, and the incrementing and checking of loop indices. "Vectorisation" is the term used for optimising algorithms to take full advantage of this very efficient processing capability. Vector registers are the fast, intermediate locations used to store operands and results to ensure fast sequential processing through the pipelines.

- Parallel Processing. In a conventional computer architecture every program instruction (including both component calculations and program control instructions) are fed sequentially through one processor. Where individual calculations can be performed independently there is scope for increasing

program performance by dividing the computational tasks between a number of processors which operate simultaneously i.e. "in parallel".

- Customisation. It is possible, depending upon resources, to construct hardware microprocessor/memory chips which are customised for a particular application. An example of this is the "cellular-automata machine" [5a] which operates on bit-level logic. Such machines were developed for the special requirements of cellular-automata algorithms which were unsuited to conventional byte/word manipulation machines.

- Hybrid Implementations. Different classes of CFD problem, or different algorithms, have differing potential and requirements for using the alternative architectures above. Individual research teams may assemble their own computing facility from a heterogeneous combination of computing components in order to "tune" the performance of their CFD algorithms.

More detail of new computer architectures may be found in [13e]. Vector registers and arithmetic pipelines, with only a very modest degree of parallelism (about 2 to 4 processors) are at the heart of today's fastest supercomputers. These (still essentially) sequentially pipelined architectures have almost reached the limits on speed for the processors, and any further improvements would be difficult and expensive to obtain. The fastest and most powerful machines are still, however, too small and too slow to provide the solution to realistic 3-dimensional flows of particular interest. Undoubtedly the most exciting implementation developments will come with advances in parallel processing architectures with optical communications rather than electronic data transfer. What is equally certain, however, is that advances in CFD due to implementation developments will be considerably slower than the increasing capabilities of the hardware simply because the excessive cost of the new machines will place them out of the reach of most research teams.

Algorithms

Innovations in algorithm design are somewhat less easy to identify simply because there tends to be more scope for "variations on a given theme" here than in the areas of representation or implementation. For example, all of the conventional techniques for CFD (figure 1.3) are simply different algorithms covering the same continuum representation of a fluid. The differences between each of the techniques (as will be seen in chapter 2) lie in the protocols used for discretisation of the Navier-Stokes equations: once discretised, the solution procedures for the solution thereafter are very much the same.

The thrust of developments in algorithm design as far as conventional representations are concerned are directed towards improving existing standard techniques to gain greater accuracy with the more or less fixed maximum resolution afforded by current computers' size and speed capabilities. Examples of current developments lie in adaptive and unstructured gridding techniques to provide and maintain high resolution in complicated areas of flow; fast near-neighbour algorithms for Lagrangian CFD description; and algorithm reorganisation to make the most efficient use of pipelined and paralleled computer processors. It may be debated whether such developments can fairly be described as "innovative"; the new directions are hardly radical, although they are, undoubtedly, more subtle.

6. THE DIRECTION OF THIS RESEARCH

Aref [3a] has noted that, "There is a pragmatic effect that one's vision with regard to what constitutes a feasible computation is very much dictated by what computing power is at one's disposal." Another prevalent attitude in the literature is that new approaches in CFD ought to be directed *to suit* the new computer architectures becoming available. Both of these outlooks reflect an unfortunate (although very understandable) short-sightedness in the field of CFD. For the quest for the "best" fluid modelling representation, algorithm, and implementation should not be influenced by existing limitations of computer power and design. Rather, it should be open to the vastly increased computing potential that the future will bring and the facility to purpose-build machines if required*. The work of this thesis represents such a quest for the "best" approach to fluid modelling using a computer. As a result of the earlier exposure to conventional CFD techniques (see section 2) it was felt that the best approach could only be one which was as "physically transparent" as possible in all stages, that is, one which modelled the physics directly with minimum obscurity being introduced by mathematical treatments. This is what is meant, then, by "A Direct Approach", in the title of the thesis.

The first decision to be made in the work was the choice of the most physically transparent representation. Now it might appear on the basis of the preceding sections that a particle or cellular automata model would have had to be the choice for they have, unquestionably, the closer parallel to the microscopic sub-structure of fluids. However, it is debatable whether such models would lead to the best physical representation in the sense of providing an insight into the behaviour of fluids on the macroscopic level which is

---

* An example (already mentioned) of adapting computer design to suit the modelling concept is in cellular-automata research. These concepts were originally explored using conventional computer architectures, although not for fluid modelling purposes, and the interest and the obvious potential of the techniques lead to the development of specialised cellular-automata machines.

of particular interest in naval architecture and engineering in general. For suppose the dream of a massively parallel cellular-automata machine were realised, say; it would then be possible to constitute the machine as a ship's towing tank and to run comparative tests on alternative hull geometries in the process of ship design for the purpose of hull form selection. However, ironically, it may still not be possible to explain *why* a particular hull was the best in terms of hydrodynamic performance for the underlying mechanics of the molecular model would be too far removed from the observable performance features to be able correlate the "causes" (namely the subtleties of the hull shape) and the "effects" (the variations of flow behaviour). With this observation it is now possible to expand upon the required capabilities needed in CFD as described in section 3. It is clear now that in addition to the facility to replace standard physical testing rigs such as wind tunnels and water tanks, CFD should ideally provide an insight to, and information for, the *understanding* of fluid behaviour on the macroscopic level. This should now be considered as a further implicit qualification of what is meant by the term "direct".

In this work, then, it was decided to develop the ideas of a "direct computer model" adhering to a continuum representation of a fluid, believing this to be the most physically suitable model for facilitating understanding of flow phenomena on an observable level. Modelling concepts and developments were to be explored using a conventional computer architecture, but with the awareness that the developed algorithms may not be suited to such sequential processing. As the basis of representation would be essentially conventional, any innovative features of the techniques developed would lie on the ALGORITHMIC LEVEL (see section 5). The principal innovative feature intended was the avoidance of mathematical interpretations and distractions, and the development of an algorithm that matched the concepts of physical transparency as closely as possible throughout.

7. CLOSURE

In this chapter the origins of the research into the development of a "direct" approach to computer modelling of fluids have been described. These lie in the recognition of an urgent need for CFD developments in engineering (particularly Naval Architecture) and what are believed to be certain shortfalls in conventional approaches where actual physical mechanisms can be obscured by intermediate mathematical models. A direct approach has been defined as one that is "physically transparent" - a term which is qualified to imply, additionally, the provision of the facility to *understand* fluid system responses. The decisions to use a (conventional) continuum representation of fluid structure and to be open-minded about implementation possibilities have been described.

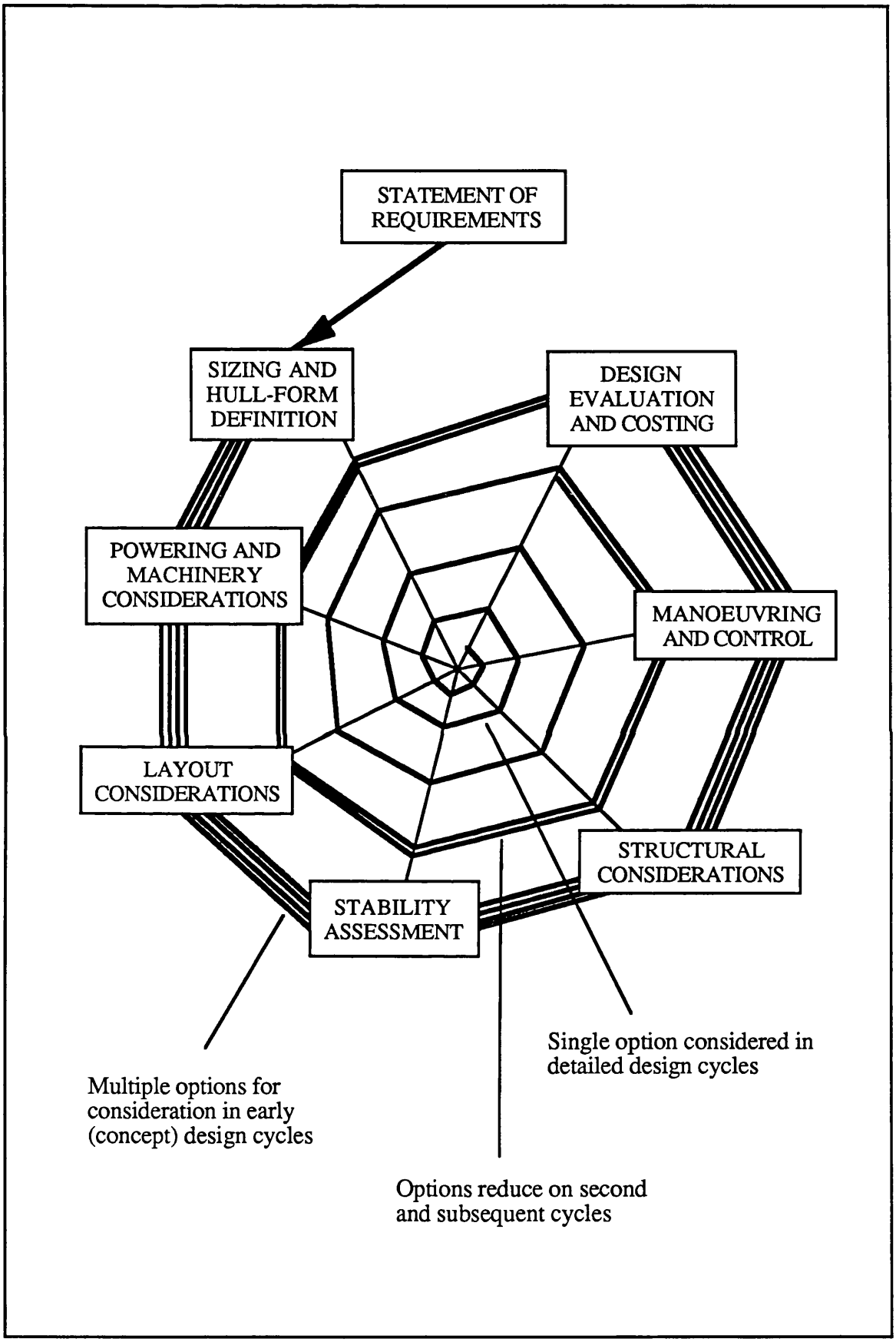

Figure 1.1 The Ship Design Process

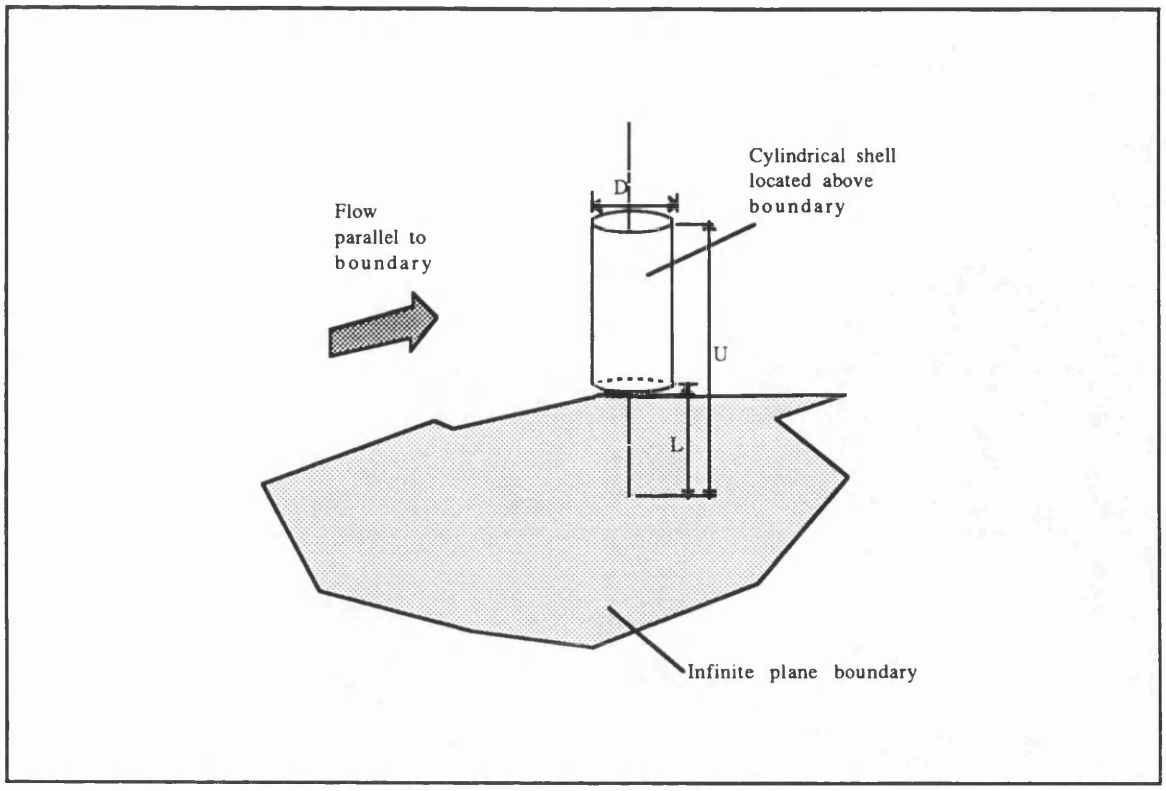

Figure 1.2 Spalding's Suggested Stepping Stone for CFD Development

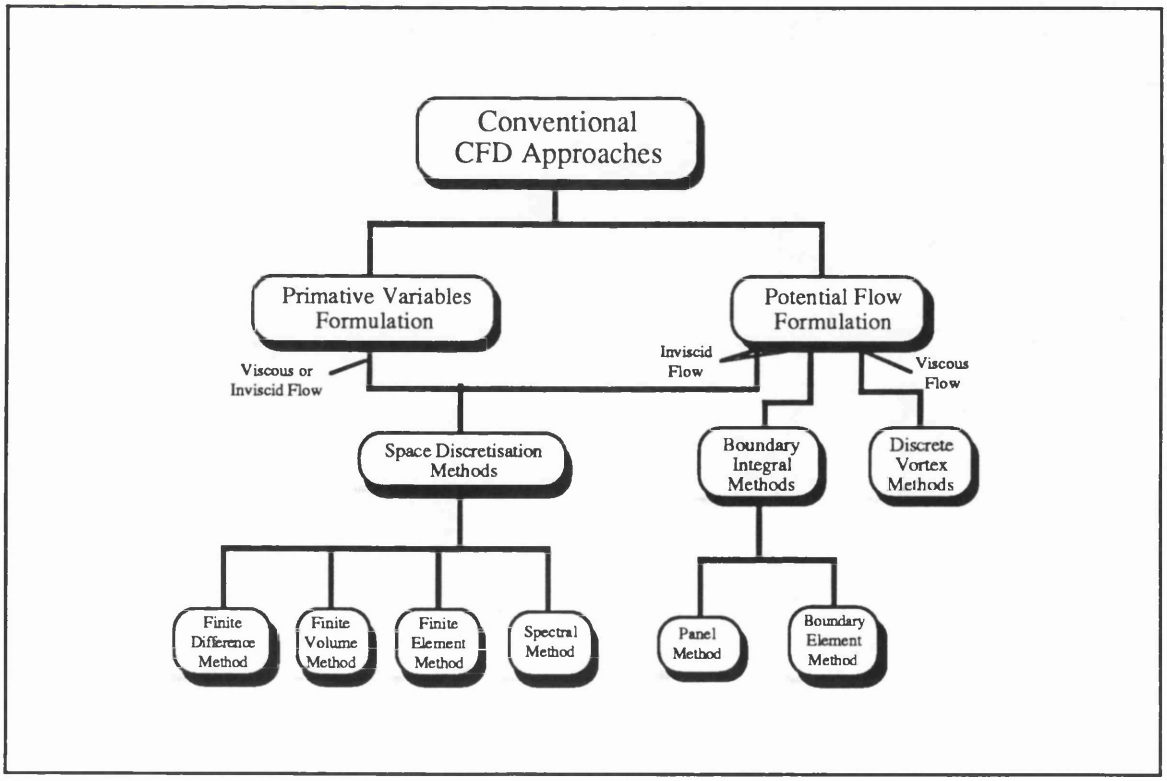

Figure 1.3 Categorisation of Conventional Approaches

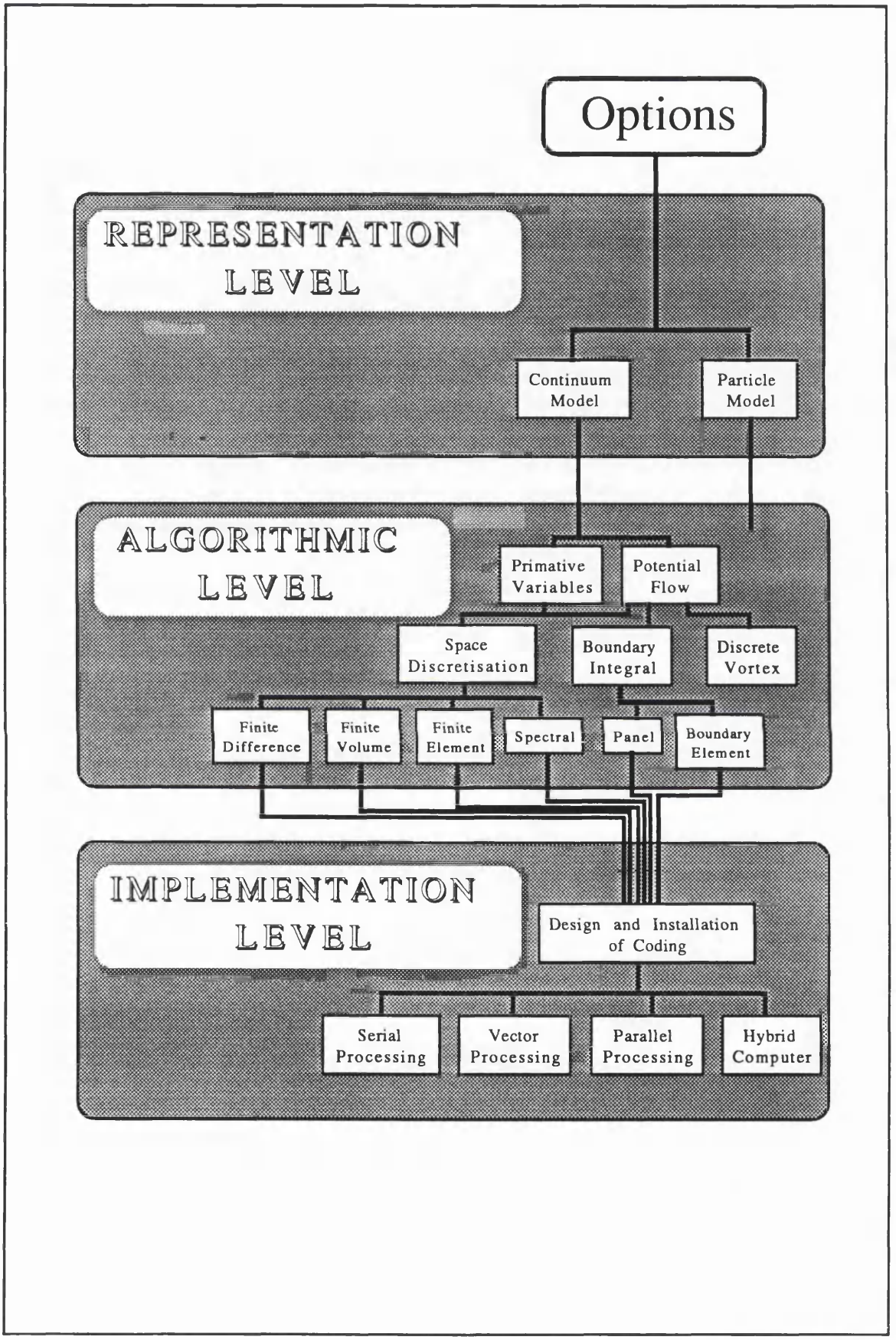

Figure 1.4 Representation, Algorithmic and Implementation Levels in Conventional Approaches

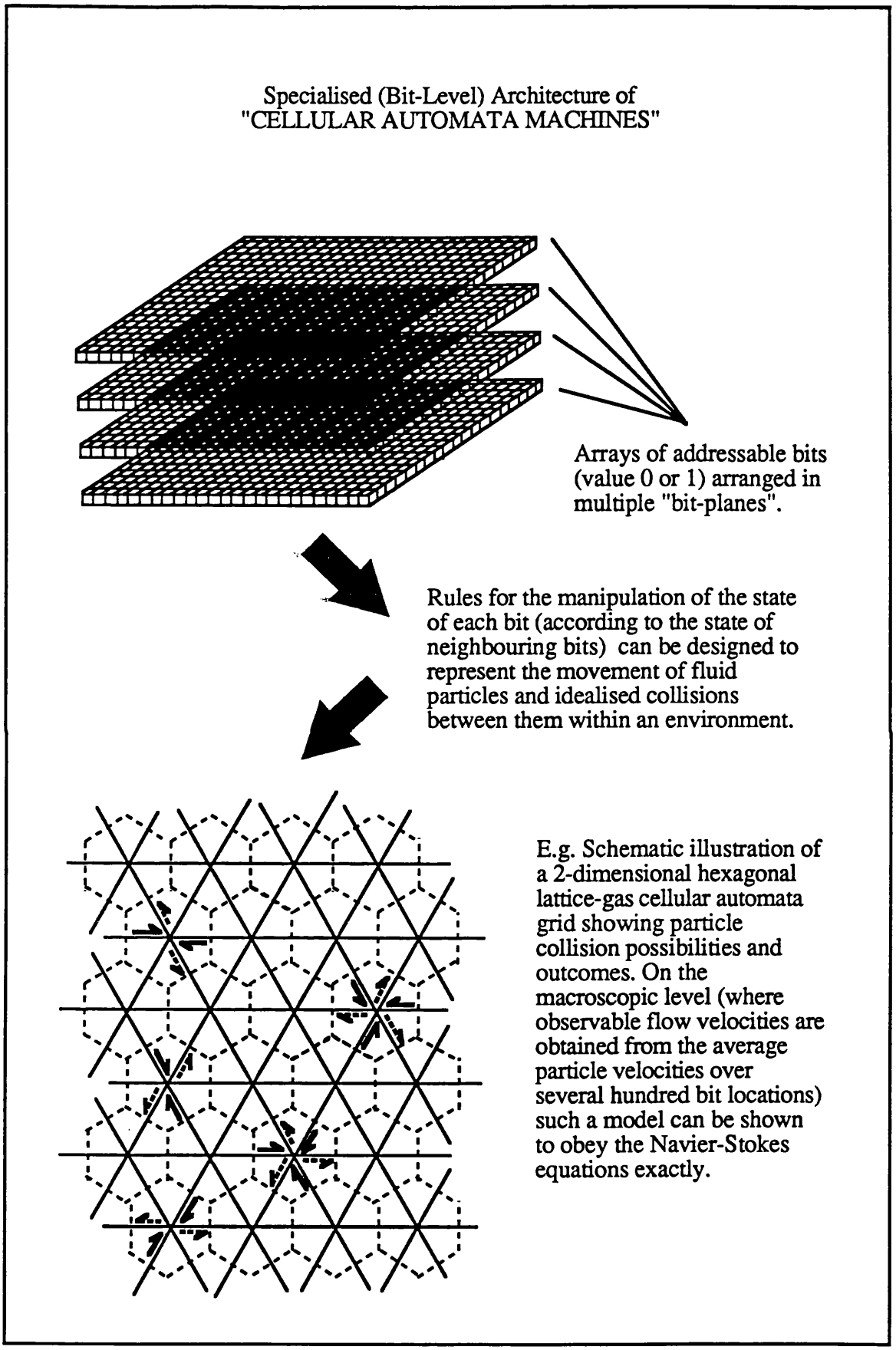

Figure 1.5 Cellular Automata Model of a Fluid

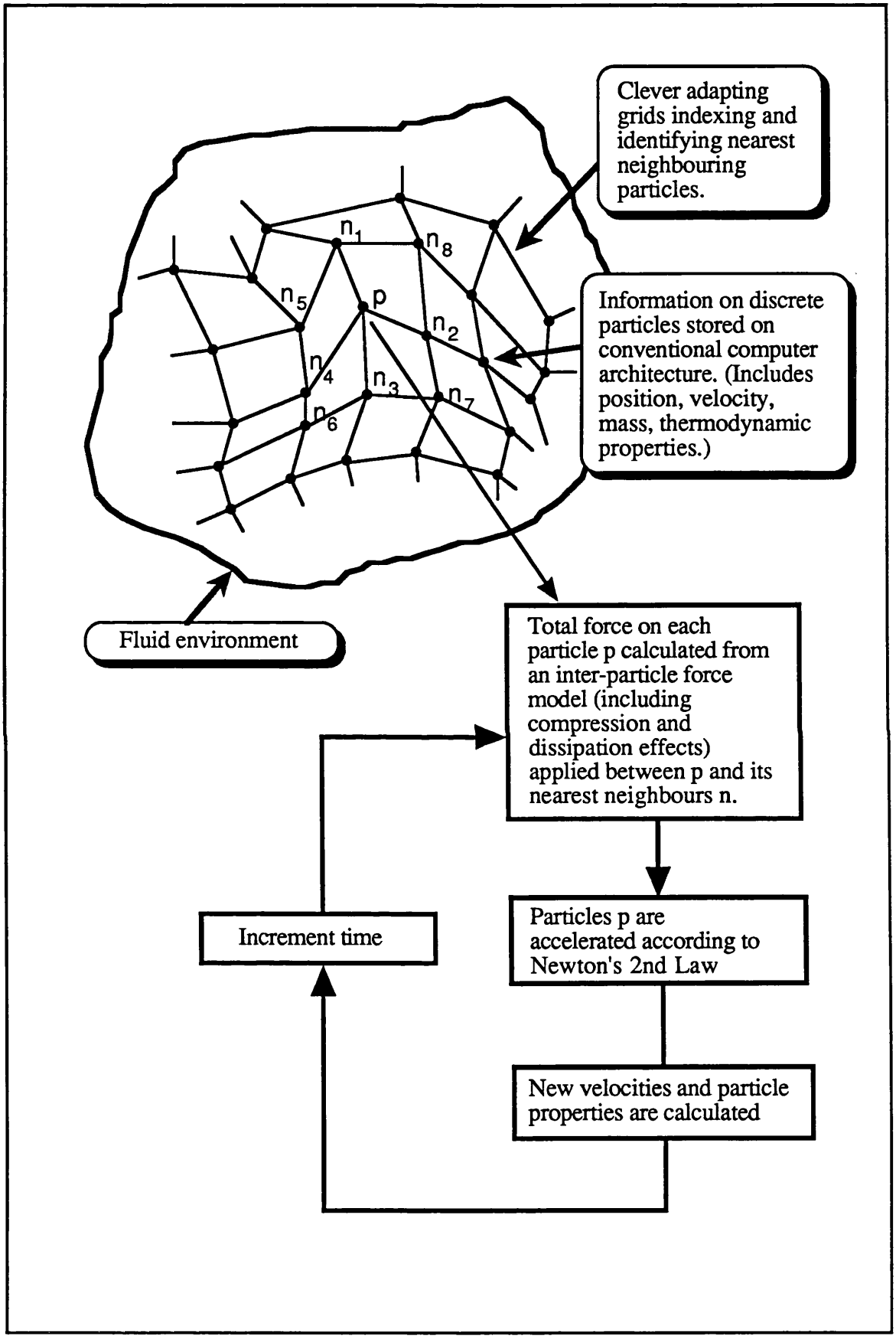

Figure 1.6 Particle Model of a Fluid

CHAPTER 2

CONVENTIONAL COMPUTATIONAL FLUID DYNAMICS

1. INTRODUCTION

In chapter 1 the need for developments in computer modelling of fluids has been established, but concern was expressed regarding *the way* in which computers are presently being used to model fluid behaviour. It was felt that there was too much emphasis on the mathematical interpretation of flow equations rather than the basic physical behavioural mechanisms involved. The direction of this research, then, was to develop a "direct" approach to modelling fluid behaviour using a computer where the techniques involved would be physically transparent throughout. In order to clarify the distinction between a "mathematical model" and a "direct" model, and to be able to gauge any achievements made in this research, this chapter presents a short review and criticism of the techniques used in conventional CFD.

2. MATHEMATICAL BASES

2.1 Continuum Hypothesis

In the normal range of engineering fluids applications the smallest significant length considered is much greater than the average distance between molecules. It is therefore justifiable to simplify the nature of a fluid and treat it as a "continuum", that is a continuous distribution of matter, rather than an (actual) conglomeration of separate molecules. The properties of a fluid may then be considered to vary continuously throughout its extent, even though these are molecular in origin, and may be represented by such attributes as temperature, pressure, viscosity, and so on. Similarly, kinematic characteristics such as velocity and acceleration are considered to vary continuously from point to point in a fluid. Where it is necessary in the development of flow equations to postulate a very small element (or particle) of fluid, this is assumed to be still large enough to contain very many molecules such that it constitutes part of the continuum.

2.2 Continuity

The principle that matter may not be created or destroyed, when applied to the flow through an infinitesimal control volume within a fluid, yields the so-called continuity equation. In a cartesian coordinate system this is

$$\frac{\partial \rho}{\partial t} = -\left[\frac{\partial}{\partial x}(\rho u) + \frac{\partial}{\partial y}(\rho v) + \frac{\partial}{\partial z}(\rho w)\right] \qquad 2.1$$

which reduces to

$$\frac{\partial u}{\partial x} + \frac{\partial v}{\partial y} + \frac{\partial w}{\partial z} = 0 \qquad 2.2$$

for incompressible fluids, i.e. fluids of constant density.

2.3 General Equations of Motion

The equations of motion using an Eulerian description for a fluid are simply a statement of Newton's Second Law of Motion as applied at a point in the flow. The mass of fluid considered is that of an infinitesimal particle of fluid passing through the point, and the force and acceleration may be conveniently resolved into components in the principal directions of an appropriate axes system.

The force on a particle of fluid is composed of "body forces" and "surface forces". A body force is one which is proportional to the mass of the particle (e.g. weight), whereas surface forces arise due to the continuous distribution of stress throughout the fluid caused by pressure and shearing influences. In a cartesian coordinate system let the body forces per unit volume be X, Y, & Z at a point in the directions of the axes. Considering surface forces, the stress at a point in the fluid is conveniently described by the 2nd order tensor

$$\begin{pmatrix} \sigma_{xx} & \tau_{yx} & \tau_{zx} \\ \tau_{xy} & \sigma_{yy} & \tau_{zy} \\ \tau_{xz} & \tau_{yz} & \sigma_{zz} \end{pmatrix} \qquad 2.3$$

and it can be shown that the resultant of the surface forces acting on the particle of fluid per unit volume is the gradient of these stress components

$$\begin{pmatrix} \frac{\partial \sigma_{xx}}{\partial x} & \frac{\partial \tau_{yx}}{\partial y} & \frac{\partial \tau_{zx}}{\partial z} \\ \frac{\partial \tau_{xy}}{\partial x} & \frac{\partial \sigma_{yy}}{\partial y} & \frac{\partial \tau_{zy}}{\partial z} \\ \frac{\partial \tau_{xz}}{\partial x} & \frac{\partial \tau_{yz}}{\partial y} & \frac{\partial \sigma_{zz}}{\partial z} \end{pmatrix} \qquad 2.4$$

Applying Newton's Second Law, then, to unit volume of fluid at a point yields the equations describing motion in each of the axes directions as

$$\begin{aligned} \rho\frac{Du}{Dt} &= \frac{\partial \sigma_{xx}}{\partial x} + \frac{\partial \tau_{yx}}{\partial y} + \frac{\partial \tau_{zx}}{\partial z} + \rho X \\ \rho\frac{Dv}{Dt} &= \frac{\partial \tau_{xy}}{\partial x} + \frac{\partial \sigma_{yy}}{\partial y} + \frac{\partial \tau_{zy}}{\partial z} + \rho Y \\ \rho\frac{Dw}{Dt} &= \frac{\partial \tau_{xz}}{\partial x} + \frac{\partial \tau_{yz}}{\partial y} + \frac{\partial \sigma_{zz}}{\partial z} + \rho Z \end{aligned} \qquad 2.5$$

where, for example,

$$\rho\frac{Du}{Dt} = \rho\left\{\frac{\partial u}{\partial t} + u\frac{\partial u}{\partial x} + v\frac{\partial u}{\partial y} + w\frac{\partial u}{\partial z}\right\}$$

which, using 2.1, can be expressed as

$$\rho\frac{Du}{Dt} = \frac{\partial}{\partial t}(\rho u) + \frac{\partial}{\partial x}(\rho u^2) + \frac{\partial}{\partial y}(\rho uv) + \frac{\partial}{\partial z}(\rho uw)$$

It is interesting to note that equations 2.5 are equally valid for solids as well as fluids. The specific form of the equations for a specific medium are obtained by introducing the relevant stress-strain relationships. This will be developed in section 2.4.

2.4 Rheology of Newtonian Fluids

Rheology is the study of stress-strain relationships covering the whole range of continuum solid and fluid media. Here, interest will be concentrated only on Newtonian fluids which are of most common interest in engineering applications.

It is expedient (and logical) in general rheological considerations to identify the isotropic and deviatoric components of stress and strain and to relate corresponding components with each other. Isotropic components are those associated with (perhaps) a change in volume of particles, but not their shape; deviatoric components are associated with a change in shape of particles but not their volume.

Consider a situation where shear stresses are zero and only direct stresses are present. Equilibrium considerations illustrate that the direct stress components must all be equal, and this provides a definition of pressure at a point in a fluid as

$$\begin{pmatrix} \sigma_{xx} & 0 & 0 \\ 0 & \sigma_{yy} & 0 \\ 0 & 0 & \sigma_{zz} \end{pmatrix} = \begin{pmatrix} -p & 0 & 0 \\ 0 & -p & 0 \\ 0 & 0 & -p \end{pmatrix} \qquad 2.6$$

When shear stresses are present equality between the direct stress components does not necessarily apply. Nevertheless, it is possible to define the pressure at a point in a viscous fluid as (the negative of) the mean of the direct stress components, and to define the isotropic and deviatoric stress components on this basis as follows:

$$-p = \frac{1}{3}[\sigma_{xx} + \sigma_{yy} + \sigma_{zz}] = \sigma_m \qquad 2.7$$

$$\text{Isotropic stress} = \begin{pmatrix} -p & 0 & 0 \\ 0 & -p & 0 \\ 0 & 0 & -p \end{pmatrix} \qquad 2.8$$

$$\text{Deviatoric stress} = \begin{pmatrix} \sigma_{xx}+p & \tau_{yx} & \tau_{zx} \\ \tau_{xy} & \sigma_{yy}+p & \tau_{zy} \\ \tau_{xz} & \tau_{yz} & \sigma_{zz}+p \end{pmatrix} \qquad 2.9$$

In tensor form the general strain condition is given by

$$\begin{pmatrix} e_{xx} & e_{yx} & e_{zx} \\ e_{xy} & e_{yy} & e_{zy} \\ e_{xz} & e_{yz} & e_{zz} \end{pmatrix} \text{ where } e_{ij} = e_{ji} \qquad 2.10$$

and the general rate-of-strain tensor by

$$\begin{pmatrix} \varepsilon_{xx} & \varepsilon_{yx} & \varepsilon_{zx} \\ \varepsilon_{xy} & \varepsilon_{yy} & \varepsilon_{zy} \\ \varepsilon_{xz} & \varepsilon_{yz} & \varepsilon_{zz} \end{pmatrix} \text{ where } \varepsilon_{ij} = \varepsilon_{ji} \text{ and } \varepsilon_{ij} = \frac{\partial}{\partial t}(e_{ij}) \qquad 2.11$$

Here

$$\varepsilon_{xx} = \frac{\partial u}{\partial x}; \quad \varepsilon_{yy} = \frac{\partial v}{\partial y}; \quad \varepsilon_{zz} = \frac{\partial w}{\partial z}$$
$$\varepsilon_{xy} = \varepsilon_{yx} = \frac{1}{2}\left(\frac{\partial v}{\partial x} + \frac{\partial u}{\partial y}\right)$$
$$\varepsilon_{xz} = \varepsilon_{zx} = \frac{1}{2}\left(\frac{\partial w}{\partial x} + \frac{\partial u}{\partial z}\right) \qquad 2.12$$
$$\varepsilon_{yz} = \varepsilon_{zy} = \frac{1}{2}\left(\frac{\partial w}{\partial y} + \frac{\partial v}{\partial z}\right)$$

Dividing these into isotropic and deviatoric components gives the following:-

$$\text{Isotropic strain} = \begin{pmatrix} \frac{e_v}{3} & 0 & 0 \\ 0 & \frac{e_v}{3} & 0 \\ 0 & 0 & \frac{e_v}{3} \end{pmatrix} \qquad 2.13$$

where

$$e_v = \text{volumetric strain} = [e_{xx} + e_{yy} + e_{zz}]$$

$$\text{Deviatoric strain} = \begin{pmatrix} e_{xx} - \frac{e_v}{3} & e_{yx} & e_{zx} \\ e_{xy} & e_{yy} - \frac{e_v}{3} & e_{zy} \\ e_{xz} & e_{yz} & e_{zz} - \frac{e_v}{3} \end{pmatrix} \qquad 2.14$$

$$\text{Isotropic rate of strain} = \begin{pmatrix} \frac{\varepsilon_v}{3} & 0 & 0 \\ 0 & \frac{\varepsilon_v}{3} & 0 \\ 0 & 0 & \frac{\varepsilon_v}{3} \end{pmatrix} \qquad 2.15$$

where

$$\varepsilon_v = \text{rate of volumetric strain}$$
$$= [\varepsilon_{xx} + \varepsilon_{yy} + \varepsilon_{zz}]$$
$$= \left[\frac{\partial u}{\partial x} + \frac{\partial v}{\partial y} + \frac{\partial w}{\partial z}\right]$$
$$= \text{div } \mathbf{q}$$

$$\text{Deviatoric rate of strain} = \begin{pmatrix} \varepsilon_{xx} - \frac{\varepsilon_v}{3} & \varepsilon_{yx} & \varepsilon_{zx} \\ \varepsilon_{xy} & \varepsilon_{yy} - \frac{\varepsilon_v}{3} & \varepsilon_{zy} \\ \varepsilon_{xz} & \varepsilon_{yz} & \varepsilon_{zz} - \frac{\varepsilon_v}{3} \end{pmatrix} \qquad 2.16$$

Consider now the stress/strain relationships for the Newtonian fluid idealisation. Here the fluid is assumed to behave elastically under hydrostatic pressure such that the isotropic components of stress and strain may be related as

$$\begin{pmatrix} -p & 0 & 0 \\ 0 & -p & 0 \\ 0 & 0 & -p \end{pmatrix} = K \begin{pmatrix} e_v/3 & 0 & 0 \\ 0 & e_v/3 & 0 \\ 0 & 0 & e_v/3 \end{pmatrix} \qquad 2.17$$

where K is the bulk modulus of the fluid. Also, it is assumed that the shear stresses are directly proportional to the velocity strains such that the deviatoric components of stress and strain may be related as

$$\begin{pmatrix} \sigma_{xx}+p & \tau_{yx} & \tau_{zx} \\ \tau_{xy} & \sigma_{yy}+p & \tau_{zy} \\ \tau_{xz} & \tau_{yz} & \sigma_{zz}+p \end{pmatrix} = 2\mu \begin{pmatrix} \varepsilon_{xx}-\varepsilon_v/3 & \varepsilon_{yx} & \varepsilon_{zxx} \\ \varepsilon_{xy} & \varepsilon_{yy}-\varepsilon_v/3 & \varepsilon_{zy} \\ \varepsilon_{xz} & \varepsilon_{yz} & \varepsilon_{zz}-\varepsilon_v/3 \end{pmatrix} \qquad 2.18$$

where μ is the shear viscosity of the fluid. On substitution of 2.12 and 2.15 the fluid stress state is related to the flow kinematics by

$$\begin{pmatrix} \sigma_{xx}+p & \tau_{yx} & \tau_{zx} \\ \tau_{xy} & \sigma_{yy}+p & \tau_{zy} \\ \tau_{xz} & \tau_{yz} & \sigma_{zz}+p \end{pmatrix} = \mu \begin{pmatrix} \left(2\frac{\partial u}{\partial x} - \frac{2}{3}\operatorname{div} \mathbf{q}\right) & \left(\frac{\partial v}{\partial x}+\frac{\partial u}{\partial y}\right) & \left(\frac{\partial v}{\partial x}+\frac{\partial u}{\partial y}\right) \\ \left(\frac{\partial v}{\partial x}+\frac{\partial u}{\partial y}\right) & \left(2\frac{\partial v}{\partial y} - \frac{2}{3}\operatorname{div} \mathbf{q}\right) & \left(\frac{\partial v}{\partial x}+\frac{\partial u}{\partial y}\right) \\ \left(\frac{\partial v}{\partial x}+\frac{\partial u}{\partial y}\right) & \left(\frac{\partial v}{\partial x}+\frac{\partial u}{\partial y}\right) & \left(2\frac{\partial w}{\partial z} - \frac{2}{3}\operatorname{div} \mathbf{q}\right) \end{pmatrix} \qquad 2.19$$

In restricting attention to incompressible Newtonian fluids, where K=infinity and $\varepsilon_v = 0$, then the div **q** terms will drop out.

2.5 Equations of Motion for a Newtonian Fluid With Constant Properties

The rheological relationships for a Newtonian fluid (2.19) may now be substituted into the general equations of motion (2.5). The component equations in the x, y and z directions then are as follows

$$\frac{\partial(\rho u)}{\partial t} + \frac{\partial}{\partial x}\left[\rho u^2 - \left(2\mu\frac{\partial u}{\partial x} - \frac{2}{3}\mu \,\mathrm{div}\,\mathbf{q}\right)\right] + \frac{\partial}{\partial y}\left[\rho uv - \left(\mu\left[\frac{\partial v}{\partial x} + \frac{\partial u}{\partial y}\right]\right)\right] + \frac{\partial}{\partial z}\left[\rho uw - \left(\mu\left[\frac{\partial w}{\partial x} + \frac{\partial u}{\partial z}\right]\right)\right] + \frac{\partial p}{\partial x} - \rho X = 0 \qquad 2.20(a)$$

$$\frac{\partial(\rho v)}{\partial t} + \frac{\partial}{\partial x}\left[\rho vu - \left(\mu\left[\frac{\partial u}{\partial y} + \frac{\partial v}{\partial x}\right]\right)\right] + \frac{\partial}{\partial y}\left[\rho v^2 - \left(2\mu\frac{\partial v}{\partial y} - \frac{2}{3}\mu \,\mathrm{div}\,\mathbf{q}\right)\right] + \frac{\partial}{\partial z}\left[\rho vw - \left(\mu\left[\frac{\partial w}{\partial y} + \frac{\partial v}{\partial z}\right]\right)\right] + \frac{\partial p}{\partial y} - \rho Y = 0 \qquad 2.20(b)$$

$$\frac{\partial(\rho w)}{\partial t} + \frac{\partial}{\partial x}\left[\rho wu - \left(\mu\left[\frac{\partial u}{\partial z} + \frac{\partial w}{\partial x}\right]\right)\right] + \frac{\partial}{\partial y}\left[\rho wv - \left(\mu\left[\frac{\partial v}{\partial z} + \frac{\partial w}{\partial y}\right]\right)\right] + \frac{\partial}{\partial z}\left[\rho w^2 - \left(2\mu\frac{\partial w}{\partial z} - \frac{2}{3}\mu \,\mathrm{div}\,\mathbf{q}\right)\right] + \frac{\partial p}{\partial z} - \rho Z = 0 \qquad 2.20(c)$$

These are the **Navier-Stokes Equations** for Newtonian fluids which, in the given form, allow for compressibility and varying viscosity. If viscosity can be considered constant then μ may be taken outside the differentials. For incompressible flows ρ may be taken outside the differentials and the div **q** terms will vanish.

There is obviously a symmetry to the components of the Navier-Stokes equations and, although this is far from distinct, use is generally made of this feature to simplify the presentation and subsequent manipulation of these equations in analytical or computational work. It is appropriate, therefore, to illustrate that the Navier-Stokes equations are usually summarised in suffix notation as follows

$$\frac{\partial(\rho u_i)}{\partial t} + \frac{\partial}{\partial x_j}\left[\rho u_j u_i - \mu\left(\frac{\partial u_j}{\partial x_i} + \frac{\partial u_i}{\partial x_j} - \frac{2}{3}\frac{\partial u_k}{\partial x_k}\delta_{ij}\right)\right] + \frac{\partial p}{\partial x_i} - \rho X_i = 0 \qquad 2.21$$

where this represents the three equations of 2.20 in one expression. In 2.21 u_i is the velocity component in the direction x_i, where i = 1, 2, 3 and corresponds to the cartesian directions x, y, z respectively. Terms involving suffix j are to be repeated within the component expression for j = 1, 2, 3. The "rules" for the interpretation of the suffix notation are best assimilated by comparing 2.21 with the components of 2.20.

3. TREATMENT OF THE EQUATIONS OF MOTION

A rigorous, general solution to the Navier-Stokes equations (2.20) is not known and, therefore, simplifications to the equations must be made (providing these are justifiable) and/or the equations must be tackled numerically (with associated approximations) to obtain specific solutions. The solution of the partial differential equations will depend upon the boundary conditions of the specific problem, which may consist of kinematic and dynamic constraints. Kinematic constraints are the more common where the velocity vectors at the boundaries must be such that:

(i) The component of the fluid velocity normal to the boundary must equal the normal velocity of the boundary.

(ii) For a viscous fluid the component of the fluid velocity tangential to the boundary must equal the tangential velocity of the boundary.

Dynamic boundary conditions may also exist where the pressure of the fluid is known at the boundary. For example, where the fluid has a free surface to air (a flexible boundary) the solution must be such that the pressure is constant and equal to the ambient air pressure.

3.1 Reynolds Averaged Navier-Stokes Equations

Although non-linear in form, the Navier-Stokes equations (2.20) look reasonably amenable to numerical solution. There is, however, a very important complication associated with most flows of engineering interest, namely turbulence. The problem appears when attempting to discretise the equations for numerical solution; for the length scale of turbulence within a fluid is extremely small and this would place extremely demanding restrictions on the discretisation in order to adequately represent the spatial variations of flow velocities. Emmons [3e] provides a useful demonstration of the severity of the computational demands of solving the full Navier-Stokes equations for turbulent

flow. He estimated that to model fully developed turbulent flow in a pipe at the very modest Reynolds number of $5x10^3$ would require about 10^{14} numerical operations. In 1970 when computer speeds were of the order of 10^5 operations per second the solution would have taken about 10^9 seconds, or 100 years. With modern day supercomputers, where typical speeds are about $400x10^6$ operations per second, the equivalent calculation would still take about 3 months with a conventional computer architecture. Although such numerical solution of the full Navier-Stokes equations is becoming possible on the most advanced supercomputers [3a,3d] the capacity and speed of past and common present day machines has demanded the incorporation within the equations of some form of "turbulence model" whereby the influences of smaller scales of turbulence affecting the gross flow behaviour can be modelled using relatively coarse discretisation.

Turbulence is characterised by the superposition of a highly irregular oscillating velocity pattern upon an underlying "smooth" or "average" flow. As the flow characteristics of direct interest are generally the more observable features, such as the mean velocity profiles and mean drag forces, etc, the approach adopted to account for turbulence in flow problems of practical interest is to re-cast the Navier-Stokes equations for the *averaged* values of velocity, stresses, density, and so on. To achieve this it is necessary to identify the time-averaged and fluctuating components of each flow parameter as

$$\begin{aligned} u &= \bar{u} + u' \\ v &= \bar{v} + v' \\ w &= \bar{w} + w' \\ p &= \bar{p} + p' \\ &\text{etc.} \end{aligned} \qquad 2.22$$

where the plain lower-case symbols represent the instantaneous values, the over-bar denotes the time-averaged values, and the primes denote the fluctuating components. By substituting for 2.22 into the Navier-Stokes equations 2.20 and taking the average of each resulting term (over a temporal period that is large compared to the characteristic period of the turbulent oscillations but still small compared to the time-scale of the basic flow) yields the time-averaged (or Reynolds averaged) Navier-Stokes equations given below.

$$\frac{\partial(\bar{\rho}\bar{u}_i)}{\partial t} + \frac{\partial}{\partial x_j}\left[\bar{\rho}\,\bar{u}_j\bar{u}_i + \bar{\rho}\,\overline{u'_i u'_j} - \mu\left(\frac{\partial \bar{u}_j}{\partial x_i} + \frac{\partial \bar{u}_i}{\partial x_j} - \frac{2}{3}\frac{\partial \bar{u}_k}{\partial x_k}\delta_{ij}\right)\right] + \frac{\partial \bar{p}}{\partial x_i} - \bar{\rho}\,\bar{X}_i = 0 \qquad 2.23$$

In the averaging process the terms which are linear with respect to the fluctuating components vanish while the quadratic terms survive. This accounts for the appearance of the Reynolds stresses which are produced by the time-averaging of the acceleration terms. Physically, the Reynolds stresses can be identified with the transport of momentum

associated with the fluctuating components of velocity. Unfortunately, there is no means of defining the Reynolds stresses by means of a distinct analytical expression of known flow properties. It is necessary, therefore, to account for these terms by treatments which rely on empiricism and experimental observation. The way in which the (six) unknown Reynolds stress components are handled constitutes the subject of turbulence modelling, about which a vast literature exists. For the present purposes of review it will suffice only to describe one of the most common, economical, and reasonably reliable treatments, the "k-ε" model [10c]. This model, in common with many others, is based upon the "eddy viscosity hypothesis" where it is assumed that the Reynolds stresses are analogous to the viscous stresses in the system and are of the form

$$-\overline{\rho}\,\overline{u'_i u'_j} = \mu_t\left(\frac{\partial \overline{u}_j}{\partial x_i}+\frac{\partial \overline{u}_i}{\partial x_j}-\frac{2}{3}\frac{\partial \overline{u}_k}{\partial x_k}\delta_{ij}\right) - \frac{2}{3}\rho k\,\delta_{ij} \qquad 2.24$$

using suffix notation. Here k is the kinetic energy of the turbulent motion given by

$$k = \frac{1}{2}\left(\overline{u'_i\,u'_i}\right) \qquad 2.25$$

and μ_t is called the turbulent (or eddy) viscosity and is some function of the dynamics of the flow. When this description of the Reynolds stress is assumed, and the term containing k is combined with the pressure, the time-averaged Navier-Stokes equations take on a form which is identical to the general Navier-Stokes equations

$$\frac{\partial(\overline{\rho}\overline{u}_i)}{\partial t}+\frac{\partial}{\partial x_j}\left[\overline{\rho}\,\overline{u}_j\overline{u}_i-\mu_{eff}\left(\frac{\partial \overline{u}_j}{\partial x_i}+\frac{\partial \overline{u}_i}{\partial x_j}-\frac{2}{3}\frac{\partial \overline{u}_k}{\partial x_k}\delta_{ij}\right)\right]+\frac{\partial \overline{p}}{\partial x_i}-\overline{\rho}\,\overline{X}_i = 0 \qquad 2.26$$

where $\mu_{eff} = \mu + \mu_t$. By this treatment the six unknown Reynolds stresses have been replaced by the single unknown μ_t.

The k-ε Model of Turbulence

In the k-ε model arguments of dimensional analysis suggest that μ_t may be represented by

$$\frac{\mu_t}{\rho} = \frac{C_\mu k^2}{\varepsilon} \qquad 2.27$$

where ε is the rate at which the kinetic energy of the mean flow is being dissipated to internal energy by the action of molecular viscosity. C_μ is an empirical constant which is expected to be constant for a wide range of flows of similar type. The two unknowns k and ε require two further equations . Exact transport equations for each may be derived but

these introduce further unknowns, and so on. To avoid the ensuing infinite system of equations, the exact equations for k and ε are modelled by equations derived from them which mimic them as far as possible while avoiding the introduction of further unknowns. The simplified equations governing k and ε, then, are

$$\frac{\partial(\rho k)}{\partial t} + \frac{\partial}{\partial x_j}\left[\overline{\rho u_j} k - \frac{\mu_t}{\sigma_k}\frac{\partial k}{\partial x_j}\right] - \mu_t C_1 + \rho\varepsilon = 0 \qquad 2.28$$

$$\frac{\partial(\rho\varepsilon)}{\partial t} + \frac{\partial}{\partial x_j}\left[\overline{\rho u_j}\varepsilon - \frac{\mu_t}{\sigma_\varepsilon}\frac{\partial \varepsilon}{\partial x_j}\right] - \frac{\varepsilon}{k}(C_1\mu_t G - C_2\rho\varepsilon) = 0 \qquad 2.29$$

where

$$G = \left(\frac{\partial \overline{u}_i}{\partial x_j} + \frac{\partial \overline{u}_j}{\partial x_i}\right)\frac{\partial u_i}{\partial x_j}$$

and C_1, C_2, σ_k and σ_ε are empirical coefficients which for the simplest model are taken as constants (see [10c]).

3.2 Reduction of the Navier-Stokes Equations

The most obvious simplification of the equations of motion is to eliminate viscosity. If viscosity is absent then there is no mechanism for generating shear stresses within the fluid and the flow is consequently irrotational. In these circumstances the velocity components can be described by a velocity potential function $\phi(x,y,z,t)$ where

$$u = \frac{\partial \phi}{\partial x}; \quad v = \frac{\partial \phi}{\partial y}; \quad w = \frac{\partial \phi}{\partial z} \qquad 2.30$$

Substituting for 2.30 into the continuity equation for incompressible flow (2.2) indicates that the velocity field may be described by the Laplace equation

$$\nabla^2 \phi = 0 \qquad 2.31$$

and therefore by solving this equation (usually numerically) with the given boundary conditions the velocities in the system may be found independently of the pressure field. The equations of motion in the absence of viscosity reduce to the Euler equations (see [1c] for a useful description of flow equations) and these now serve to provide the solution to the pressure field in the fluid.

Potential flow solutions can only be assumed to be reasonable approximations to flow systems where the velocity gradients in the flow are small. Such solutions, therefore, have limited direct application in engineering, but may be used in the overall synthesis of a flow solution in a number of ways. For example, recognising that the highest velocity gradients exist in the boundary layers of viscous flows, a suitable treatment in some circumstances is to deal with the boundary layer and mainstream flows semi-independently in a technique sometimes described as "zonal decomposition" of the flow: here the mainstream flow is treated as a potential flow problem, and the Navier-Stokes equations need only be applied in the boundary layer regions - and even then, perhaps, with simplifications [2b]. The use of such zonal approaches, however, is generally restricted to flow systems where very limited flow separation takes place.

To simulate the *effects* of viscous flows where significant separation occurs it is possible to extend the technique of potential flow modelling by including discrete and distributed vortex elements in the potential field (see[9a]). Such methods can produce good pictures of separating flow where the points of likely separation and the generation of the dominant vortices in the flow are known. However, they are less successful for flow *predictions* where points and strengths of separation are to be determined in perhaps novel system geometries. And so, for general modelling of viscous flows, then, it is necessary to tackle the full Navier-Stokes equations.

3.3 Detail

In sections 4 and 5 the typical numerical treatments of the equations of motion will be described in more detail. The purpose is to review the techniques involved in conventional approaches in CFD in order to clarify the distinction between these and the form of the "direct" model proposed in this work. Section 4 will examine computational techniques for tackling the Reynolds Averaged Navier-Stokes equations for general complex flow. Section 5 will look at computational methods used for flow systems where the Navier-Stokes equations can be simplified or avoided. The reason for starting with the treatment of general flow problems is that some of the techniques described in section 4 can also be used for the simpler flow models; simple reference can therefore be made to them from within section 5.

4. COMPUTATIONAL METHODS FOR SOLVING THE NAVIER-STOKES EQUATIONS

There is a logic to the development of the solution procedure adopted for any given flow problem using conventional CFD. This is illustrated in figure 2.1. Starting from the basic set of differential equations the first decision to be made is the choice of the principal dependent variables (i.e. the appropriate flow parameters) and the independent variables (i.e. the coordinate system) for the algorithm. Having selected the working differential equations, a discretisation procedure must be adopted to transform the (infinite degree of freedom) differential equations to (finite degree of freedom) algebraic form, where the continuous variations of flow variables are now represented by values at discrete locations in time and space within the system. Next, the details of the solution algorithm must be chosen and coded as a computer program. Finally, the program results must be checked for accuracy and limitations before any real confidence can be placed in the coding.

4.1 The Basic Differential Equations

The basic differential equations involved in CFD (and developed in sections 2 and 3) are summarised in figure 2.2. The time averaged Navier-Stokes (momentum) equations, employing the k-ε turbulent viscosity model (see section 3.1), are shown as equations A. The continuity equation is given in equation B. The associated equations governing the kinetic energy of turbulence and the rate of dissipation of the same are given by equations C.

In three dimensions for turbulent flow, then, we have (so far) six equations (three in A for i = 1,2,3, plus B, plus two in C) and six unknowns, $\bar{u}_i$ (i=1,2,3), $\bar{p}$, k, and ε. Compressible flow problems will involve at least these six equations with the associated equation of state D linking the pressure and density in the flow. If significant changes in temperature or chemical reactions occur, then further scalar conservation equations for total energy and chemical species will become involved. For the flows of interest to Naval Architecture constant density, temperature and composition are usually valid assumptions and just the first six equations described would need to be solved. For laminar flow (seldom encountered in Naval Architecture) k and ε are zero and the total number of equations reduce by two.

Although the principal interest of this thesis is in incompressible flow modelling, the equations will be left in general (compressible) form in order to review all available CFD techniques. For it could be argued that compressible flow algorithms could be applied to

incompressible flow problems; and so for completeness these need to be covered. It is convenient to note that all of the equations described so far can be represented by the generalised equation E in figure 2.3. For the purposes of representing the discretisation of the equations in sections 4.2 to 4.5 these general variables will be used. Figure 2.3 summarises the interpretations of the generalised equation for the individual equations A to D in figure 2.2..

4.2 Choice of Dependent Variables

There is a certain amount of choice available in the selection of the principal dependent variables in the algorithm for solving the equations of motion. The most obvious options are either velocity and pressure, or velocity and density. By choosing the latter one is immediately restricted to compressible flow problems, as density ceases to be a variable in incompressible flow. The choice of velocity and pressure is general in applicability, but suffers somewhat in that the pressure has no obvious equation of its own.

Less obvious as a choice of dependent variable is the vector potential and vorticity of the flow (see [1a]). This was once the most popular selection because only two equations were required for the 2-dimensional flows studied in early work. However, as vector potential can only be defined if the density is constant, the formulation is only suitable for incompressible flow. Furthermore, the extension of the concepts to 3-dimensions is difficult, and the imposition of kinematic and dynamic boundary conditions is awkward. More details of this representation may be found in [2b].

4.3 Selection of Independent Variables

The independent variables in any computation are the coordinates of the discrete points used to represent the continuous variations of flow parameters (velocity, pressure, etc.). The arrangement of these coordinates constitutes the computational mesh or grid, and the choice of this will determine the geometrical flexibility of the model as a whole and, to some extent, the choice of the discretisation process.

With the governing equations of motion most usually expressed (as here), and most easily recognisable, in cartesian from, the most obvious mesh arrangement would be rectangular as shown in figure 2.4(a). The representation of flow derivatives, then, could be in terms of differences between grid points (nodes) along the principal directions of the

grid. However, it is considered that such mesh arrangements are inflexible, particularly with respect to mesh distribution where the need to refine the mesh (by subdivision) results in crowding in irrelevant regions. For general application, then, rectangular mesh arrangements are not recommended by computational fluid dynamicists [2d,10b].

With rectangular meshes being dismissed for general application, more elaborate schemes must be employed for the coordinate arrangements. The principal possibilities are illustrated in figure 2.4. The increased flexibility of the alternative arrangements comes at a cost of; (i) increased complication with the likely need to re-cast the equations in a form compatible with the mesh coordinate system; (ii) increased effort in defining the mesh and fitting it to complex geometries. The latter problem has become almost a discipline in its own right [4]. A review of procedures adopted in mesh generation may be found in [4b].

Despite the limited application of rectangular mesh arrangements, the remainder of this description of CFD principles and techniques will continue with treatment of the equations of motion in cartesian form.

4.4 Discretisation of the Governing Equations

Having selected the governing equations (in a form suited to the chosen mesh arrangements), it is now necessary to transform the (continuous) differential conservation equations to algebraic form with a finite number of degrees of freedom (dependent on the number of nodes in the system). The procedure involves approximating space and time derivatives of dependent variables at discrete locations in the mesh to algebraic functions of the values of the respective variables at the given node and a selection of its neighbours. There are four principal strategies that can be adopted to do this. These are:-

- Finite Difference Method
- Finite Volume Method
- Finite Element Method
- Spectral Method

In practice time derivatives are always represented by finite difference approximations, whilst spatial derivatives may be represented by any of the four. These different strategies will now be briefly outlined. In the following sections concentration will be placed on the finite volume method with which the author has had more experience [10d].

The process of discretisation by any of the above strategies reduces the differential equations of motion to algebraic form where the values of the variables ϕ at node point p are related to the values of neighbouring nodes by an expression which combines the effects of accumulation, transport and sources within the system - see figure 2.5. Whatever method is used to perform this discretisation, the subsequent solution procedure is essentially independent of the means of discretisation.

Finite Difference Method

This is the most direct and the most obvious means of discretising any differential equation governing a variable ϕ. The variation of ϕ is approximated by some function of distance in the coordinate directions and is fitted to the selected nodes. Figure 2.6 illustrates one implementation of such a scheme as applied to a simplified form of the prototype equation of figure 2.3. Here the time difference has been represented by a forward differencing approximation, and the spatial derivatives by a centred differencing approximation. Other differencing schemes are possible, such as upwind differencing, hybrid and blended techniques; the details of these may be followed up in [2a]. It should be noted that the choice of whether the spatial derivatives are evaluated at the old timestep or at the new timestep has important consequences for the nature of the solution algorithm (see section 4.5).

The finite difference method is very easy to implement. However, its adaptability is constrained by the type of mesh used: orthogonal meshes are straightforward to use, but other types need some considerable effort in formulation of the finite difference scheme. The technique requires low to moderate computing effort, with relatively low storage requirements. The principal failing of the method is that conservation is not ensured.

Finite Volume Method

In this technique the governing differential equations are integrated over control volumes surrounding each node. This results in integral flux and source expressions which again may be approximated using the various differencing schemes. Figure 2.7 illustrates an implementation of the process as applied to a simplified form of the prototype equation.

Again this method is straightforward to implement, yet unlike the finite difference method it is easy to adapt to different mesh configurations. The computing effort and storage requirements are similar to the finite difference method. The main strength of this method is that, since fluxes are employed, conservation can be ensured.

Finite Element Method

The finite element method achieves discretisation of the governing equations in two stages. Each stage involves errors, but these are not always additive. First an assumption is made about the spatial variation of ϕ within each element by means of a "trial function". This is essentially a local interpolation applied over an element, linking the solution at a point within the element to the nodal values. The second stage uses a weighted residual method (see [2b]) to obtain algebraic equations for the relationships between nodal values. The details of the technique will not be described further here, suffice it to say that the resulting discretisation yields algebraic equations of the form illustrated in figure 2.5. More details of the technique may be found in [2d].

The finite element method is much more complex than the finite volume or difference techniques. The main attraction of the method is said to be its ability to handle complex geometries with ease. (Proponents of the finite volume method argue that this formulation is similarly versatile [2d].) The computing effort and storage is generally much higher than the finite difference or volume techniques and, because flux continuity is difficult to maintain between elements, conservation is seldom ensured.

Spectral Method

In this, relatively new, technique the spatial variation of each dependent variable throughout the system is represented by an infinite series (such as a Fourier Series, Chebyshev Polynomial, or a Legendre Polynomial) truncated to a finite number of terms. As the series applies over the whole domain, the method is said to be global. By substituting the series approximations into the governing partial differential equations, relationships between the series coefficients can be obtained. Specialised methods, such as fast Fourier transforms, may be used to determine the coefficients. More details of this approach may be found in [2a,2b].

The spectral method is very complex and has a high storage and computing effort requirement. Nevertheless, when it works(!) it is very accurate, and indeed is probably the most cost effective of all the methods in terms of accuracy. A principal drawback is that the technique of matching series expansions is very much removed from the physics of the problem: physical constraints on the flow, for similar reasons, are difficult to enforce.

4.5 Solution Algorithms for the Discretised Equations of Motion

The discretisation process produces algebraic forms of the equations of motion as summarised in figure 2.8. In each of the discretised equations the terms resulting from spatial discretisation have been unassigned to any particular time level. The reason for this is because the choice of time level in the description of these terms has a radical influence on the solution algorithm - indeed, the choice will classify the nature of the solution algorithm as one of three main types EXPLICIT, SEMI-IMPLICIT, or FULLY IMPLICIT. These terms describe the way in which the dependent variables are accessible from the equation formulation.

Before continuing to describe the three classes of algorithm, it is worth noting the main features of the system of governing differential equations. Neglecting the scalars, there are 4 equations in 4 unknowns $\tilde{u}_1$, $\tilde{u}_2$, $\tilde{u}_3$, $\tilde{p}$ (or $\tilde{\rho}$). The equations are "two-way coupled", both linearly and non-linearly. The major feature of the equations is the linear coupling between the momentum and continuity equations through the pressure (although this ceases when flows are treated as "incompressible" and then leads to a rather uncertain role for the continuity equation). The main non-linear coupling is through the dependence of the discretisation coefficients a_p and a_j on the velocities and densities.

Fully Explicit Algorithm

The fully explicit formulation of the equations of motion is illustrated in figure 2.9(a). The discretised spatial terms are expressed entirely with respect to the old (known) values at the old time level. At the start of the process these values must be prescribed as initial conditions. The velocities and densities/pressures at the new time level are then given explicitly in terms of the old time level values, and a simple timestepping procedure for the flow development can then be adopted as illustrated in figure 2.9(b).

Although this is the most straightforward of all the algorithms to construct and use, it suffers from significant drawbacks. The most obvious restriction is that the algorithm is limited to compressible flows for the density must feature as a dependent variable in the equations in order to yield direct values of pressure through the equation of state. The economy of the method also turns out to be poor because the explicit driving of the flow by the pressure imposes a severe restriction on the permissible timestep in order to ensure stability of the solution. This restriction is given by the Courant-Friedrichs-Lewy (CFL) condition (see figure 2.9(b)) which, physically, may be interpreted that a particle of fluid should not travel more than one spatial step size δx in one timestep δt. This restriction means that the method can be up to 1000 times slower than implicit schemes, and its

usefulness is found to be limited to rapidly evolving flows for which $u_{max} > c$. The most widely used explicit algorithm for the compressible Navier-Stokes equations is the MacCormack Scheme; more details of this may be found in [2a,2b].

Semi-Implicit Algorithm

A typical semi-implicit formulation of the equations of motion is illustrated in figure 2.10(a). The difference between this and the fully-explicit formulation is that the pressure derivative terms in the momentum equations are now expressed with respect to the new time level. This means that the new velocities are now described implicitly because the new pressure values are dependent on the new velocities, etc. In order to obtain the new velocities it is necessary to first determine the new pressure levels. This is achieved by solving the discretised pressure equation (obtained from combining the momentum and continuity equations) using standard matrix techniques for linear simultaneous equations. Note that the remaining spatial terms in the momentum equations and all the spatial terms in the scalar equations remain in explicit formulation (hence the name "semi-implicit"); the solution for velocities then follows by direct substitution of the calculated pressures (see figure 2.10(b)).

The implicit treatment of the pressure means that the semi-implicit algorithm can be applied to both compressible and incompressible flows. Furthermore, it significantly eases the CFL restriction on the timestep (see figure 2.10(b)), limiting now only the convection "waves" which are still explicitly described. Note that a further restriction on the timestep exists to limit the movement of diffusion waves to within the smallest mesh interval (see [2c]); this may become dominant for fluids of high diffusivity. Examples of semi-implicit implementations are the MAC (Marker And Cell) Method (see [2b]), and the ICE (Implicit Continuous Eulerian) Method (see[10b]). Although such methods are more flexible and economical than the fully explicit scheme, some significant restriction on the allowable timestep remain which can be considered expensive compared to "fully implicit" methods.

Fully Implicit Algorithm

The fully implicit formulation is illustrated in figure 2.11(a) where it can be seen, with reference to figure 2.8, that all the spatial discretisation terms are now assigned to the new time level. There is now complete coupling between the nodes and the variables at the new time level. The major two-way coupling between the pressure and velocity is generally solved by an iterative procedure (see figure 2.11(b)) which also handles the non-linearities of the equations. The fully implicit formulation removes the timestep restrictions associated with explicit convection and diffusion; the problem now shifts to ensuring that the iterative matrix solution procedures produce a converging result.

Many different fully implicit solution algorithms have been developed: the fully implicit approach is now the most widely used method in CFD. A very useful overview of some of the better known algorithms is provided in [10b].

5. COMPUTATIONAL METHODS FOR SIMPLIFIED FLOW

In section 4 various techniques for attacking the full mathematical model of a fluid have been described. It will be appreciated that the complexity of these methods means that they have been developed and implemented only relatively recently and that their scale of application is still limited even on state-of-the-art supercomputers in view of the computational effort involved in 3-dimensional calculations. Proponents of fluid modelling before the advent of the digital computer were forced to categorise flows and consider simplifications of the general equations of motion that would allow hand calculations to be made. These techniques, and offshoots from them, still remain in application and, when computerised themselves, can still constitute powerful flow prediction tools. Indeed, in Naval Architecture, simplified flow techniques still dominate the field and are likely to do so for some time to come [3f]. In this section an overview of such "simplified" techniques will be made.

The complexity of the full Navier-Stokes equations is associated with the characteristics of the actions of viscosity. All of the simplified techniques stem from the observation that the dominant viscous influences tend to be very localised in most flow systems and therefore it is acceptable to consider the fluid as inviscid in all or a large part of the flow. If a flow can be considered as inviscid and irrotational then this allows the use of a single scalar velocity potential function ϕ to describe all three components of velocity simultaneously. Potential flow solution techniques are therefore at the heart of all the simplified approaches. In section 5.1 a review of Potential Flow Theory is made. Section 5.2 describes the techniques used to obtain solutions to the potential flow equations, and in section 5.3 techniques involving the introduction of localised viscous effects are discussed. It can be seen, therefore, that this section will be concentrating on techniques involving the use of the potential function. The (perhaps) more obvious alternative approach for inviscid flows would be to solve the Euler equations which involve a primitive variable formulation. The Euler equations, of course, may be considered as simple cases (μ=0) of the Navier-Stokes equations, solutions of which using various space discretisation techniques have already been been described in section 4.

5.1 Review of the Bases of Potential Flow Theory

Equations of Motion (Refer to figure 2.12)

If a flow is inviscid and irrotational it can be shown (eg [12b]) that the velocity components can be described by the gradients of a single scalar function ϕ known as the "velocity potential" (equation A). Substituting for A in the continuity equation yields the Laplace Equation, B, which expresses the conservation of fluid mass in steady flow (or constant density flow) whilst simultaneously providing the governing equation to be solved for flow velocities. Laplace's equation for the velocity potential, in association with appropriate boundary conditions for the flow, completely determines the velocity distribution in a flow that can be considered to be inviscid and irrotational. The pressure in the flow can be obtained subsequently from the Euler equations or, more usually and more directly, from the Bernoulli equation C which can be derived by substitution of A in the Euler equations.

Boundary Conditions (Refer to figure 2.12)

Kinematic boundary conditions are straightforward to specify and apply as shown in figure 2.12, equation D. Such specification can apply to solid boundaries in the system or to virtual boundaries - for example, upstream or downstream where uniform flow velocities can be prescribed.

Kinematic boundary conditions do not always completely describe the behaviour of a boundary to the flow in a system. This is particularly obvious in the case of a "free-surface" boundary where waves can be generated. In these circumstances the free-surface distortion is not known *a priori*: although the kinematic boundary condition D applies on the free-surface, the problem is that the velocity of the surface is not known. It is necessary to account for this unknown with an extra equation, and the appropriate physical condition for water/air interfaces (particularly relevant to Naval Architecture problems) is that the pressure must be equal to atmospheric pressure on the free surface. Implementing such "dynamic" boundary conditions is much more difficult than the kinematic boundary condition alone. The conditions which must apply are given by relations E. Physically the first states the kinematic requirement that the free-surface elevation must be matched to the variation of the disturbance of a fluid particle at the surface: the second is a statement of the dynamic condition that the pressure of the fluid particles at the free-surface must equal the pressure of the adjacent atmosphere. The latter equation is obtained by applying the Bernoulli equation to the free-surface streamline.

5.2 Solution Techniques for Potential Flow

Early analytical work, before the advent of computers, was limited to 2 dimensional (or axi-symmetric flow). The linearity of the governing equation of motion allowed the superposition of complex potential functions describing basic flow elements which individually satisfied Laplace's equation (sources, sinks, dipoles, and vortices) to generate irrotational flow patterns around fairly simple body shapes. (For examples, see [1a].) Conformal transformation techniques allowed more complicated flow geometries to be interpreted from the simpler flow systems, although the range of possible shapes was limited by the available mathematical transformations. Very useful design tools were developed for 2-dimensional thin aerofoils using the principal of superposition of vortex elements as a continuous chordwise distribution of vortex strength along a mean line to predict loading distributions, etc. [7e]. The extension of these ideas laterally to represent finite aspect ratio wings as spanwise distributions of vortex strength lead, for example, to Lerbs' lifting line theory for marine propeller design [7f]. Methods based on such principles of superposition of flow elements are still the most common techniques used for tackling potential flow problems using modern day computers.

Panel Method

In the panel method the surface of a body is divided into N contiguous panels. On each of these panels j is placed a panel source of strength σ_j (as yet unknown), as illustrated in figure 2.13. The value of the potential at any point in the system is then given by an integration of the contributions from each of the panel sources. By referring to control points associated with each of the N panels an expression for the gradient of the potential function at each control point can be obtained. Substitution of the boundary conditions (no flow normal to the body surface) at each control point yields a set of N linear simultaneous equations in the N unknown panel source densities. These equations can be solved either directly or iteratively using standard techniques and once the source strengths are known the velocities and pressures at any point in the system can be determined.

Panel methods originated in the aircraft industry from non-lifting potential flow theory [7g]. The technique was extended to lifting flows with the inclusion of doublet distributions [7i]. Higher order methods have since been introduced where curved panels and distributions of source density may now be used, and the field has been reviewed recently by one of the original proponents [7j]. The panel method is most suited and effective for "external" flows about isolated bodies in otherwise unrestricted uniform streams. For "internal" flows an alternative formulation based on Green's theorem turns out to be more convenient in most cases. In Naval Architecture, then, simple source panel

methods can be used for deeply submerged submarines (or in some applications, with care, for shallow running conditions [7b]). For surface ship applications, the extension of the panel method in the attempt to cover the complication of the free-surface boundary conditions has involved less elegant additional source distributions; for example, on the mean free-surface to represent wave distortion effects for wave resistance predictions [7c], or the use of pulsating sources in wave excitation problems [7d].

Boundary Integral (or Boundary Element) Methods

The panel method is effectively a simple implementation of a more comprehensive boundary integral formulation based on Green's theorem. The boundary integral method seeks solutions of the potential at a point in the system directly, without introducing the intermediate source panel concept. Figure 2.14 illustrates the boundary integral formulation.

For internal flows (i.e. flows past bodies in channels and in the presence of free-surfaces, etc.) it is usually computationally advantageous [11b] to replace the simple source element distribution by modified source potentials called "Green Functions" which satisfy the Laplace equation and all the solid and free-surface boundary conditions other than that of the body in the flow. A large selection of Green Functions is available from [11f].

Space Discretisation Methods

The various space discretisation techniques (finite difference, finite volume, finite element, spectral) have already been described in the context of solving the Navier-Stokes equations (see section 4). These methods can, of course, be applied to the equation governing the velocity potential in inviscid flow. The question of which approach, space discretisation or boundary integral, is most efficient depends upon the application. In many situations the physical quantities are only required on the boundaries and therefore space discretisation techniques would appear inefficient and wasteful since they yield a great deal of interior data that are usually of minor interest. Yeung [11b] provides a rational formula for comparison of the computational effort that may be involved in the various alternative techniques, but points out that the boundary integral methods are always superior in terms of data storage requirements.

Hybrid Techniques

Although boundary integral techniques are superior in terms of computer storage requirements, the integration of the derivatives of Green Functions over relatively complicated body shapes can be difficult to deal with. For this reason "hybrid methods" have become popular where different solution procedures are employed in different sub-

regions of the system. A common hybrid approach is to take advantage of analytical solutions in the outer regions of a flow where the geometry is simple and matching this to an interior numerical solution such as the finite element method which is more suited to arbitrary or complicated system geometries [11b]. The hybrid technique can, of course, be extended to any combination of individual methods: for example the use of a coupled element technique involving finite elements for the inner solution and boundary integrals for the outer solution has been advocated in [7a] for the calculation of wave resistance of ships.

5.3 The Introduction of Localised Viscous Effects

The usefulness of potential flow analysis stems from the observation that viscous effects are very localised in many engineering problems and therefore potential flow solutions can describe the fluid behaviour over most of a fluid system. The observation by d'Alembert in classical hydrodynamics (d'Alembert's Paradox)*, however, underlines the need to somehow represent the influences of viscosity in order to obtain useful engineering information such as lift and drag on bodies in flow.

Boundary-Layer Theory

The "discovery" of the boundary-layer by Prandtl in 1904 gave birth to Boundary-Layer Theory. The observation that the most significant velocity gradients, and therefore effects of viscosity, were contained within a relatively thin layer of fluid adjacent to the boundary walls meant that a model for viscosity only needed to be applied in this fairly well defined sub-region of the flow; the bulk of the flow outside the boundary-layer could be assumed to be inviscid and therefore predictable using potential flow solution techniques. As boundary-layers were observed to be mostly very thin, the viscous equations of motion could be considerably simplified since the pressure could be assumed to be constant across the boundary-layer normal to the body surface. The resulting boundary-layer equations (see figure 2.15), being parabolic in nature, can be solved by a single march in the direction of the boundary flow. The solution requires a knowledge of the flow characteristics on the outer edge of the boundary-layer and the initial profile of the flow entering the boundary-layer. The outer edge details are supplied by a potential flow analysis, to begin with over the bare boundary, but possibly corrected in a subsequent iteration for the displacement thickness of the computed boundary-layer.

Before the advent of the digital computer 2-dimensional boundary-layer problems were usually tackled via the "momentum integral equation" interpretation of the boundary-layer equations (see [1b]). This approach was very effective for determining, with

* d'Alembert's Paradox:- Steady flow of an ideal fluid past a totally immersed body will exert zero net hydrodynamic force on the body.

reasonable accuracy, the overall characteristics (such as the skin friction or the separation point of the flow) rather than the details of the flow in the boundary-layer. For more general 3-dimensional boundary-layer flow problems the various numerical schemes outlined in section 4 can be applied to the boundary-layer equations. Fletcher [2b] outlines the most common numerical schemes used for boundary/potential flow zonal decomposition.

The main limitation of boundary-layer theory is that it can only be applied where the boundary-layer flows remain "attached" to the boundaries in the flow. Although the technique can predict roughly the points of separation of flow from the surface, it cannot continue the boundary-layer solution downstream from this position. To obtain details of highly separated flow systems, the full Navier-Stokes equations must be solved.

The Use of Discrete Vortex Elements

In many cases of engineering interest when boundary-layers separate from the solid surfaces in a flow the vorticity generated by the action of viscosity is contained only within a small fraction of the total fluid volume as discrete vortices shed from the body surface. To determine the principal characteristics of the fluid behaviour, even in complex and unsteady separating flow, it is necessary, then, only to follow the evolution of the relatively simple vorticity field represented by a series of discrete vortex elements. Roughly, the elements are sections of a vortex tube and are convected at or near the local fluid velocity. The vorticity vector associated with each element is strained by the local velocity gradient and each vortex element contributes to a "distortion" of the nominal velocity field. The scheme is illustrated in figure 2.16. Leonard [9a] reviews the various discrete vortex formulations available for simulating incompressible viscous flows. It must be stressed that in general these methods can only provide essentially qualitative descriptions of flows as they depend largely on empirical/intuitive information regarding the locations of the flow separation points on the boundaries and other major regions of vortex shedding.

In Naval Architecture applications discrete vortex elements have been used for some time in the lifting surface theories for marine propeller design and performance prediction [9c,9d]. Here the shed vortex filament roots and trajectories are relatively easy to define. More recently the modelling of separated flow over manoeuvring submarines has been attempted [9e]: this research is still very much in its infancy.

6. CRITICISMS OF CONVENTIONAL CFD

It is easy to criticise those techniques involving the use of a flow potential function for they sacrifice, to a large extent, physical significance in the variables used for mathematical expediency in the solution procedure. Associated with this, then, is the danger of losing "feel" for the actual fluid behavioural mechanisms that are involved in flow development. Hybrid schemes for viscous flow analysis (as used in zonal approaches and vortex modelling approaches), although perhaps slightly less abstract than the pure potential analysis, are additionally very cumbersome in their formulation.

Criticism of those methods which tackle the Navier-Stokes equations directly and work with the physically identifiable variables of velocities and pressure is less obvious, but nevertheless there is still much scope. This is the main concern of this section and it will be tackled under the following three interrelated headings; Criticism of (i) General Approach, (ii) Mathematical Bases, and (iii) Presentation.

6.1 Criticism of General Approach

The emphasis in conventional Navier-Stokes approaches is in ***solving*** the "governing" equations of motion. The question is: Is this what a fluid does? Superficially it seems clear that it is not. A fluid does not compute a "solution" to given flow boundary conditions and an equation of motion and then move accordingly. Rather, it moves under the direction of a number of influences, some of which are external to the fluid (such as the presence or movement of solid boundaries in the system) and some of which are internal (such as viscous mechanisms). Movements induced by the prevailing influences will alter the levels of those influences or will bring more influences into play. For example, when a viscous fluid is caused to move from rest, initially there are no viscous influences acting since there is no motion, let alone relative motion, within the flow. Once motion begins, then so too do the influences of viscosity.

The motion of a real fluid, then, develops through a series of cause and effect recursive stages, and it can be argued that a "direct" computer model of a fluid should imitate the logic of this process in a similarly modular way. It may *seem* that conventional techniques effectively do this - it is just that all the influence "modules" are combined within the governing equations. This is potentially true, but it depends upon the way in which the equations are used, that is, whether they are treated as equations of balance (which must be "solved"), or as driving equations for the solution. Only the latter use conforms to the logic of cause followed by effect. Examining the different strategies in

conventional approaches to fluid modelling (section 4.5) it can be seen that only fully explicit algorithms satisfy this logic - although perhaps more by accident rather than design. For as soon as methods become semi- or fully-implicit then the problem as implemented on a computer changes from being a model of the physics to become a mathematical exercise in solving simultaneous equations by matrix manipulation - something that a fluid certainly does not do. Although the physical mechanisms are *represented* in the equations of motion, they are not modelled as such in implicit solution algorithms. The extreme example of this is where, using fully implicit algorithms, steady state solutions of flows can be achieved without recourse to the time domain: in that they *allow* such steady state solutions to be obtained directly clearly indicates the compromise of the physics for mathematical expediency involved.

The reason for suggesting that explicit algorithms perhaps satisfy the logic of cause and effect "by accident rather than by design" is based on a general impression gained by descriptions of the various CFD techniques in the literature. The explicit algorithm is always described merely as one of the possible ways of tackling the equations, never (in the author's experience) as the most physical way of modelling fluid behaviour. Further support for the impression that mathematics too quickly dominates CFD is gained from the observation that no fully explicit scheme has been suggested or pursued for "incompressible" flows, as far as the author is aware. The reason for this is that for so-called incompressible flows it is immediately stated that the density is constant. The effect of this mathematical "simplification" is that the continuity equation is decoupled from the momentum equations which in turn denies the possibility of any truly physical model of pressure within the subsequent numerical code, for the *mechanism* of pressure generation has been removed. CFD approaches to incompressible flows, then, are always implicit, at least in the treatment of pressure. A more physical approach to modelling incompressible fluids would be to make use of the bulk modulus concept as a pressure generation mechanism. It will be seen in Chapter 5 that this is attempted in this work.

In section 4.5 fully explicit algorithms have been reported as being too demanding of computing effort in order to ensure stability of the developing flow. The speed of a "direct" flow modelling algorithm is not a principal concern of this study for the reasons outlined in chapter 1, section 6, and so explicit type approaches will not be discounted. For the interest lies in developing a modelling strategy that is simple to understand and implement: if any speed penalties are perceived in comparison with other methods then these may be considered as compromises that should diminish with the increased capabilities of future computing machines. Whether conventional explicit techniques are the best way of modelling the true cause and effect logic of fluid behaviour is a question that will be addressed in the development chapters of this work.

6.2 Criticism of Mathematical Bases

It is not the intention to criticise the details of the mathematical models used in the formulation of the Navier-Stokes equations, but rather to recall the general observation that approximations and assumptions are easily forgotten once an equation has been derived and has been well used. It is easy to place too much faith in the equations and more reliance on the predictions from those equations than may actually be merited by the formulation, or indeed to set too much store in the quest to solve such equations *exactly*.

The approximations and assumptions in the derivation of the Navier-Stokes equations are listed here for reference.

- The representation of pressure.
- The model of viscous actions.
- Representation of the effects of turbulence in the time-averaged equations.
- Constant density assumption for incompressible flow problems.

One of the questions that this work asks is: Is it necessary to formalise a problem as an equation of motion where a certain "tidiness" is always sought? Would it not be more realistic and flexible to leave the specification in modular form, with adaptable modules to model the various influences affecting flow behaviour?

6.3 Criticism of Presentation

Apart from the distinct sacrifices in representing the physics in some of the methods, all of the conventional CFD techniques suffer considerably from the point of view of presentation. Presentation is critical in order to encourage engineers to use CFD in the interest of validation and future development. Conventional presentation appears to suffer on two major counts. The first lies in the formulation of the problem as a composite equation of motion with all the behavioural mechanisms embedded within it. When the equations are discretised to algebraic form (figure 2.8) the various coefficients contain contributions from each of the behavioural influence models and are therefore rather obscure; the physics becomes somewhat intangible from this stage onwards in the presentation of the solution procedure. The second problem that arises is probably due to convention. It seems to be expected in CFD publications to represent every stage of the development from the equations in mathematical form. This involves clever abreviations of equations and the use of index conventions to represent repeated or non-repeated subscripts - see figure 2.3. These are fine if the reader is familiar with the conventions *and*

well used to them; however, they can be very unhelpful, off-putting and confusing to the novice.

It is believed that these problems of presentation could again be improved by adopting a modular description of the system "inputs" and the use of more diagrams/flowcharts to illustrate discretisation procedures, overall algorithms and suggested computer coding structures.

7. CLOSURE

In this chapter the elements of conventional approaches to Computational Fluid Dynamics have been described and criticised in order to be able to formulate specific guidelines for the development of a "direct" approach to computer modelling of fluids. These guidelines are presented in chapter 3. This short review will also serve as the basis for discussing the achievements of the overall project (chapter 6).

The critical observations made of conventional techniques in computer modelling of fluids are as follows:-

(i) There is too much emphasis on *solving* the governing equations of motion throughout the system. This means that CFD techniques have become either wholly, or in part, ***computer models of the mathematics*** of the physics, rather than direct computer models of the physics *per se*.

(ii) The concepts involved in certain treatments of the equations of motion can be far removed from the reality of actual physical phenomena. This can inhibit progress in understanding fluid behavioural mechanisms, and thereby restricts research development.

(iii) There is a predominance of complex mathematics in the various CFD techniques. This arises from the range of different discretisation strategies and differencing schemes that are possible, and from the favouring of implicit algorithms which demand iterative matrix solution methods with all the associated subtleties concerning stability and convergence. Such mathematics presents a severe obstacle to users of CFD codes who need to know the limitations of application of the software. Unfortunately, to understand these limitations it is necessary to be reasonably familiar with the mathematical treatments involved. To have to master CFD subtleties in

order to use CFD software is very resource-wasteful and off-putting for design engineers.

(iv) Tradition in the presentation of most scientific research seems to demand "neatness" of all mathematical descriptions. This convention in both analytical fluid dynamics and CFD results in combined descriptions of different fluid behavioural mechanisms in one equation. With the process of discretisation then, the contributions from each mechanism to the resulting flow response can be lost - thereby diminishing the success of the approaches for the purposes of really *understanding* flow behaviour.

(v) A particle of fluid knows nothing about the details of numerical schemes for solving the Navier-Stokes equations, potential flow, rotational flow, etc, and therefore it *must* be possible to develop a *direct* model of the physics of a fluid's behaviour without recourse to such concepts. (This is probably the most important observation since it underlies all the others.)

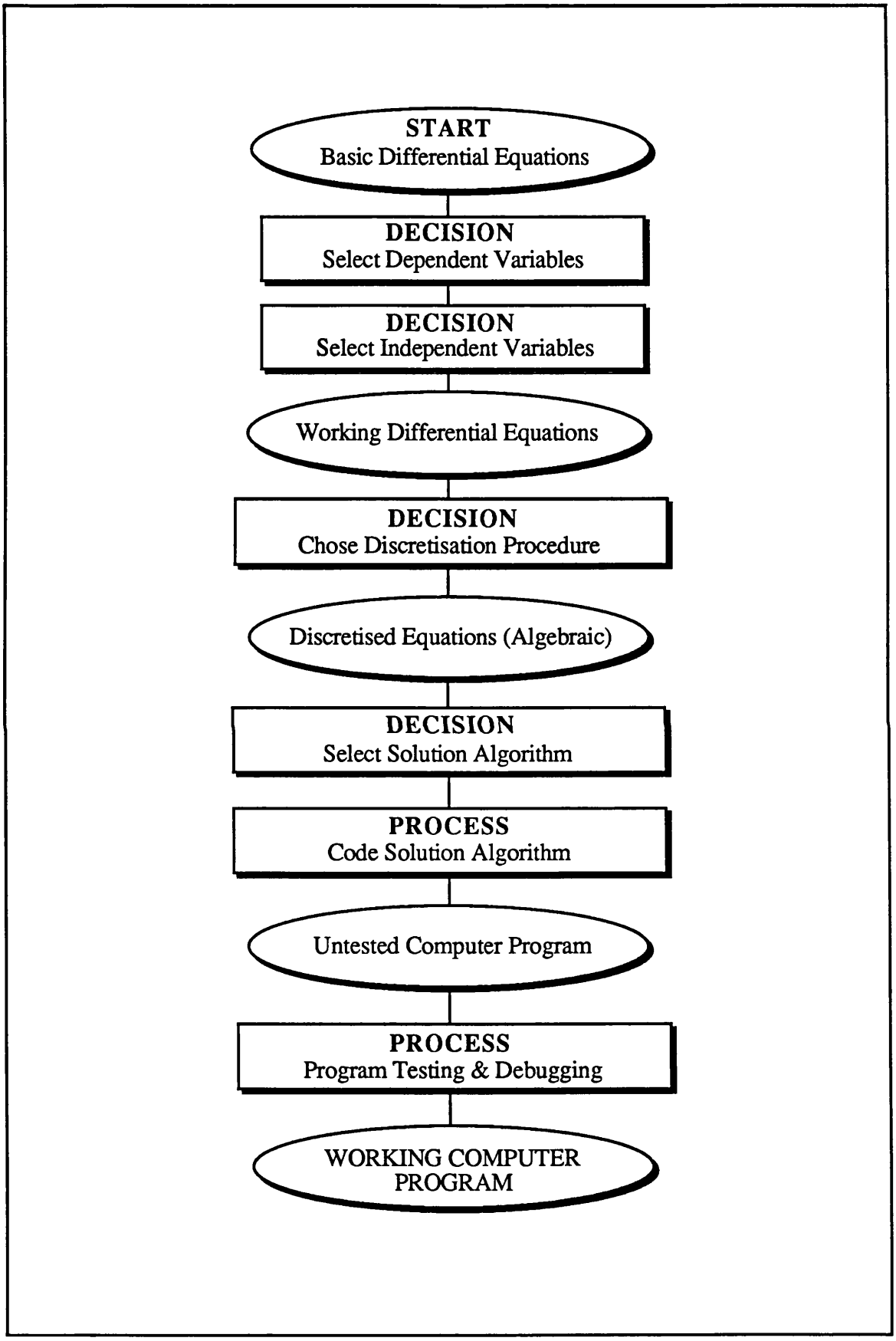

Figure 2.1 Logic of the Development of a Solution Procedure in CFD

MOMENTUM

$$\frac{\partial(\bar{\rho}\bar{u}_i)}{\partial t} + \frac{\partial}{\partial x_j}\left[\bar{\rho}\,\bar{u}_j\bar{u}_i - \mu_{eff}E_{ij}\right] + \frac{\partial \bar{p}}{\partial x_i} - \bar{\rho}\,\bar{X}_i = 0 \qquad \textbf{A}$$

$$\text{where} \quad E_{ij} = \left(\frac{\partial \bar{u}_j}{\partial x_i} + \frac{\partial \bar{u}_i}{\partial x_j} - \frac{2}{3}\frac{\partial \bar{u}_k}{\partial x_k}\delta_{ij}\right)$$

CONTINUITY

$$\frac{\partial \bar{\rho}}{\partial t} + \frac{\partial}{\partial x_j}(\bar{\rho}\bar{u}_j) = 0 \qquad \textbf{B}$$

k-ε TURBULENCE MODEL

$$k = \frac{1}{2}\left(\overline{u'_i\,u'_i}\right)$$

$$\varepsilon = \frac{\mu_t}{\rho}\left(\overline{\left(\frac{\partial u'_i}{\partial x_j}\right)\left(\frac{\partial u'_i}{\partial x_j}\right)}\right)$$

$$\frac{\mu_t}{\rho} = \frac{C_\mu k^2}{\varepsilon}$$

$$\frac{\partial(\rho k)}{\partial t} + \frac{\partial}{\partial x_j}\left[\bar{\rho}\bar{u}_j k - \frac{\mu_t}{\sigma_k}\frac{\partial k}{\partial x_j}\right] - \mu_t C_1 + \rho\varepsilon = 0$$

$$\frac{\partial(\rho\varepsilon)}{\partial t} + \frac{\partial}{\partial x_j}\left[\bar{\rho}\bar{u}_j\varepsilon - \frac{\mu_t}{\sigma_\varepsilon}\frac{\partial \varepsilon}{\partial x_j}\right] - \frac{\varepsilon}{k}(C_1\mu_t G - C_2\rho\varepsilon) = 0 \qquad \textbf{C}$$

$$\text{where} \quad G = \left(\frac{\partial \bar{u}_i}{\partial x_j} + \frac{\partial \bar{u}_j}{\partial x_i}\right)\frac{\partial u_i}{\partial x_j}$$

EQUATION OF STATE

$$\bar{p} = \bar{\rho}\,R\,T \qquad \textbf{D}$$

Figure 2.2 Summary of Basic Equations Used in CFD

GENERALISED EQUATION:-

$$\frac{\partial(\bar{\rho}\phi)}{\partial t} + \frac{\partial}{\partial x_j}\left(\bar{\rho}\,\bar{u}_j\,\phi - \Gamma_\phi \frac{\partial \phi}{\partial x_j}\right) - S_\phi = 0 \qquad \mathbf{E}$$

INTERPRETATIONS:-

Equation	Principal Variable ϕ	Exchange Coefficient Γ_ϕ	"Source" Term S_ϕ
Momentum	$\bar{u}_i$	μ_{eff}	$\bar{\rho}\,\bar{X}_i + \frac{\partial}{\partial x_j}\left[\mu_{eff}\left(\frac{\partial \bar{u}_j}{\partial x_i} - \frac{2}{3}\frac{\partial \bar{u}_k}{\partial x_k}\delta_{ij}\right)\right] - \frac{\partial \bar{p}}{\partial x_i}$
Continuity	1	0	0
Turbulence Energy	k	$\frac{\mu_t}{\sigma_k}$	$\mu_t C_1 - \rho\varepsilon$
Energy Dissipation	ε	$\frac{\mu_t}{\sigma_\varepsilon}$	$\frac{\varepsilon}{k}(C_1\mu_t G - C_2\rho\varepsilon)$

Figure 2.3 Generalised Equation and Interpretations

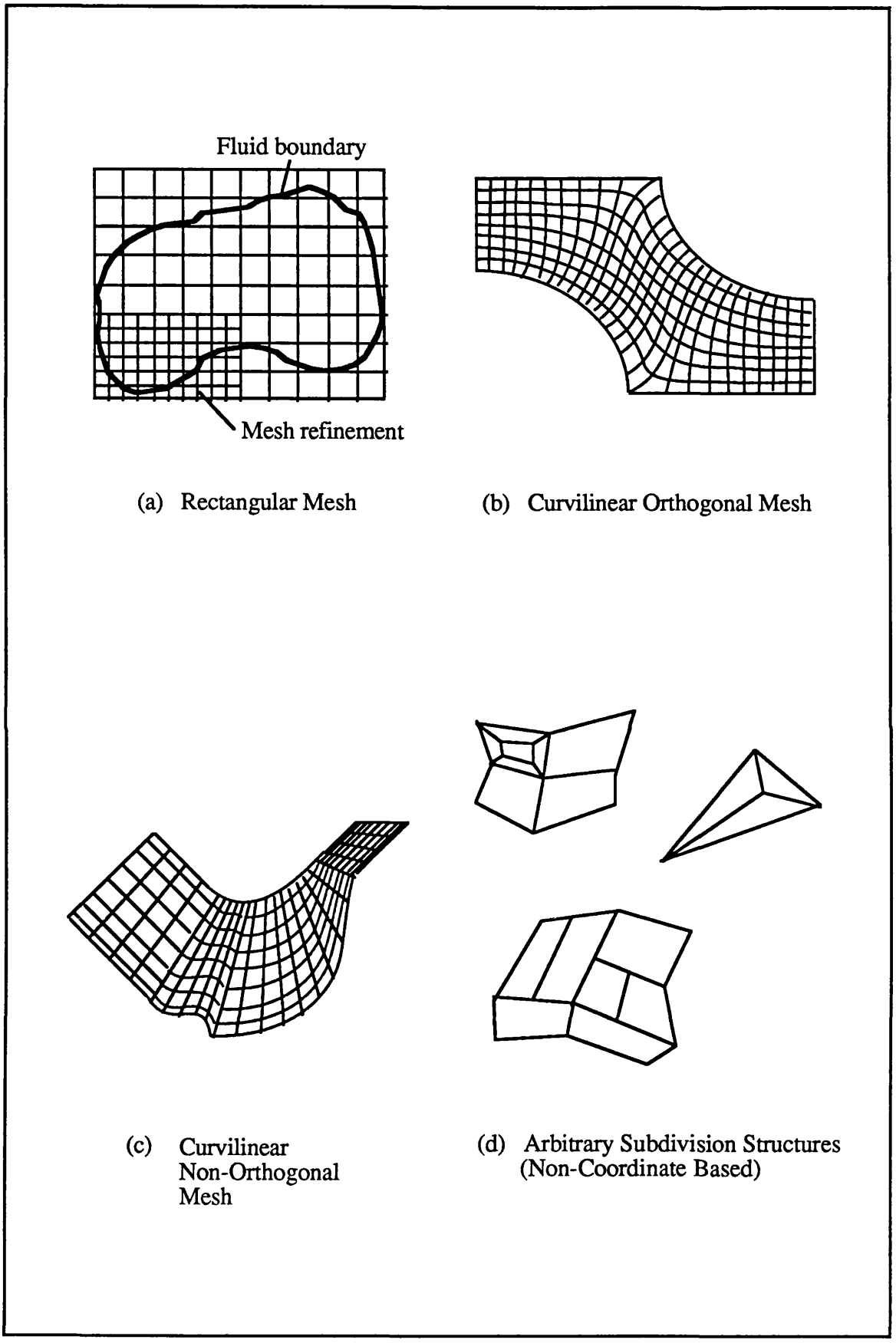

Figure 2.4 Schemes for Coordinate (Mesh) Arrangements

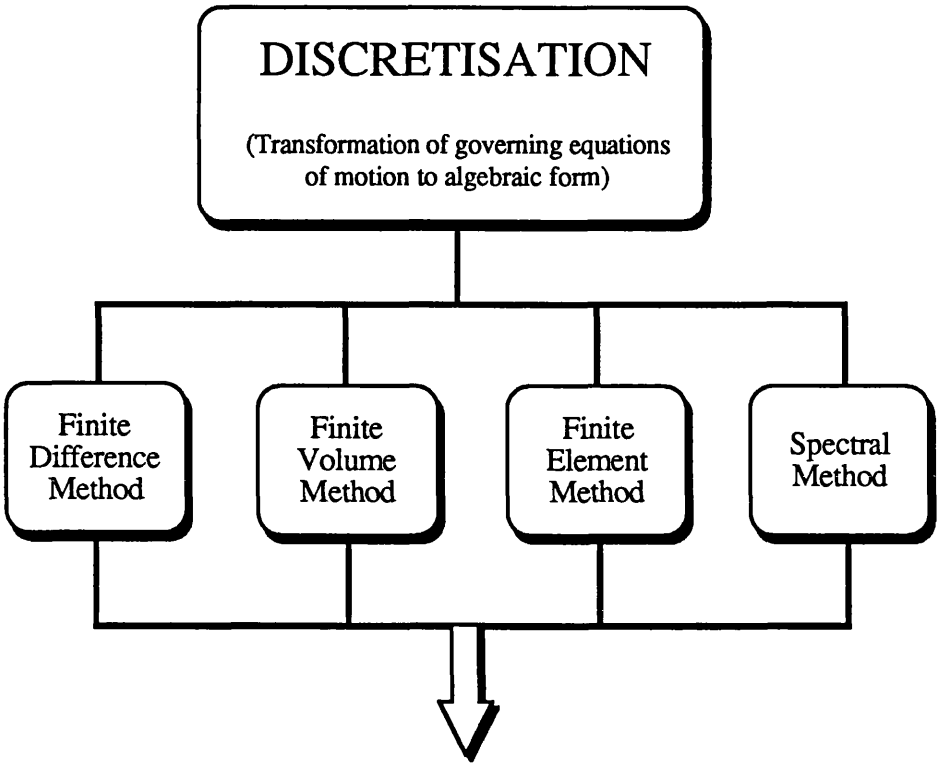

Discretisation Result

(General form for each node p)

$$a_p \phi_p = \sum_j a_j \phi_j + b$$

Summation over selected neighbours.

"a" values come from combined effects of accumulation, transport and some source terms, and depend upon how the partial derivatives are modelled.

From parts of the source term.

Figure 2.5 Generalised Result of Discretisation

ILLUSTRATIVE EXAMPLE

Approximation of the one-dimensional form of the generalised equation

$$\frac{\partial(\bar{\rho}\phi)}{\partial t} + \frac{\partial}{\partial x}\left(\bar{\rho}\,\bar{u}\,\phi - \Gamma_\phi \frac{\partial \phi}{\partial x}\right) - S_\phi = 0$$

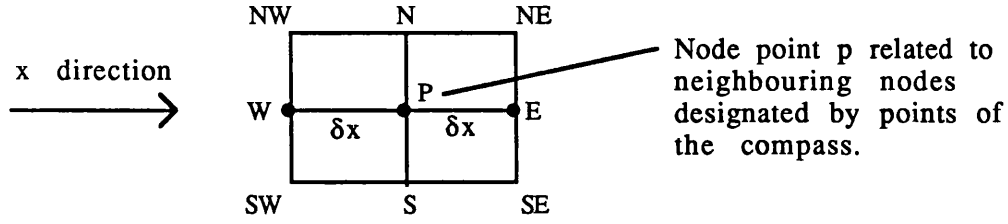

Approximating Functions in the x and t dimensions:-

$$\phi_E \approx \phi_P + \left(\frac{\partial \phi}{\partial x}\right)_P . \delta x + \left(\frac{\partial^2 \phi}{\partial x^2}\right)_P . \frac{\delta x^2}{2!} + \ldots.$$

$$\phi_W \approx \phi_P - \left(\frac{\partial \phi}{\partial x}\right)_P . \delta x + \left(\frac{\partial^2 \phi}{\partial x^2}\right)_P . \frac{\delta x^2}{2!} - \ldots.$$

$$\phi_P^n \approx \phi_P^o + \left(\frac{\partial \phi}{\partial t}\right)_P^o . \delta t + \left(\frac{\partial^2 \phi}{\partial t^2}\right)_P^o . \frac{\delta t^2}{2!} + \ldots.$$

} Taylor Series Expansion

$$\left(\frac{\partial \phi}{\partial x}\right)_P \approx \frac{\phi_E - \phi_W}{2\,\delta x} \quad \text{(note truncation error)}$$

$$\left(\frac{\partial^2 \phi}{\partial x^2}\right)_P \approx \frac{\phi_E + \phi_W - 2\,\phi_P}{\delta x^2} \quad \text{(note truncation error)}$$

} Centred Differencing

$$\left(\frac{\partial \phi}{\partial t}\right)_P \approx \frac{\phi_P^n - \phi_P^o}{\delta t} \quad \text{(note truncation error)}$$

} Forward Differencing

Substituting for Derivative Approximations:-

$$\bar{\rho}_P \frac{(\phi_P^n - \phi_P^o)}{\delta t} + (\bar{\rho}\,\bar{u})_P \frac{(\phi_E - \phi_W)}{2\,\delta x} - (\Gamma_\phi)_P \frac{(\phi_E + \phi_W - 2\,\phi_P)}{\delta x^2} - (S_\phi)_P = 0$$

Figure 2.6 The Finite Difference Method of Discretisation

ILLUSTRATIVE EXAMPLE

Approximation of the one-dimensional form of the generalised equation

$$\frac{\partial(\bar{\rho}\phi)}{\partial t} + \frac{\partial}{\partial x}\left(\bar{\rho}\,\bar{u}\,\phi - \Gamma_\phi \frac{\partial \phi}{\partial x}\right) - S_\phi = 0$$

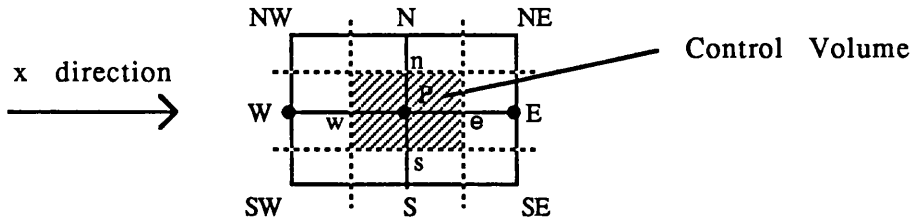

Integrate the equation over the control volume for each node p

$$\int_w^e \frac{\partial(\bar{\rho}\phi)}{\partial t}\,dx + \left[\bar{\rho}\,\bar{u}\,\phi - \Gamma_\phi \frac{\partial \phi}{\partial x}\right]_w^e - \int_w^e S_\phi\,dx = 0$$

Assume variation between nodes and approximating function in the x-direction

For example:-

$\phi = ax + b$ (linear profile assumption) between nodes.

S_ϕ , $\frac{\partial(\bar{\rho}\phi)}{\partial t}$ are constant over the control volume.

$$\left(\frac{\partial \phi}{\partial x}\right)_P \approx \frac{\phi_E - \phi_W}{2\,\delta x} \quad \text{(note truncation error)} \quad \Big\} \text{ Centred Differencing}$$

$$\left(\frac{\partial \phi}{\partial t}\right)_P \approx \frac{\phi_P^n - \phi_P^o}{\delta t} \quad \text{(note truncation error)} \quad \Big\} \text{ Forward Differencing}$$

Substituting for Approximations

$$\bar{\rho}_P \frac{(\phi_P^n - \phi_P^o)}{\delta t}\,.\,\delta x + \left[(\bar{\rho}\,\bar{u})_e \frac{(\phi_P + \phi_E)}{2} - (\bar{\rho}\,\bar{u})_w \frac{(\phi_P + \phi_W)}{2}\right]$$
$$- \left[(\Gamma_\phi)_e \frac{(\phi_E - \phi_P)}{2\,\delta x} - (\Gamma_\phi)_w \frac{(\phi_P - \phi_W)}{2\,\delta x}\right] - S_\phi.\delta x = 0$$

Figure 2.7 The Finite Volume Method of Discretisation

Illustration Based on Finite Volume Method For 2-Dimensional Flow

X Momentum:-

$$d^n \bar{u}_P = d^o \bar{u}_P + \Sigma a_j \bar{u}_j - a_P \bar{u}_P + (p_W - p_P) A_{ew}$$

where aj values depend on the specifics of the discretisation of the spatial derivative terms and

$$d = \frac{\bar{\rho} V_P}{\delta t}$$

Y Momentum:-

Similar to x momentum.

Continuity:-

$$d^* \bar{\rho}_P^n = -D_P + d^* \bar{\rho}_P^o$$

where

$$D_P = [(\bar{\rho}\bar{u})_e - (\bar{\rho}\bar{u})_w] A_{ew} + [(\bar{\rho}\bar{v})_n - (\bar{\rho}\bar{v})_s] A_{ns} \quad \text{and} \quad d^* = \frac{V_P}{\delta t}$$

Scalars:-

$$d^n \phi_P^n - d^o \phi_P^o = \Sigma a_j \phi_j$$

Figure 2.8 Discretised Form of the Governing Equations of Motion

(a) FORMULATION

Momentum:-

$$d^n \bar{u}_P^n = d^o \bar{u}_P^o + \Sigma a_j^o \bar{u}_j^o - a_P^o \bar{u}_P^o + (\bar{p}_W^o - \bar{p}_P^o) A_{ew} \quad (1)$$

and similarly for v and w.

Continuity:-

$$d^* \bar{\rho}_P^n = -D_P^o + d^* \bar{\rho}_P^o \quad (2)$$

plus

$$\bar{p} = \bar{\rho} R T \quad (3)$$

Scalars:-

$$d^n \phi_P^n = \Sigma a_j^o \phi_j^o - d^o \phi_P^o \quad (4)$$

(b) SOLUTION PROCEDURE

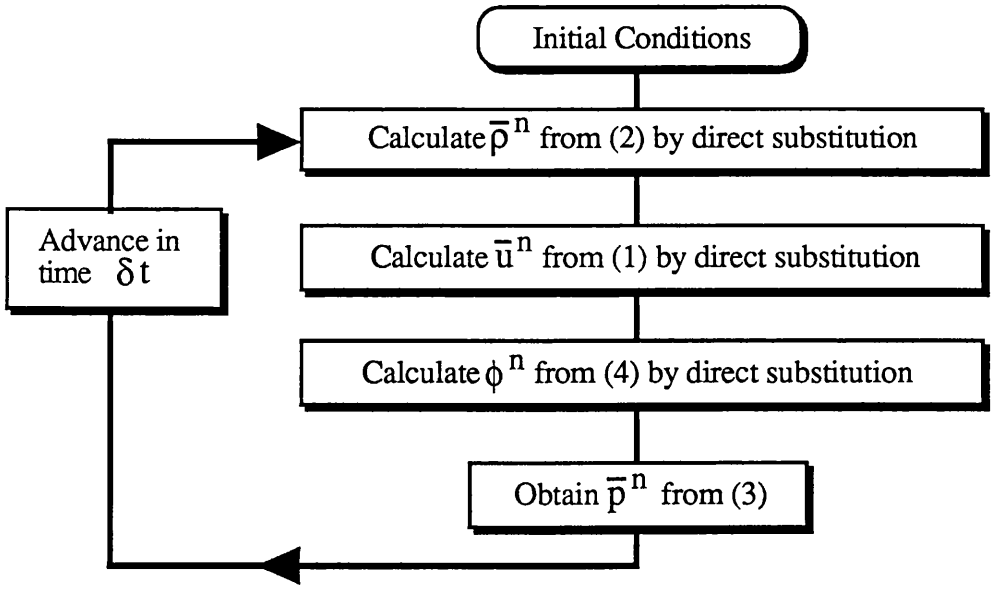

Stability restriction on δt:- $\quad \delta t \leq \dfrac{\delta x}{(|\bar{u}|_{max} + c)}$

Figure 2.9 Example of Fully-Explicit Formulation and Solution

(a) FORMULATION

Momentum:-

$$d^n \bar{u}_P^n = d^o \bar{u}_P^o + \Sigma a_j^o \bar{u}_j^o - a_P^o \bar{u}_P^o + (\bar{p}_W^n - \bar{p}_P^n) A_{ew} \quad (1)$$

and similarly for v and w.
(In this example all terms are explicit except for the pressures.)

Continuity/Pressure:-

$$a_P \bar{p}_P^n = \Sigma a_j \bar{p}_j^n + D_P^n - D_P^o - \Sigma H_j^o \quad (2)$$

(This is the discretised form of the pressure equation obtained from combining the continuity and momentum equations. The H_j's are the combined flux terms from the momentum equations.)

Scalars:-

$$d^n \phi_P^n = \Sigma a_j^o \phi_j^o - d^o \phi_P^o \quad (3)$$

(In this example the scalars are described in fully explicit form.)

(b) SOLUTION PROCEDURE

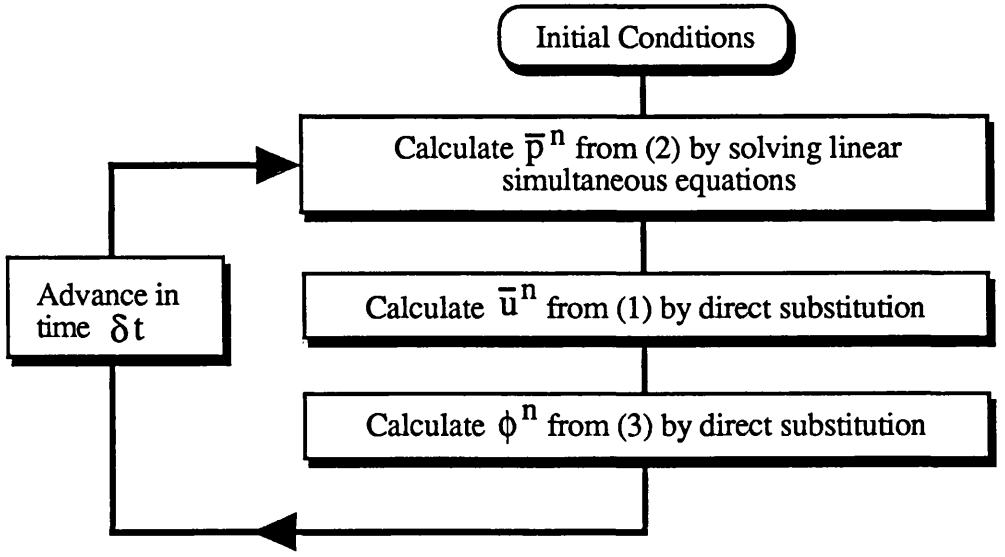

Stability restriction on δt:- $\quad \delta t \leq \dfrac{\delta x}{|\bar{u}|_{max}}$

Figure 2.10 Example of Semi-Implicit Formulation and Solution

(a) FORMULATION

Momentum:-

$$\left(d^M + a_P^M\right)\bar{u}_P^{M+1} = d^o\bar{u}_P^o + \Sigma\, a_j^M\,\bar{u}_j^{M+1} + \left(\bar{p}_W^M - \bar{p}_P^M\right)A_{ew} \qquad (1)$$

and similarly for v and w.

Continuity/Pressure:-

$$a_P^M\,\bar{p}_P^{M+1} = \Sigma\, a_j\,\bar{p}_j^{M+1} + D_P^{M+1} - D_P^o - \Sigma\, H_j^{M+1} \qquad (2)$$

(This is the discretised form of the pressure equation obtained from combining the continuity and momentum equations. The H_j's are the combined flux terms from the momentum equations.)

Scalars:-

$$a_P^M\,\phi_P^{M+1} = \Sigma\, a_j^M\,\phi_j^{M+1} - d^o\,\phi_P^o \qquad (3)$$

(N.B. M is an iteration counter within a given timestep.)

(b) SOLUTION PROCEDURE

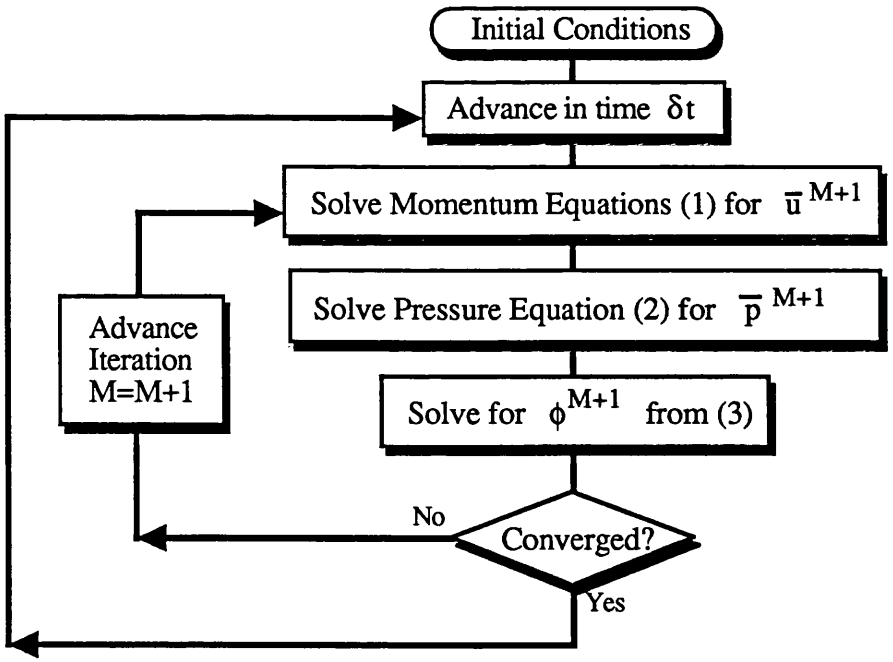

Figure 2.11 Example of Fully-Implicit Formulation and Solution

Velocities in Terms of Potential Function ϕ

$$u = \frac{\partial \phi}{\partial x} \; ; \qquad v = \frac{\partial \phi}{\partial y} \; ; \qquad w = \frac{\partial \phi}{\partial z} \qquad \mathbf{A}$$

Laplace's Equation

$$\nabla^2 \phi = \frac{\partial^2 \phi}{\partial x^2} + \frac{\partial^2 \phi}{\partial y^2} + \frac{\partial^2 \phi}{\partial z^2} \qquad \mathbf{B}$$

Bernoulli's Equation

$$\frac{\partial \phi}{\partial t} + \frac{1}{2} q^2 + \frac{p}{\rho} + gz = \text{constant} \qquad \mathbf{C}$$

(where $q^2 = u^2 + v^2 + w^2$)

Kinematic Boundary Conditions

$$\frac{\partial \phi}{\partial n} = \mathbf{U} \cdot \mathbf{n} \qquad \mathbf{D}$$

where **U** is the velocity of the physical boundary and **n** is the local unit normal to the boundary surface.

Free-Surface Dynamic Boundary Conditions

$$\left.\begin{aligned} \frac{D\eta}{Dt} &= \frac{Dz}{Dt} \\ \eta &= -\frac{1}{g}\left(\frac{\partial \phi}{\partial t} + \frac{1}{2} \nabla \phi \cdot \nabla \phi\right) \end{aligned}\right\} \text{ On the free Surface} \qquad \mathbf{E}$$

Figure 2.12 Review of Potential Flow Theory

Example of 2-Dimensional Flow Past a Body:-

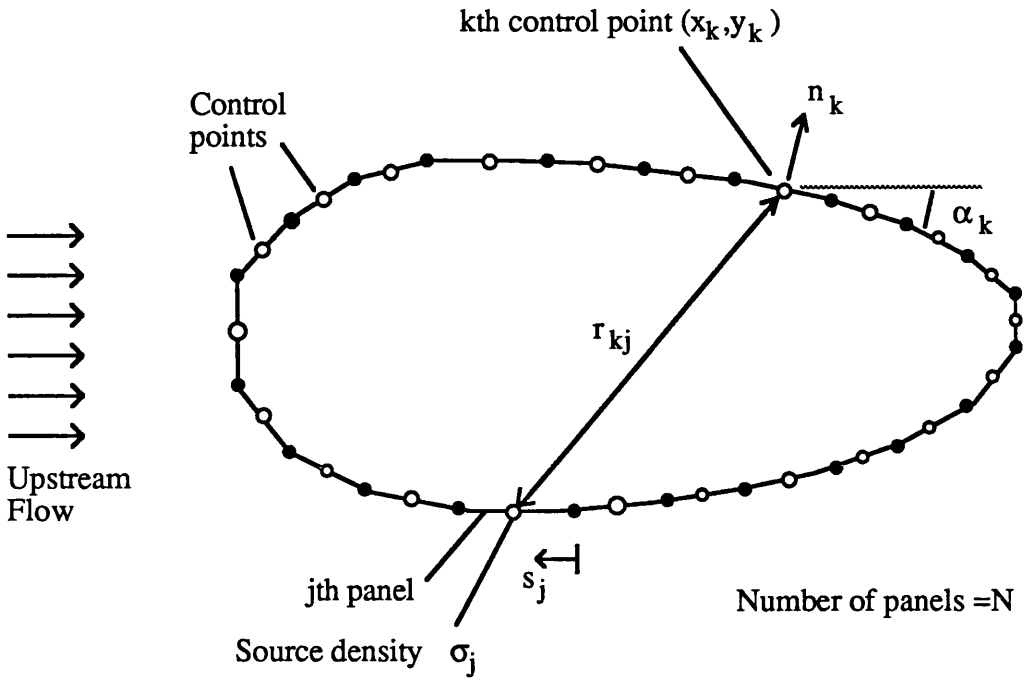

Potential at Control Point k:-

$$\phi(x_k,y_k) = U_\infty x_k + \frac{1}{2\pi}\sum_{j=1}^{N} \sigma_j \int \ln r_{kj}\ ds_j$$

Boundary Conditions:-

$$v_n = \frac{\partial\phi}{\partial n_k}(x_k,y_k) = -U_\infty \sin\alpha_k + \frac{1}{2\pi}\sum_{j=1}^{N} \sigma_j \int \frac{\partial}{\partial n_k}(\ln r_{kj})\ ds_j = 0$$

which, applied to each control point, leads to a linear system of N equations for the unknown source strengths σ_j (j = 1 to N).

Figure 2.13 Panel Method

Example of "Internal Flow" - Flow Past a Body in the Presence of Definite Boundaries:-

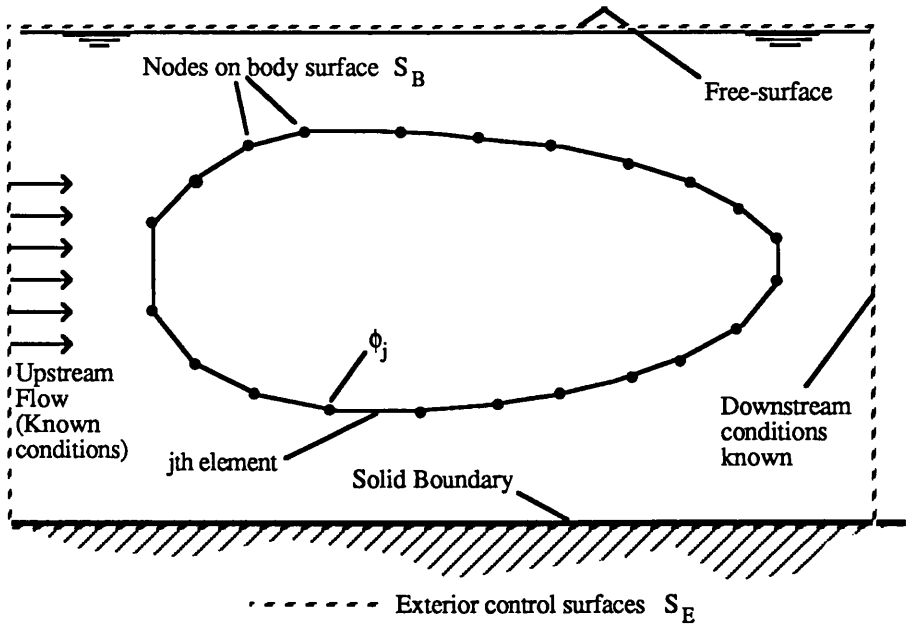

Potential at a General Point k in the Fluid:-

The potential at the point (x_k,y_k) in the general fluid domain is expressed in terms of an appropriate Green Function G chosen to satisfy the exterior boundary conditions on S_E:-

$$\phi(x_k,y_k) = \frac{1}{2\pi}\int_{S_B+S_E}\left(\phi \cdot \frac{\partial G}{\partial n} - \frac{\partial \phi}{\partial n} \cdot G\right) ds \qquad \text{(A)}$$

Boundary Conditions on S_B:-

The variation of ϕ on the control surfaces is represented by a series of interpolating functions N_j linking the node values ϕ_j:-

$$\phi(s) = \sum_j N_j \cdot \phi_j \qquad \text{(B)}$$

Solution:-

Substituting for (B) in (A) and demanding that the resulting equation is exactly satisfied at the boundary nodes produces a linear system of equations leading to a direct solution for ϕ_j.

Figure 2.14 Boundary Integral Method

Example of Flow Over a 2-Dimensional Streamlined Body:-

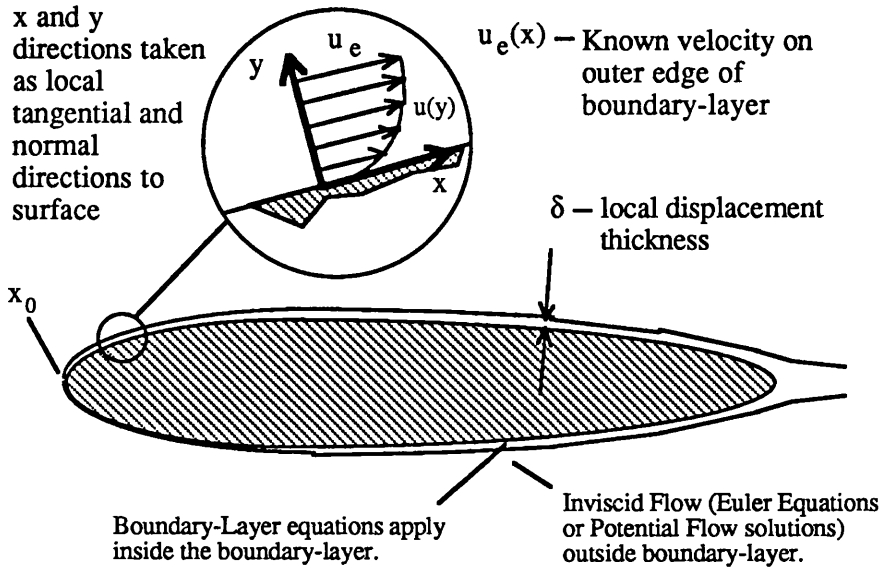

Assumptions:-

- No separation.
- Boundary-layer is thin.

Governing Equations:-

For 2-dimensional, incompressible, laminar, steady flow:-

$$\frac{\partial u}{\partial x} + \frac{\partial v}{\partial y} = 0 \qquad \textbf{Continuity}$$

$$u\frac{\partial u}{\partial x} + v\frac{\partial u}{\partial y} = u_e\frac{\partial u_e}{\partial x} + \nu\frac{\partial^2 u}{\partial y^2} \qquad \textbf{Momentum}$$

(Note that the pressure is predicted from a calculation of inviscid flow over the body - although possibly with iterative surface geometry corrections to take account of the computed boundary-layer thickness.)

Boundary Conditions:-

$u(x_0,y) = u_0(y)$	(Initial profile)
$u(x,0) = 0$	(No-slip condition)
$v(x,0) = 0$	(Tangential flow)
$u(x,\delta) = u_e(x)$	(Outer velocity from inviscid solution)

Figure 2.15 Boundary-Layer Theory

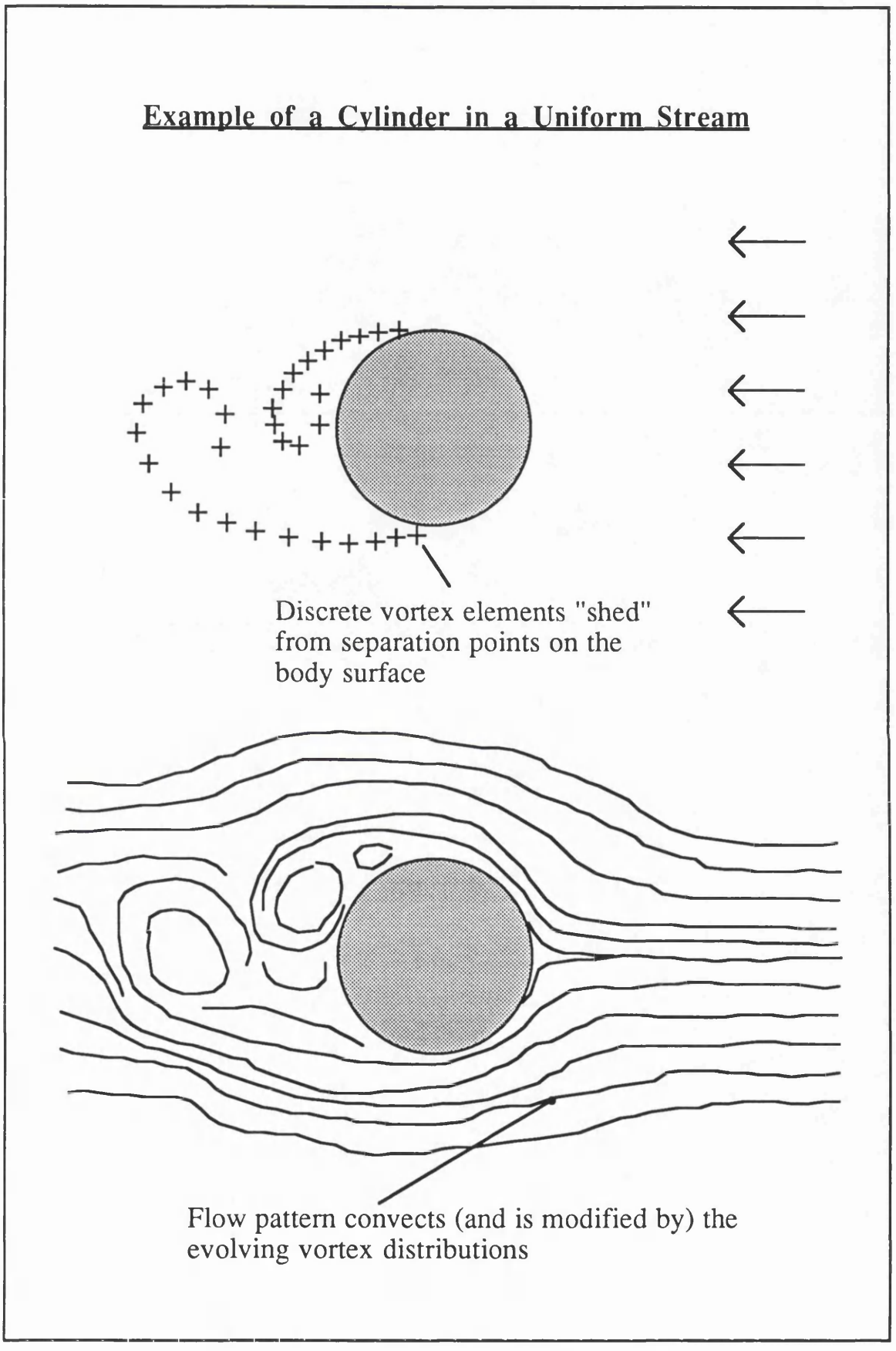

Figure 2.16 Use of Discrete Vortex Elements

CHAPTER 3

GUIDELINES AND PRELIMINARY STUDIES

1. INTRODUCTION

Chapter 1 has identified the capabilities that are ideally required of a computer model for fluids. These were rather more than merely a more efficient alternative to physical model testing facilities such as wind-tunnels and water tanks. The important "extra" that the ideal computer model should provide is an insight into the *understanding* of fluid behaviour. In order to have any hope of providing this extra facility it was concluded that the representation of the fluid and the algorithms used to model the flow behaviour would, at the very least, have to be "physically transparent" - in other words, unobscured by complex intermediate mathematical models or techniques. This is what is meant by a "direct" model for fluid flow.

On the basis of the arguments of chapter 1 it was decided that the continuum model was the the most physically transparent representation of fluid structure on the observable level. The more detailed critical examination of conventional CFD techniques in chapter 2 was necessary to be able to provide guidelines for the development of physically transparent algorithms for fluids' behaviour. It should be noted, however, that from the outset that it was unclear how the "extra" facility of insight into understanding fluid behaviour could be ensured; the best that could be done would be to be as faithful as possible to the ideals of physical transparency and thereby, hopefully, the insight into understanding would follow.

In section 2 of this chapter general rules for the development of a direct computer model are presented, as synthesised from the conclusions of chapters 1 and 2. In section 3 certain common flow modelling concepts are assessed against these general rules. Section 4 presents the specific objectives for the work of this thesis and the original scope of the research. In section 5 the overall modelling strategy, where flow influences are treated in modular form, is outlined. Finally, in section 6, important early studies are described that helped in the formulation of the ideas for this research and provided encouragement for embarking on the research development.

2. RULES FOR THE DEVELOPMENT OF A DIRECT COMPUTER MODEL OF FLUIDS

On the bases of chapters 1 and 2 the original rules formulated for the development of the coding for a direct (physically transparent) computer model of a fluid are as follows:-

(i) A Continuum representation should be adopted.

(ii) Speed and "efficiency" considerations should not influence the algorithm design. (A conventional computer architecture may not be the most suitable for implementation.)

(iii) "Solution seeking" procedures for global relationships, couched as equations of balance, must not be involved.

(iv) Equations describing basic individual physical relationships may be used, but only to drive the computer model. Equations combining more than one physical mechanism should not be involved.

(v) Engineering approximations to describe certain physical influences within a fluid may be used. These, as the physical laws in (iv) above, must only be used to drive the computer model and could therefore be treated as replaceable modules within the driver algorithms of the program.

(vi) All driving influences used within the model must be physically and/or logically justifiable, as opposed to mathematically justifiable.

(vii) The techniques employed should not be sensitive to the number, nature, or relative motions of the bodies/boundaries within the fluid.

It must be emphasised that these were the original rules for development, which were drawn up before the arguments of chapters 1 and 2 were fully established (see Foreword). The looseness of guideline (vi), which permitted "physical and/or *logical*" (instead of just physical) mechanisms to be considered, reflects this. Indeed it will be seen that (vi) caused such problems in the development work that this necessitated a review of these rules during the course of the research (see chapter 4, section 6).

3. ADMISSIBLE CONSIDERATIONS IN A DIRECT MODEL

In chapters 1 and 2 the concept of a direct approach to fluid modelling has been described and in section 2 of this chapter rules for developing algorithms for such a technique have been presented. Here it is worth stating the admissible and inadmissible considerations that could be made in accordance with those rules.

System Discretisation

Dividing the fluid into finite sized regions or control volumes was considered to be perfectly acceptable. Such regions would be fixed in space and flow fields could be described by flow rates across all the region boundaries. From these flow rates, representative region velocities could be deduced. The discretisation process, however, had to be simple and should not be sensitive to the nature of geometries in the system. Too much effort in conventional CFD generally has to be directed towards this aspect of modelling.

Timestepping

Discretisation in the time domain, just as in the space domain, was considered to be a perfectly acceptable concept.

Steady State Solutions

In conventional CFD analyses it is generally possible to obtain a steady-state solution to a viscous flow problem directly (see chapter 2, section 4.5). This generally involves proposing a first guess to the solution and then numerically balancing the discretised system so that the appropriate equations of motion are satisfied at each discretised location in the flow. It may be wondered whether in such techniques the *correct* solution has been found, as the Navier-Stokes equations can have more than one solution for any given set of boundary conditions.

The idea of trying to deduce a steady state solution directly contradicts the ideals of physical transparency. In the technique to be proposed here the fluid must decide for itself how it shall move with given influences in the system. As the viscous influences are clearly time-dependent, the only logical means of developing a flow is through a time-stepping sequence. For this reason this work could not consider algorithms for the direct solution of a steady state flow.

Impulsive Motion

Impulsive starts to systems were considered to be acceptable (although only in Phase 1 of the research). This may seem like a contradiction to the previous statements on the

generation of steady state solutions but there was a distinct difference between the two considerations. The impulsive motion refers only to the boundaries in a system. If such boundary motions were to take place in an incompressible flow then the instantaneous response of the fluid would be, essentially, an inviscid flow pattern since viscosity mechanisms would have no time to interfere with the flow. To develop the steady state viscous flow response, it would be necessary to timestep the model to build up the effects of the viscous influences. Impulsive motion systems may then be thought of as inviscid flow patterns developing from time t = 0 when the viscous mechanisms are "switched on" suddenly.

4. OBJECTIVE AND SCOPE OF RESEARCH

Although the overall goal associated with the theme of this research was to develop a physically transparent computer model that will handle any fluid for any geometry, it was necessary to be rather less ambitious for the work of this thesis. The original objective, then, was more simply *to demonstrate and realise the principles of such a direct modelling approach.*

Certain system simplifications were considered to be expedient to be able to satisfy (without interfering with) this objective. Modelling considerations were to be restricted to

- Viscous, incompressible flow
- Flow in the absence of free-surface distortion
- 2 dimensions

This original scope for development applies to the preliminary studies which are discussed in section 6, and to Phase 1 of the main research effort described in chapter 4. It will be seen that just as the rules for algorithm development had to be revised at the end of Phase 1, so too did this scope of treatment.

5. MODULARISING FLOW INFLUENCES

One of the most important design requirements for the direct computer model was the modularisation of all the influences and mechanisms affecting the flow and, where possible, modularisation of all the resulting flow attributes (such as pressure and velocity components). This was to retain physical transparency of all of the mechanisms throughout the modelling process. In any fluid system of the restricted type considered here (see

section 4) it was straightforward to distinguish, at least superficially, between "external" and "internal" influences. The external influences were simply the motions of solid boundaries, whilst an example of an internal influence was the action of viscosity. In order to be able to synthesise physically transparent and modularised algorithms for modelling the flow of a real fluid it was necessary to consider carefully and isolate the component causes and their effects in such systems.

For illustration purposes consider the motion from rest of a flat plate in a stationary fluid (see figure 3.1). Suppose the plate accelerates from rest and then maintains a steady speed. How does the fluid respond? When the plate just starts to accelerate the incompressible fluid will respond immediately with a temporally accelerating flow pattern. Within an instant the fluid must decide where to go and furthermore the mechanisms for influencing this immediate response from the rest condition must be entirely inviscid since no actual velocity yet exists in the fluid. When flow begins, however, then the viscous mechanisms come into play and these will continue to influence the system until flow ceases.

The modular model conceived for incompressible flow as a starting point and template for the development of the computer coding is illustrated in figure 3.2. This is an influence diagram for a fluid, not a computer flowchart (although one may be derived from it), for it simply represents the structure of the identifiable causes and effects within the development of a flow. It will be noted that the only external influence considered was the acceleration of solid boundaries within the fluid. This might appear to neglect some of the more common boundary condition inputs considered in conventional modelling, such as applied pressures or upstream and downstream flow velocity conditions. However, for the types of flow systems being considered within the given scope (see section 4) it was argued that all of these alternative inputs could, ultimately, be traced back to the acceleration of some boundary surface or surfaces.

It is important to realise that figure 3.2 illustrates the earliest model for the flow influence structure and as such it is by no means comprehensive or entirely adequate. As it stands the model only really covers the development of simple stream flows as illustrated in figure 3.3(a). By the same token, of course, it also describes the equivalent acceleration of single bodies parallel to parallel boundaries in a stationary fluid as illustrated in figure 3.3(b); however, the mechanisms are less easy to visualise in these situations since it is traditional and more usual to transfer the frame of reference to the moving body. The model of figure 3.2 does not, for example, cover the more complicated situations as in figure 3.3(c) where the boundary accelerations actually lead to a change in the overall system geometry. Such complexities are considered (conceptually at least) during the

course of the research development and a more comprehensive modular model for flow behaviour will be presented in chapter 6.

Consider now the system depicted in figure 3.3(a). Following the influence diagram of figure 3.2 for the flow developing from rest shows that the initial boundary accelerations in the system will give rise to a sympathetic temporal acceleration field (and corresponding temporal pressure field) in the fluid which will induce finite velocities of the fluid. These velocities then give rise to two phenomena. The first is the generation of convective pressure in the system which is the pressure field associated with the convective acceleration (i.e. the spatial variation of velocity) of the flow*. The second is the action of viscosity, which is dependent upon the velocity gradients in the system. If the boundaries in the system continue to accelerate, there will subsequently be two contributions to the total temporal acceleration of the fluid. The first component is the direct or pure acceleration response to the instantaneous boundary accelerations which should be independent of the existing velocities in the flow and must be entirely inviscid in its mechanism. The second is the contribution from the shearing actions of viscosity which will, of course, be related to the velocity levels within the flow. Flow velocity increments will arise from each of these temporal acceleration influences and the flow field and convective pressure levels will be modified accordingly.

It is worth noting that the overall modular breakdown, as described above, illustrates certain obvious expectations. For inviscid flow, for example, it can be seen that no change in the velocity or convective pressure field will take place without boundary accelerations being experienced. That is, for a final steady motion of the boundaries the flow will be sustained by the convective pressure developed during the acceleration phase. For steady motions of the boundaries in viscous flows, on the other hand, there is a potential source of temporal acceleration from the viscous shear influences which may lead to unsteady phenomena such as vortex shedding in otherwise steady conditions.

---

* "Temporal" and "convective" pressures are not terms commonly found in fluid dynamics, even though temporal and convective acceleration components are. The approach of this work demanded that such a distinction of pressure components be made at an early stage. In chapter 5, section 3.8, the interplay between these pressure components will be discussed in detail.

6. PRELIMINARY STUDIES

6.1 Introduction

The preceeding sections of this chapter have presented the guidelines that were established for the work of this research in the form of rules, objective, scope and structure for the development of the computer coding. These were formulated with the aid of some preliminary studies that were performed to clarify the concepts involved and verify that the proposed modelling approach had some possibility of success. A simple algorithm had been conceived for the temporal acceleration response module of the overall model (see figure 3.2) and a sound justification for embarking on a full research program would be if this could be applied to a simple fluid system and could be shown to produce results that compared favourably with a known "solution".

The need for justification of the concepts was strong, not only for the purposes of seeking research funding, but also in recognition of the fact that a fully working computer modelling system would require the development of many relatively straightforward but extensive program segments (for example, the setting up of the program menu structures, and the description of the system boundaries and fluid characteristics, etc.) before any testing and development could be performed on the "heart" of the computer model - namely, the behavioural modelling routines. Consideration of only a single system geometry would mean that a simple pilot program could be written around this geometry and that the behavioural modelling routines could be written and tested quickly. This section, then, describes the form of, and the results from, the proposed temporal acceleration algorithm implemented in such a pilot program.

6.2 The Pilot Program

6.2.1 Implementation

The test program was written in BASIC on a BBC microcomputer (with 6502 second processor). This system was chosen because of its simple-to-use, though relatively powerful, graphics capability. The system modelled was the linear acceleration in a radial direction of an infinitely long cylinder within a concentric annulus of fluid, bounded by a fixed cylindrical wall (see figure 3.4). The reasons for choosing this particular geometry were as follows:-

(i) An analytical solution was available.

(ii) The system was "closed" in that the fluid had distinct limits. Therefore no complications, such as the consideration of free-surfaces or flow "at infinity", needed to be addressed.

6.2.2 Algorithm for the Temporal Acceleration Field Resulting from Boundary Accelerations

The fluid was divided into a series of elemental "regions", conveniently annular in shape (in this case), as shown in figure 3.5. Fluid acceleration within the system was represented by the rates of change of volume flux across the region boundaries. From this flow information the average normal and tangential acceleration components for a region could be deduced by averaging the rates of change of volume flux per unit area for the relevant boundaries of the region.

Consider an instantaneous acceleration of the inner cylinder with respect to the fluid regions. The acceleration response of the fluid to the body movement was synthesised from a logical consideration of what would happen within an instant of time, as follows. The initial effect of the cylinder's acceleration would be to cause a sympathetic effective acceleration of the flow across the region boundaries which are coincident with the cylinder surface as shown in figure 3.6(a). This would mean that there would be a rate of build-up of fluid within the regions adjacent to the cylinder. This was quantified by means of a "squeeze factor" defined as:-

$$\text{SQUEEZE FACTOR (SQF)} = \frac{\text{Rate of change of volume flux into region}}{\text{Region volume}}$$

(Note that SQF could be positive or negative.) With regions "stressed" in this way*, the logical reaction would be to attempt to relieve the tended flow build-up; and since a particle of fluid would not be "aware" of restrictions to flow, other than solid boundaries, then it was considered logical that a region should exhaust (or relax) evenly across all free boundaries in accordance with the level of SQF - i.e. the same rate of change of volume flux per unit area was impressed upon all a region's boundaries, except those which were coincident with the cylinder. The relaxation of one region, of course, altered the SQF of its neighbours; and by repeating the process as summarised in figures 3.6 and 3.7, the initial acceleration disturbance from the boundaries in the system was spread throughout the fluid to produce the fluid's temporal acceleration response.

---

* Note that the term "stressed" above is in quotes because no *actual* compression of the fluid has taken place. Indeed, the use of the term "squeeze factor" is rather a misnomer for this same reason.

It can be seen that the only underlying constraint on the development of the flow in the given example was to achieve continuity of flow acceleration in accordance with the cylinder's acceleration. This was achieved by considering what must logically happen during an instant of time. No high level mathematical equations were used or solved.

6.2.3 Interpretation of Flow Patterns Produced

The algorithm as described produces acceleration patterns which represent the temporal acceleration field resulting from instantaneous accelerations of the solid boundaries in the system. It should be remembered that this may not be the total temporal acceleration in a real fluid since further accelerating influences are produced from viscous actions once velocities build up in the flow (see figure 3.2). For inviscid fluids, however, the patterns produced *do* represent the total temporal acceleration of the flow and by the same token, therefore, they also reflect inviscid *velocity* patterns for given velocities of the system boundaries. This latter interpretation was not of direct interest to the development of the physically transparent computer model, but did serve to allow comparison of the acceleration fields produced here (and later) with analytical flow solutions which were all traditional velocity formulations.

6.3 Results from the Pilot Program

The acceleration patterns produced by the pilot program were qualitatively encouraging. An example is shown in figure 3.8 of the fluid's acceleration response to a linear acceleration of the inner cylinder. A potential flow solution is available for the given system geometry and this provides the comparison for quantitative assessment of the computer model results. The analytical solution for the symmetrical configuration used here can be obtained from the well known "2d cylinder in an infinite uniform flow" (velocity) solution by manipulating the usually neglected flow description within the cylinder (see appendix 1). This analysis agrees with a more general formulation of this solution which can be found in reference [13f].

Radial and tangential components of acceleration were directly available from the program output for positions corresponding to the "centres" of the fluid regions. Graphs could, therefore, be simply constructed from the results to show the radial and circumferential variations in the acceleration components. Analytical results from the potential flow solution were superimposed on these graphs, and examples are shown in

figures 3.9 and 3.10 for one particular ratio of inner to outer cylinder diameter. Other configurations were examined. Very close agreement between the pilot program results and the analytical solution was obtained, even with the limited discretisation that could be achieved with the small memory of the BBC microcomputer.

6.4 Conclusions

The level of agreement between the computer results and the analytical solutions was considered adequate justification for continuing with the research. This would obviously require the use of a rather more powerful computer system and the development of system set-up modules in the modelling program to allow exploration of more general flow configurations. This main development of the work is covered in chapters 4 and 5.

The results of these preliminary studies seemed to highlight the sort of confusion that can arise in the understanding of "cause" and "effect" in fluid behaviour which is sometimes aggravated by traditional teaching of fluid mechanics. In the model described here, the driving influence was the acceleration disturbance to the flow as caused by the movement of the cylinder: this disturbance had to be logically relaxed to achieve continuity of acceleration in the system. Traditional teaching might suggest that the irrotationality condition must also be a driving influence in the development of the flow; but the results here seemed to illustrate that this was actually a consequence of the fluid's logical behaviour. A proper recognition of "influences" and "consequences" was to be very important for the development of a program that conformed to the concepts of a direct computer model of a fluid. This recognition was by no means complete at this stage of the work, as will be seen from the subsequent chapters. For example, at this stage embedded in the algorithm designed was the erroneous statement that the pressure distribution in the system was a "consequence" in fluid behaviour and, therefore, that both temporal and convective pressure should result from a logical consideration of how the fluid must behave in response to a geometrical disturbance to the system. This lead directly to the development of what were essentially kinematic models for modelling fluid behaviour as described in chapter 4, which were later found to be restricting and deficient.

7. CLOSURE

This chapter has presented the original rules that were formulated for the development of a direct computer model of fluids. Although the aim of the *theme* of the research was to develop a comprehensive program along these lines, it was necessary to

be rather less ambitious for the work within the confines of this thesis. The objective of this research, then, was simply to demonstrate and realise the principles of such an approach. In terms of scope of study, consideration was to be restricted to 2-dimensional, viscous, incompressible flow, in the absence of free-surface distortion; this scope was considered to be sufficient for the stated objective. The modelling strategy has been described with reference to an influence diagram showing the cause and effect structure of the influences and reactions occurring within a developing fluid flow. This influence diagram (figure 3.2), although not comprehensive nor entirely adequate at this stage, illustrates the type of modular structure that had to be aimed for in the overall design of the computer model. Finally, preliminary studies have been outlined, the results of which hinted at the viability of the main research effort. These studies provided the basis for a successful application for research funding.

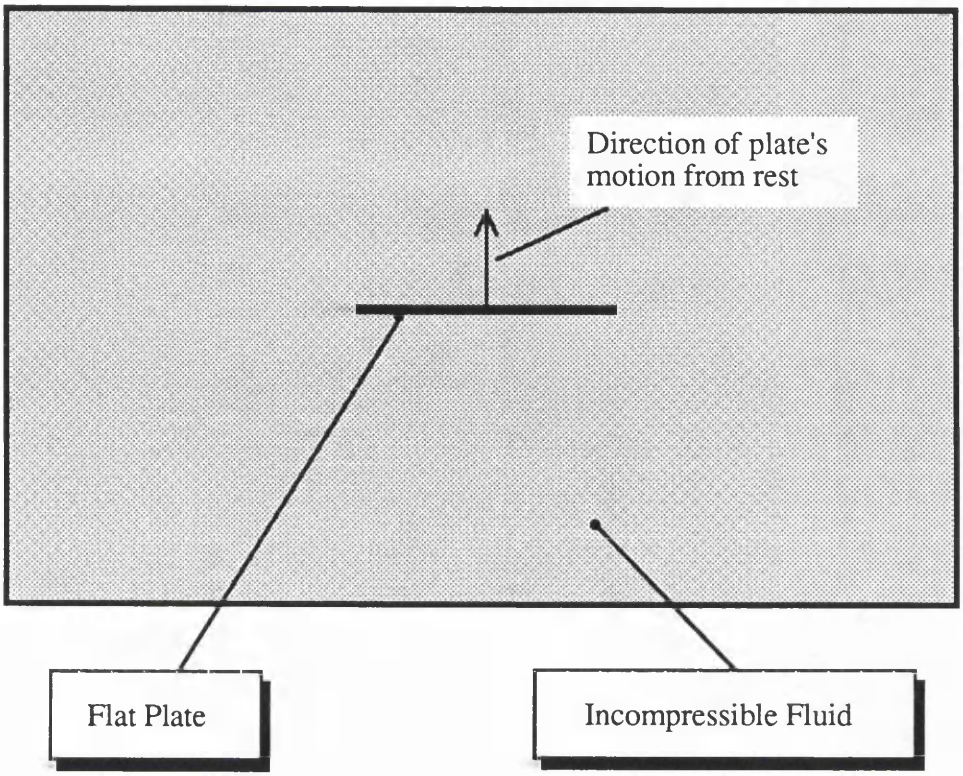

Plate Motion Time History

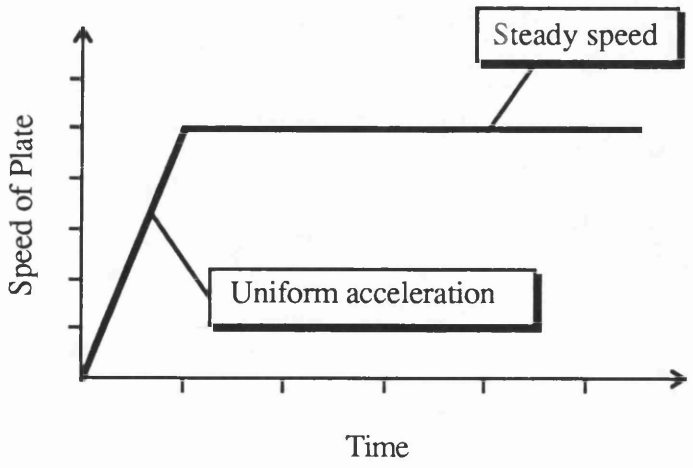

Figure 3.1 Flat Plate Accelerating from Rest in a Stationary Fluid

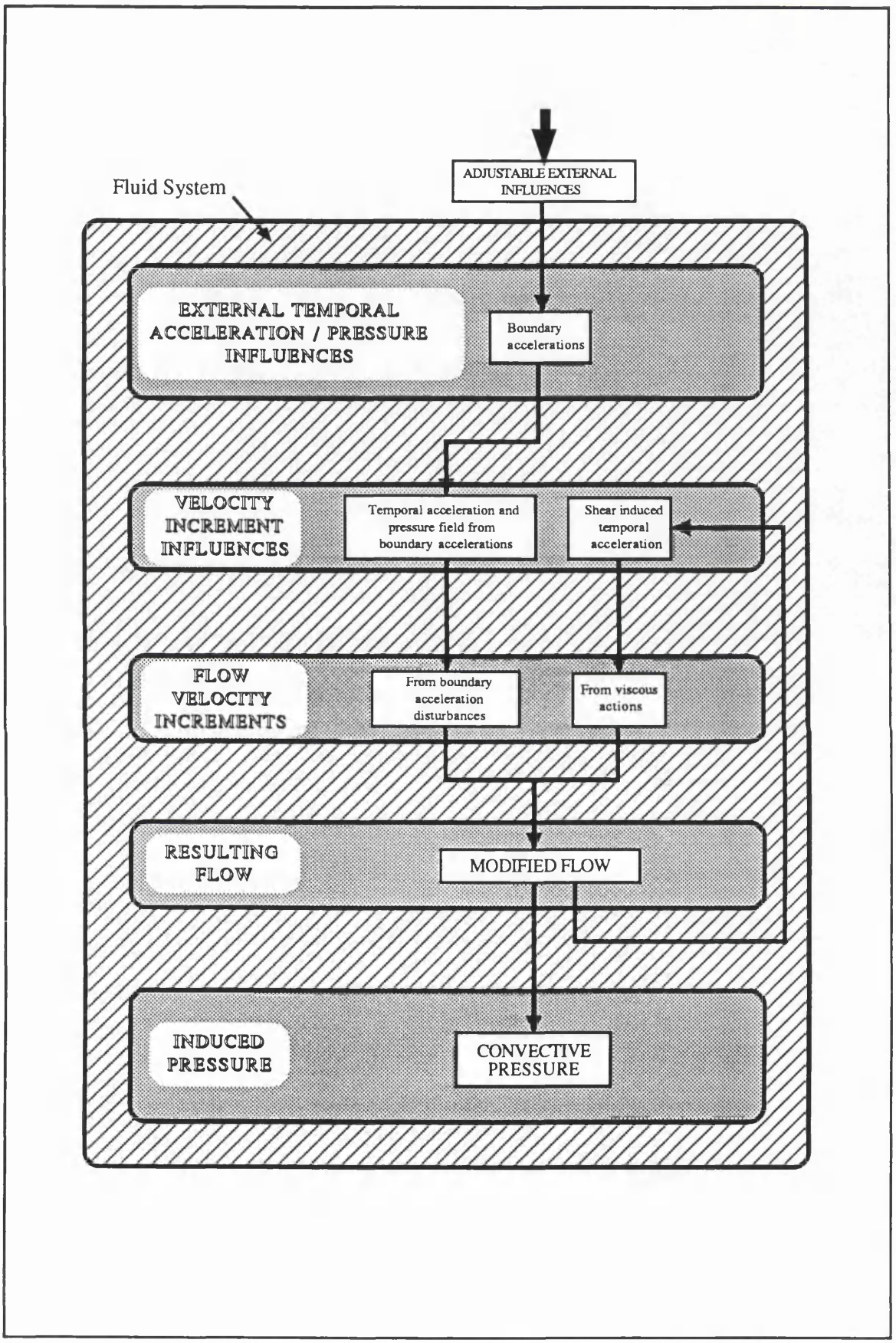

Figure 3.2 Modular Influence Diagram for Flow Development

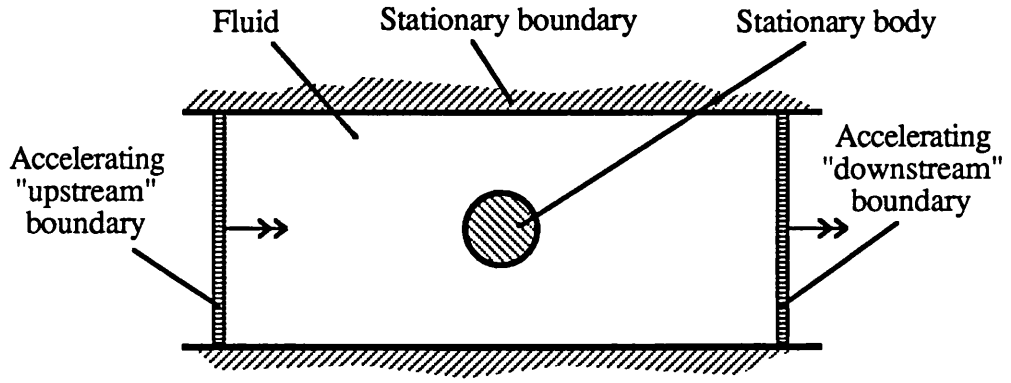

(a) Accelerating Stream Past a Stationary Body

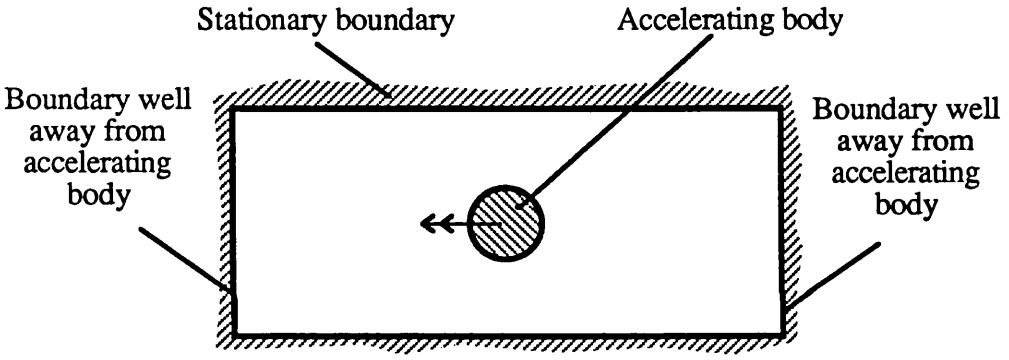

(b) Acceleration of a Body Between Parallel Walls

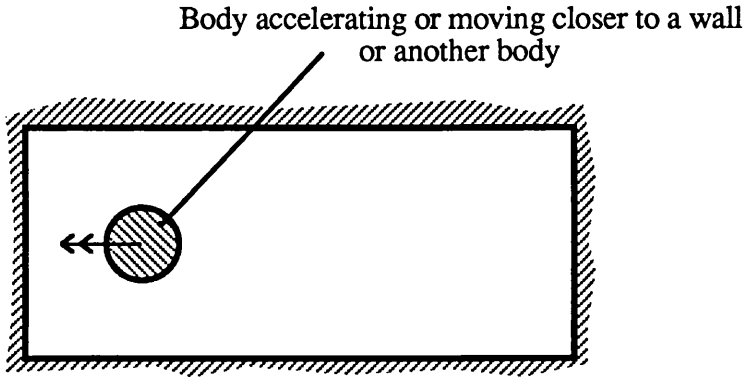

(c) More Complicated System

Figure 3.3 Representative Flow Systems

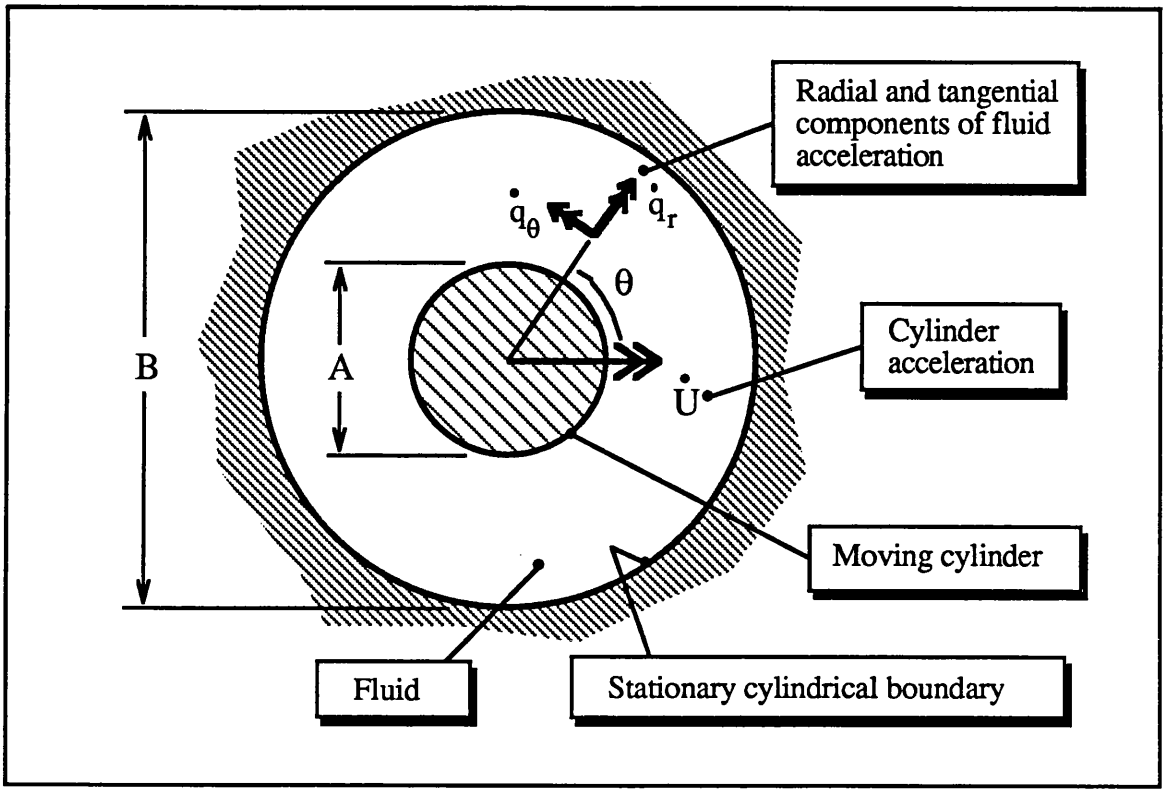

Figure 3.4 Infinite Cylinder in an Annulus of Fluid

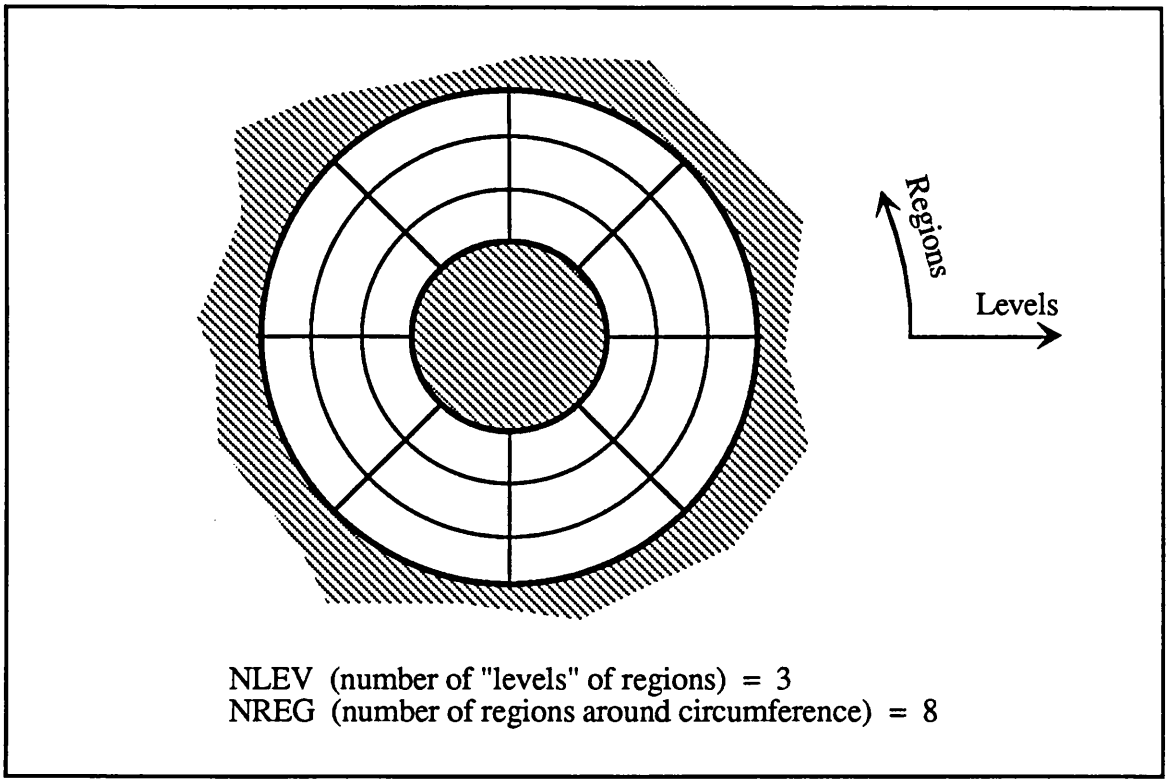

Figure 3.5 Example of Simple Discretisation of Fluid

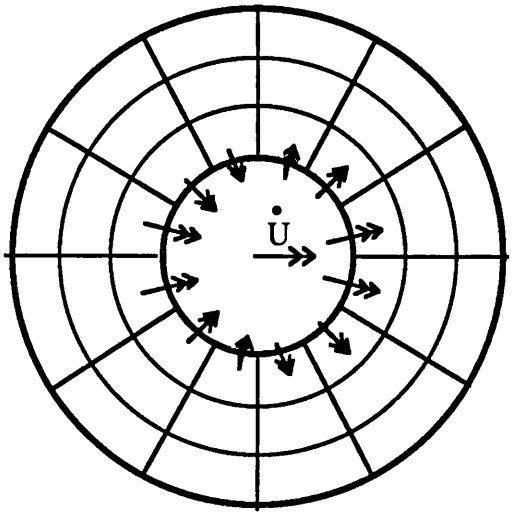

(a) INITIAL DISTURBANCE:- The acceleration of the cylinder is equivalent to a fixed rate of change of flux across the region boundaries which are coincident with the cylinder wall. There is thus a tended build-up of fluid within the regions adjacent to the cylinder.

Volume of region

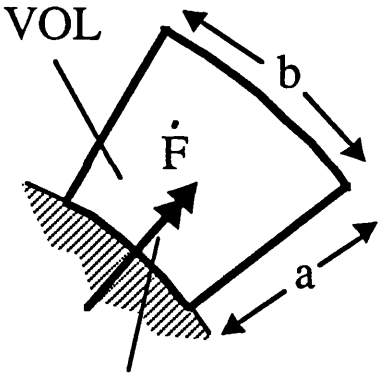

Total rate of change of flux across boundary

(b) The "stress state" of a region from (a) may be described by the "squeeze factor" definition. Here, the initial value for such a region is given simply by:-

$$SQF = \dot{F} / VOL$$

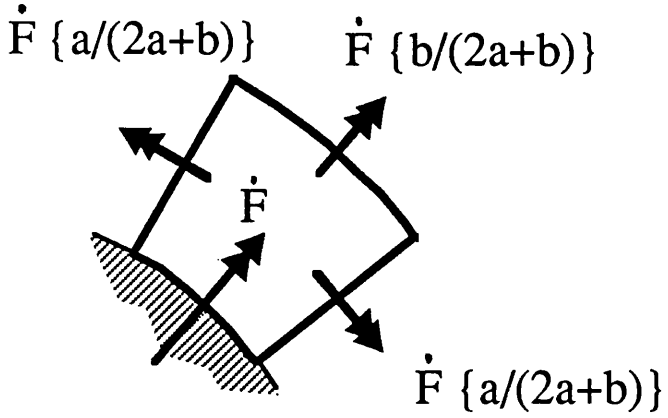

(c) The tended build-up of fluid must be exhausted from the region evenly via all free sides. In the given case, relaxation gives the increments to the flow accelerations as shown. Note that this affects the SQF levels in neighbouring regions, and that such relaxation must be repeated throughout the system until the SQF levels are (near) zero.

Figure 3.6 The Initial Disturbance and Relaxation Process

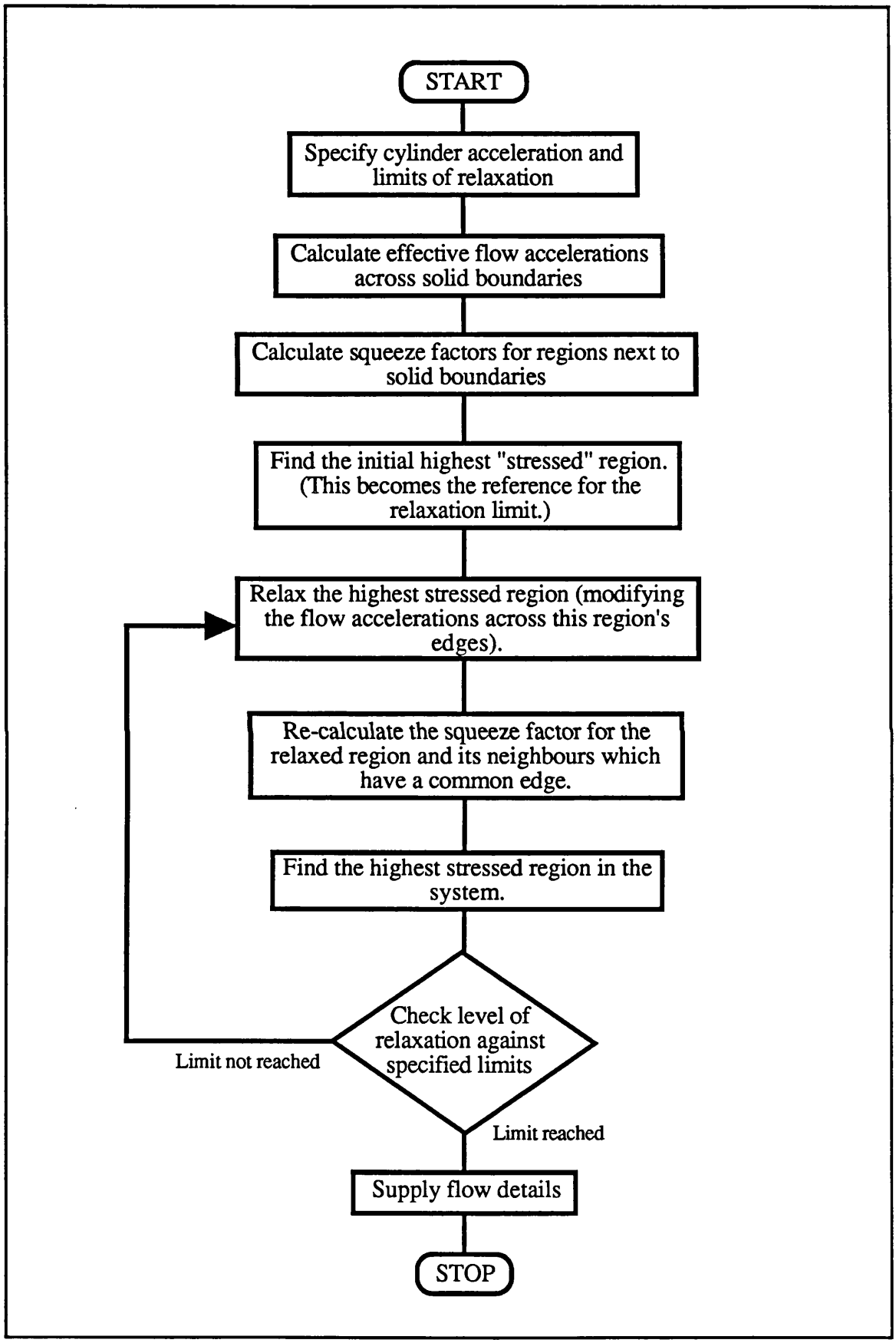

Figure 3.7 Flow Diagram of Pilot Program for Temporal Acceleration Response

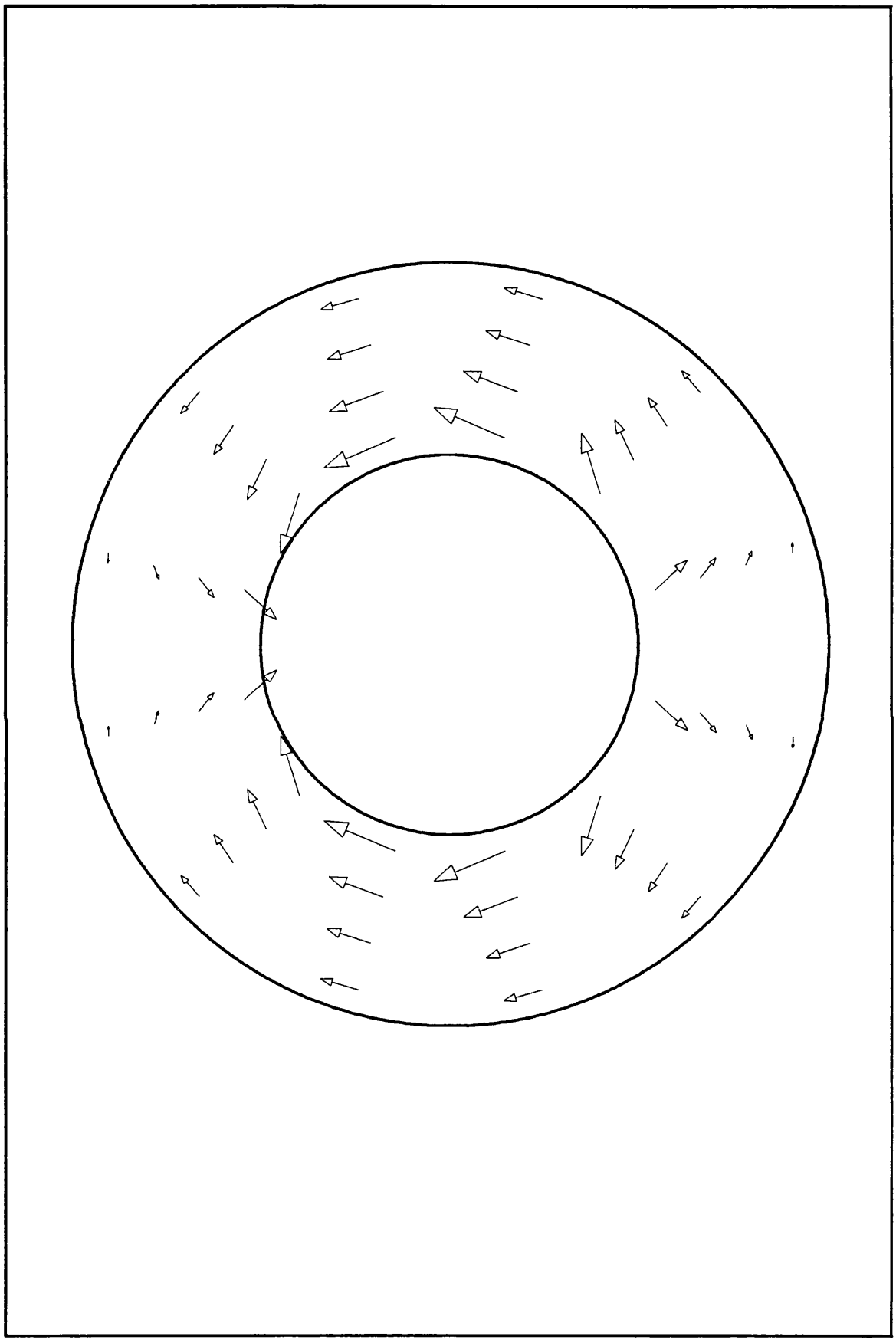

Figure 3.8 Acceleration Patterns from the Pilot Program

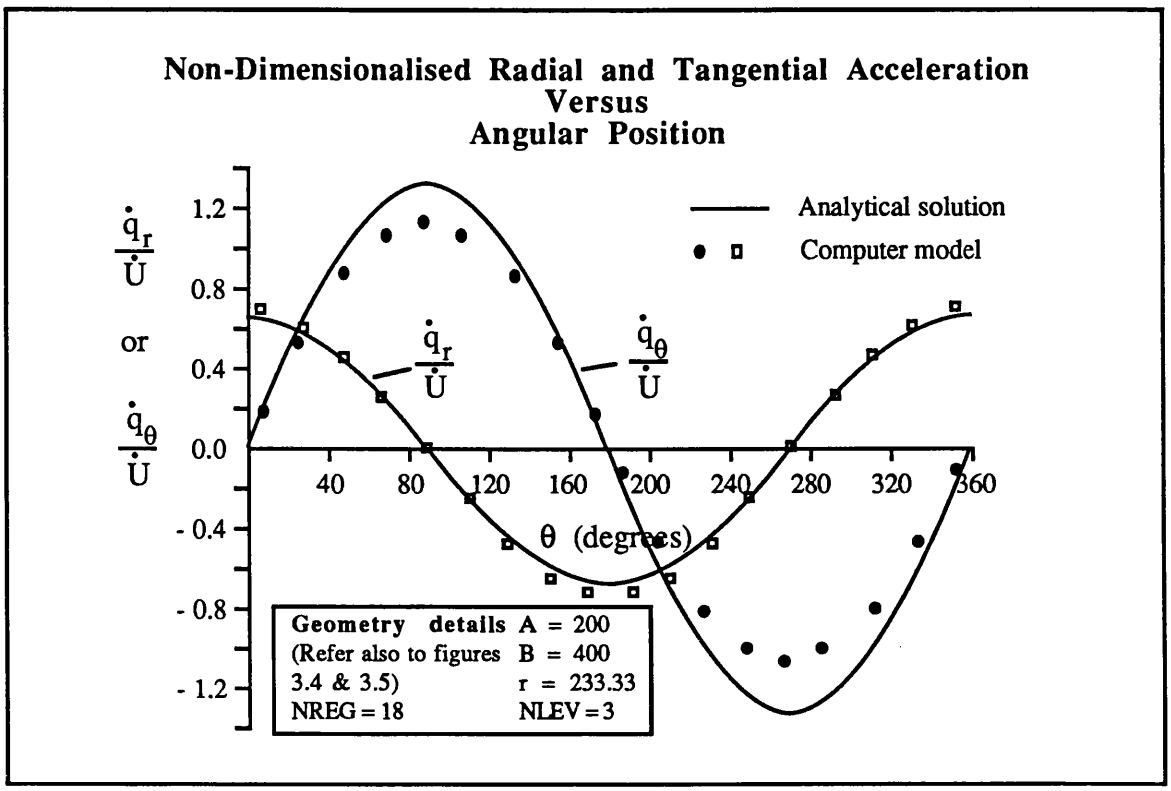

Figure 3.9 Variation of Radial and Tangential Acceleration with Angular Position

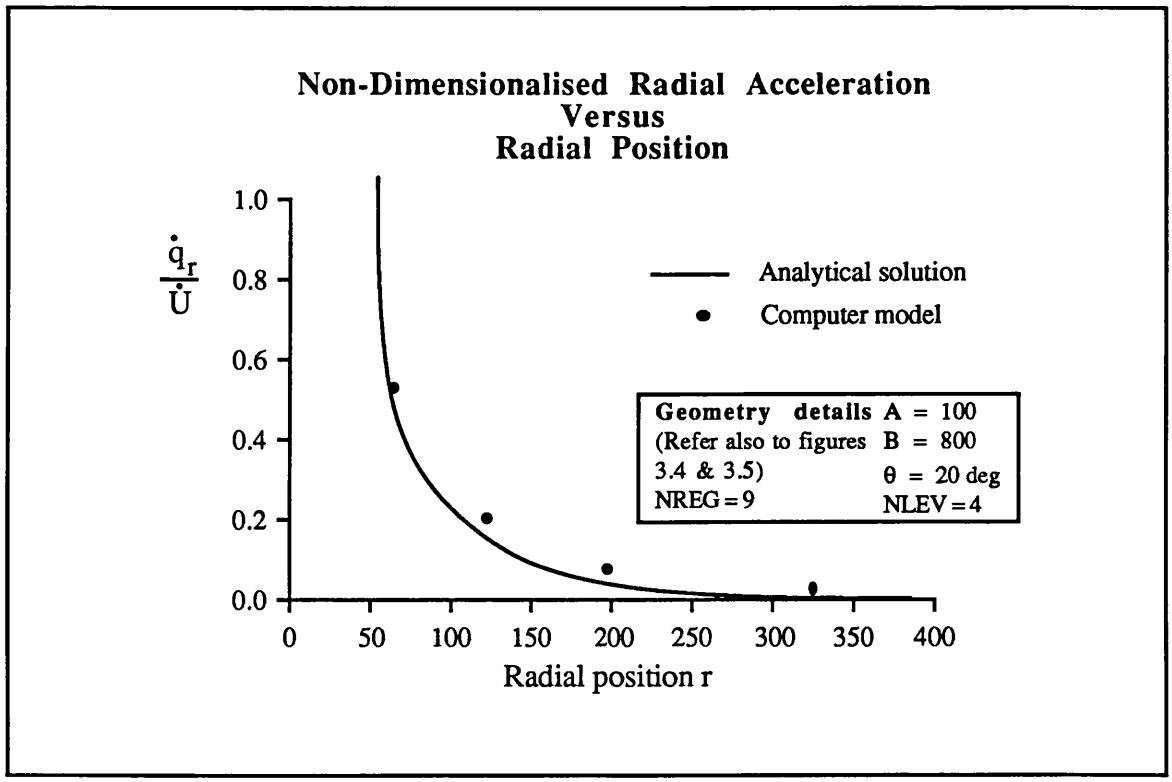

Figure 3.10 Variation of Radial Acceleration with Radial Position

CHAPTER 4

DEVELOPMENT OF A DIRECT COMPUTER MODEL OF FLUIDS (PHASE 1)

1. INTRODUCTION

Chapter 3 has described the guidelines that were formulated for the development of coding and some preliminary studies that were performed to explore the viability of the proposed direct approach to modelling fluid flow on a digital computer. In that work the original scheme devised for modelling the principal inviscid mechanism within a real fluid flow - namely the generation of the temporal acceleration response to boundary accelerations - was tested on a flow system for which an analytical solution was available. Encouraging results were obtained. This was considered sufficient justification for embarking on the synthesis of a general flow modelling program where it was recognised that, in addition to the development of the modelling algorithms for real (viscous) flow, significant effort would be involved in designing algorithms just to describe the system set-up. This chapter, then, describes Phase 1 of the research - the early development work carried out in an attempt to realise a direct computer model of a viscous fluid. It includes a description of the computer system used and details of the system set-up algorithms, as well as the various flow modelling strategies that were explored.

2. FLOW SYSTEMS CONSIDERED

For the purpose of demonstrating the viability of the direct approach to fluid modelling it was considered expedient to base explorations on the simplest realistic type of flow system (see chapter 3, section 4). The flows to be considered then were 2-dimensional, viscous, incompressible, and in the absence of a free surface. The requirement for simplicity in the modelling processes meant that mechanisms developed for 2-d flow should be readily transferable to 3-d situations, requiring only extra programming effort rather than adjustment of the intrinsic method of the algorithms. The restriction to flows in the absence of a free surface seemed most reasonable at the time since the reliable modelling of viscous flows alone was a significant task.

3. HARDWARE AND SOFTWARE

The fluid modelling test program, which was called FLOW2D, was written and developed on a DIGITAL MICRO-VAX GPX computer. The colour graphics capability of this machine was invaluable for debugging purposes within the design of algorithms as well as, of course, for clear presentation of program results. Hardcopies of screen displays were obtained using a DIGITAL LN03R laser-jet printer. Many of such hardcopies are provided as figures in this thesis and being restricted to black and white these do not reflect the full capabilities of the graphics modules of the developed program.

The program was written in FORTRAN 77 and the graphics modules use the GRAPHICS KERNAL SYSTEM (GKS) standard software. Consequently the developed program should be transportable with minimal conversion effort required. An overview of the program structure is shown in figure 4.1 and is described in more detail in section 4.

4. SYSTEM SET-UP ROUTINES

In view of the requirement to test the robustness of any flow modelling algorithms, it was necessary to be able to define different systems/geometries with ease. This meant that in the early stages of the work considerable attention had to be given to "system set-up" routines. These routines effectively define the system - its geometries, its motions and the discretisation required. They may be thought of as the "apparatus" for the research since they provided the program structure into which adaptable flow modelling test routines could be slotted. The algorithms developed for flow modelling are described separately in section 5.

4.1 Body and Environment Geometries

The 2-dimensional fluid systems can consist of up to 4 separate bodies in a fluid constrained by one environment surface. The default environment is a rectangle which can represent infinity by adjusting its dimensions so that it lies suitably far from all the bodies in the system. If a definite constraining environment exists then this can be separately defined.

Both bodies and (non-default) environment surfaces can be defined by a series of segments which may be a combination of straight-line and circular-arc segments (see figure 4.2). Surfaces are defined with respect to their own axes system and must be closed so that

"solid" and "fluid" areas in the system may be analytically determined. Options are available for enlarging and orientating surfaces with respect to a world axes system.

4.2 Fluid Discretisation

Depending on body shapes in the system, it is tempting to consider matching region shapes to the body curves. This type of approach, which is extensively used in conventional CFD [4b], can lead to all sorts of difficulties when complex geometries are to be considered. For a fluid modelling technique which was to be general in its application it was believed to be more logical to adopt a simple regular lattice to describe fluid "regions"; and because of the need to have a more closely defined system near to boundaries - and therefore sub-division of the lattice - a square grid system was considered most appropriate (see figure 4.3). Note that this decision was made despite the general mainstream feeling against such arrangements (chapter 2, section 4.3). It should be remembered that an emphasis in this work was in simplicity of the model (in order to keep it physically transparent) rather than speed and efficiency of the developed program (chapter 2, section 6). Certainly, the ideals of the work demanded that the success of the technique should not be highly sensitive to the discretisation process.

A system may be discretised by specifying a coarse grid size and a coarse region's centre coordinates with respect to the world axes system. A coarse grid is then automatically defined which just extends to envelop the environment surface. An option is then provided to allow subdivision of individual coarse regions down to seven further levels. (See figure 4.4.) (The subdivision process was not automatic since such a feature would have involved extensive programming effort beyond that needed for the purpose of proving the modelling concept.) Having discretised the whole system with a sensible grid it is then necessary to determine the "solid" and "fluid" regions in the system. This is discussed in section 4.3.

4.3 Region Definition

This involved the most extensive (but necessary) programming effort in the set-up routines. Because the program had to accommodate a wide range of system geometries, the arrays describing the fluid regions had to be generated from scratch from the body and environment geometry details and the discretisation grid. Fluid regions are described by a series of edges, one (or more) of which may be solid edges (as part of the body or environment surfaces), the others being fluid edges which are common with adjacent fluid

regions. Figure 4.5 illustrates the principal data items that are generated for each region in terms of setting up the discretised system. Clearly this information had to be consistent throughout and it can be appreciated that this region definition process requires fairly considerable computational effort in order to determine the full interconnections for flow within the system. Figure 4.6 illustrates the principal variables and arrays required to define the *flow*; this will be discussed in more detail in section 5.

4.4 Motion Description

The bodies and/or the environment surface may be given motion descriptions consisting of linear and angular acceleration time histories. The accelerations are assumed constant and prevail over a specified time interval given by a start time and a stop time. Motions will (logically) start from rest and at the end of the acceleration phases the system boundaries will be in constant motion (i.e. constant velocities of bodies or far field free-stream). The motion descriptions are used by the time-stepping controller of the analysis section of the program (see section 4.5).

4.5 Control of Model

A time-stepping controller subroutine governs the calling of the viscous flow modelling routines which will be described in section 5. Some set-up routines are required to initialise certain parameters associated with the timestepping sequence and processes involved in the modelling.

4.6 Miscellaneous Routines

The principal program components for set-up have been described in sections 4.1 to 4.3. Associated with these are the more mundane but essential routines which add to the flexibility and user-friendliness of the program to facilitate testing of the algorithms. Examples are the display routines both for representing results and for displaying intermediate processes for illustrative and debugging purposes.

5. FLOW MODELLING

The strategy for structuring the computer model in a modular fashion to retain the identity of the component influences in flow development has been described in chapter 3, section 5. From the influence diagram constructed there (figure 3.2) it was possible to construct the high-level flowchart for the coding of the required computer program and this is shown in figure 4.7. Two principal program segments are high-lighted in figure 4.7. The first contains the inviscid algorithms to determine the temporal acceleration response of the fluid to instantaneous accelerations of the boundaries in the system. The second contains the viscous algorithms to calculate the magnitudes of the direct viscous actions within the existing flow at a given time and to determine the component of temporal acceleration in response to these actions. The development of the contents of only these two segments was attempted in Phase 1 and the following sub-sections describe the details of the approaches explored.

Before passing figure 4.7 it is worth explaining one feature more explicitly. Stage 0 indicates that the time-stepping process commences from a given flow field condition. This condition could either be (i) rest (in which case the viscous modelling routines will do nothing in the first timestep since no flow exists); (ii) a previously determined steady state viscous flow; or (iii) an inviscid flow corresponding to the immediate response of the fluid to an impulsive motion of the system boundaries.

Within the discretised system flow accelerations/velocities were represented in the computer program by the average flow accelerations/velocities *normal* to each edge or averaged accelerations/velocities for each region. These variables have been shown in figure 4.6. There is clearly a simple relationship between the averaged flow description for each region and the average normal flow rates at its edges; depending on the algorithm it may be more directly relevant to work with the edge flows rather than region flows, or vice-versa.

5.1 Modelling Inviscid Influences

5.1.1 The Technique

The scheme devised for modelling inviscid influences has already been described in chapter 3, section 6.2.2, where it was applied to a system discretisation in the form of annular elements. The principles of the technique used with the square grid system of discretisation are identical and figures 4.8 and 4.9 review the method by applying it to the

example of the flat plate accelerating from rest in a stationary fluid (see figure 3.1) using the variable names defined for the program in figure 4.6.

The process described is clearly a relaxation technique but is based on a logical balancing of physically identifiable quantities (flow accelerations) rather than mathematical concepts such as the flow potential function. Two adjustable parameters are indicated in the flowchart of figure 4.9, the "relaxation factor" (RFACT) and the "squeeze factor reduction limit" (RLIMIT). The former is the ratio of exhausted flow to inflow and was found to lead to optimum convergence rates at values of around 1.6 (see figure 4.10). The latter is the test ratio for convergence, defined as the ratio of the maximum squeeze factor within the system at the current stage of the relaxation process divided by the maximum squeeze factor in the system at the beginning of the relaxation process. Efficient convergence occurred down to squeeze factor reduction fractions of about 0.01 and convergence was small thereafter (see figure 4.11).

5.1.2 Inviscid Results

Figures 4.12 to 4.21 illustrate the results obtained for a series of inviscid runs of the program. The vectors drawn should be interpreted as instantaneous temporal accelerations of the fluid, though in some cases they may be interpreted as a steady state inviscid velocity field (see chapter 3, section 6.2.3). Where available, analytical solutions have been superimposed as dashed line vectors. The accuracy can be seen to be very good, the worst discrepancies being about 5-10%, though this may be improved by finer discretisation. Some discrepancies are evident with very small regions next to the body and in locations of transfer from small to large grid size. This was due to some numerical subtlety in the relaxation process from small to large regions and vice-versa, and would have required more study. However, in the interests of pursuing the concepts of the approach rather than the details, greater effort was directed towards the physical problem of viscous modelling.

5.1.3 Applications

The principal application of the inviscid modelling routines was, of course, as the boundary-influence driver for the fully viscous flow modelling process (see figure 4.7). However, some side applications were of interest.

AC Field Analogy

In the field of non-destructive testing a technique used for detecting surface cracks in metal components is to monitor the distortion in an applied AC voltage distribution on the surface of the metal [13d]. As AC fields and inviscid flows are analogous, the inviscid algorithms of this program could produce useful results for exploring expected AC field distortion with different shaped cracks. Figure 4.21 illustrates the flow of a mainstream over a semi-circular ditch. This can alternatively be interpreted as the magnetic field associated with a uniform AC voltage applied on the surface of a metal specimen and normal to a semi-circular crack. (Here half of the crack is "folded out" into the plane of the specimen surface.)

Added Mass

The most obvious direct application of the inviscid results obtainable was in the calculation of added masses of 2-dimensional body sections. A sub-program option was included to calculate added masses using the kinetic energy approach (see [1d] for example) interpreting the inviscid vectors as fluid velocities. The sub-program simply summed the fluid kinetic energies of all the regions based on their representative velocities, and evaluated the added mass in the usual way*. Figure 4.22 illustrates the added mass variation calculated for varying geometries of the cylinder-in-fluid-annulus system (eg figure 4.12). The results show good correlation with the analytical solution which is included in appendix 1.

5.2 Modelling Viscous Influences

The model of flow influences (chapter 3, section 5) seemed to have identified a distinct sequence of events that were associated with the viscous distortion of a flowing fluid. First, flow had to be generated for there to be any relative motion within the flow to cause shearing influences in the first place. Once shear motions appeared, so too would shear stresses within the fluid which would want to create a sympathetic viscous acceleration increment to the flow. It was clear, however, that in most flow situations this initial viscous acceleration tendency, obtained directly from the existing flow field, would not satisfy continuity requirements. Some further flow distortion influence would, therefore, be experienced as a result of any finite flow increments arising from the initial viscous acceleration. The combination of the initial viscous acceleration and the necessary

---

* This, of course, is not the way that the direct model should calculate added masses and it should be stressed that this sub-program option was simply an add-on for interest's sake at this stage of the development.

modification to this to satisfy continuity would constitute the resulting temporal acceleration component arising from viscous influences.

Two problems needed to be addressed, then, with respect to the time-stepping model. The first was how to calculate the initial viscous acceleration tendency at a given timestep (this effectively describes the contents of process 3 of figure 4.7). The second was how to determine the nature of the consequent mechanism dealing with the continuity problem (process 4 of figure 4.7), which constituted an effective blockage to the flow. The modelling algorithms tested for these phenomena will be described in sections 5.2.1 and 5.2.2.

Throughout the viscous modelling development, work concentrated on the single system configuration of flow of water onto a flat plate whose plane was normal to the mainstream (figure 4.23). This was because bluff flow onto a flat plate constituted a severe geometry and any viable algorithm had to work for such a case.

5.2.1 Relaxing the Initial Viscous Distortion of a Fluid

Only one technique was conceived and used to adjust the continuity clashes set up by the initial viscous acceleration of the flow. That was, by using the same relaxation process as for the inviscid modelling of boundary influences. The relaxation process (the means of satisfying continuity) was the same (see section 5.1) but the nature of the distorting influence was different. Whereas the boundary distortion to the flow could be considered as a "hard" input in that the flow acceleration was fixed at a boundary wall, the distortion due to viscosity was considered as a "soft" input in that it could be altered subsequently in the relaxation process. Having determined the initial viscous acceleration then, it was simply to be a case of calculating the associated "squeeze factor" values for this disturbance to the flow in the system and relaxing this by the technique outlined in section 5.1. The resulting (modified) viscous contribution to the temporal acceleration could then be added to the contribution from boundary accelerations to form the total temporal acceleration field from which flow velocity increments could be deduced.

5.2.2 Determining the Initial Viscous Flow Increments

A series of 5 schemes were explored for generating the initial viscous acceleration. These will be described briefly, with greater emphasis on scheme 5 which, although not

properly producing the expected separation behind the test plate, looked qualitatively promising.

Scheme 1. Shear Stress Distortion

This scheme involved the calculation of velocity gradients throughout the existing flow and the calculation of corresponding shear stresses acting on the fluid in individual regions. The shear forces acting on each region were summed to give resulting viscous forces: these lead directly to the initial viscous acceleration of each fluid region. Difficulty with this approach was in defining the shear stress at the wall and a representative velocity gradient based on the adjacent region velocity had to be selected rather arbitrarily.

Typical results from this scheme (figure 4.24) indicated an upstream and downstream symmetry with no tendency for reverse flow to be generated. This symmetry problem implied that convection of shearing effects was not being properly modelled. The absence of reversed flow indicated that shearing stress influences should be much greater at the plate walls.

Scheme 2. Shear Stress Distortion with Downstream Bias

In scheme 1, having calculated the initial viscous accelerations, these had to be transformed into averaged edge accelerations for the subsequent relaxation process. The edge accelerations were determined from the accelerations in the upstream and downstream regions associated with each edge. With that scheme there was no apparent mechanism for convecting the effects of the shear influence downstream. Scheme 2 attempted to overcome this deficiency, and the need to concentrate shear influences towards the wall. Viscous accelerations, then, were assumed only to be significant in wall regions; and having evaluated the total viscous force on a wall region this was converted directly into a decrease to the accelerating outflow from the region. An example of the results is shown in figure 4.25, and although a slight asymmetry could be observed it was not significant enough to be encouraging.

Scheme 3. The Influence of Adverse Pressure Gradients at the Wall

Scheme 3 was an exploration rather than a proper attempt at modelling the viscous behaviour. From the early success of the algorithm for inviscid influences it had been felt that it should be possible to deduce flow from consideration of kinematics alone, the pressure distribution being believed to be a consequence rather than a cause of fluid motion. Nevertheless, in an attempt to see if the "soft" relaxation method (see 5.2.1) could sustain a reversed flow, scheme 3 was devised where only flow in wall regions with an adverse pressure gradient would show a noticeable viscous acceleration. In such regions the flow was (rather drastically) brought to rest and then re-accelerated in the opposite

direction in accordance with the pressure differential. The results produced (see figure 4.26) were encouraging in that recirculating zones could be seen to be set up after the soft relaxation of the viscous disturbance. However, there was no logical way in which the influence could progress; and furthermore, the size of the separation zone was directly influenced by the size of the discretisation grid.

Scheme 4. Separation of Inviscid Flows?

At this stage in the work it was wondered whether viscosity alone causes the separation phenomenon to appear as quickly as it does in real flow systems. Scheme 4, then, was a "sideways" diversion from the consideration of viscosity which asked the question: how else could fluid flows separate?

Bearing in mind that a high Reynolds number (where separation effects would be large on the flat plate example being considered) implies large inertia forces compared with viscous forces, what is implied in the limit as viscous forces tend to zero? The extrapolation to an inviscid flow would be a very dubious process, but it is tempting to ask why can an inviscid flow not separate? Scheme 4 was a "conceptual search" for alterations to the relaxation method for inviscid analysis which could produce a separated type flow as illustrated in figure 4.27. Although no logical algorithm was conceived, the concept remains challenging. It was satisfying to discover subsequently that Saunders [12a] had described such a concept, although not in the context of fluid modelling, unfortunately.

Scheme 5. A "ROTATION" Model

In scheme 5 attention was directed towards explicit consideration of diffusing and convecting the predominant shear influence at the wall. Descriptions given in standard texts of the reasons for separation behaviour on the downstream side of bodies describe the convection and diffusion of vorticity. When Reynolds numbers are high, convection of this quantity "vorticity" is more effective than diffusion and more vorticity is carried around to the downstream side of the body. Eventually there is more vorticity at the rear of the body for the satisfaction of the "no-slip" condition at the wall there, and a backward flow is induced near the surface. This reversed flow counters the forward moving fluid and deflects it away from the rear of the plate. (See [1a].)

The mathematical concept of point vorticity (in terms of definition and description) was somewhat abstract and therefore was considered inappropriate for inclusion in this work. Nevertheless, it was thought possible to construct a model of the diffusion and convection of a more physically agreeable shear induced quantity. A quantity which was called ROTATION in the program was set up: this was described as a rotation *influence* rather than an actual rotation of the fluid in any region and it was considered to be

generated by the tendency of the fluid flowing in regions adjacent to a solid boundary to be "tripped up" as indicated in figure 4.28. ROTATION was only to be generated at the wall, its prevailing magnitude there being related to the representative velocity in the wall regions and the lengths of the wall boundaries for each region. As flow developed with time the ROTATION generated would spread throughout the fluid by convection and viscous diffusion. The distribution of ROTATION would therefore change as the flow developed and at each timestep the change in ROTATION level in each region must somehow cause the initial viscous acceleration.

Modelling Diffusion of a Quantity: This algorithm made use of the concept of "diffusion distance" of predominant shear effects in a time interval, which in analytical terms may be derived from the Rayleigh Problem (see [1b]). The application of this concept to the viscous diffusion of any fluid-bound diffusable quantity is summarised in figure 4.29. It should be noted that the concept placed a restriction on the timestep allowable in the modelling process.

Modelling the Convection of a Quantity: Again this algorithm was simple. Considering each region in turn, it involved a proportional transfer to neighbouring downstream regions of the amount of the quantity in the region concerned in accordance with the existing flow rates downstream and the timestep. This process placed a second limitation on the maximum value of the timestep as illustrated in figure 4.30.

Modelling the Generation and Effects of Rotation: The formula used to define the level of ROTATION maintained in a wall region is illustrated in figure 4.31. The units of ROTATION from this formula were s^{-1} and therefore could be related in some way to the average vorticity level within the region. However, because of the lack of physical "feel" still in the nature of this quantity, an arbitrary factor was included which could be varied in the tests. The proposed effect of a change of a region's ROTATION level on the surrounding flow is illustrated in figure 4.32. The assumption made was that the change in ROTATION manifested itself as a circulation acceleration through the neighbouring regions in accordance with the "sense" of the ROTATION - whether clockwise or anti-clockwise. However again, because of the poor physical interpretation associated with the ROTATION quantity, an arbitrary factor was included for varying the magnitude of the induced initial accelerations. The summation of the circulation flows induced by all the regions experiencing ROTATION changes resulted in the total initial viscous acceleration for this scheme.

Results Produced By Scheme 5: Figures 4.33 and 4.34 illustrate the best results for two runs using this scheme for an impulsive motion start of the stream onto the flat plate. A

plate of length 0.1m in water was chosen. Figures 4.33 correspond to an upstream speed of 0.01m/s (equivalent Re=1000); figures 4.34 correspond to an upstream speed of 0.1m/s (equivalent Re = 10000). The results were disappointing in the sense that they showed no recirculating flow on the downstream side of the plate, although a tended separation effect was observable and greater for the higher Re case at time t = 2 seconds as would be expected (see figures 4.33(k) & 4.34(i)). On the other hand, the results were quite encouraging in that they demonstrated a relaxed viscous velocity increment to the flow which did appear to have, at least, the correct qualitative characteristics in the form of recirculating zones which grow behind the plate (see figures 4.33(g) & 4.34(e)). Comparing figures 4.33(i) and 4.34(g)* illustrates the difference in ROTATION distribution caused by differing rates of convection: also, in the higher Re case proportionally less diffusion of ROTATION has taken place upstream.

6. DISCUSSION

Although the success of the inviscid influence algorithms developed in Phase 1 was encouraging, the shortcomings of the viscous algorithms were clearly evident. It was necessary, then, at this stage in the work to review the modelling concept and all of the developed algorithms in order to proceed to the next phase of the research.

Certain deficiencies with the algorithms became clear. First, there was no obvious physical reason why the initial viscous acceleration disturbance had to be relaxed by the same relaxation process as that for the boundary acceleration disturbance. Second, the algorithms used throughout, being essentially kinematic in nature, did not provide a direct value for the associated pressure disturbance in the flow, and without this the extension of the techniques described to flows with free-surfaces, for example, would not be possible. Furthermore, without a direct model of the pressure in the fluid, added masses, for example, had to be calculated by a kinetic energy approach: this was contrary to the ideals of a "direct" approach where added mass loadings should be measurable from pressures acting on body surfaces as a result of acceleration. These shortfalls in the form of the techniques developed so far were considered to be due to the misguided acceptance of the term "logical" as a description for permissible driving influences in the original rules for developing algorithms (see chapter 3, section 2). For example, fundamental to the work so far was the acceleration relaxation process. This process was based on a logical

* "3-dimensional" diagrams such as these will appear regularly from now on and so their interpretation needs to be clarified. They illustrate the distribution of some scalar flow property (in this case ROTATION) within the flow system where the averaged value of the property over each discretisation region is represented by a step having a height proportional to that value. In some of the figures of chapter 5, where such step diagrams are used to illustrate the distributions of pressure within the system, it is sometimes tempting, *but erroneous*, to see these as surface wave distortions.

balancing of tended flows within the discretised system yet, although very good results were obtained, the *physical* interpretation of the relaxation process was obscure.

It was decided, therefore, that in the next phase of the research the inviscid flow algorithms would have to be re-developed along strictly physical lines. Work on viscous influence algorithms could only proceed once the foundations of the inviscid influence modelling were firmly laid. The aim would be to synthesise fluid pressure and motion *together* in the flow model rather than, for example, invoking the momentum equation once motion has been defined. It was realised that in order to synthesise pressure levels in this way account had to be taken of the fluid compressibility, however small. Too much emphasis on the supposedly "simplified" problem of an incompressible fluid in the early stages of the work had obscured this necessity. The second phase of the research, therefore, was to concentrate on 2-dimensional inviscid flow. However, to ensure generality of the techniques developed the possibility of free-surface distortions would have to be accommodated.

7. CLOSURE

The results achieved in Phase 1 of the research, as described in this chapter, gave support to the *concept* of a direct approach to computer modelling of fluids but they were far from the *realisation* of such a technique. Much work was still required to develop a general modelling algorithm along these lines. With hindsight it was easy to identify the weaknesses in the algorithms developed. These arose from the allowable consideration of "logical" algorithms in the original rules for modelling (see chapter 3, section 2) rather than purely physical algorithms when modelling fluid influence mechanisms, as well as a pre-occupation with "incompressible" flow. The essentially kinematic models of behaviour developed as a result proved to be inadequate for the prediction of pressure by "physically transparent" means. Criticism of the results of Phase 1, however, usefully indicated the direction for Phase 2 (described in chapter 5) where the emphasis would be on synthesising both pressure and motion by purely physical algorithms. In one direction the scope of the research would have to be restricted to inviscid flow since work on viscous influences could only sensibly proceed once the foundations of the inviscid algorithms were firmly laid. In another direction the scope would be extended slightly to admit the possibility of free-surface distortion: this was to ensure that the algorithms developed would *properly* model pressure in a developing flow.

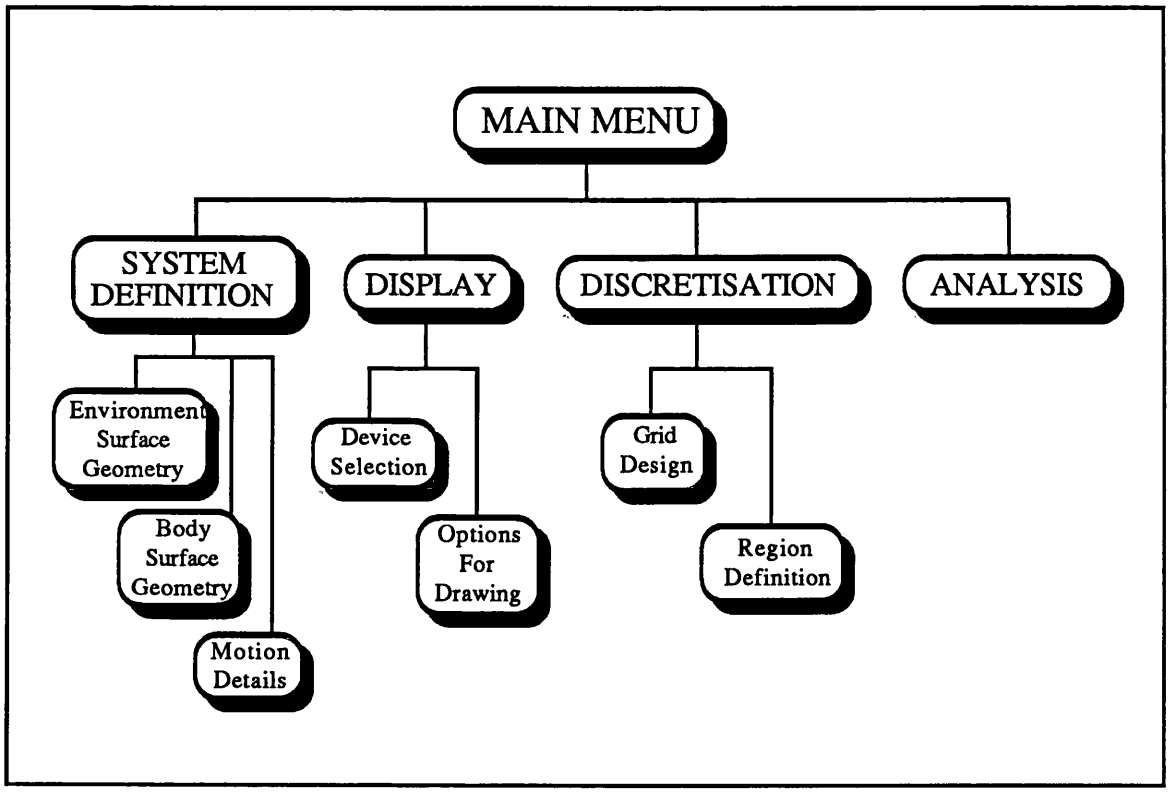

Figure 4.1 Overview of Program Structure

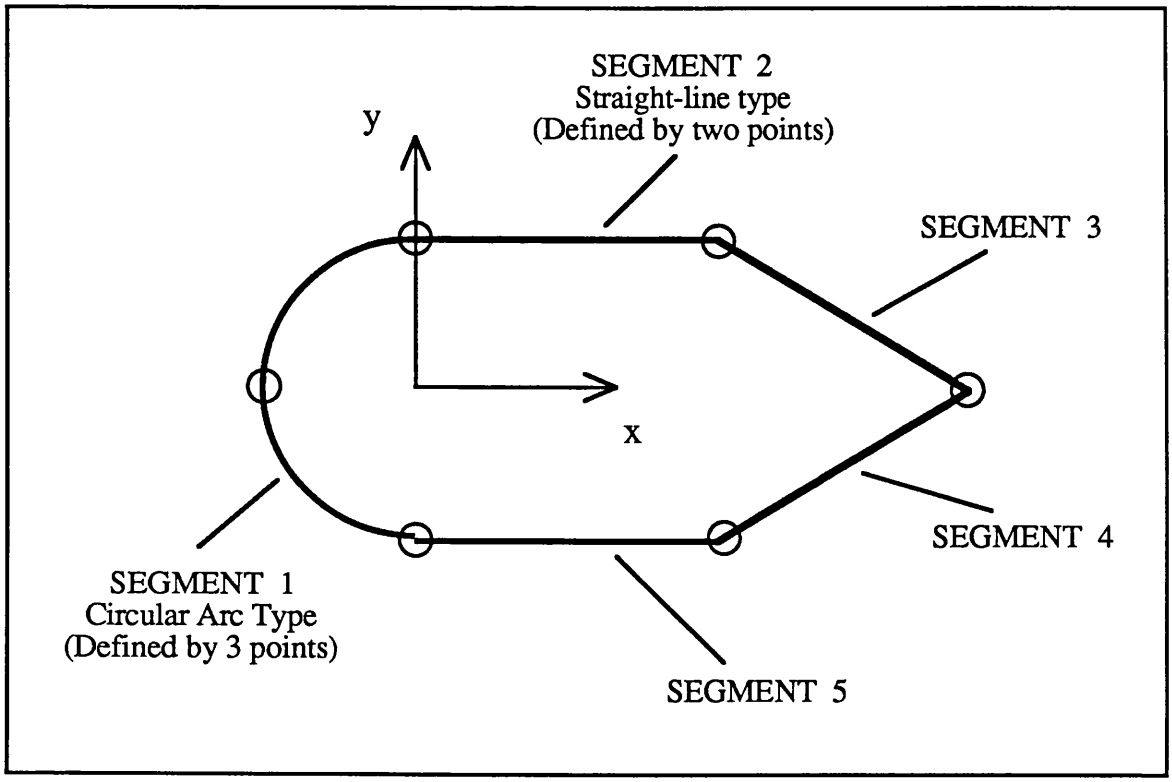

Figure 4.2 Example of Body Definition as a Series of Connecting Line Segments

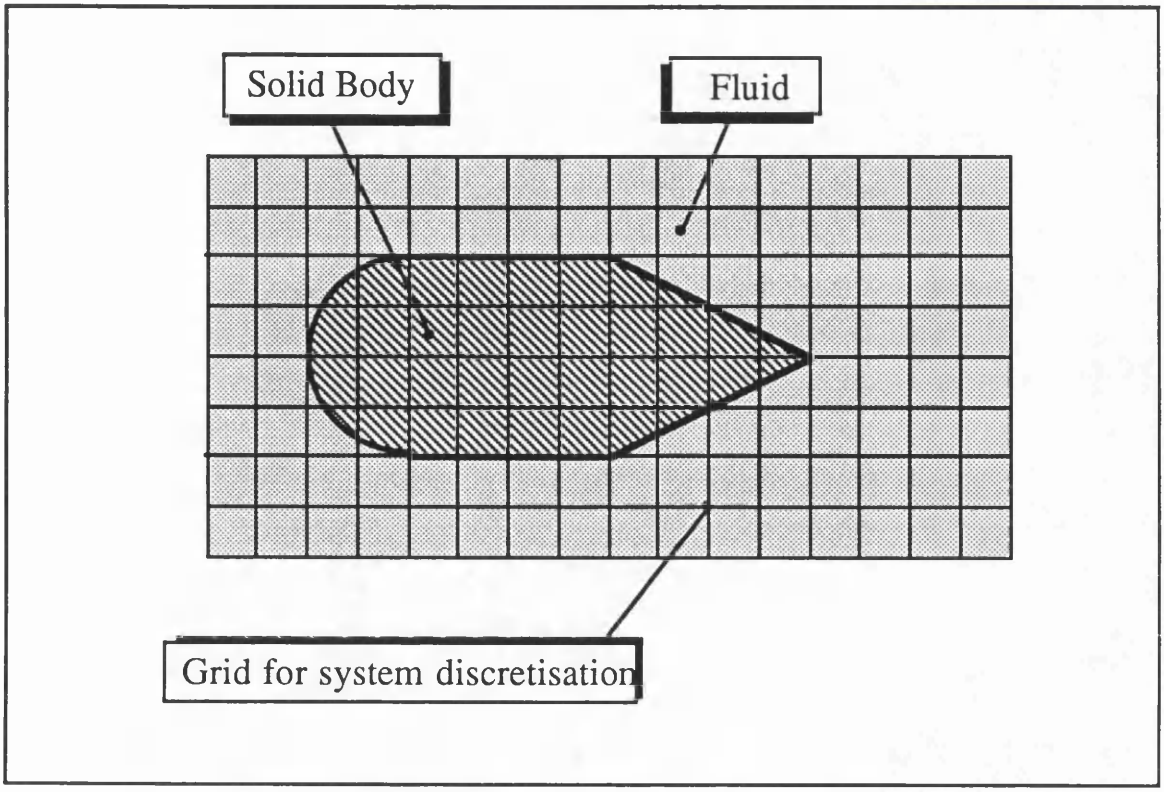

Figure 4.3 Simple Square Grid Chosen for System Discretisation

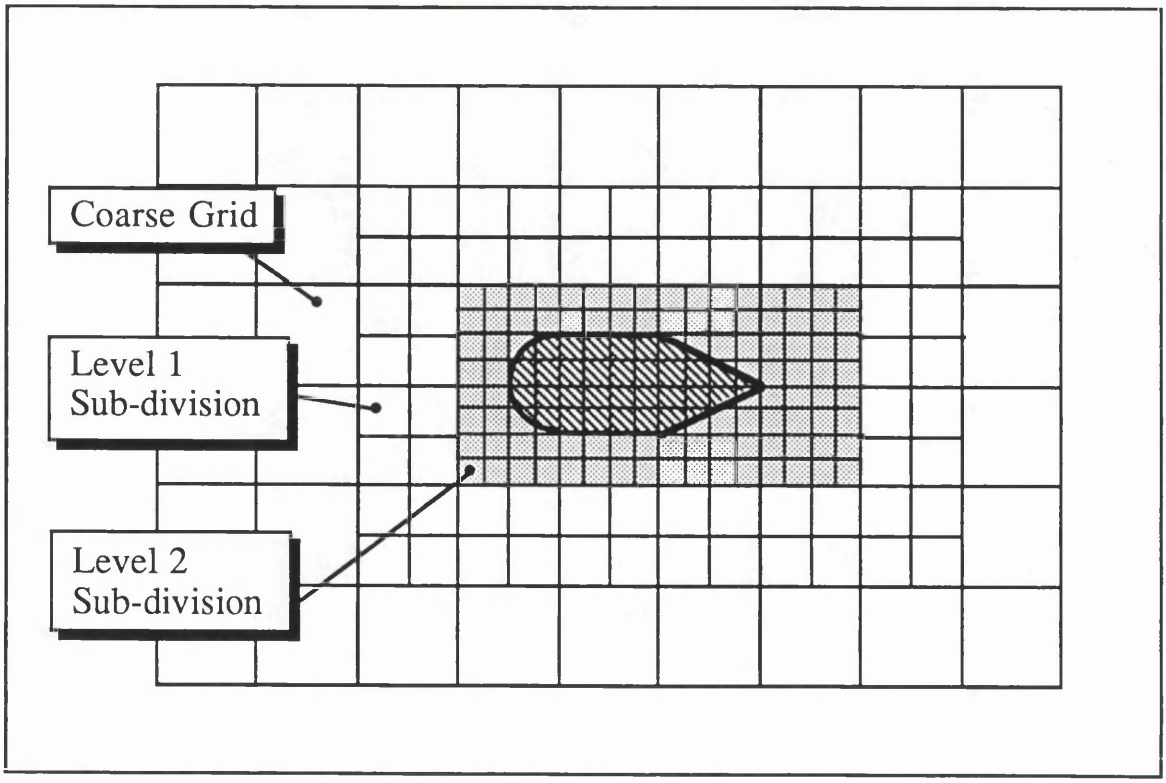

Figure 4.4 Coarse Grid Plus Two Levels of Sub-division

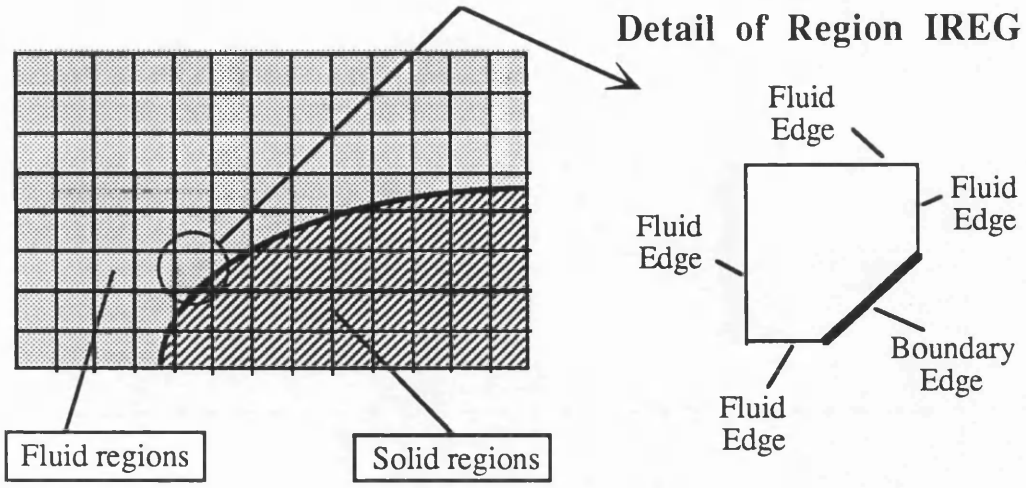

Regions are numbered 1 to NOREG
Edges are numbered 1 to NOEDG

Principal Set-Up Data for Region IREG

IDEDGE(IREG,10)	Edge reference numbers for up to ten edges associated with region IREG.
IDNEIG(IREG,10)	Region reference numbers for up to ten adjacent (neighbouring) regions.
CENTRD(IREG,2)	x, y components of region centroid.
VOLUME(IREG)	Volume (per unit depth) of 2-dimensional region.

Principal Set-Up Data for Edge IEDG

COEDGE(IEDG,2,2)	x,y coordinates for each end of edge.
IDREG(IEDG,2)	Region reference numbers for the two regions associated with edge IEDG.
NTYPE(IEDG)	Index to signify the type of the edge (i.e. whether a fluid or boundary edge).
AREA(IEDG)	Area (per unit depth) of 2-dimensional edge.

(Refer to Notation section for full array structure)

Figure 4.5 Description of Set-Up Variables Associated with System Definition

Part of a Discretised System

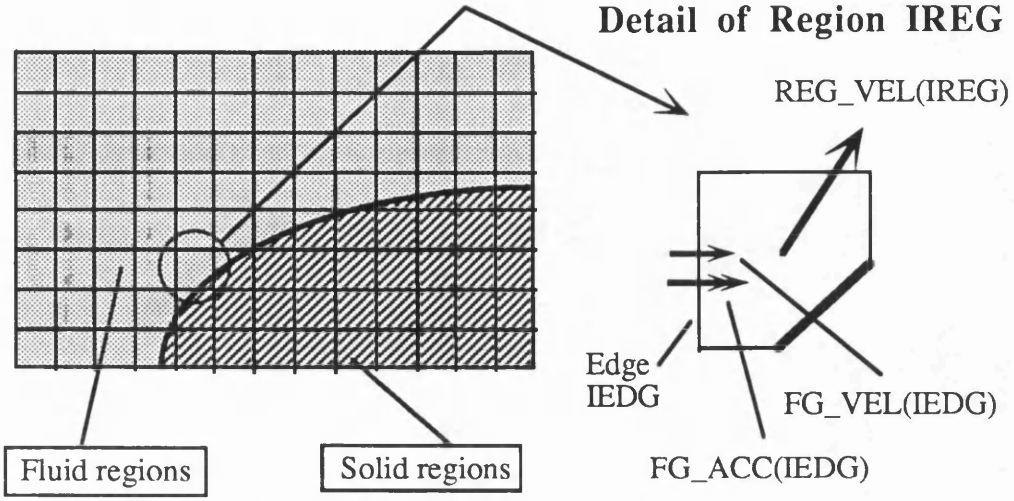

Regions are numbered 1 to NOREG
Edges are numbered 1 to NOEDG

Principal Dynamic Data for Region IREG

REG_ACC(IREG,2)	x, y components of average region acceleration.
REG_VEL(IREG,2)	x, y components of average region velocity.
PRESS(IREG)	Total pressure.
PRESS_T(IREG)	Temporal pressure.
PRESS_C(IREG)	Convective pressure.
ROTATION(IREG)	A viscosity induced quantity.
SQF(IREG)	"Squeeze factor" associated with pressurising mechanisms.

Principal Dynamic Data for Edge IEDG

FG_VEL(IEDG)	Averaged normal velocity at edge.
FG_ACC(IEDG)	Averaged normal acceleration at edge.

(See Notation section for full array structures.)

Figure 4.6 Description of Flow Variables Associated with Region and Edge Definition

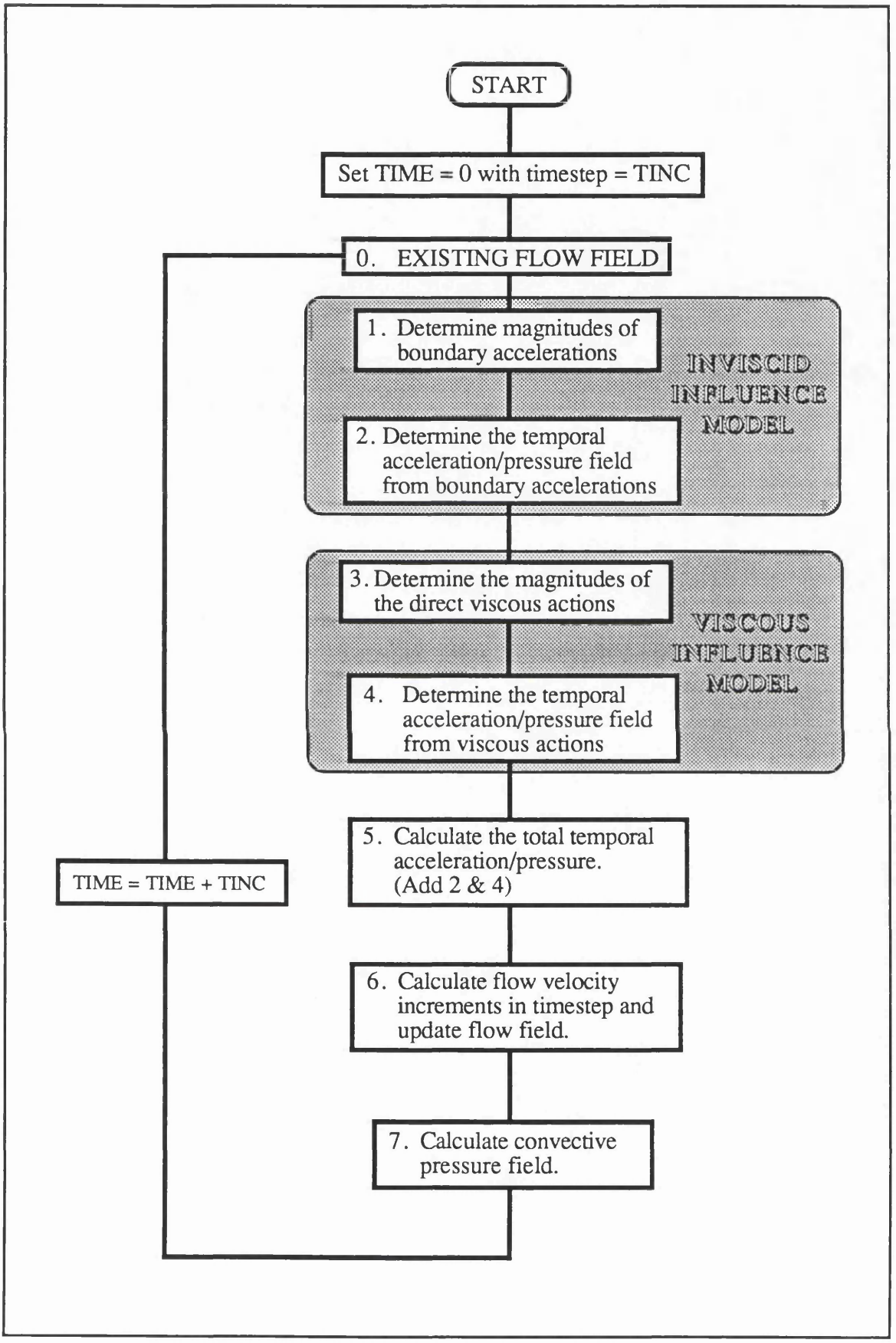

Figure 4.7 Flowchart of the Logic for Flow Modelling of a Real Fluid

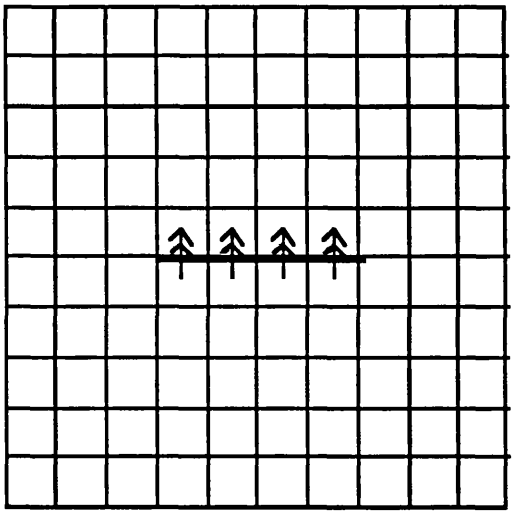

(a) INITIAL DISTURBANCE:-
The acceleration of the plate is equivalent to a fixed rate of change of flux across the region boundaries which are coincident with the plate surface. There is thus a tended build-up of fluid within the regions adjacent to the plate.

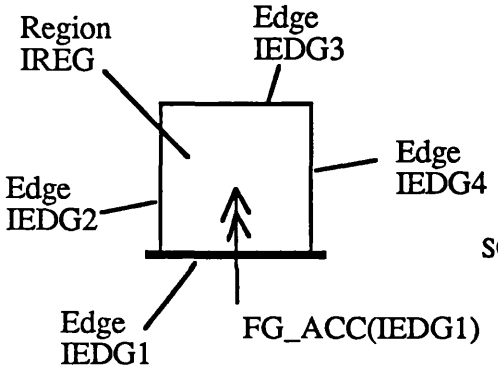

(b) The "stress state" of a region from (a) may be described by the "squeeze factor" definition. Here, the initial value for such a region is given simply by:-

$$SQF(IREG) = \frac{FG\_ACC(IEDG1) * AREA(IEDG1)}{VOLUME(IREG)}$$

(c) The tended build-up of fluid must be exhausted from the region evenly via all free sides. In the given case, relaxation gives the increments to the flow accelerations as shown. Note that this affects the SQF levels in neighbouring regions, and that such relaxation must be repeated throughout the system until the SQF levels are (near) zero.

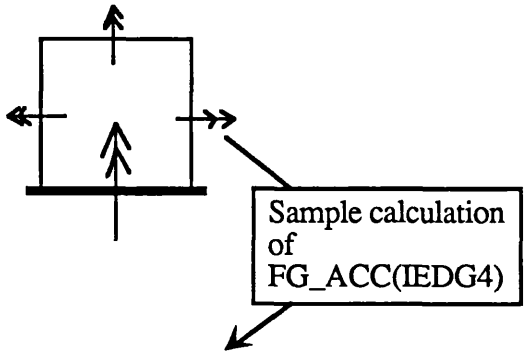

$$TAREA = AREA(IEDG2) + AREA(IEDG3) + AREA(IEDG4)$$

$$FG\_ACC(IEDG4) = FG\_ACC(IEDG4) + (SQF(IREG)*VOLUME(IREG)) * \frac{AREA(IEDG4)}{TAREA}$$

Figure 4.8 INVISCID MODELLING:-
Boundary Influences and the Relaxation Process

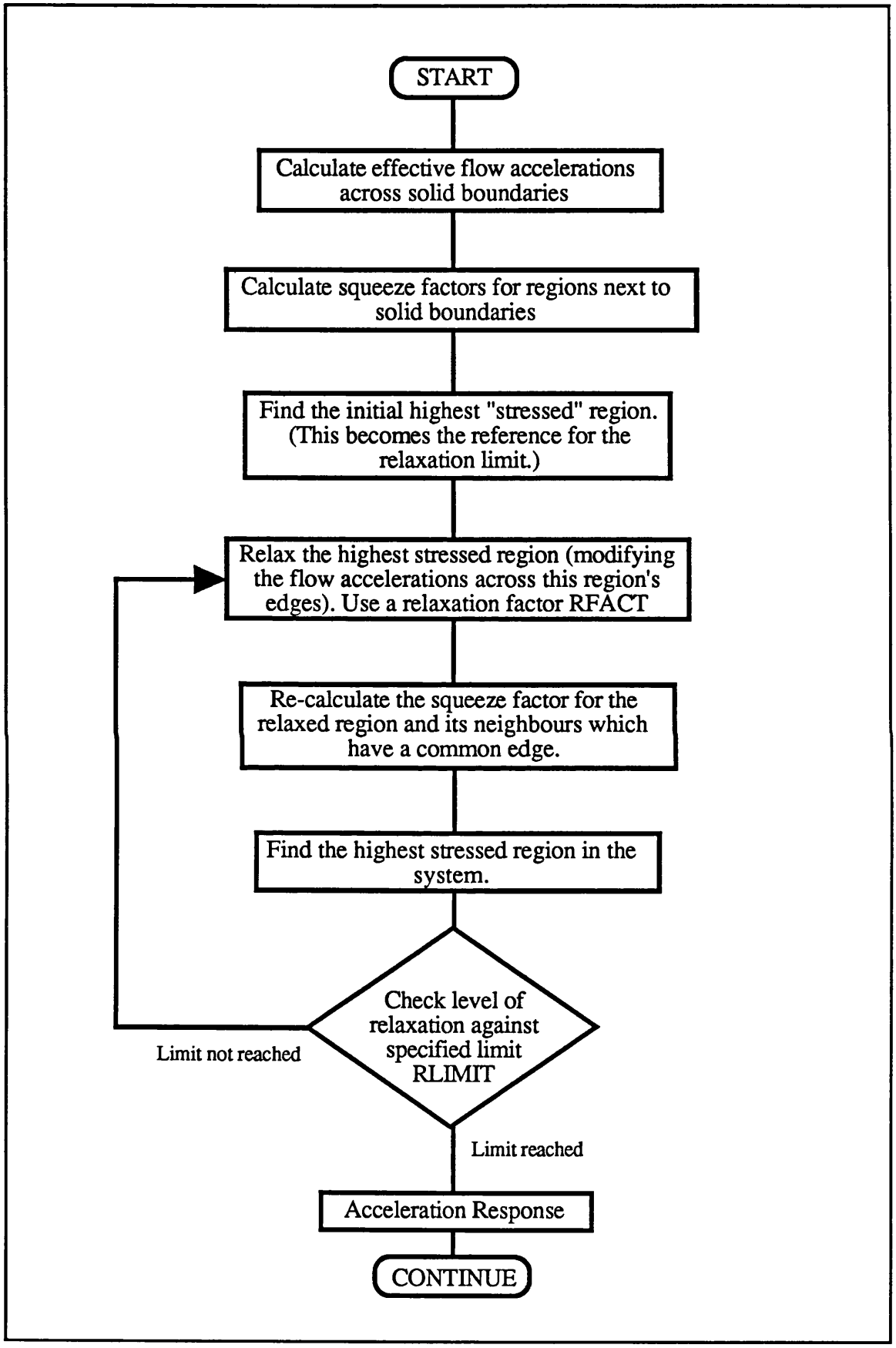

Figure 4.9 Flowchart of the Relaxation Technique for Relaxing Boundary Acceleration Disturbances

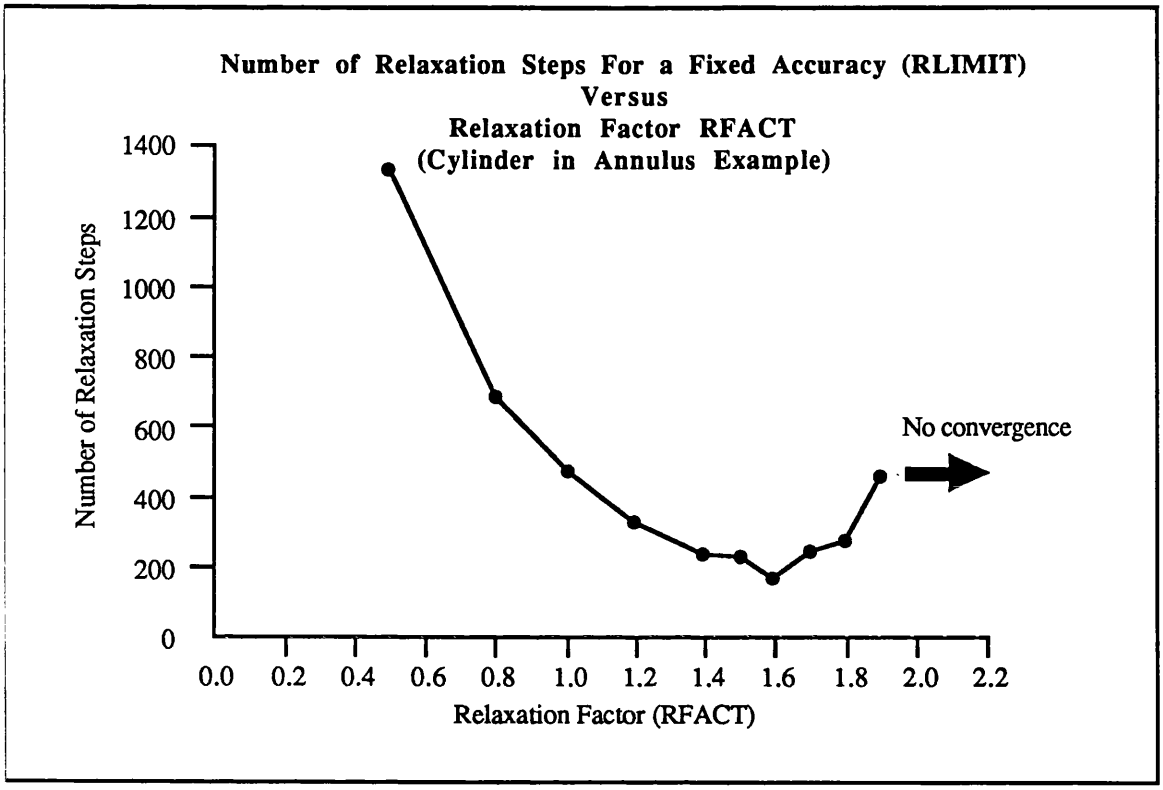

Figure 4.10 Speed of Convergence with Variation in Relaxation (or Exhaust) Factor

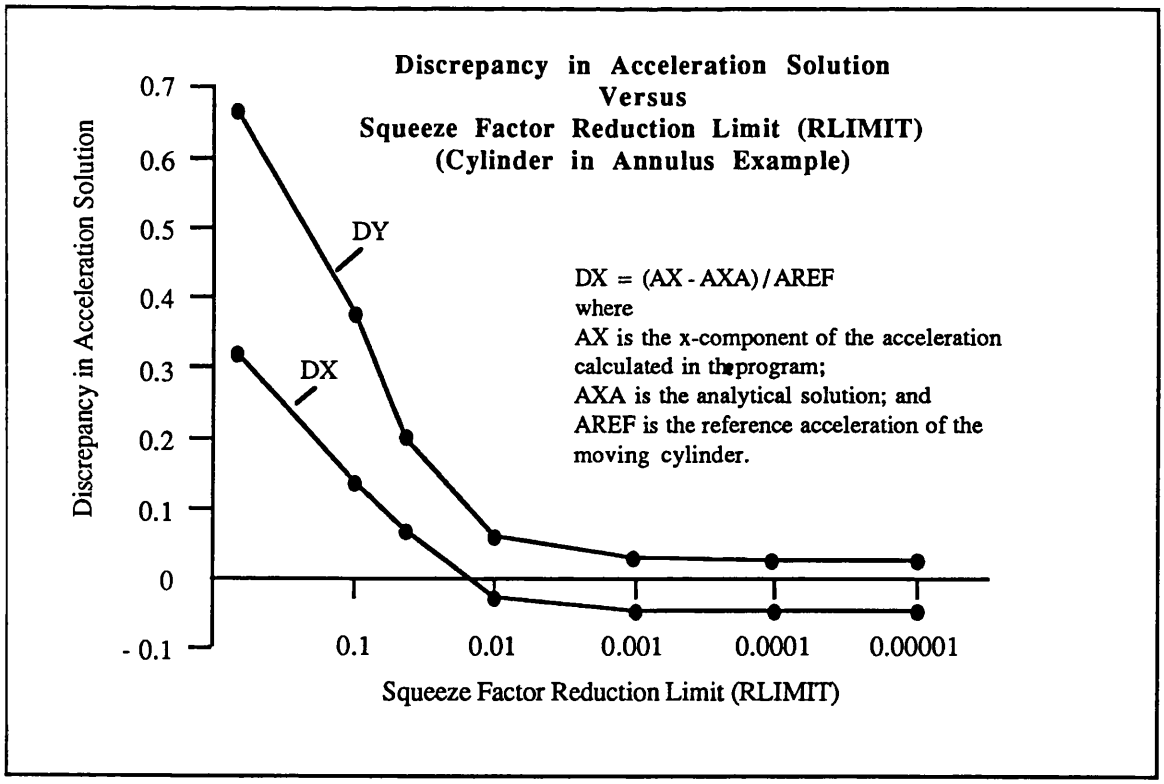

Figure 4.11 Solution Convergence with Variation in Relaxation Limit

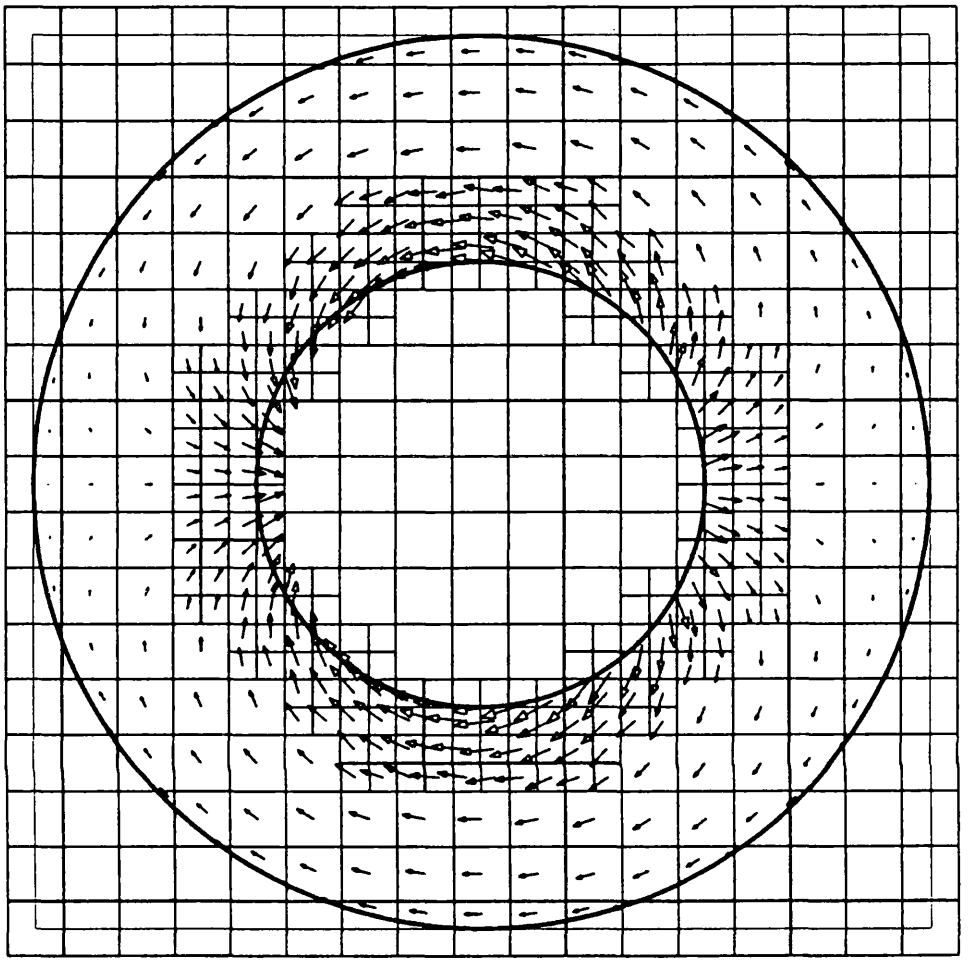

(a) Overall view of results.

Figure 4.12 Inviscid Result for a Cylinder Moving Within a Cylindrical Environment

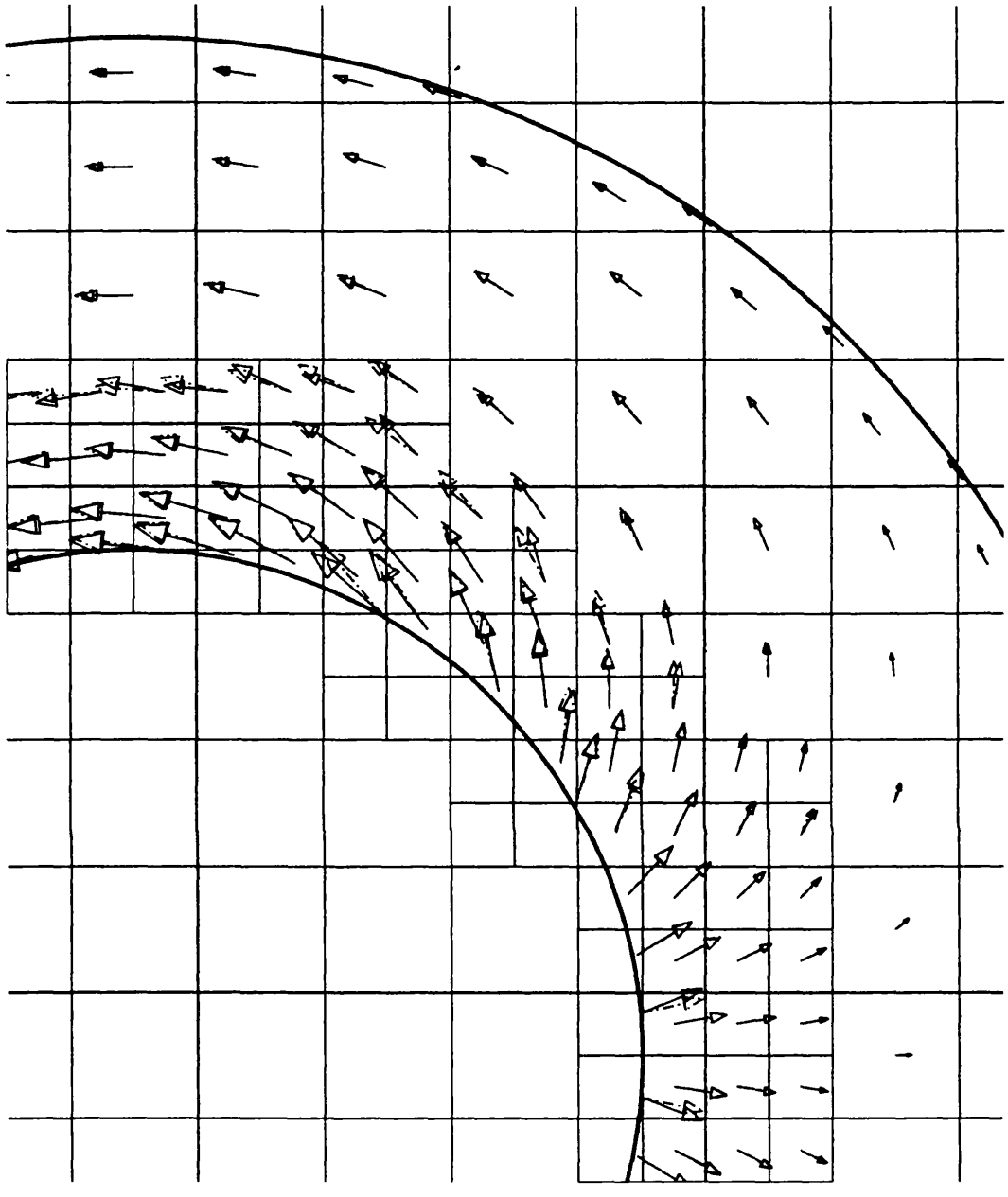

(b) Close-up of results showing analytical solution as dashed vectors.

Figure 4.12 (Continued)

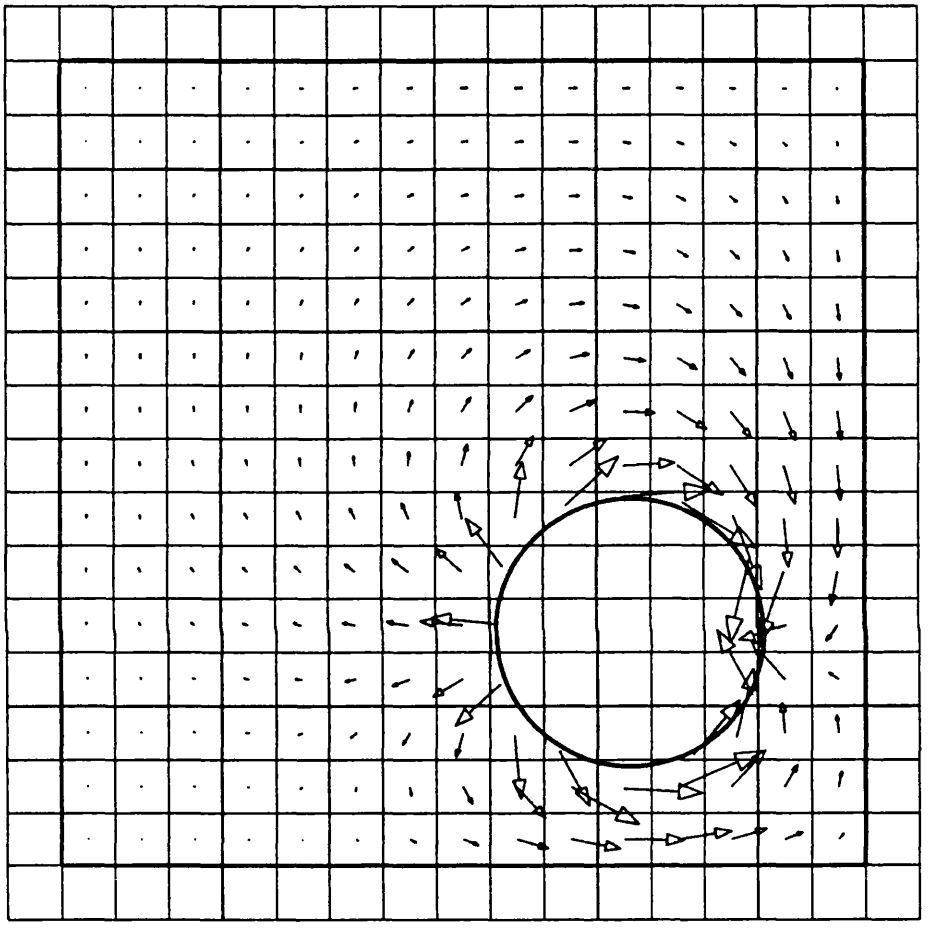

Figure 4.13 Inviscid Result for a Cylinder Moving Close to a Corner

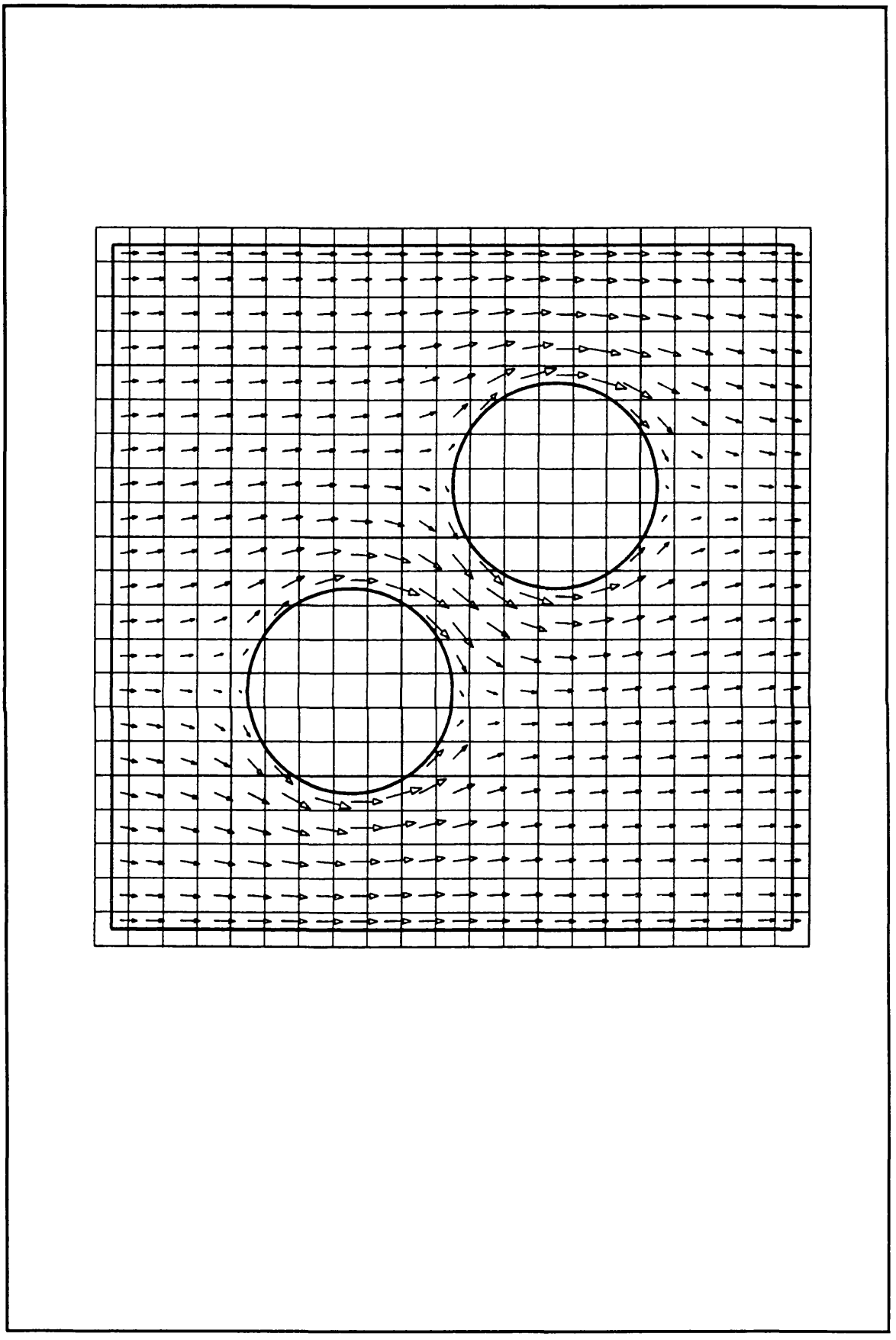

Figure 4.14 Inviscid Result for Constrained Flow Past Two Cylinders

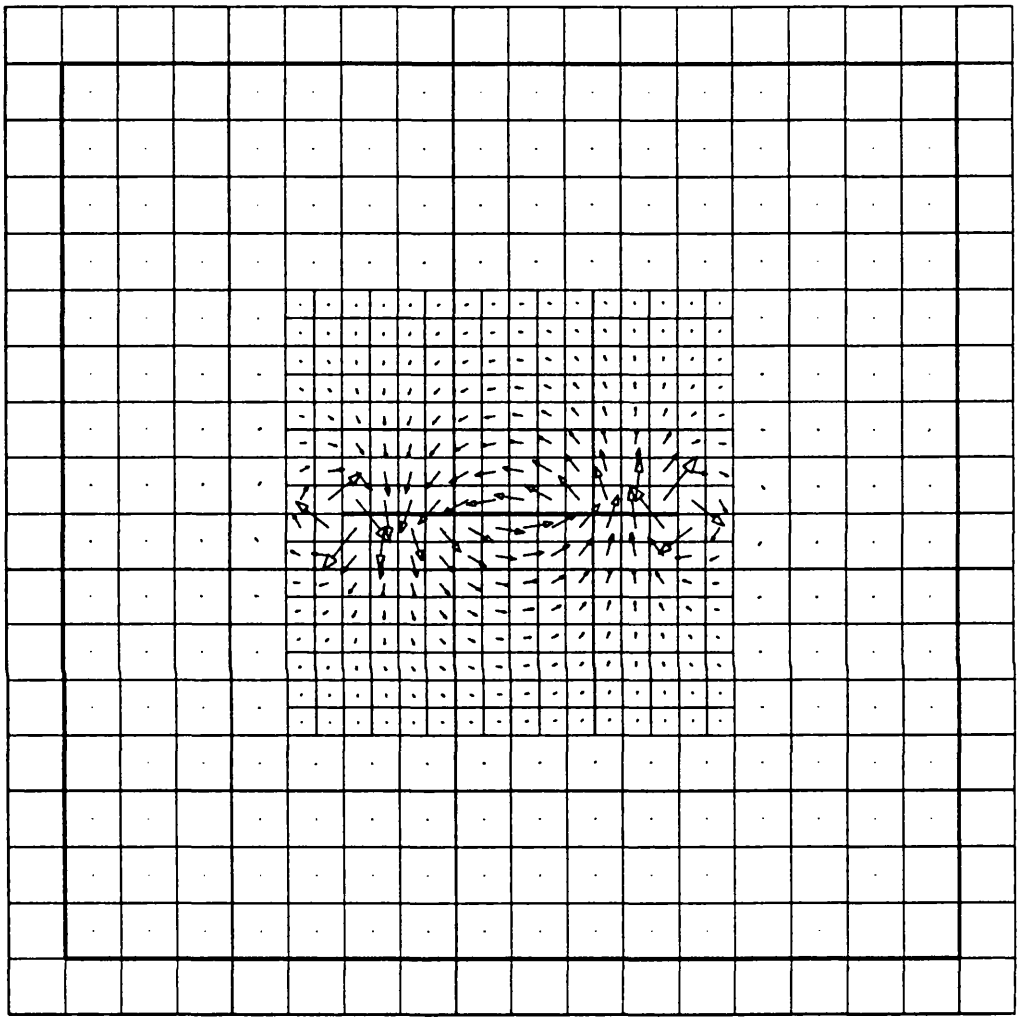

Figure 4.15 Inviscid Result for a Plate Rotating about its Centre

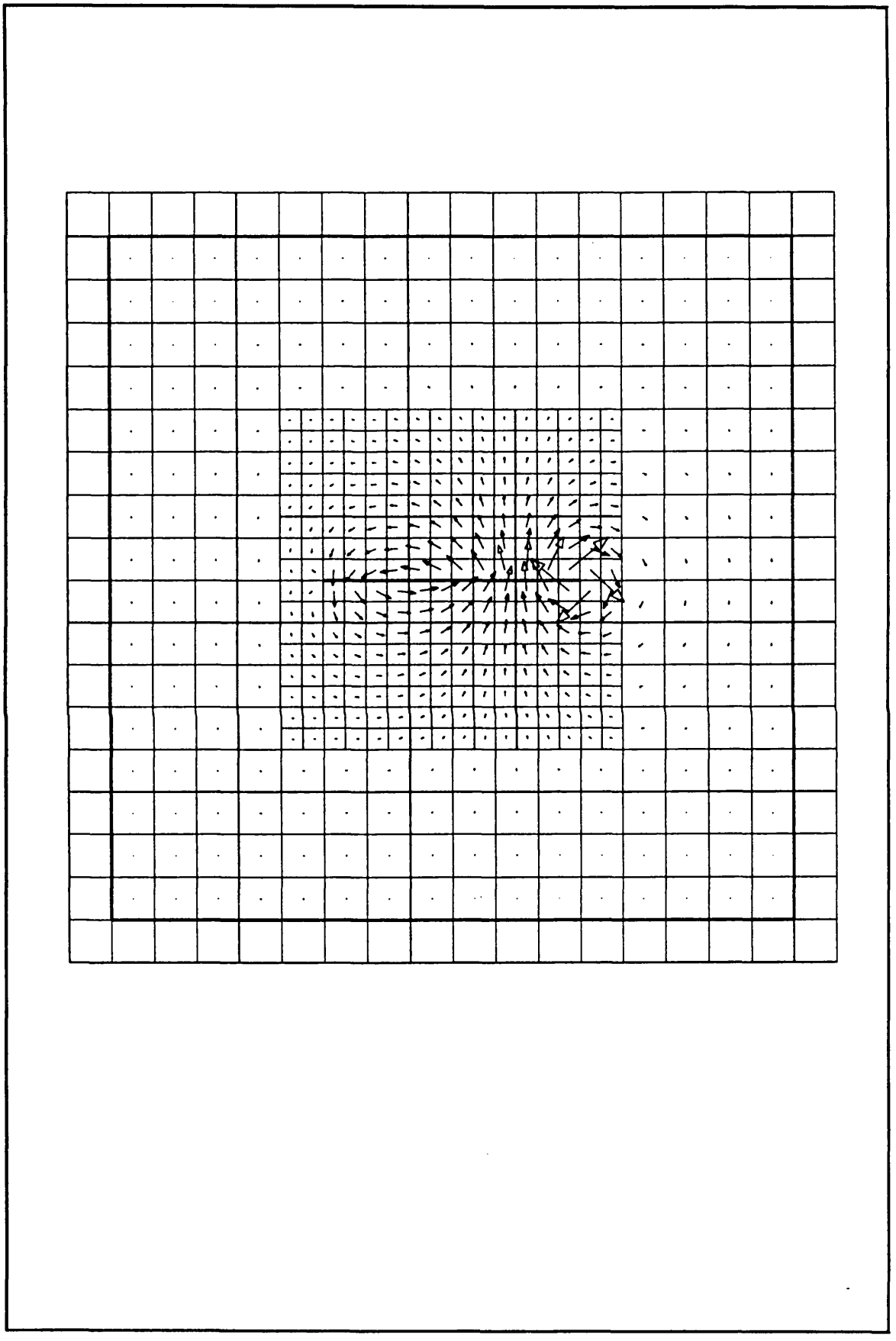

Figure 4.16 Inviscid Result for a Plate Translating and Rotating

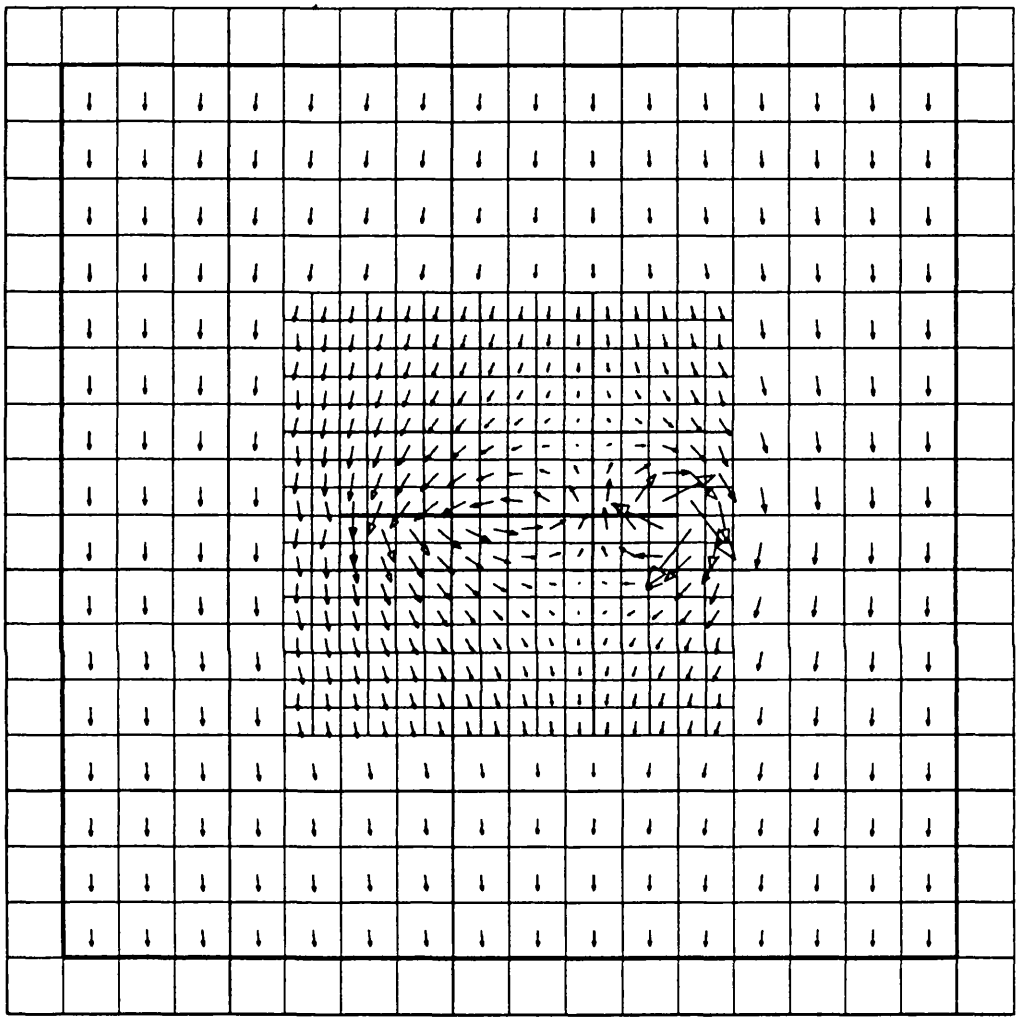

Figure 4.17 Inviscid Result for a Plate Accelerating in Rotation about its Centre in an Accelerating Stream

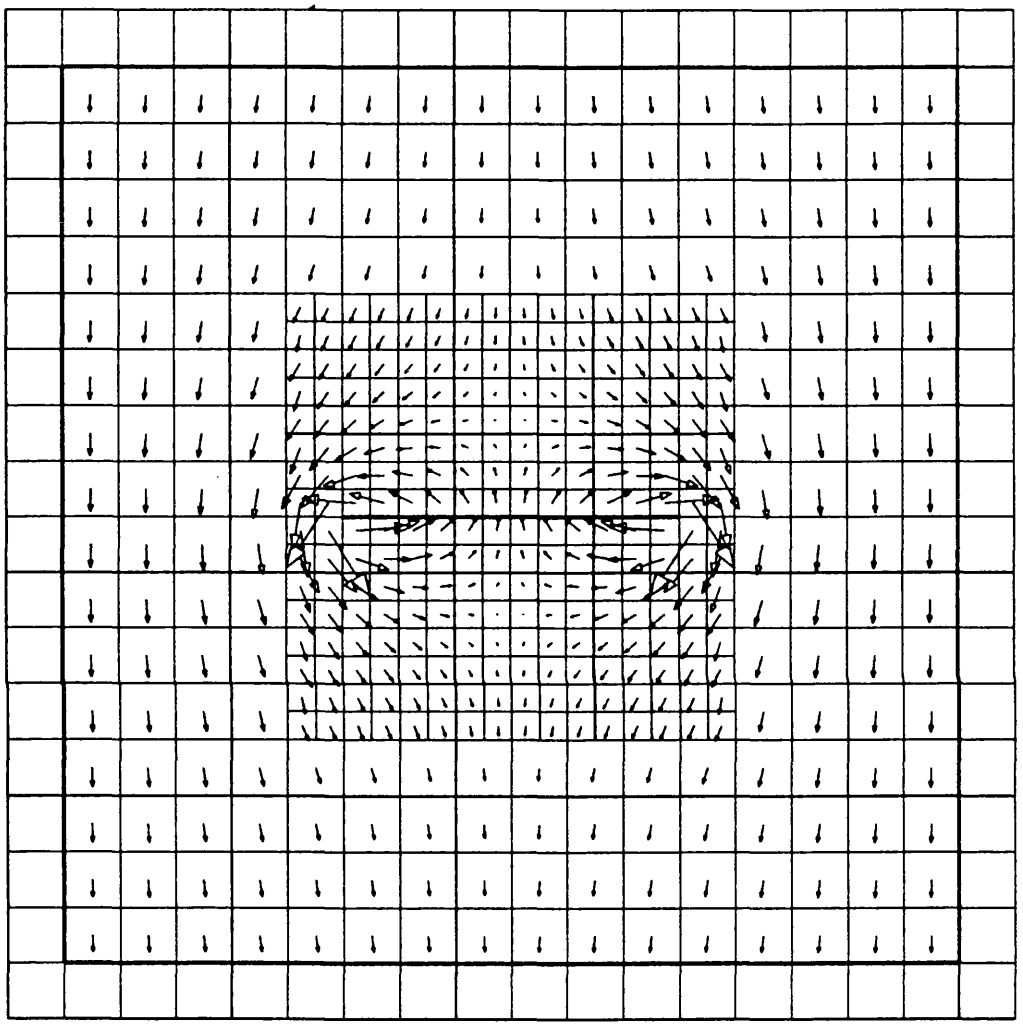

Figure 4.18 Inviscid Result for a Plate Accelerating Towards an Accelerating Stream

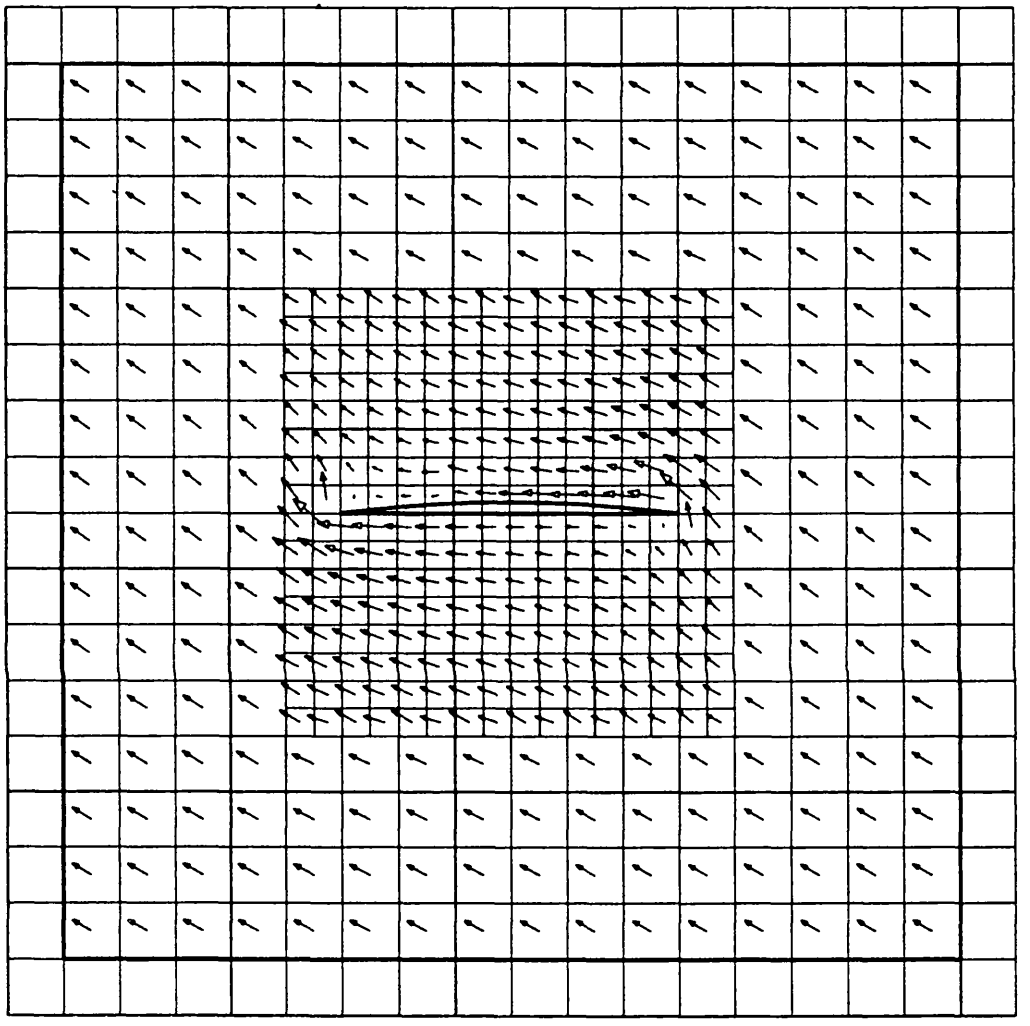

Figure 4.19 Inviscid Result for Flow Over a Hydrofoil Section at an Angle of Incidence

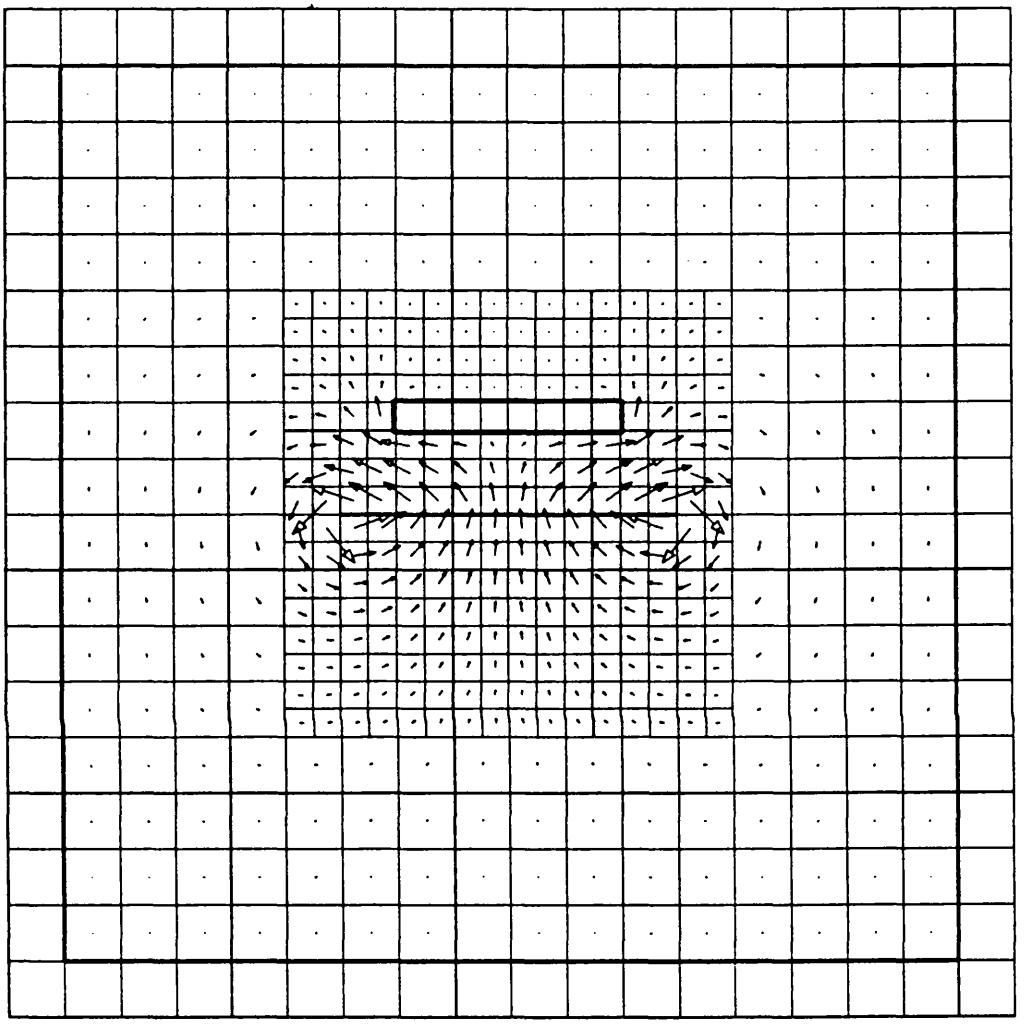

Figure 4.20 Inviscid Result for a Flat Plate Moving Towards a Stationary Wall

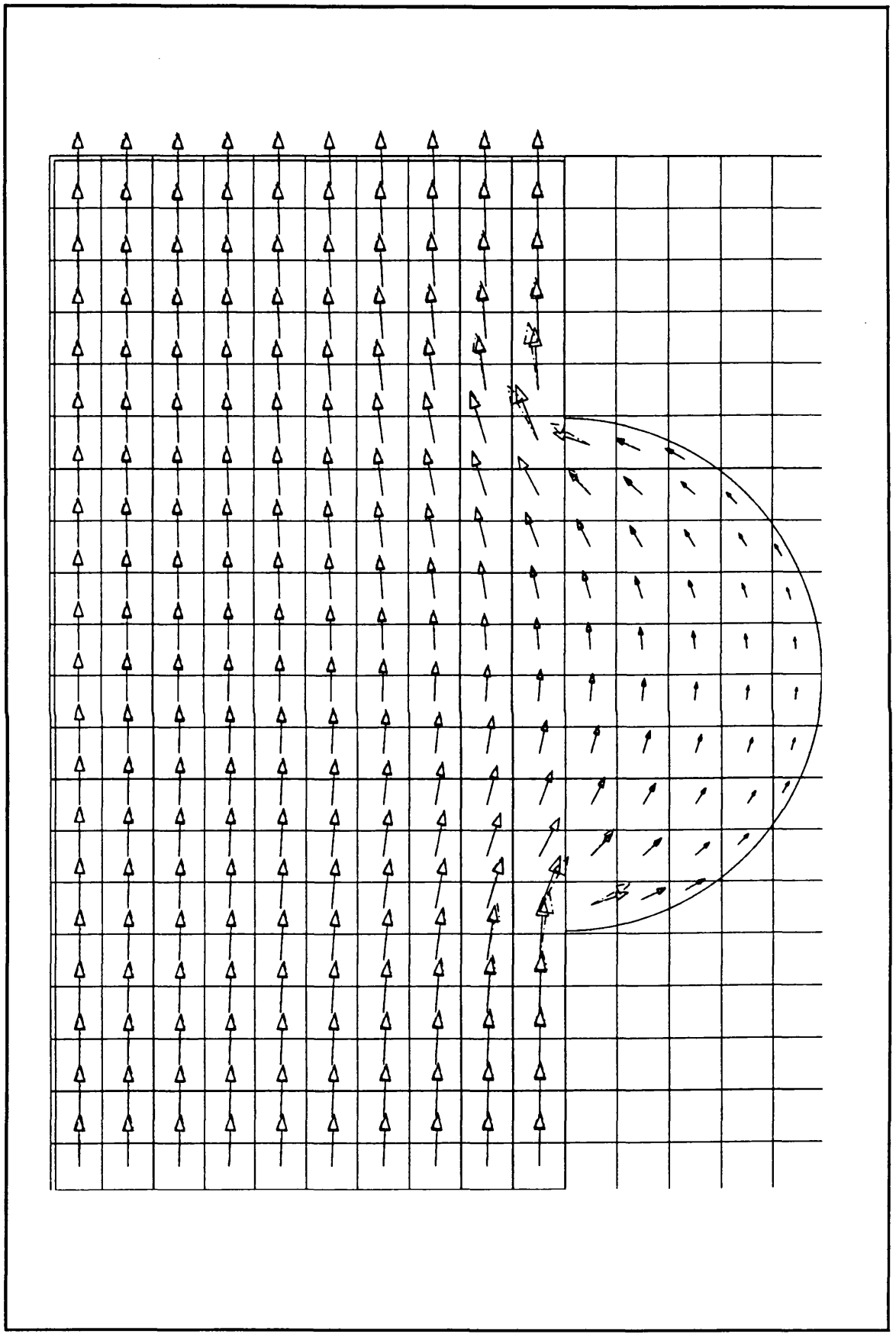

Figure 4.21 Inviscid Result for Flow Over a Semi-Circular Ditch

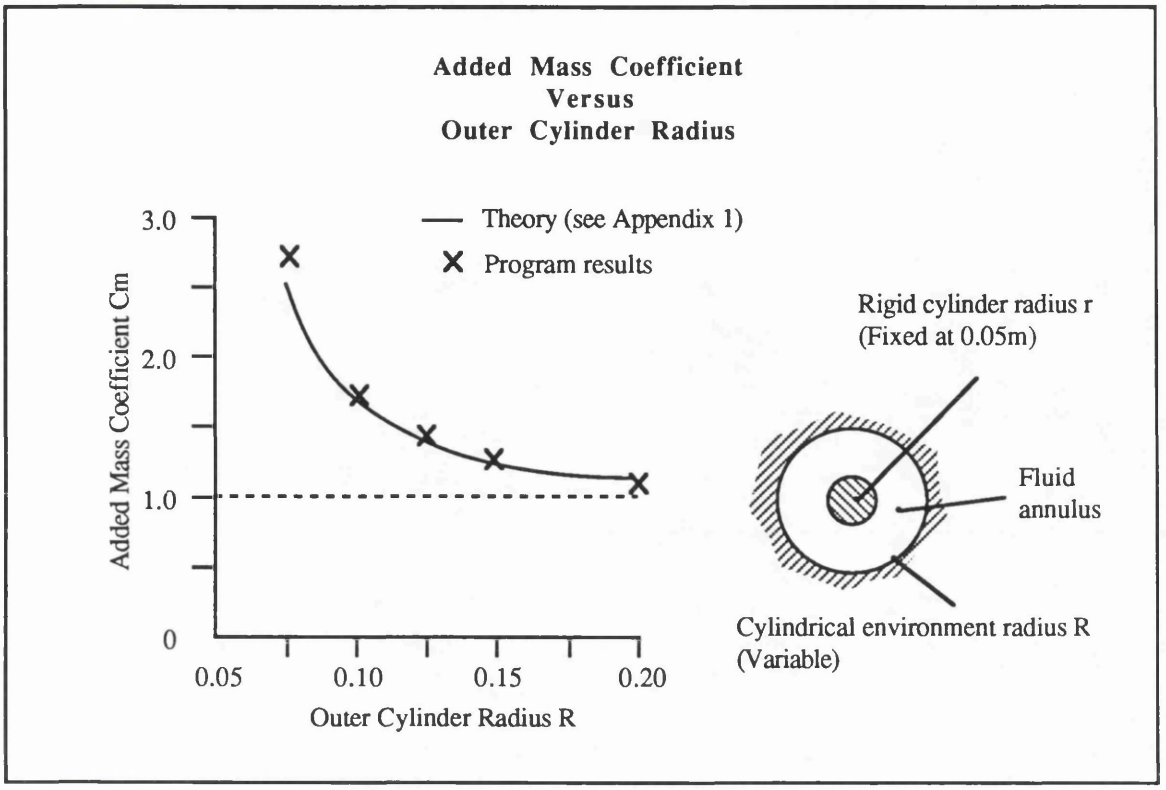

Figure 4.22 Added Mass Results for a Circular Cylinder Moving Within a Circular Annulus of Variable Size

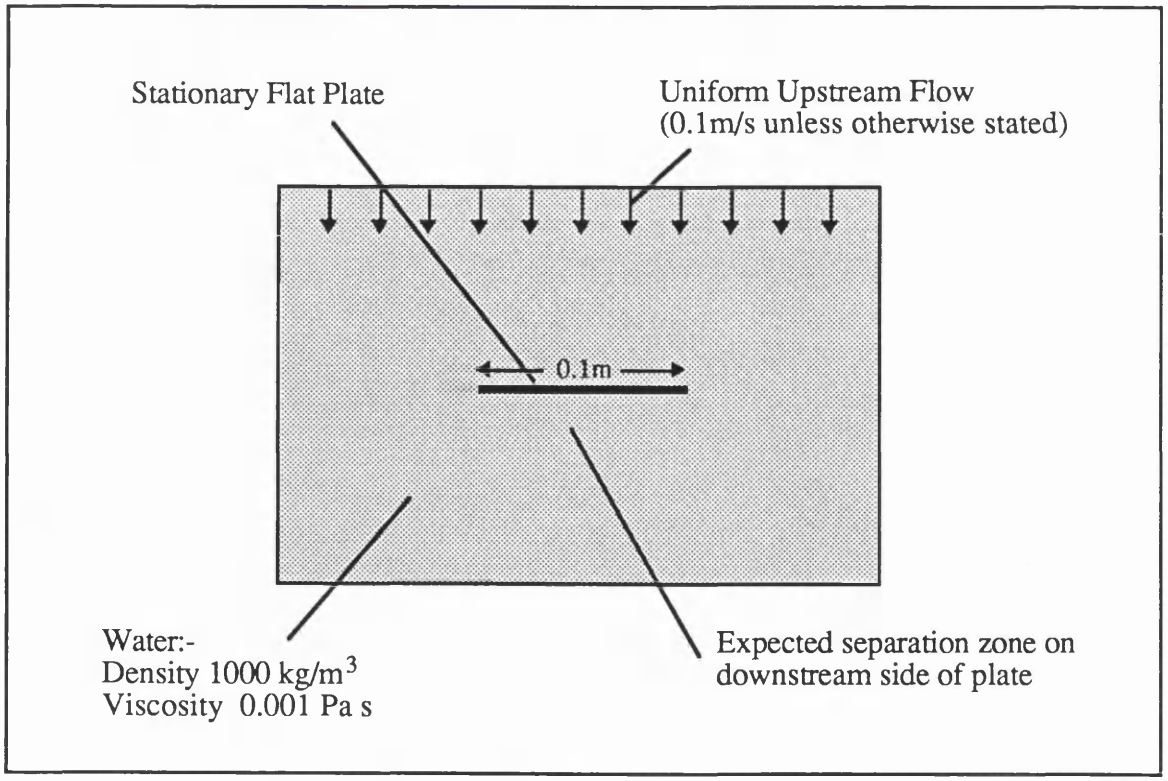

Figure 4.23 Impulsive Flow Onto a Flat Plate

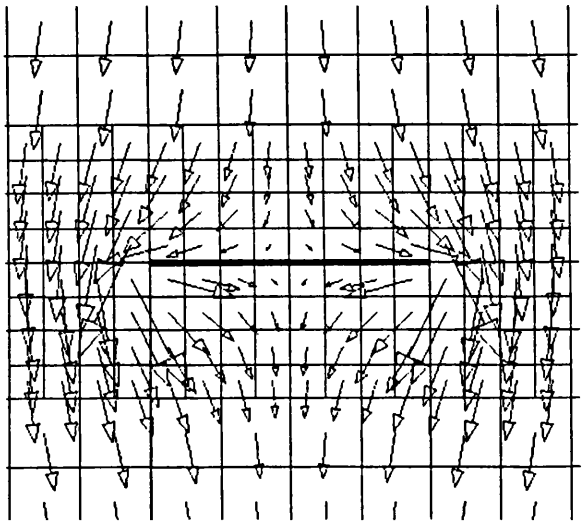

(a) Nature of the inviscid flow from an impulsive start.

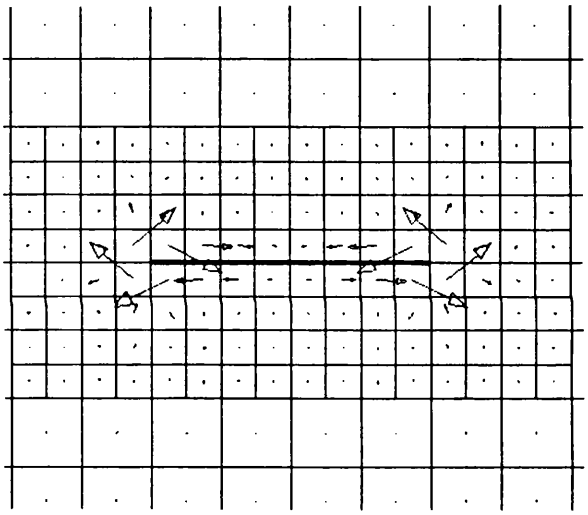

(b) Nature of the initial viscous acceleration.

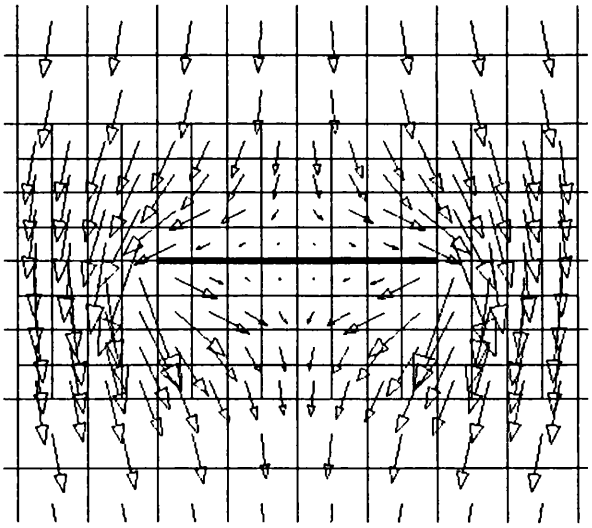

(c) Nature of the modified flow pattern.

Figure 4.24 Viscous Modelling Scheme 1

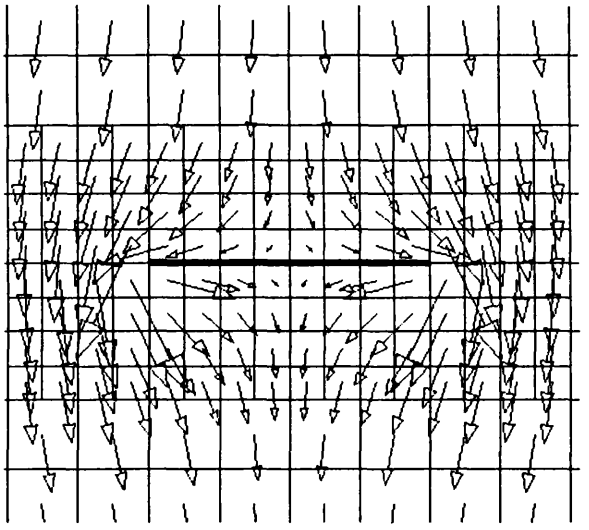

(a) Nature of the inviscid flow from an impulsive start.

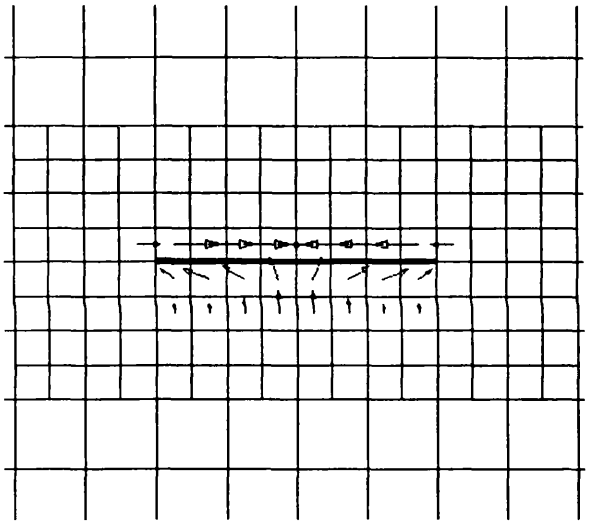

(b) Nature of the initial viscous acceleration.

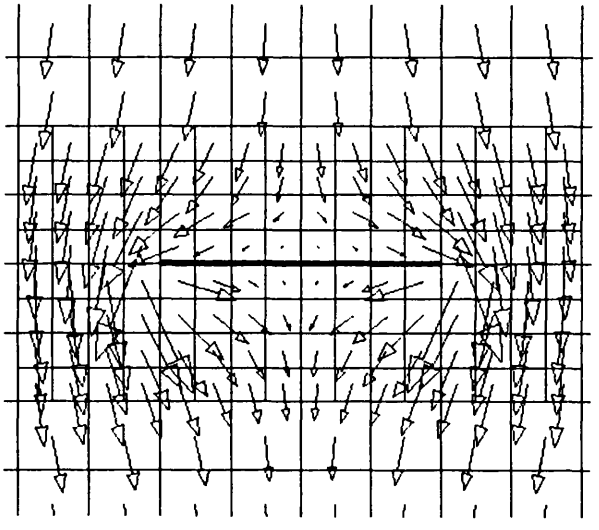

(c) Nature of the modified flow pattern.

Figure 4.25 Viscous Modelling Scheme 2

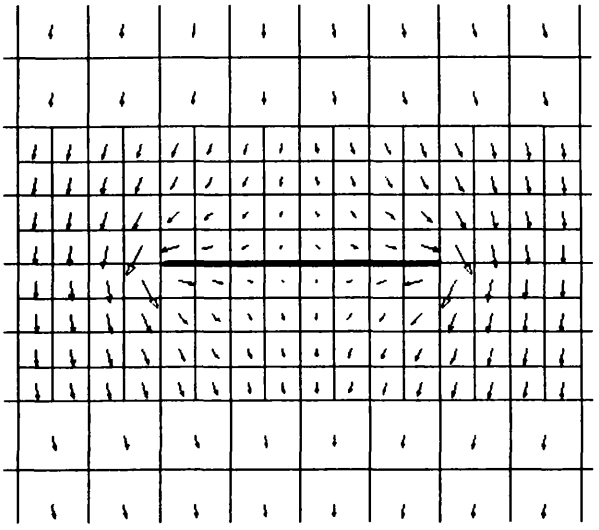

(a) Nature of the inviscid flow from an impulsive start.

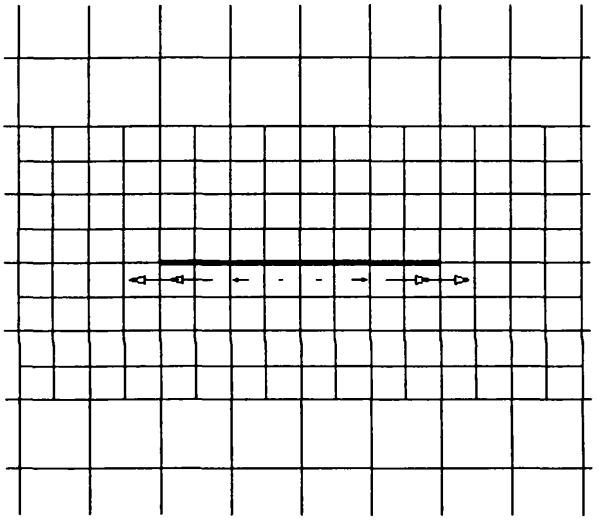

(b) Nature of the initial viscous acceleration.

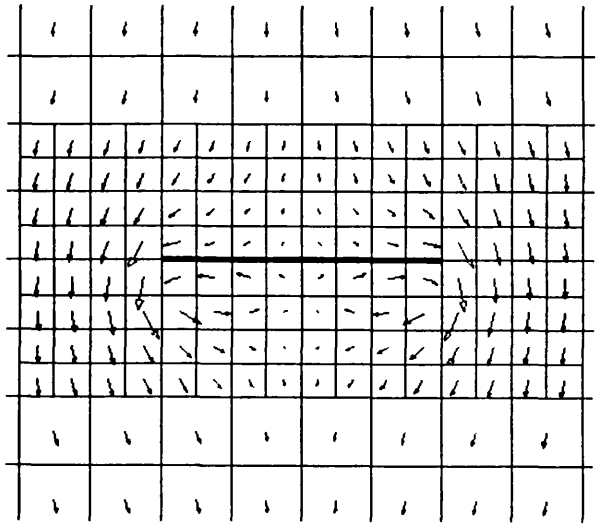

(c) Nature of the modified flow pattern.

Figure 4.26 Viscous Modelling Scheme 3

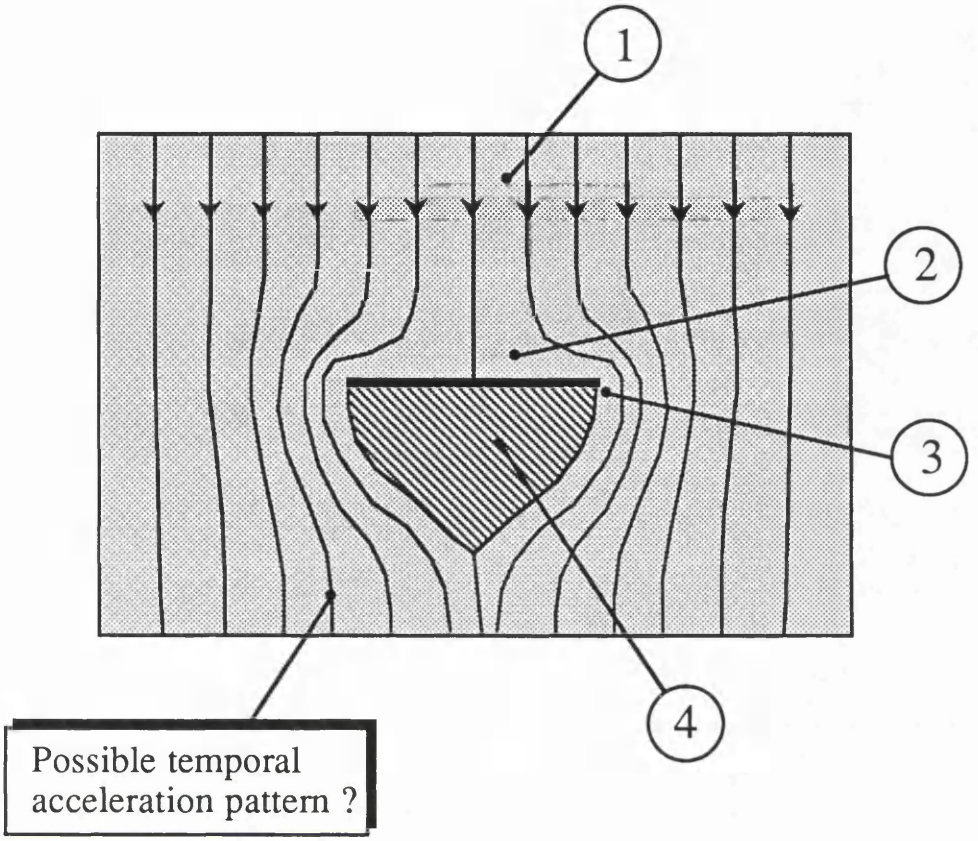

1. Disturbance logically propagates from upstream.

2. Here the developing flow has no choice of where to go. It finds the plate and must deflect to the side.

3. Here, however, perhaps the flow*has* got a choice. Why should the developing flow tend to go around the back of the plate? Could there be other possibilities (e.g. as shown) where a region of stationary fluid acts like an extension to the body? Once finite velocities are developed the discontinuities of pressure on the separation streamline may be such as to modify the pattern of flow. Nevertheless, could this be a valid temporal acceleration pattern?

4. Proposed inviscid separation zone. Stationary fluid, not accelerating with the rest of the fluid.

Figure 4.27 Separation of Inviscid Flow ?

The small velocities set up initially in a developing flow will reflect an inviscid pattern.

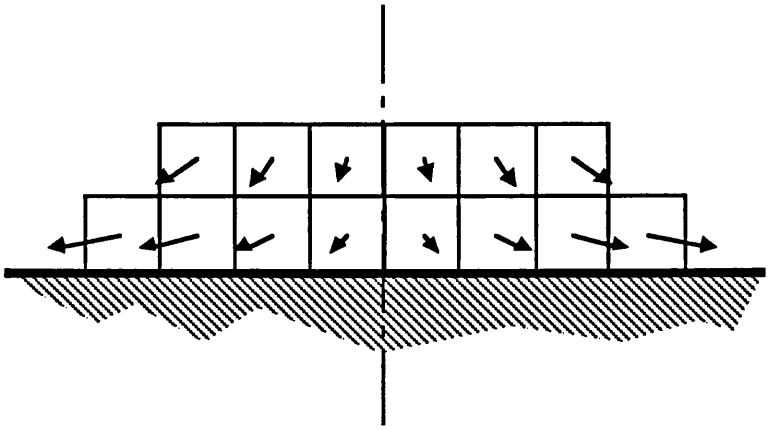

As the velocities become finite shearing mechanisms come into play. In Viscous Scheme 5 the no-slip condition at the wall was assumed to "trip" the fluid in the adjacent boundary regions. An influence on the flow was therefore modelled which tried to effect a block rotation of the fluid in each boundary region as shown below. The magnitude of this rotation tendency was called ROTATION in the computer program.

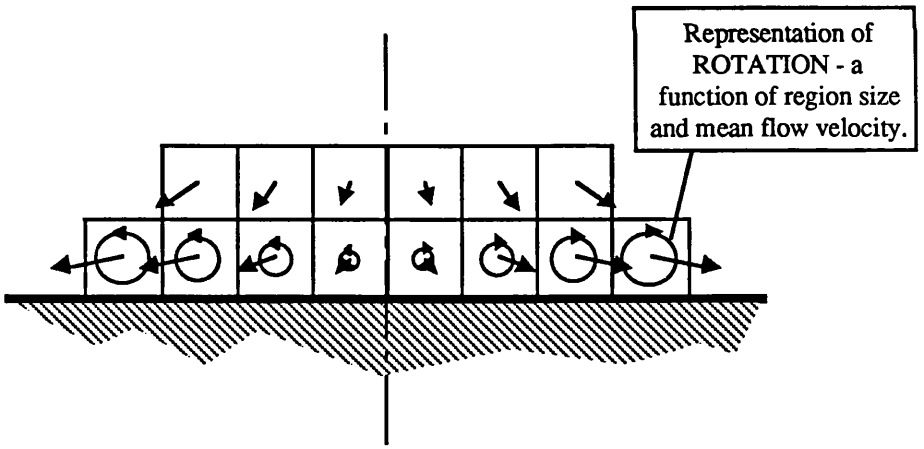

ROTATION described the shear influence generated in boundary regions. This shear effect would diffuse and convect in the system. Changes in ROTATION within the fluid would be associated with the component of the temporal acceleration of the fluid due to the action of viscosity and would lead to the viscous distortion of the flow.

Figure 4.28 Tripping Action of the Wall Generating ROTATION

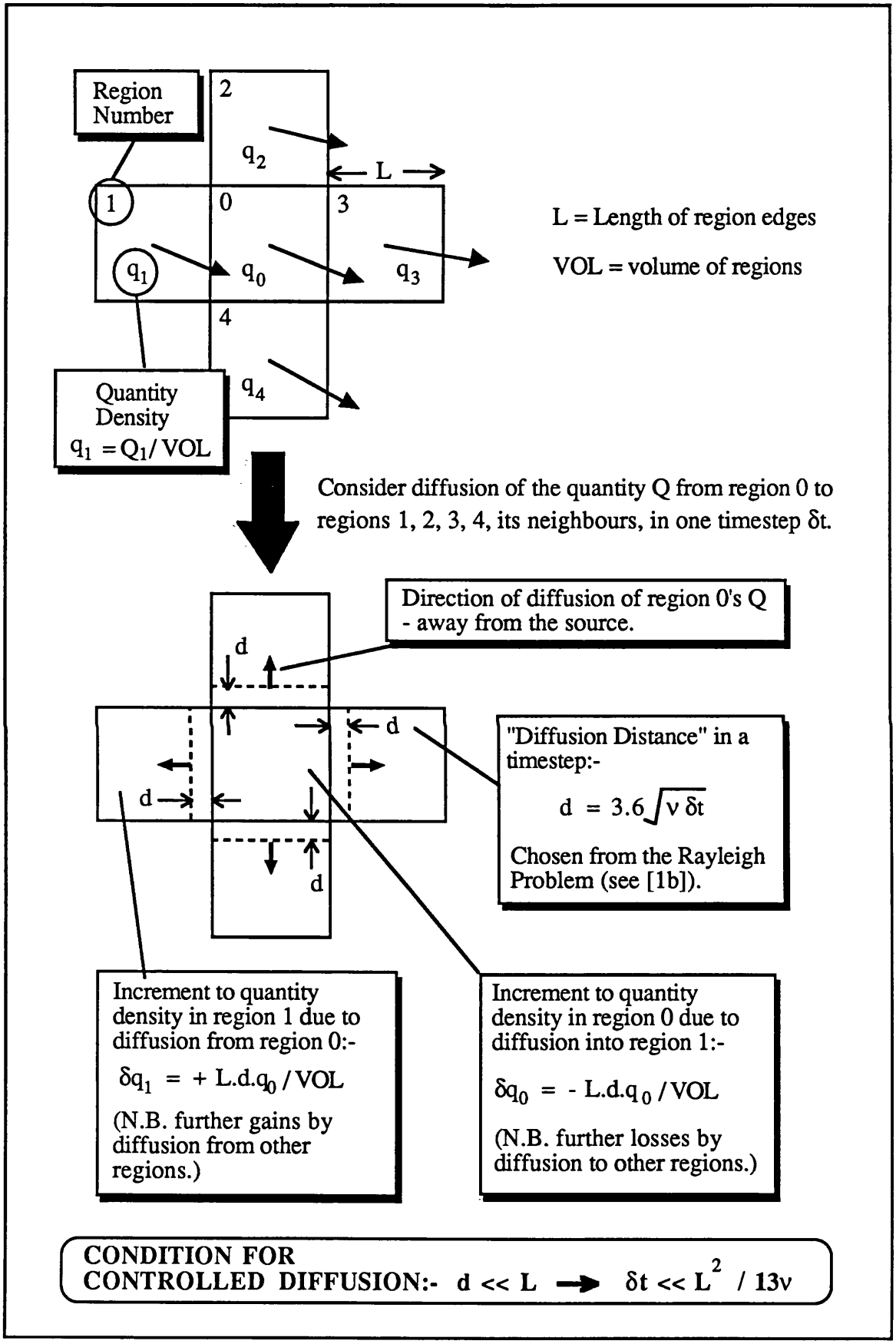

Figure 4.29 Diffusion of a Fluid-Bound Quantity Q

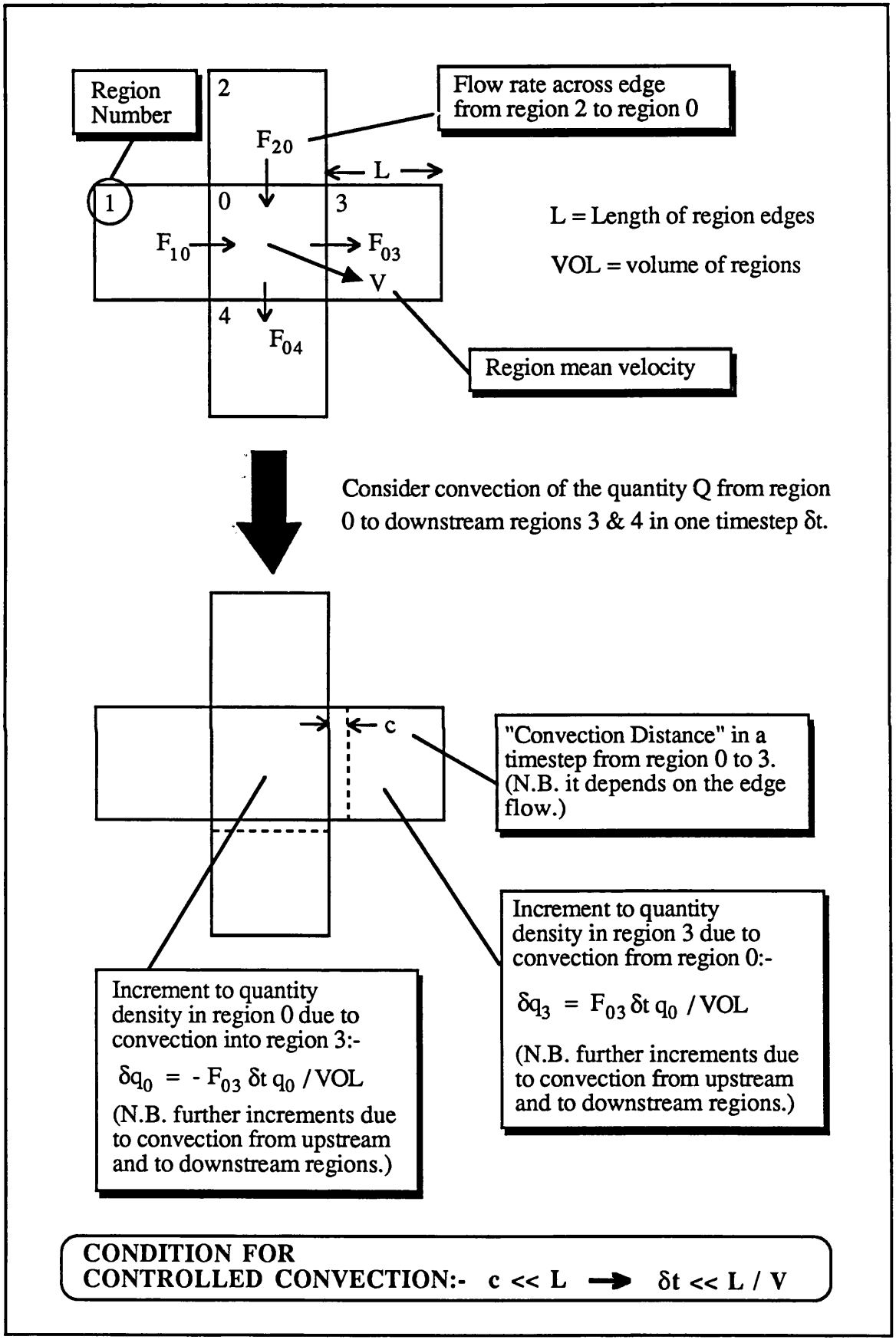

Figure 4.30 Convection of a Fluid-Bound Quantity Q

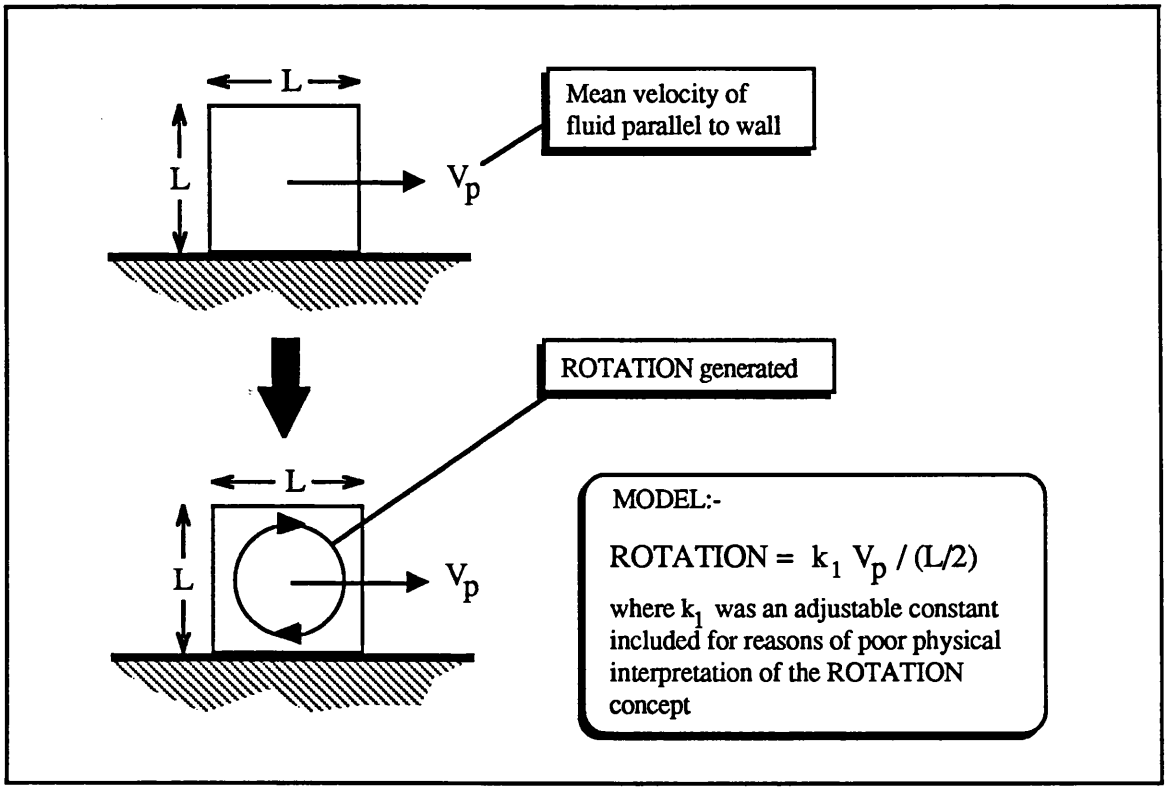

Figure 4.31 Generating ROTATION

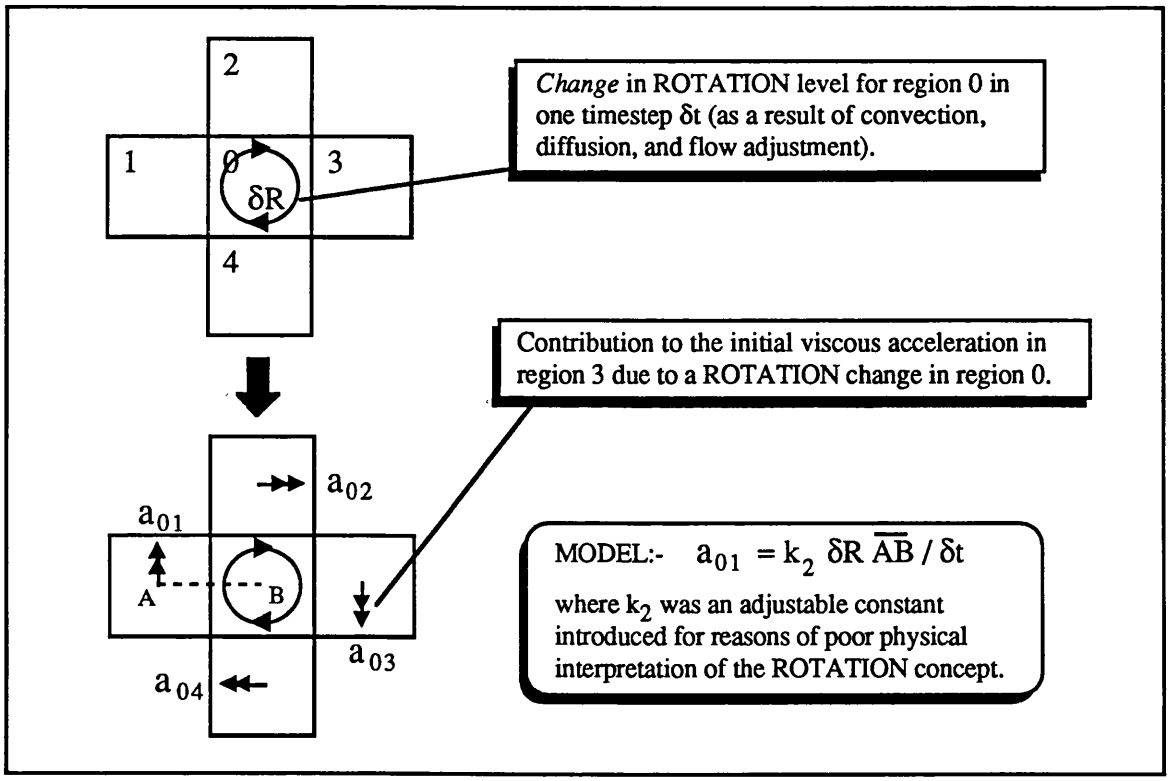

Figure 4.32 The Tended Effects of ROTATION on the flow

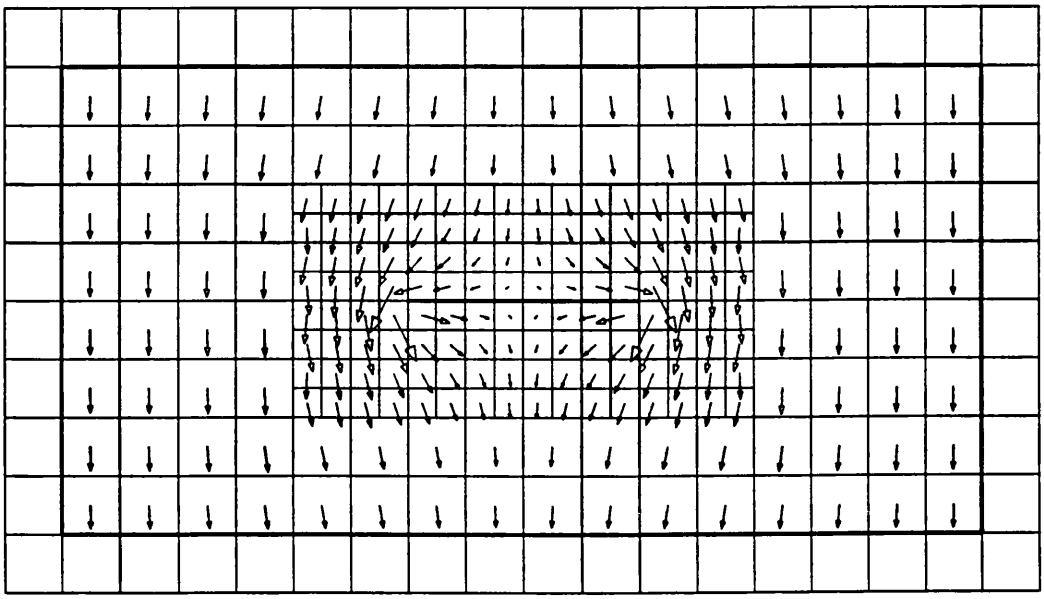

MODELLING PARAMETERS:-

Upstream speed 0.01 m/s
Timestep 0.1 s
Reynolds Number 1000

(a) Impulsive motion start.
(Scale = 1.0 for vectors.)

Figure 4.33 Viscous Modelling Results
(Reynolds Number = 1000)

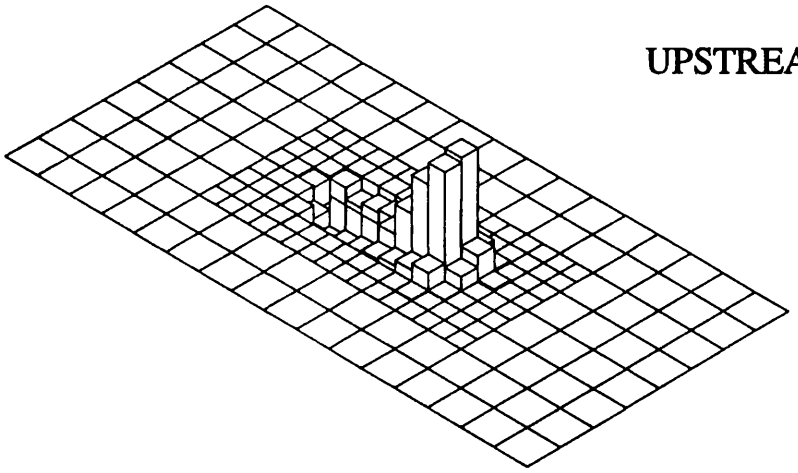

(b) ROTATION spread by convection and diffusion at time t = 0.1 s.

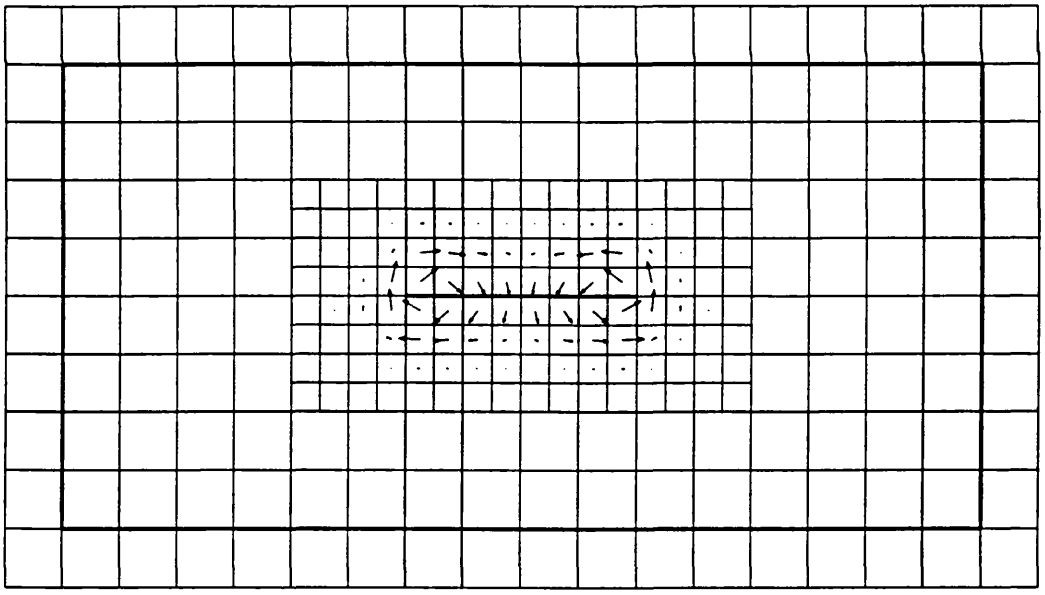

(c) Initial viscous acceleration at t = 0.1 s.
(Scale = 0.1)

Figure 4.33 (Continued)

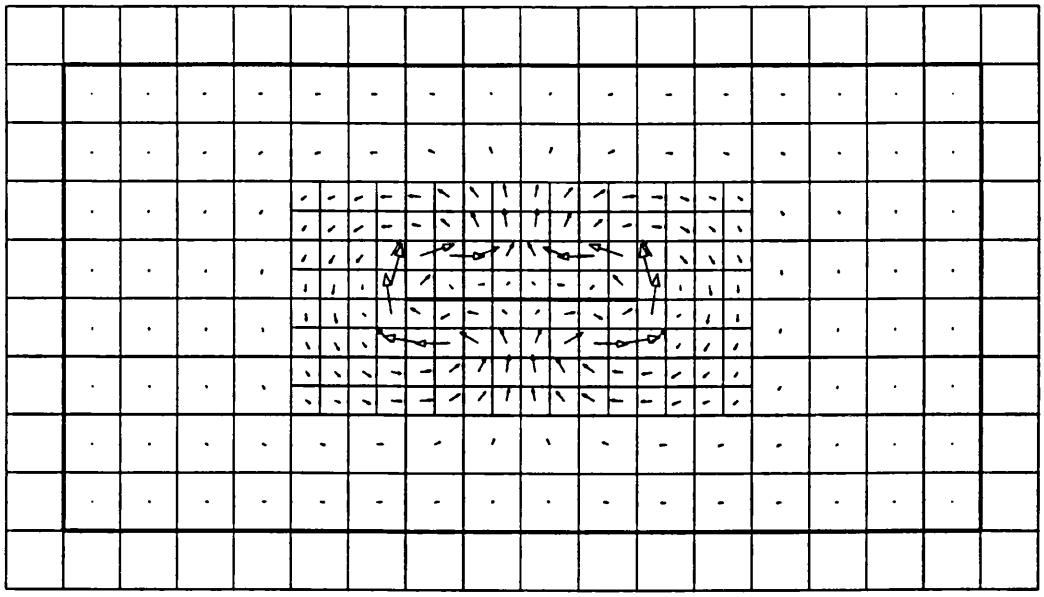

(d) Relaxed viscous acceleration at t = 0.1 s.
(Scale = 0.4)

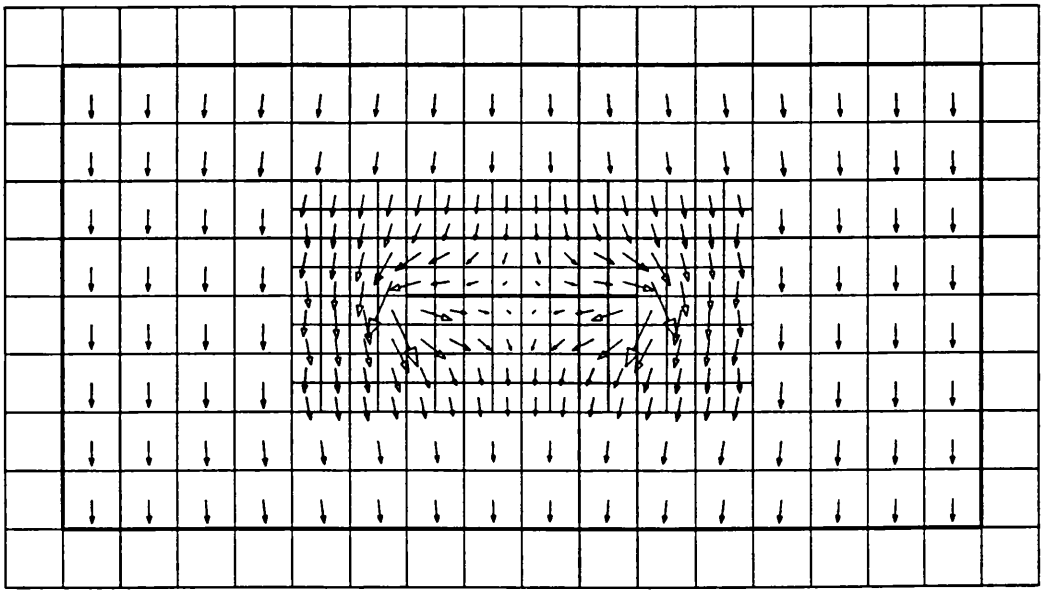

(e) Modified flow velocities at t = 0.1 s.
(Scale = 1.0)

Figure 4.33 (Continued)

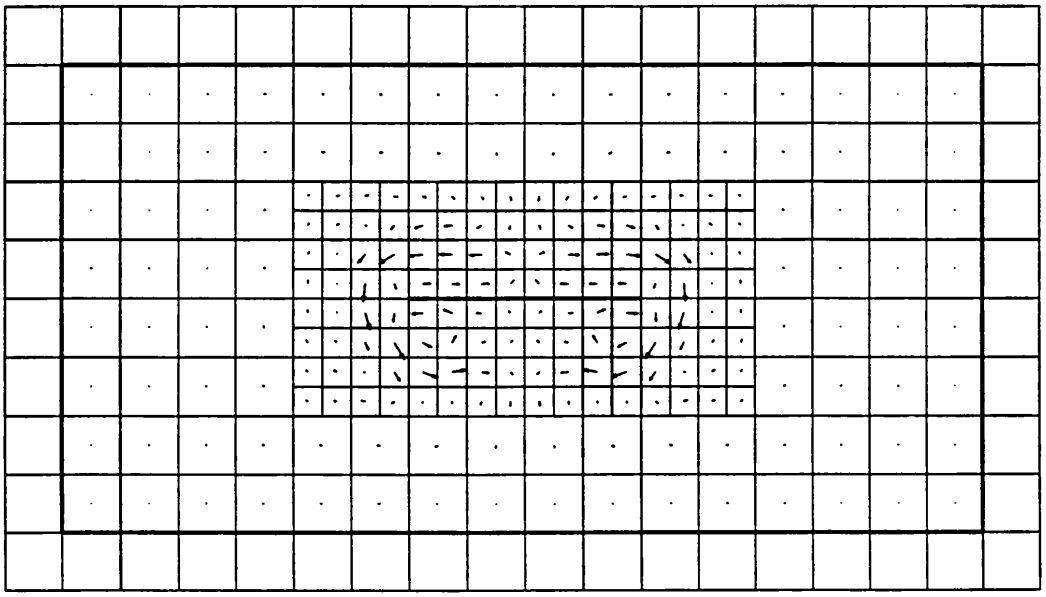

(f) Relaxed viscous acceleration at t = 0.2 s.
(Scale = 1.0)

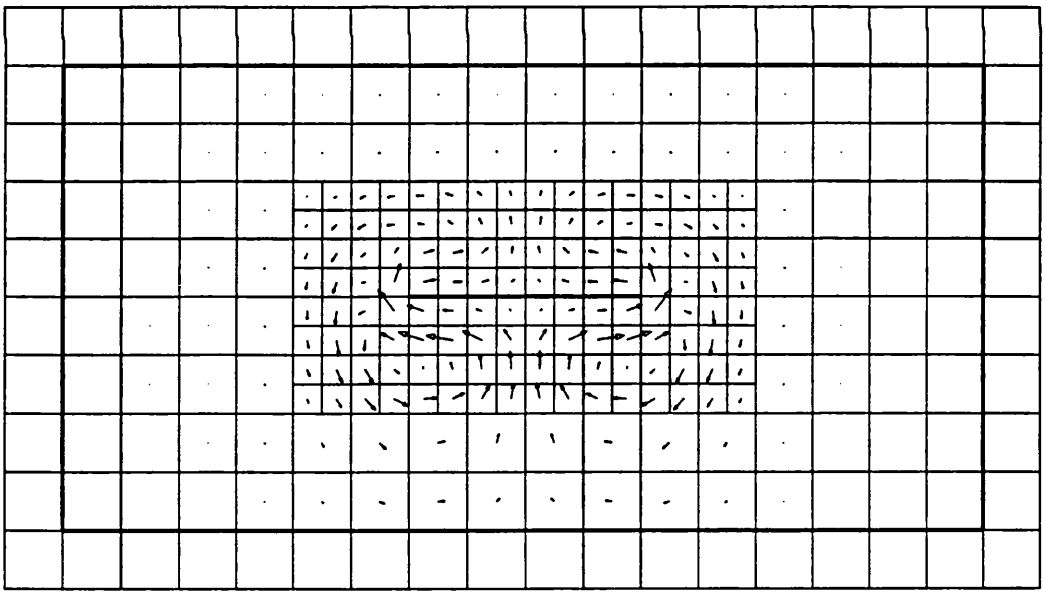

(g) Relaxed viscous acceleration at t = 1.0 s.
(Scale = 5.0)

Figure 4.33 (Continued)

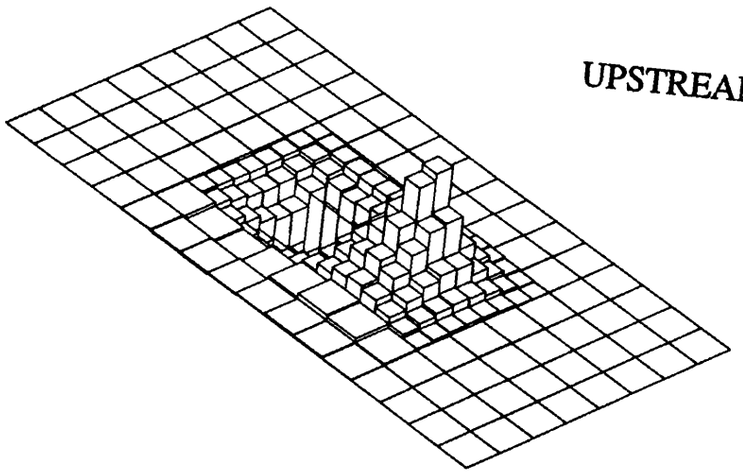

(h) ROTATION spread at t = 2.0 s.

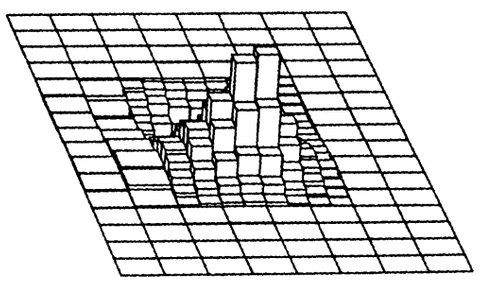

(i) ROTATION spread at t = 2.0 s. (Side view.)

Figure 4.33 (Continued)

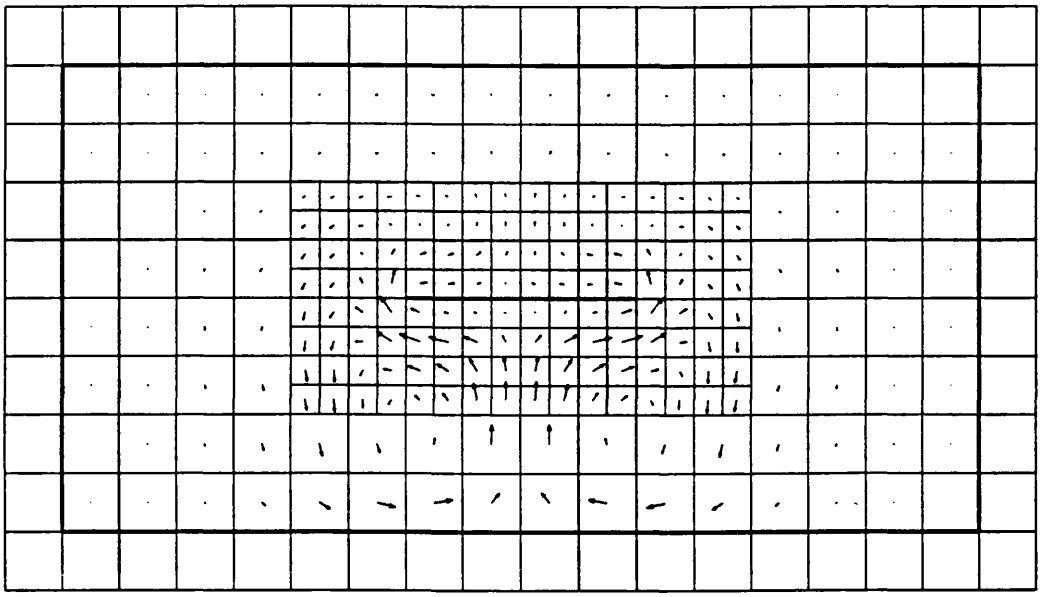

(j) Relaxed viscous acceleration at t = 2.0 s.
(Scale = 10.0)

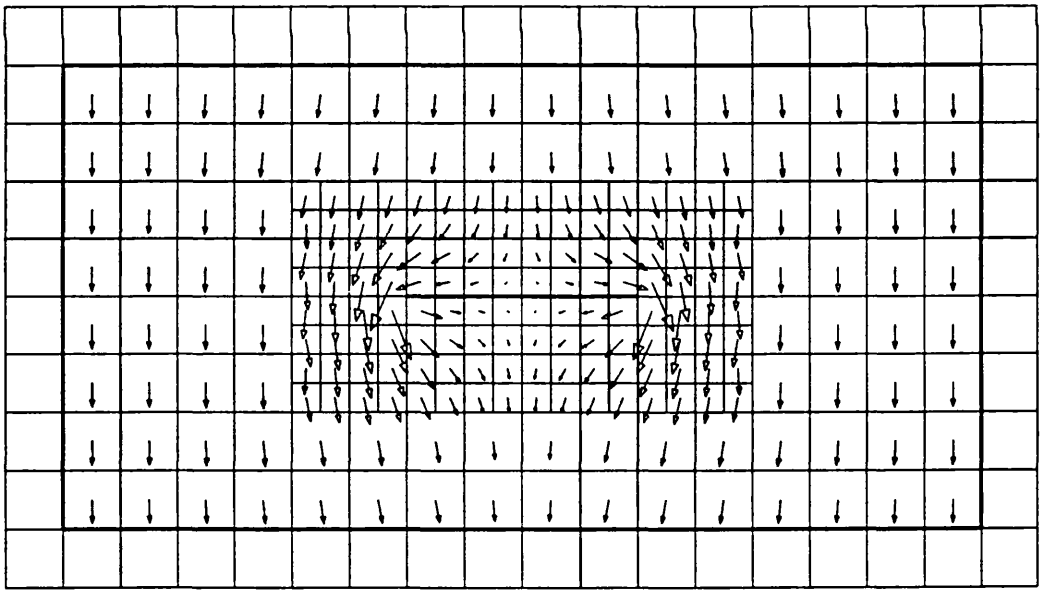

(k) Modified flow velocities at t = 2.0 s.
(Scale = 1.0)

Figure 4.33 (Continued)

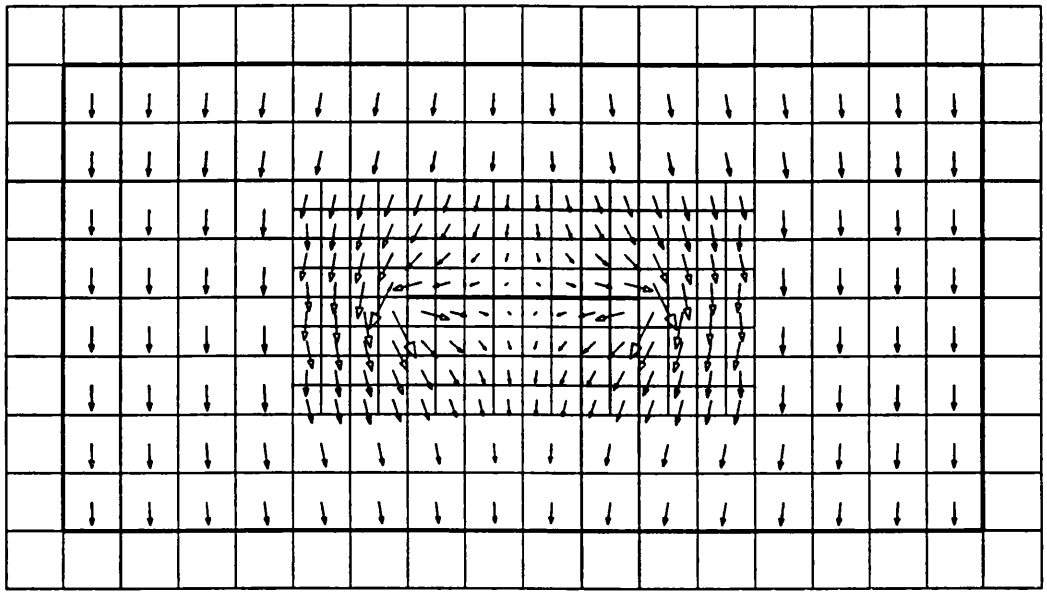

MODELLING PARAMETERS:-

Upstream speed 0.1 m/s
Timestep 0.02 s
Reynolds Number 10000

(a) Impulsive motion start.
(Scale = 0.1 for vectors.)

Figure 4.34 Viscous Modelling Results
(Reynolds Number = 10000)

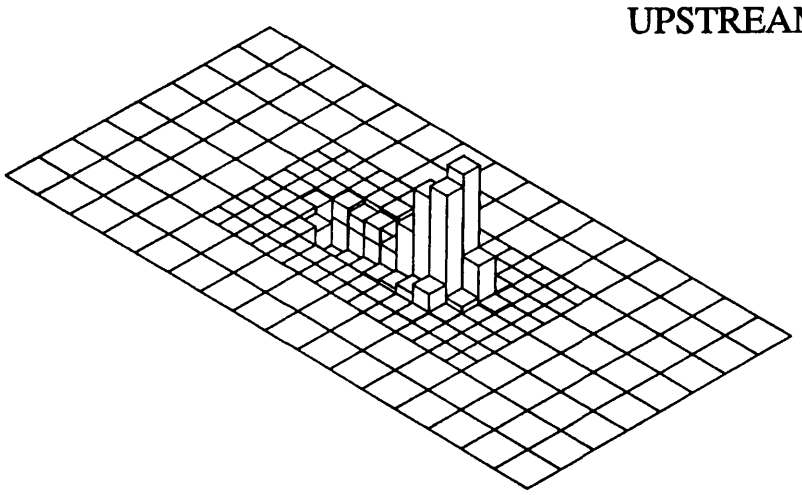

(b) ROTATION spread by convection and diffusion at time t = 0.02 s.

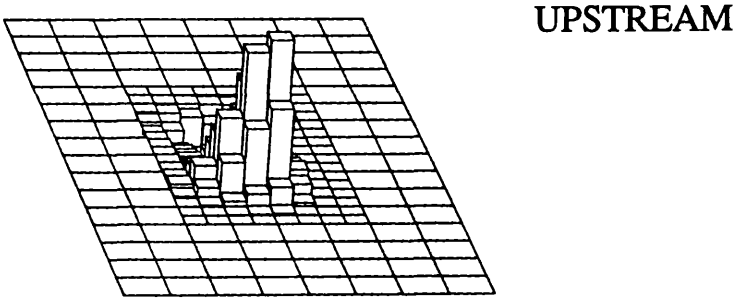

(c) ROTATION spread at time t = 0.1 s.

Figure 4.34 (Continued)

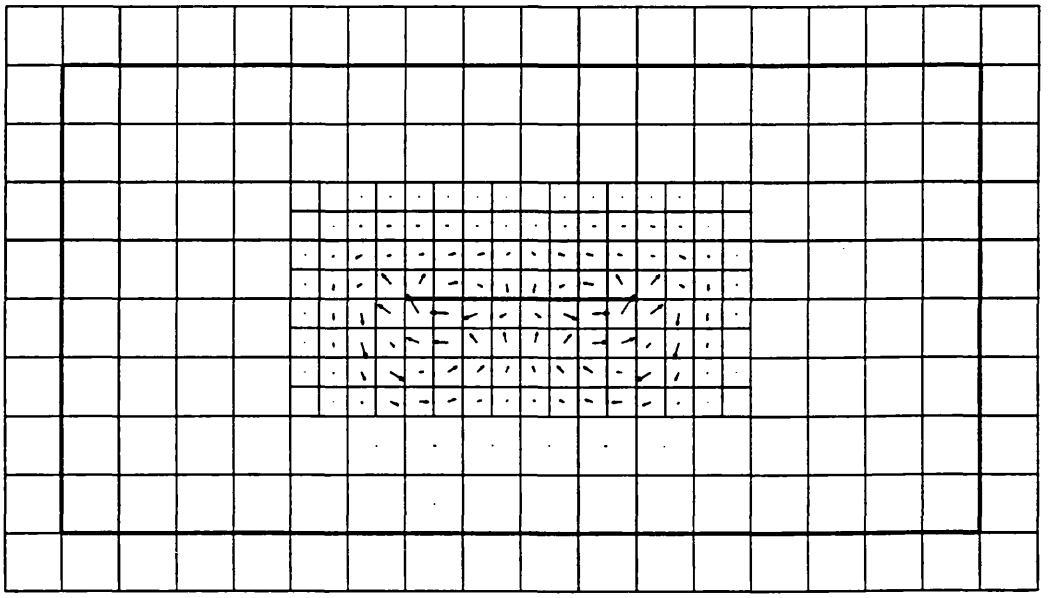

(d) Initial viscous acceleration at t = 0.1 s.
(Scale = 0.02)

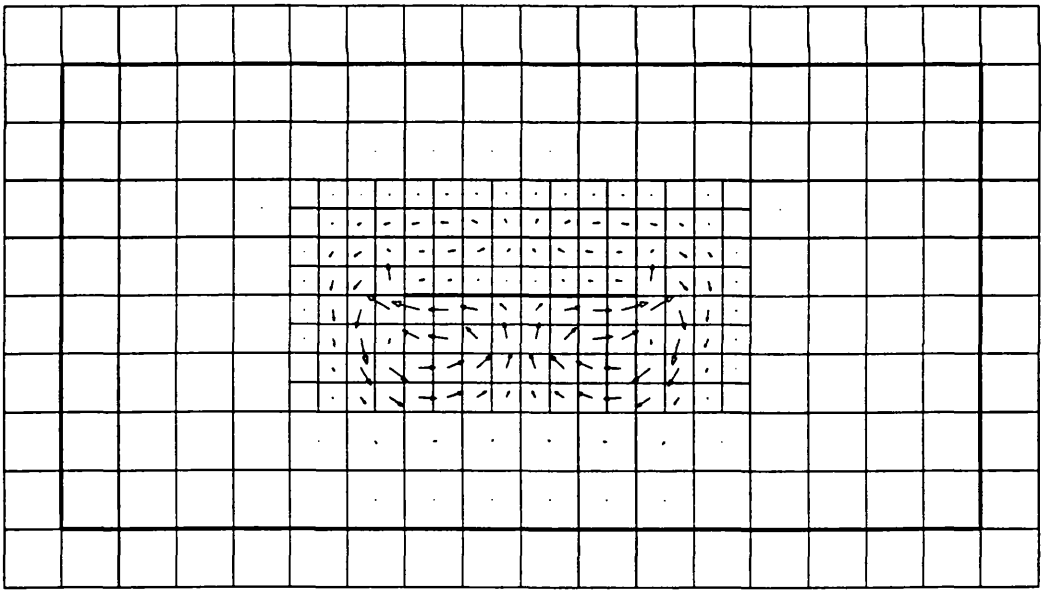

(e) Relaxed viscous acceleration at t = 0.1 s.
(Scale = 0.04)

Figure 4.34 (Continued)

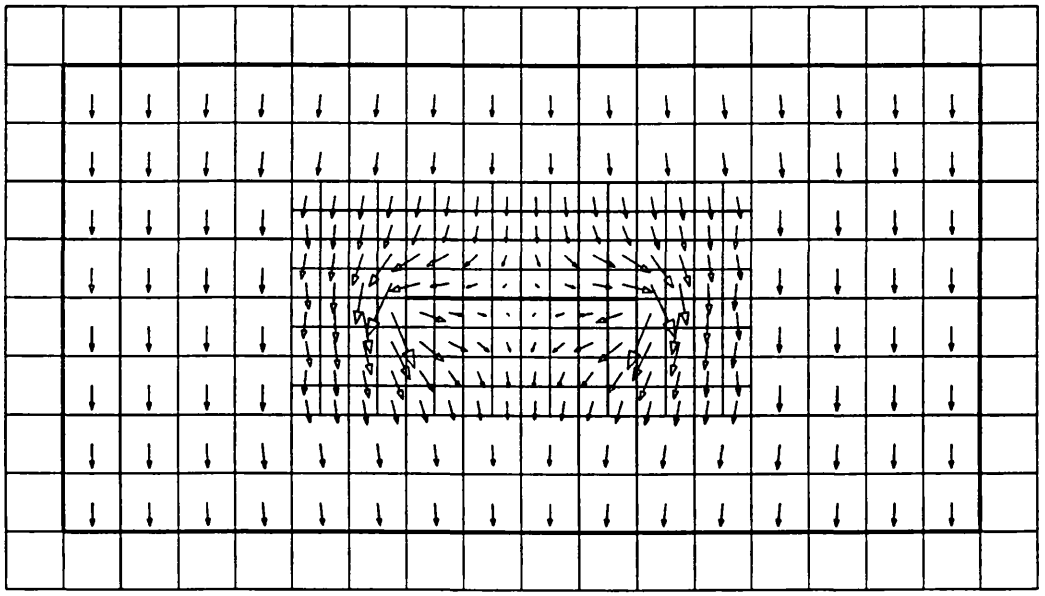

(f) Modified flow velocities at t = 0.1 s.
(Scale = 0.1)

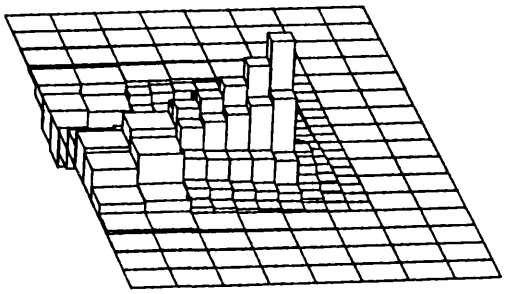

(g) ROTATION spread at t = 2.0 s.

Figure 4.34 (Continued)

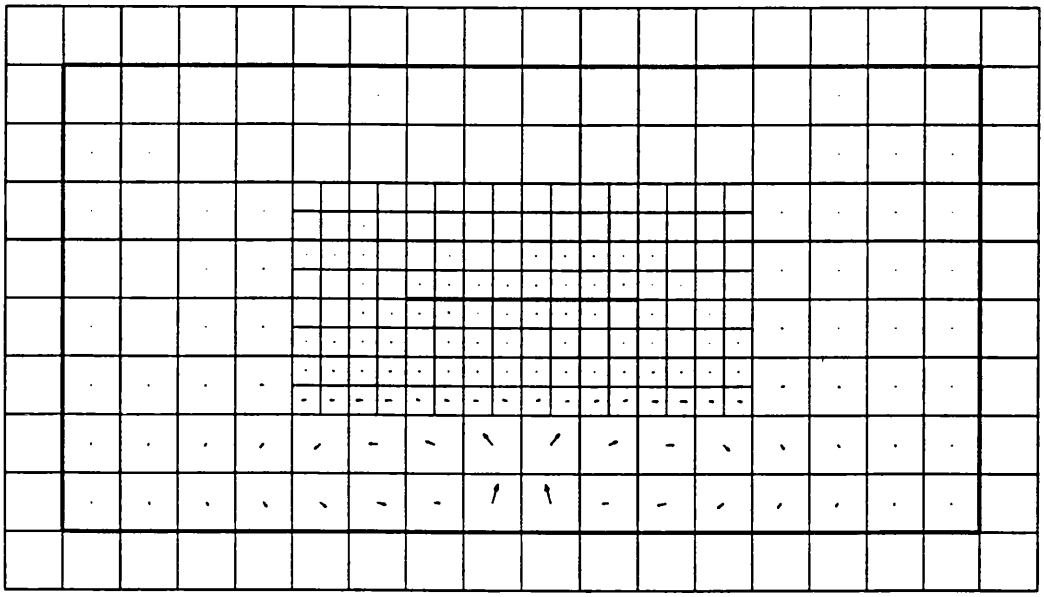

(h) Initial viscous acceleration at t = 2.0 s.
(Scale = 4.0)

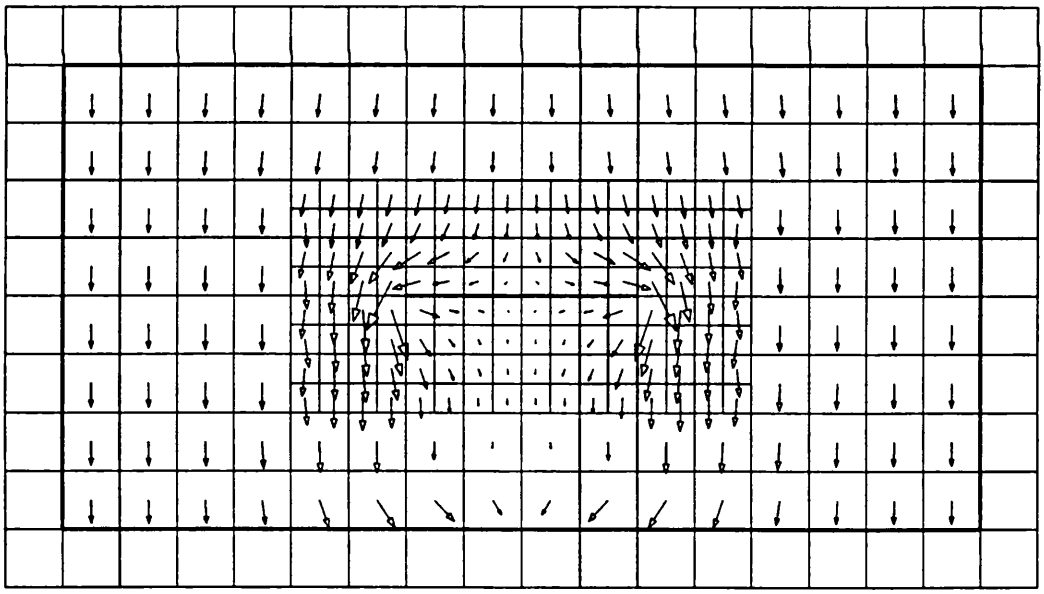

(i) Modified flow velocities at t = 2.0 s.
(Scale = 0.1)

Figure 4.34 (Continued)

CHAPTER 5

DEVELOPMENT OF A DIRECT COMPUTER MODEL OF FLUIDS (PHASE 2)

1. INTRODUCTION

Despite the success of certain aspects of the modelling of Phase 1 of the research, as described in chapter 4, distinct deficiencies in the algorithms were recognised. The principal shortcoming was that the algorithms were entirely kinematic in nature and, as a consequence, no direct value of fluid pressure was provided. Although it would have been possible to invoke the momentum equation to deduce the pressure, this would have been contrary to the aim of the research: for a fluid does not invoke the momentum equation to work out what pressure it should exhibit with a given flow field - and therefore a direct computer model of a fluid should not either. The purpose, then, of Phase 2 was to re-work and validate the inviscid modelling algorithms of Phase 1 along strictly physical lines. It was felt that no sensible progress could be made in viscous modelling until the inviscid model was sound.

2. REVISED GUIDELINES FOR PHASE 2

The revised scope of the second phase of the research was as follows:-

- To concentrate on inviscid flow and to re-develop the inviscid algorithms of Phase 1 of the research along strictly physical lines.
- To synthesise fluid pressure and motion *together* within the modelling algorithms.
- To accommodate the possibilities of free-surface distortions and the actions of gravity on the fluid.

The revision to the rules for algorithm development (see chapter 3, section 2) was to disallow "logical" driving influences from being considered (guideline (vi)). These modifications are based on the conclusions of chapter 4.

3. DEVELOPMENT

3.1 Review of Inviscid Flow Modelling of Phase 1

The algorithm for developing inviscid flows in Phase 1 of the research was based on a consideration of what must happen "in an instant" when a solid body or boundary begins to move from rest within an incompressible stationary fluid. The instantaneous disturbance to the fluid was given by the acceleration of the body/boundary surfaces and by using a logical procedure for relaxing this initial disturbance throughout the fluid discretisation an acceleration response of the fluid could be obtained.

The algorithm used in Phase 1 is summarised in figures 5.1 and 5.2 where, for illustration, the response of a fluid to the acceleration from rest of a flat plate is considered*. The initial effect of the plate's motion was to cause a *tended* "squeezing" of the fluid in the regions adjacent to the plate. (The qualification "tended" here is important since the disturbances are calculated on the basis of accelerations: no *actual* distortions of the fluid have actually taken place.) This tended build up of fluid had (logically) to be exhausted from the stressed regions, thereby spreading the disturbance through the fluid. The state of "squeeze" of a fluid region was given by the variable SQF ("squeeze factor"). The relaxation process was driven by the continuity requirement for incompressible fluids: flow acceleration rates across fluid edges within the system had to be adjusted during the process in such a way as to reduce the SQF values to zero everywhere in the system.

3.2 Parallel Relaxation to Replace Sequential Relaxation

It can be seen from figure 5.2 that the relaxation process of Phase 1 was *sequential* in the sense that only the highest "stressed" region was relaxed in one relaxation step. This had been found to produce faster convergence of the final acceleration pattern when compared to the alternative, more physical, scheme of parallel relaxation, where all regions relax in each step of the process (see figure 5.3). Despite the penalty in terms of convergence rate, it was felt that a parallel scheme had to be adopted for development in order to adhere to the aims of the work.

---

* These diagrams are copies of figures 4.8 and 4.9 and are reproduced here for convenience.

3.3 A New Definition of Squeeze Factor

Although the name "squeeze factor" suggests some sort of pressurising influence there are clear inadequacies associated with the variable as used in Phase 1. A clear manifestation of these is that the old inviscid algorithm described in section 3.1 ended with a state of zero "squeeze", whereas we now require a distribution of the temporal pressure associated with the accelerating fluid. The problem lay in the actual definition of the variable which was then in terms of *rate of change of volume flux into a region per unit volume* (see chapter 3, section 6.2.2). As the only physical way of synthesising pressure within the algorithms is to consider and use the compressibility of the fluid (even for the cases of so-called "incompressible" fluids) then clearly a squeeze factor defined as a straight proportional increase in fluid volume was required. This new physical definition is illustrated in figure 5.4 but its use is dependent upon the modelling strategy followed, as is now discussed in section 3.4.

3.4 Approaches to Temporal Acceleration/Pressure Response Prediction

In Phase 2 the identifications of "cause" and "effect" in fluid behaviour had to be more closely examined. In Phase 1, based on the observations of a pilot study to that work, the rather simplistic view that pressure could be considered as a consequence of fluid motion was implied. This lead to the subsequent limitations of application of the algorithms developed. Here it must be asked more carefully; what comes first, pressure or motion? Certainly, when considering the macroscopic development of a flow it is obvious (though not easy to describe) that pressure and motion are being generated and are interacting *simultaneously*. However, when developing physical algorithms to drive a discretised system representation of a fluid (in the space and time domain) it becomes necessary to identify and describe explicitly the "horses" and the "carts" of the system. Unfortunately, because of the discretisation, there are several different cause-and-effect strategies that can be followed. Two of these approaches have been explored in this work and are now described in section 3.5: there may be more.

3.5 Synthesis of Temporal Pressure: Pressure-FOR-Acceleration Approach

This strategy was essentially a continuation of that used in Phase 1. The objective was to predict the acceleration response of a fluid to the instantaneous accelerations of the

solid boundaries in the system and this was to be achieved by a two stage process: first, to determine the temporal pressure field associated with the boundary accelerations; and second, to use the pressure field so calculated to *drive* the acceleration response of the fluid. (See figure 5.5.) In the first stage, in order to achieve a true pressurising influence, it was necessary to consider displacements of the fluid edges for all the regions so that the new SQF definition could be employed (figure 5.4). These displacements were conceived as virtual displacements arising from the (input) boundary accelerations, along similar lines to the "tended" motions concept used in Phase 1 where balancing of accelerations was effected. They would not be used to represent motion response as this would be driven from the resulting pressure field. However, an interesting observation would be whether the fluid displacement distortions obtained from the pressure field calculation gave the same representation of the fluid's acceleration response as that produced subsequently from the driving influence of the pressure field.

The breakdown of the modelling strategy into the two components was based on the conventional idea that pressure disturbances travel very quickly in "incompressible" fluids This means that a temporal pressure field will be fully established well before any significant velocities are observed in the fluid. The discretisation grid in this method, therefore, is used for two purposes and has two corresponding interpretations (figure 5.6). The first is a network to "balance" very small tended distortions to the bulk of the fluid arising from accelerations of the boundaries. The second is then simply a reference system for the flow kinematics driven by the pressure field obtained.

It can be seen that once the pressure field has been determined in this method then the second stage of accelerating the fluid is a straight-forward application of Newton's Second Law using forces from differential pressures. The principal algorithm associated with this strategy, then, is that which develops the temporal pressure field. Two approaches were tried: both were relaxation techniques and the proposed interpretation of the SQF "response" during the relaxation process is illustrated in figure 5.7. The details of the two techniques are now described and the results obtained are discussed.

3.5.1 Old Relaxation Approach - Equal Exhaust Across Edges

This first approach was to use a similar relaxation process to that used in Phase 1, but this time parallel relaxation and the new definition of SQF were employed (figures 5.3 and 5.4). Accordingly the inputs to the system were the *displacements* of the solid boundaries in a given time interval, and these displacements were to be relaxed throughout the discretised system. The process is illustrated in figure 5.8. As the relaxation process

was driven by the need to reduce SQF to zero throughout the system, the pressures arising from the boundary accelerations would have to be related to the *average* SQF levels for each of the fluid regions during the relaxation process, as illustrated in figure 5.7.

The sort of results obtained with this algorithm are shown in figure 5.9 which shows 3-dimensional representations of the integrated SQF values over the relaxation process for various system geometries. It can be seen that the bulk of this integrated SQF field is certainly qualitatively correct in its form. However, problems were apparent with localised discrepancies, mainly associated with partial and subdivided regions, which indicated a failing of the relaxation algorithm. This failing directed effort towards the second and more physically recognisable relaxation algorithm which is described in section 3.5.2. More fundamental, however, was the difficulty experienced when trying to scale the pressure levels from the integrated SQF values; for the relaxation process was asymptotic and the choice of averaging parameters was found to be obscure, particularly with the physical ambiguity of the "relaxation factor". It was hoped that the new relaxation algorithm might improve the means of interpreting the temporal pressure values. As it turned out, however, the new approach exhibited similar problems and these will be discussed further in section 3.5.3.

3.5.2 New Relaxation Approach - SQF Driven Exhaust

Early efforts (in Phase 1) to modify the relaxation process such that outflows were proportional to the differential levels of SQF across the edges of a region were unsuccessful. They had not been attempted, however, with the parallel relaxation technique where obvious redundancies in the old relaxation process could be more easily identified. An example of such redundancy is illustrated in figure 5.10, where exhausting of fluid from one region to another which has an equal SQF level is seen to be a cancelling and (arguably) computationally wasteful process. A new relaxation technique which used the differential SQF/pressure levels during the relaxation process was required, and this had also to solve the problems observed in section 3.5.1 and to succeed in smoothing the SQF/pressure fields produced in way of partial and subdivided fluid regions. The algorithm devised will now be described. It was developed essentially, by an iterative process of trial and error greatly facilitated by the graphics capability of the computer program "testbed". The problem of partial regions in a single level of discretisation was tackled first, and then the problems of subdivision were addressed.

The nature of the developed algorithm is outlined in figure 5.11. Considering the relaxation of one region in any given relaxation step, the first task was to calculate the

displacement increment for each of the region's edges assuming that these individually were to equalise SQF/pressure between the two associated regions. These tended displacements were multiplied by the area of the respective edges and were summed to get a total tended flow transfer for the region given by the variable S_DINC_AREA. The individual edge displacements were then moderated by this factor in proportion to their contributions to the S_DINC_AREA value.

The problem of inconsistent SQF/pressure levels being generated in partial regions was solved by normalising all regions of a given discretisation level to the standard sized region for that level. Rather than using the actual volumes and edge areas of partial regions in the relaxation algorithm, effective volumes and edge areas were used as illustrated in figure 5.12. The success of this modification is shown in figure 5.13.

The treatment of subdivided regions was more difficult than simply regarding them as partial regions. Figure 5.14 shows the effects on both the SQF levels and the displacements for a simple channel flow system where subdivision was introduced. This uneven relaxation was improved by allowing the subdivided regions to relax 4 times (amongst themselves) for each single relaxation step of the next highest discretisation level. This higher level addition to the algorithm is illustrated in figure 5.15. Figure 5.16 shows that the results were reasonable - but not perfect. The algorithm was developed further, although within the context of a different cause-and-effect strategy (see section 3.6).

3.5.3 Discussion of the Pressure-FOR-Acceleration Technique

As mentioned in section 3.5.1, the principal problem of the two-stage Pressure-For-Acceleration technique lay in the scaling of the SQF values to pressure. Figure 5.7 has shown the intended interpretation of the SQF response. It can be seen, however, that the expression described for the pressure will tend towards zero as the number of relaxation steps increases rather than a finite value of pressure as required. It was necessary, then, to determine the effective limit to the relaxation process. The difficulty lay in defining this limit for the integration or the plateaux to which the integrated SQF values approached in the asymptotic relaxation technique. Figure 5.17 illustrates this problem. It was also found that the relaxation factor used to increase the speed of convergence of the relaxation process affected the final values of SQFINTEG. Although these problems could, perhaps, have been tackled analytically, the need for that sort of "adjustment" process would have been contrary to the revised guidelines of Phase 2 (see section 2).

Only at this stage of the work did it become evident that the relaxation approaches used so far were flawed (although with hindsight it was obvious). For they allowed the use of a relaxation factor, the choice of which was, to some extent, rather arbitrary and was based on considerations of numerical convergence of the process rather than a clearly defined physical objective. Despite this observation, the qualitative picture of the pressure synthesis was very encouraging. For although the magnitudes of the temporal pressures could not be reliably evaluated, the directions and *relative magnitudes* of the accelerations that these would produce were very promising. Figure 5.18 shows the comparison between three pictures of the acceleration response for the well used example of a cylinder moving within a cylindrical annulus of fluid. The first comes from the relative levels of the integrated SQF values using the differentials in levels across a region to produce an average acceleration for that region in the given direction. The second comes from the final edge displacement values after relaxation, interpreted as being proportional to the acceleration. It can be seen that for the main body of the fluid these two pictures are geometrically similar: irregularities can be seen clearly in regions adjacent to the boundaries, but this was because with the simple algorithm used for "accelerating" the fluid the pressure at the boundary was simply taken as being equal to that of the adjacent region, and accuracy at the boundary, therefore, was not expected. The third picture of the acceleration comes from the analytical solution for this particular problem.

The encouraging observations described above, ironically, gave support to the feeling that the Pressure-For-Acceleration strategy itself was fundamentally flawed. For if its results indicated that accelerations could be synthesised at the same time as the pressure, then why could this not be done directly? However, a clearer criticism of the strategy had become apparent. For although the techniques used a quasi-transient compressibility of the discretised fluid, the final SQF state, being reduced to zero, did not allow for the possibility of *observable* compressibility as exhibited by fluids of low bulk modulus. Although compressible flow considerations were not specifically of interest in this research, the failure of the methods being developed to allow for extension in this direction was an indication of deviation from a properly physical model. For this reason effort was redirected towards an alternative strategy where pressure and acceleration were to be synthesised simultaneously. The development of this technique is described in section 3.6.

3.6 Synthesis of Temporal Pressure: Pressure-AND-Acceleration Approach

The relaxation techniques employed with the Pressure-FOR-Acceleration approach (section 3.5) have been described as "quasi-transient". They attempted to model a pressure spreading/balancing process that must occur within a short period of time, but they worked without any explicit consideration of *actual* times involved. Such consideration would be essential if truly compressible flows were to be modelled, and therefore such consideration should also be made for analysis of "incompressible" flows. Concern had also been felt for the rather simplistic visualisation of the disturbance in the Pressure-FOR-Acceleration approach. A distinctly finite block movement of the system boundaries was considered to occur first and the relaxation process *then* spread this distortion throughout the fluid. What actually happens in practice is that infinitesimal movements of the boundaries occur in infinitesimal time intervals, and each of these has a pressurising influence which spreads with the sonic velocity throughout the fluid. The aim of the Pressure-AND-Acceleration approach was to model this cumulative pressure generation/spreading process with specific reference to the time domain. In section 3.6.1 the implications for such time domain modelling are described and in sections 3.6.2, 3.6.3 and 3.6.4 alternative approaches for such modelling are described.

3.6.1 Disturbance Spreading in the Time Domain

So far in the work spreading of the SQF/pressure disturbance from one region to its neighbour has been carried out in one "relaxation step" without any explicit consideration of the time that such a step would take. A nominal figure to take for this time interval may be taken as the distance between centres of neighbouring regions divided by the sonic velocity for pressure waves in the given fluid, although the actual time interval would depend upon the detailed mechanism of the disturbance spreading process*. If specific time intervals can be identified, then, in each of these intervals not only should spreading of pressure take place between adjacent regions, but also additional increments to the disturbance to the fluid should occur with cumulative displacements of the moving solid boundaries in the system. Such a model is illustrated in figure 5.19 where it can be seen that the discretisation grid is treated as an Eulerian reference system, and flow kinematics, represented by average velocities and accelerations at every fluid edge in the system, are now true functions of time during the process. Also, the fluid displacements at the edges

* It is interesting to note that this nominal time interval is consistent with considerations of pressure "conditioning" limitations in a discretised system if the response of the fluid were to be driven explicitly by Newton's Law - see Appendix 2.

are no longer "virtual" values and this is designated by a change in the variable name used from DINC to FG_DISP. It is important to note that the interpretation of pressure from the SQF values is now different from the Pressure-FOR-Acceleration approach. Here the SQF values are directly proportional to the actual pressure in the fluid at the given time during the pressure spreading process, and as the spreading proceeds these values do not necessarily tend towards zero. Rather, these should tend towards observably well-behaved values, giving the total pressure in the flow - a combination of the temporal and convective pressure.

The time interval identified above was to be referred to from this stage on as a *sub*-timestep, for it is very small for "incompressible" fluids. Its use was expected to be neccessary only to model the microscopic transients involved in determining the temporal pressure/acceleration field. Macroscopic transients would be modelled using a much coarser timestep over which interval the temporal acceleration could be taken as constant.

3.6.2 Edge Transfer Method

The edge transfer method for spreading pressure disturbances involved incrementing an edge's kinematics according to the existing states of pressure within the associated regions but WITHOUT consideration of transfers occurring across other edges of those regions. In this approach, the increments to the flow were made by applying Newton's law explicitly to the fluid in the vicinity of the edge as illustrated in figure 5.20. At any given sub-timestep in the process, the fluid's temporal acceleration at each edge could be calculated from the difference between the total pressure differential across the edge and the convective pressure differential across the edge (the latter being inferred from the convective acceleration as calculated from the spatial variation of velocity across the edge). These temporal accelerations for the timestep were then used to increment the fluid's velocity values at the edges during the sub-timestep. Using the accelerations and velocities across edges, effective fluid displacements taking place across the edges were then determined and these adjusted the SQF (and therefore the pressure) levels in all the regions.

This scheme was applied to the simple case of the development of channel flow. A rectangular (2-dimensional) "tank" of still water, of dimensions 0.2m x 0.1m, was set up within the computer model. At each end of the tank a "flowplate" having a uniform

acceleration of 0.01m/s^2 was defined*. A discretisation grid size of 0.02m was specified. The whole system is illustrated in figure 5.21. The edge transfer algorithm described above and in figure 5.20 was set to run for 1000 transfer steps and the resulting motions and pressure levels were monitored throughout the process. Tests were carried out for varying the specified sub-timestep and the aspect ratio of the tank and the results of these investigations are now discussed.

The Effects of Altering the Sub-Timestep

With the given tank discretisation the nominal time interval for one transfer step worked out to be 1.31×10^{-6}s. It was found, however, that within the given algorithm this lead to a numerical instability, the form of which will be described later. By reducing the sub-timestep by a factor of 0.5, a well-behaved response of the system was achieved. The nature of this response is shown in figure 5.22 where the graphical output from the program for the given test has been collated. The results show that, with a continuing acceleration of the flowplates, a steady state picture of the pressure in the system is reached after about 800 transfer steps corresponding to 5.22×10^{-3} seconds and that the pressure gradient in the channel is consistent with the accelerations of the flowplates and, therefore, the temporal accelerations of the fluid. The graph of the variation of pressure (for one particular region) against transfer step exhibits a decaying oscillatory transient of frequency 5 cycles per 200 transfer steps, which translates to 3828Hz. This frequency can be shown to be consistent with the travel and return along the length of the channel of a pressure pulse at the sonic velocity in water.

The results obtained were certainly physically plausible. Reducing the sub-timestep was found to proportionally reduce the frequency of the oscillations with respect to transfer steps, but maintained the same frequency when related to the scaled time. Indeed, from this observation that the frequency of oscillations is independent of time-step it can be seen that the oscillatory response actually yields the value of the sonic velocity of the fluid. (Note that the calculation of the nominal sub-timestep is effectively redundant other than indicating a margin of instability.) The damping ratio of the oscillations was, however, found to change and the significance of this was unclear initially. What was most encouraging from the results was the observation that "steady" acceleration conditions *were* attained after relatively few sub-timesteps. This meant that the sub-timestep approach could be used to determine the temporal acceleration characteristics of

---

* A flowplate is a virtual moving boundary which imposes an acceleration time history on a fixed plane in the fluid. Although it accelerates and may attain velocity, its position is artificially held fixed in order to preserve the system geometry. It is thus a device to impose kinematic boundary conditions at fixed planes in the fluid. This is discussed further in section 3.7.

the flow, and this, in turn, could be used to determine the changes in kinematics occurring within the main (observable) timestep of the overall modelling process.

The Effects of Changing the Channel Aspect Ratio

Altering the length of the channel was found to affect the frequency of the transient oscillations, but consistently with the period of travel and return of a pressure pulse along the tank. A longer tank produced a slower decay rate for the oscillations - i.e. a longer time to establish "steady" conditions. See figure 5.23.

Smoothing Effects on the Integrated SQF Values

As well as recording the variations of SQF with sub-timestep, values of the integral of SQF (SQFINTEG) were monitored. It can be seen that interpretation of these values could provide an earlier estimate of the "steady state" pressure values, as illustrated in figure 5.24.

Convective Pressure

It is worth pointing out here that the pressures only reached a steady state in this example because of the simplicity of the geometry. With no variation of the channel width, no convective pressures should be manifest after the transient oscillations, although convective effects were accounted for in the algorithm (figure 5.20). It is fair to say, though, that the details of the mechanisms of convective pressure generation had not been fully thought out at this stage (see section 3.8).

Density Changes

In the algorithm used, no explicit consideration was made of changes in density that occur as a result of the compression that is being modelled in the process. These would be very small, of course, for the water tank being modelled here. Such density changes from the datum level are accounted for tacitly as they relate directly to the SQF values.

Modelling the Action of Gravity

The explicit nature of the edge driving algorithm made it simple to include a forcing influence caused by the actions of gravity. In keeping with the aims of the research, it had to be possible to model gravity directly rather than by invoking the $p=h\rho g$ balance expression. A pressure variation with depth had to be synthesised by a pressure-and-acceleration process after gravity was "switched on". This mechanism is illustrated in figure 5.25, and the results of the algorithm applied to "stationary" water in the test tank (but now orientated in the vertical plane) are shown in figure 5.26. The results show that the expected variation with depth is achieved after transient oscillations similar to the case of linearly accelerating flow.

The Nature of the Instability Observed

Attempts to increase the sub-timestep significantly above 0.5 times the nominal value caused an instability of the response. The nature of the instability was interesting but it was clearly a numerical instability associated with the discretisation of the system. Figure 5.27 shows the pressure response of a region in the given system where the response goes unstable. The instability can be seen to be oscillatory, but of a much higher frequency than the frequencies associated with reflections in the tank. A closer study of these oscillations showed that they were consistent with reflections taking place within a length of the order of the size of the discretisation grid. Figure 5.28 shows the correspondingly rapid breakdown of the whole pressure field that occurred within a few transfer steps.

Unfortunately when attempting to model other more interesting systems this type of instability seemed to occur no matter what sub-timestep was chosen. Figure 5.29 shows results obtained for the cylinder within a cylindrical annulus problem. The resulting degeneration of the pressure field was the same, although the instability grew more slowly - presumably because of the multi-directional characteristics of the flow.

It was easy to see how the oscillatory distortions to the pressure field would be amplified once they arose, but identifying their source was not so straightforward. The cause was believed to be the rather harsh nature of the edge transfer method for spreading the pressure - for this was done without any consideration of how the pressure of the regions associated with any given edge were being affected by simultaneous transfers across other edges. At this point in the work, in order to try to take account of these simultaneous transfers and to moderate the transfers across edges, an alternative technique was explored for synthesising the temporal pressure field before returning to develop the direct edge transfer method as described in the remainder of this section. This was a "region transfer technique", similar to the region relaxation techniques described in section 3.5.2, and this is described in section 3.6.3.

Numerical Damping

It has been remarked that the significance of the variation of damping ratio in the pressure response was initially unclear. It was not certain whether the decay of oscillations was a physical characteristic associated with a uniformly accelerating flow or simply numerical damping. An exercise to "tidy up" the kinematic descriptions in the program confirmed the latter. It had been noticed that within the coding actually written the grid displacements were computed using the old velocities. By swapping the lines (so that the program now used the new accelerations and velocities) the oscillatory pressure response indicated no damping at all (see figure 5.30). A series of tests was then performed to

examine the variation of the pressure response with varying degrees of artificial damping in the temporal pressure synthesis model. This was achieved by means of a "GROWTH" factor in the velocity contribution to the grid displacement distortions as illustrated in figure 5.31. It was found that by decreasing the GROWTH factor to zero (i.e. a total suppression of the velocity synthesis in the algorithm) lead to a critically damped temporal pressure response (and the fastest settling to "steady" acceleration conditions) as shown in figure 5.32, while not affecting the steady values of the pressure and acceleration obtained. It was found also that by suppressing the velocity in this way it was possible to achieve temporal pressure synthesis for the more complex geometries that had previously exhibited instability. For example, figure 5.33 illustrates the results obtained for the cylinder-in-annulus configuration. It is important to note, however, that suppressing the velocity in this way did not ease the restriction on the timestep to allow values appreciably above 0.5 times the nominal value (see figure 5.34).

The results of pressure synthesis using no velocity suppression show that undamped oscillations will occur in an inviscid fluid. This should not be considered as a limitation of the temporal pressure modelling technique, but rather a limitation associated with the *concept* of an inviscid fluid. For it would be impossible to *drive* an inviscid fluid from rest without setting up continuous oscillations within the fluid (the frequencies of which would depend upon the exact geometry of the system). Conversely, of course, it can be argued that in order to synthesise temporal pressures within a real fluid it would be necessary to involve the viscosity of the fluid to damp out the pressure oscillations. This is true if an exact picture of the pressure wave characteristics is required; however, the results here have shown that if only the final "settled" pressure condition is of interest then it is only necessary to *represent* the action of viscosity in some way. The velocity suppression technique would serve this purpose since it has illustrated that the steady temporal pressure field is independent of the level of viscosity of the fluid.

Despite the observed expediency, the interpretation and justification for suppressing the velocity in the explicit edge transfer method needs to be considered. Suppressing the velocity response by differing degrees has been shown to have no effect on the final levels of temporal pressure computed (figure 5.32) but serves the purpose of speeding up the settling to steady values. Figure 5.35 illustrates the contributions made to the fluid displacement increments in a given sub-timestep during the synthesis of pressure. It shows that contributions from velocity generation must ultimately be associated with convective pressure in the system and that it is the contributions from the fluid accelerations that are directly responsible for moulding the final settled form of the temporal pressure field which may be considered to be superimposed upon whatever convective pressure field exists. The important additional observation was that because the

convective acceleration field is (obviously) dependent upon the time history of the acceleration field, then, by the same token the convective pressures in the system must be dependent upon the time history of the temporal pressure field. This strongly suggested that the two pressure generating mechanisms should be decoupled in the algorithm. The suppression of velocity, then, should not be considered so much as expedient, but rather as *necessary* for the aims of the research in terms of providing the required insight to the understanding of fluid behaviour. For leaving the synthesis of the two pressure components together within the model would disguise the origins and significance of both in the usage and presentation of the algorithm.

3.6.3 Region Transfer Method

During the development of the Edge Transfer Approach (3.6.2) the early problems of instability in the response of any system other than a simple rectangular tank indicated that the technique was too harsh and unrepresentative when spreading pressure within a discretised system. The Region Transfer Approach, then, aimed to moderate the edge transfers by calculating them indirectly based on the tendency of a region and its neighbours to *equalise* their pressures. The technique is illustrated in figure 5.36 and uses similar principles to those described in section 3.5.2. Note that here two moderating factors S_DINC_A_OUT and S_DINC_A_IN had to be employed. The acceleration fields obtained were reasonable, but not perfect (see figure 5.37) and the algorithm would need further attention in this area. More seriously, however, the pressure levels were not correctly predicted and varied with the chosen timestep. It appeared that explicit consideration of time for the process was important to correctly model the synthesis of pressure and unfortunately the process of equalisation of pressure in the Region Transfer method was ambiguous in this respect. Much more effort would have been required to set this technique to work and it was decided to continue the research using the Edge Transfer Technique. This decision was also based upon the indicated comparative speeds of the two methods in obtaining the "steady" acceleration responses. The variations of SQF for the same region using the two different techniques are shown in figure 5.38. Although the Region Transfer Method appears to be about 3 times faster in terms of transfer steps, each step in the Region Transfer method involves about 3 times more calculations than the Edge Transfer technique.

3.7 Pressure Driven Flow

Section 3.6 reports the decision to continue the research using the Edge Transfer Method for synthesis of temporal pressure within a discretised fluid system. Before progressing to consider the synthesis of convective pressure it was necessary to incorporate a facility to drive the flow using pressure differences rather than accelerating boundaries. In Phase 1 of the research, and up until now in Phase 2, all acceleration fields have been generated as a response to moving boundaries in the system - i.e. using kinematic boundary conditions as inputs. Artificial moving boundaries called "flowplates" were devised (see section 3.6.2) in order to represent in certain cases *the effects* of pressure planes in the fluid and to avoid the complications of changing geometries in modelling steady flow configurations. However, these modelled the pressure boundary conditions only indirectly (see figure 5.39) and, of course, in a truly physical computer model it should be possible to insert such conditions directly.

The structure of the Edge Transfer Method made the incorporation of pressure driven flow very straightforward (indeed a feature that supports the validity of the approach). Any defined surface within the system can be designated as a pressure surface and assigned a constant pressure level. The discretised "edges" of such surfaces are treated similarly to edges within the fluid in that flow accelerations across them are driven by the SQF/pressure gradient in way of the edge as shown in figure 5.40. This gradient is simply calculated from the SQF/pressure level for the region associated with the boundary edge, the set pressure of the constant pressure surface, and the distance from the centre of the region to the centre of the edge. It is important to note that the pressures assigned to any pressure surface in the system should be considered as total pressures comprising the sum of temporal pressure and convective pressure at the pressure plane. This distinction will be discussed in more detail in section 3.8 where the synthesis of convective pressure is considered. In this section, where the interest is in generating initial acceleration/temporal pressure fields (from a state of rest), the assigned surface pressure levels may be considered to be purely temporal pressure values.

Some results of the pressure driving algorithm are illustrated in figures 5.41. Figure 5.41(a) shows the significant influences of the actual pressure levels used to create the same overall pressure difference along a rectangular channel. The fastest attainment of the steady temporal conditions is achieved by specifying (equal magnitude) positive and negative pressures upstream and downstream respectively. This ensures that flow is driven in the right direction from both ends throughout the pressure spreading process. Figure 5.41(b) illustrates the plausible outcome of a mistaken input! It had been intended to specify upstream and downstream pressures for the flow past a circular cylinder; by

mistake the cylinder was designated as the high pressure surface rather than the upstream flowplate. Figure 5.41(c) shows the corrected outcome.

3.8 Synthesis of Convective Pressure

One of the most basic yet most demanding concepts in fluid behaviour is that of pressure, particularly in the context of "incompressible" fluids. Because it is so basic it is too easy simply to regard it as just one more flow parameter rather than recognise or question its source. The indirect "implicit" treatment of pressure in the more common CFD approaches as described in chapter 2, where pressure becomes merely a variable in an equation balancing exercise, reflects this. In this research the concept and treatment of pressure had caused the most problems. In Phase 1 (chapter 4), pressure was regarded rather carelessly as *a consequence* of how a fluid flow is constrained in development within the system boundaries. This description is true, up to a point, but too ambiguous to lead directly to a true physical algorithm of the fluid behaviour, as the results of Phase 1 have shown. In Phase 2, then, the concept and treatment of pressure were fundamental to the research.

3.8.1 Breakdown of Pressure

Very early in this work pressure had been categorised as two sub-components, Temporal Pressure, and Convective Pressure (see chapter 3, section 5). Very seldom are such terms used in the literature of fluids and CFD (in fact the author has never come across the terms). The reason for their introduction was simply because even from the preliminary stages of the research it seemed clear that the principal inputs to any fluid system were the boundary accelerations or the equivalent thereof. The immediate fluid response was temporal acceleration, associated with which must be a temporal pressure field. Once fluid velocities were developed, then convective pressures would arise. It seemed sensible, therefore, to retain the identities of the pressure components associated with these clearly identifiable influences in the development of the direct model of fluid behaviour. Subsequent development of the temporal pressure algorithm supported the view that these components should be treated separately (see section 3.6.2). And so, once temporal pressures had been successfully generated in the research, it was necessary to direct attention to the synthesis of convective pressure and flow velocities.

3.8.2 The Origin of Convective Pressure

Bernoulli's equation, applied to steady "incompressible" flow in a varying section duct (see figure 5.42), is commonly used in fluid dynamics texts to "explain" pressure variations in pipes, and so on. From the discussion of chapter 2 it is clear that this is not a true explanation of the convective pressure phenomenon as such, but rather an illustration that such convective pressure variations *must exist* in order to satisfy Newton's Second Law of Motion. Such steady state descriptions of flows cannot hope to explain truly how the convective pressure arises; it can only be inferred that it must be there. For steady state conditions do not provide any *mechanism* for the generation of pressure; prevailing continuity means that there is no actual (or tended) build-up of fluid anywhere in the system. This observation supported the earlier arguments of section 3.6.2 that the only possible source of convective pressure must be associated with the temporal pressure field acting during the acceleration of the flow to steady conditions.

An explanation for the development of convective pressure will now be presented as a necessary pre-cursor to the description of the algorithm devised for the computer model. Use will be made of a specific example, illustrated in figure 5.43, where the complete description of the synthesis of pressure in an **inviscid** flow developing in a long, horizontal, uniform section pipe between two very large (and, therefore, essentially "constant head") reservoirs is considered.

At time $t<0$ the fluid is at rest and the valve connecting the pipe to reservoir B is shut. The total pressures in reservoirs A and B at the respective ends of the pipe are p_A and p_B where $p_A>p_B$ and, because of the position of the valve, the pressure within the pipe is also p_A. At time $t=0$ the valve is opened instantaneously and immediately the downstream end of the pipe is exposed to the lower pressure p_B. The temporal pressure generation mechanism described in section 3.6 creates a linear variation of total pressure along the pipe as shown in figure 5.43(b)* . At this instant in time the fluid is still (macroscopically) at rest. The temporal pressure distribution (which may at this stage be considered simply as the total pressure distribution shown in figure 5.43(b)) has a uniform gradient within the pipe which, of course, is associated with a uniform (temporal) acceleration of the fluid in the pipe. This in turn will give rise to a uniform velocity of flow along the pipe which will develop with time. As the flow is inviscid, then, if the constant heads h_A and h_B are

---

* The scale of the diagram cannot show it very clearly, but the actual pressure at the inlet to the pipe would be slightly less than p_A and that at the outlet end slightly greater than p_B because of the spreading of pressure within the reservoirs. That is, there would be a smooth curve joining the uniform pressure gradient in the pipe to the plateaux of pressure in the reservoirs away from the pipe openings. Since the reservoirs are very big and the pipe is long, then assuming the pressures to be p_A and p_B at the ends of the pipe is a reasonable approximation.

maintained, the fluid in the pipe will have a constant acceleration and the velocity in the pipe would tend to rise indefinitely**. With no friction in the system, steady flow conditions will only be achieved if the temporal pressure influence is removed - for example, if the level of the fluid in reservoir B, say, is somehow raised to, and maintained at, the level of reservoir A. Supposing this steady condition is achieved at some time $t=t_{steady}$, the pressure picture, from what Bernoulli's equation indicates, will be as shown in figure 5.43(c). The level of the pressure drop Δp_{steady} in the pipe will depend upon the velocity attained in the pipe which, of course, will depend upon the history of the temporal pressure field which induced the motion. The task here is to describe physically how the pressure drop Δp_{steady} comes about.

Consider the picture of the total pressure distribution at some time $0<t<t_{steady}$ during the flow development as shown in figure 5.43(d). Along the pipe the total pressure lies below the original total pressure level (at t=0) by an amount Δp. Splitting the total pressure into components, then, a temporal pressure field, a base pressure field and a convective pressure field can be identified as shown in figure 5.43(e). Note that the choice of base pressure is somewhat arbitrary but has been made here with a knowledge of how the temporal influence was effected in the first place and how it may be removed. (The opening of the valve was equivalent to the sudden lowering of the fluid level in reservoir B from h_A to h_B, and the temporal pressure influence may be removed by raising the level in reservoir B to h_A.) Also, note that pressures are referred to a pressure datum which is the atmospheric pressure at the reservoir surfaces: in this example the absolute values are not critical, only the relative values being important. As long as $h_A>h_B$ a temporal pressure field will remain; and assuming that h_A and h_B are constant, then the temporal pressure field will be invariant with time t=0 to $t=t_{steady}$. During that time, however, the convective pressure will continue to decrease. When the temporal field is removed the convective pressure will remain at its final value; it will not recover to zero. And so, some action of the temporal pressure field will somehow have effected an expansion of the fluid in the pipe relative to the bulk of the fluid in the reservoirs. Note further, however, that in the steady state the fluid in the pipe will be continuously replaced and so the temporal pressure field effects local depressurisation *zones* within the system. As this depressurisation can only be associated with the fluid medium (since the boundaries to the flow are not changing) it is possible to be more specific. The action of the local temporal pressure field at a point in the system must somehow cause an expansion of the fluid passing that point, and once that expansion is created it is *preserved* thereafter by the kinetics of the fluid.

** The suggestion that the velocity in the pipe would continue to rise indefinitely here requires qualification. Of course it will only continue to rise in an ideal inviscid fluid as long as certain known and real physical limitations are avoided. These limitations include: vapourisation (which would introduce two-phase flow and eventually compressible flow effects); breakdown in the continuum model of the fluid (which introduces the restriction on pressure drops only to absolute zero pressure!); and the attainment of such high velocities in the pipe that would tend to change the reservoir levels at a noticeable rate.

To explain the mechanism of depressurisation of an "incompressible" fluid by the temporal pressure field it is necessary to consider the compressibility of the fluid, even though this is very small. Figure 5.43(f) shows a series of control volumes of the fluid within the pipe which are subjected to the same uniform temporal pressure gradient. The temporal pressure field has been synthesised by a redistribution of fluid in the pipe in order to smoothly connect the originally out-of-balance pressure levels p_A and p_B at each end. Associated with this pressure field, then, a variation of density (albeit very small) will have been set up, the density decreasing on progression from reservoir A to reservoir B. The temporal acceleration set up by the constant pressure gradient, although observably uniform, will actually increase slightly at successive positions along the pipe due to the small decreases in density. Correspondingly, the velocities set up in the pipe, although again observably uniform, will similarly increase slightly with position along the pipe. It can be seen that these very small variations of velocity (caused by the temporal variations in density) cause the depressurisation of the moving fluid which is manifested in the convective pressure field. The effect can be seen to be cumulative in time, as the temporal pressure field is superimposed upon the base plus convective pressure of the fluid at any instant. When the temporal field is removed the total depressurisation due to the convection of the fluid in the temporal field up to that time is preserved. The temporal density variation along the pipe (associated with the temporal pressure) is removed, and with it the small variations of velocity and density associated with temporal effects. No further depressurisation will occur until a further temporal pressure influence is applied.

Figure 5.43(g) shows that the convective pressure increment in one sub-timestep could be deduced in one of two ways. The first would be to identify a fixed mass of fluid and to calculate the pressure change caused by the volume expansion of that fluid. The second would be to identify a fixed volume of fluid and to calculate the pressure change by the mass accumulation of fluid in that volume. The former technique requires a knowledge of the small variations in velocity which occur as a result of the presence of a temporal pressure gradient in the flow, whereas the latter requires a knowledge of the small variations in density that occur. Since the variations in density are directly available from the temporal pressure levels, and a fixed region volume is readily identifiable, then the second approach was adopted for the algorithm for convective pressure synthesis (see section 3.8.4).

Before leaving this section a further note on the example chosen for describing the interplay between the temporal and convective components of pressure is appropriate. Some readers may have found the idea that the velocity in the pipe tends to continue rising when the difference in reservoir levels is maintained somewhat contrary to their

expectations. In part this is because it is sometimes difficult to appreciate how an (imaginary) inviscid fluid would behave, and in this example it is particularly important to remember that the flow will not issue from the downstream end of the pipe as a jet but will spread smoothly into reservoir B, effectively mirroring conditions upstream at inlet to the pipe. This is, essentially, where the current example is different to the case of a reservoir venting to atmosphere through a pipe (or orifice) where it is well known that a conventional inviscid analysis would indicate that the velocity of the flow issuing from the pipe *is* limited (see [1d] for example). This latter example is more complicated than the one chosen but it can still be explained by the current arguments.

3.8.3 Pressure Smoothing

Up until this stage of the work it had been sufficient to work with the averaged region pressure levels (as represented by the SQF values). Accordingly, no effort was directed towards smoothing the pressure levels and this has been reflected by pressure fields being represented by step diagrams in the various figures presented so far. While the convective pressure algorithm was being designed (see section 3.8.4) it was clear that temporal pressures at region edges were required. For "internal edges" these could simply be obtained by interpolation of pressure at the edge from the two regions associated with the given edge (figure 5.44). This simple interpolation would not work, however, for solid boundary edges and a more sophisticated algorithm was required for these edges. This required development of a pressure smoothing algorithm would also serve to enable forces on bodies to be determined with more exactitude than the step pressure picture allowed.

A constraint on the smoothing algorithm was that it had to be "local", involving a region and its nearest neighbours only, or an edge and its two associated regions only. This would be in keeping with the ideals of the research where only information from direct physical connectivity of regions could be used in the modelling. The current state of the algorithm is illustrated in figure 5.45 and in its development it was found that the synthesis of convective pressure was extremely sensitive to the degree of smoothing achieved in the temporal pressure field. Examples of the comparison between the "stepped" and "smoothed" representations of pressure fields will be given in the figures presented in sections 3.8.4 and 3.8.5.

3.8.4 Algorithm for Convective Pressure

Figure 5.43(g) has shown the basis of the algorithm used for general bi-directional flow within the program FLOW2D which is illustrated in figure 5.46. Note that in the calculation of convective pressures actual areas of edges and volumes of regions must be used for partial regions. (In the synthesis of temporal pressure it was found to be necessary to use effective areas and volumes for such regions (see section 3.5.2).)

Figures 5.47 illustrate the results of the convective pressure generation algorithm. Figure 5.47(a) shows the development of convective pressure in a simple channel (and the effects of introducing subdivision). Figure 5.47(b) shows the results of the synthesis of convective pressure in the fluid flowing around a rectangular cylinder.

When the algorithm was applied to the classical example of flow around a circular cylinder (in order to verify the magnitudes of the convective pressure being predicted) unfortunate problems were uncovered (see figures 5.48). In certain partial regions the algorithm implemented did not synthesise the convective pressure drop as intended. In regions on the body surface where it did, however, it can be seen that the pressure levels predicted agree very well with the analytical solution (see figure 5.48(e)). By examining the various views of the convective pressure field in figure 5.48 it can be seen that the problem is localised to partial regions which are formed adjacent to the cylinder surface. The problem is similar to that experienced with the early temporal pressure algorithm (see section 3.5.1 and figure 5.9). Some considerable time had to be spent in solving those discrepancies and it is believed that the problems experienced here would be equally soluble in time. Additional tests have shown that the current algorithm for the smoothing of the temporal pressure is not robust enough in the way of partial regions and further attention in this area is believed to be the key to the reliable synthesis of convective pressure.

3.8.5 Convective Pressure Created by Accelerating Bodies

The description of convective pressure generation so far has been directed to flows in pipes or channels, or past bodies located in a uniform stream. This type of flow arrangement does not, however, cover the more common flow problem encountered, for example, in Naval Architecture where the bulk of the fluid is stationary and the *body* moves. Traditional analytical treatment of this situation for steady motion of the body is simply to change the frame of reference and observe the flow from on board the body - by which effect the flow pattern now becomes that for a steady steam. Such a trick goes

"against the grain" of the principles of developing a physically transparent fluid model and it was considered to be necessary to show that convective pressure could be generated from the temporal pressure field associated with an accelerating body.

There were two possible approaches to this problem. The first was that which had been deliberately avoided in the work so far which would involve the movement of the body with respect to the discretisation grid. (This had been avoided because of the distracting effort that would be required to develop grid re-generation routines - see chapter 4, section 4.2). This approach would definitely be necessary for systems where the geometry changed significantly during the motion as illustrated in figure 5.49(a). The second possible approach would be to consider the discretisation grid as moving with the body, a scheme which would be suitable for bodies moving in unrestricted or uniformly restricted space - see figure 5.49(b).

Each of the above approaches to the problem involves a more complicated motion interaction than the case of the fluid stream accelerating with respect to a stationary temporal pressure field. In the first case the temporal pressure field is accelerating with respect to the discretisation grid (and the fluid discretised by the grid), and the fluid is accelerating with respect to the discretisation grid. In the second case the temporal pressure field is stationary with respect to the discretisation grid, but now the frame of reference is accelerating, as well as the fluid accelerating with respect to fixed space. The effort involved in developing grid re-generation algorithms precluded applied consideration of the first approach, although this will be discussed further in chapter 6. The consideration of the second approach, however, was feasible.

The task faced, then, is described in figure 5.50. The convective pressure algorithm had to be adapted to produce the same picture of convective pressure with respect to a body from two quite different temporal pressure fields and subtly different motion characteristics. It could be seen immediately (by considering the upstream pressure conditions) that the absolute convective pressures would not be *identical*; the relative pressure levels produced, however, should be so.

The algorithm devised was essentially the same, with convective pressurisation being effected by the movement or relative movement of the fluid through the temporal pressure gradient. The modifications made to the algorithm had to involve a more careful consideration of the velocity of the fluid with respect to the temporal pressure field. Originally only two components were identified:-

(i) the absolute velocity of the fluid

(ii) the absolute velocity of the temporal pressure field

The algorithm for synthesis of convective pressure was accordingly adjusted as illustrated in figure 5.51(a) but the results produced (figure 5.51(b)) clearly indicated that something had been overlooked. The missing term was the one that distinguishes the moving body problem from the moving stream problem. For in the former case, as well as the relative velocity of the fluid past a "fixed picture" variation of the temporal pressure so far considered, the temporal pressure gradients at the chosen location in the flow are also changing as the fluid passes the given location. The latter term, then, may be represented in the algorithm as illustrated in figure 5.52(a) and the resulting convective pressure field is more promising (see figure 5.52(b) and compare it with 5.47(b)).

3.8.6 Implicit Momentum Balance

Finally, it is interesting and important to note that the model for convective pressure generation has not explicitly considered or involved a spatial momentum balance. This is effected implicitly by deriving the convective pressurisation levels directly from the temporal pressure field which, of course, dictates the spatial variations in momentum flux. Discretisation errors within the program will mean that periodically during the development of a flow a momentum balance check and correction of the flow of some sort may have to be performed. This is discussed further in chapter 6.

3.9 Modelling Free-Surfaces

3.9.1 Acceleration Responses

While incorporating the features for pressure driven flow (as described in section 3.7) it was realised that these effectively enabled modelling of the first stage of free-surface distortion. For in terms of acceleration response, a free-surface is simply a surface of constant pressure. It should have been possible, then, to obtain the temporal acceleration responses for systems accelerating in the vicinity of a free-surface without any further modifications to the program being necessary. This turned out to be true. It was not clear initially what effect the acceleration due to gravity would have on the synthesis of acceleration responses associated with a surface of zero gauge pressure (to represent the atmosphere), but tests quickly showed that there was none. Figure 5.53 shows one system used for study of free-surface distortion effects. A rectangular surface piercing body is located within a rectangular tank (of water). Figures 5.54 show the results of accelerating this floating body in the vertical mode with respect to the water surface (a) with no consideration of the action of gravity and pressure variation due to depth; and (b)

with the static variation of pressure with depth and the acceleration due to gravity activated (section 3.6.2). The acceleration and temporal pressure fields produced can be seen to be identical, as indeed are the values of added mass interpreted by integrating the temporal pressure over the submerged surface of the floating body. This result is hardly surprising since the temporal acceleration mechanisms do not affect the balance between the fluid's weight distribution and the static variation of pressure with depth. Where the action of gravity will become significant will be when the static equilibrium becomes upset - that is, when a free-surface *actually* distorts. This is discussed further in chapter 6.

Figure 5.55 shows the temporal acceleration and pressure responses obtained for horizontal oscillations of the floating body of figure 5.53. The agreement of the values of added masses obtained for both the horizontal and vertical acceleration modes with analytical values (obtainable from [11d]) is very good. These values were found to be independent of the magnitude of the acceleration applied and correspond to the analytical values of added mass calculated for the body oscillating at infinite frequency where, theoretically, no actual distortion of the interface would occur. The variations of added masses calculated at lower frequencies, therefore, should be associated with averaged components of temporal pressure loading when the free-surface is actually distorted. It was thought that this effect could not be studied further until the facility for effecting actual free-surface distortions and body movements with respect to the discretisation grid were incorporated in the test program FLOW2D. However, this matter is discussed further in chapter 6.

Figure 5.56 shows the temporal acceleration and pressure responses obtained for a combination of horizontal and vertical oscillations of the floating body. The values of added masses obtained from the vertical and horizontal resolution of the temporal pressure forces on the body illustrate the linearity of the added mass characteristics.

3.9.2 Wave Disturbances Around a Body in a Stream

Figure 5.57 shows the acceleration response obtained whilst attempting to determine the initial free-surface distortion around the same body as figure 5.53, but this time in a free stream. What happens, of course, when accelerating the stream with respect to the body in the presence of the free-surface is that a tended wave distortion (quite reasonably) occurs in the vicinity of the upstream and downstream "pressure plates" as well as at the body. This is, perhaps, a promising example of how the "direct" approach to fluid modelling does not allow you to do anything which is unphysical. Certain "fiddles" to this problem were briefly envisaged. For example, it might have been possible to create a

virtual accelerating stream whose temporal pressure would not distort the interface, and then introduce the body separately with only the resulting disturbances influencing the free-stream. Again, of course, this was against the ideals of the research. Besides, with the promising convective pressure results obtained from accelerating bodies (section 3.8.5), it looked as if such fiddles should be (quite rightly) unnecessary.

4. DISCUSSION

Referring back to the guidelines for this phase of the work presented in section 2, rather more effort than expected was required to re-develop the inviscid temporal pressure generation algorithm and to synthesise convective pressure. This meant that rather less progress was made on the free-surface distortion problem than was hoped. Nevertheless, it is believed that as a result of the effort involved a clearer insight has been gained into the "workings" of fluids, and that as hoped for in chapter 3 (section 1), by being faithful to the principles of physical transparency, the extra facility for understanding fluids using a computer model has begun to be realised. In chapter 6 a summarising presentation and discussion of the overall computer model that has been written should convey this, perhaps more demonstrably than the raw development work described in this chapter.

5. CLOSURE

This chapter has presented the work involved in re-developing the inviscid influence algorithms of Phase 1 along strictly physical lines. A new algorithm which synthesised temporal pressure and accelerations together was designed. Support for the algorithm was manifested by the fact that it allowed extension to pressure driven flow and flow in the presence of free-surfaces without any modifications. It could also be used to physically create a gravitational variation of pressure with depth in a fluid.

Much effort was spent on designing the algorithm to synthesise convective pressure in a system which was consistent for the "equivalent" cases of streaming flow past a stationary body and motion of a body in a stationary fluid. The results of this part of the work were probably the most significant product of the work of this thesis for they demonstrated that the non-linear problem of fluid pressure can be approached in a "modular" form. The results also show that this direct treatment (or at least the presentation of it), where individual mechanisms affecting flow behaviour are modelled separately, can lead to a greater understanding of fluid dynamics than the traditional composite equation approach.

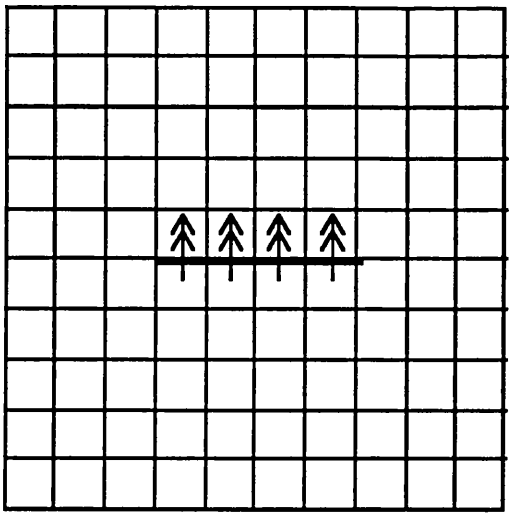

(a) INITIAL DISTURBANCE:-
The acceleration of the plate is equivalent to a fixed rate of change of flux across the region boundaries which are coincident with the plate surface. There is thus a tended build-up of fluid within the regions adjacent to the plate.

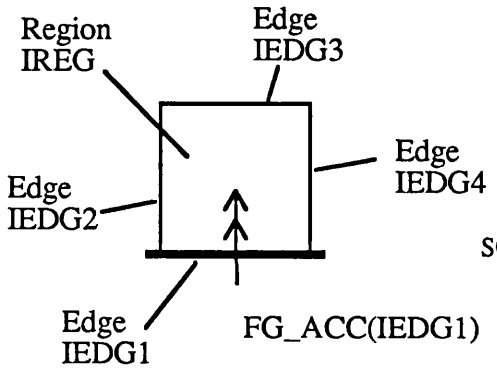

(b) The "stress state" of a region from (a) may be described by the "squeeze factor" definition. Here, the initial value for such a region is given simply by:-

$$SQF(IREG) = \frac{FG\_ACC(IEDG1) * AREA(IEDG1)}{VOLUME(IREG)}$$

(c) The tended build-up of fluid must be exhausted from the region evenly via all free sides. In the given case, relaxation gives the increments to the flow accelerations as shown. Note that this affects the SQF levels in neighbouring regions, and that such relaxation must be repeated throughout the system until the SQF levels are (near) zero.

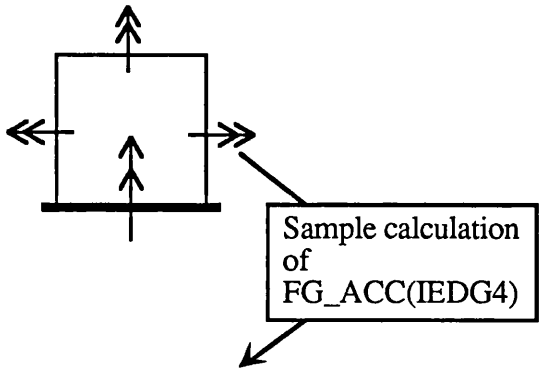

$$TAREA = AREA(IEDG2) + AREA(IEDG3) + AREA(IEDG4)$$

$$FG\_ACC(IEDG4) = FG\_ACC(IEDG4) + (SQF(IREG)*VOLUME(IREG)) * \frac{AREA(IEDG4)}{TAREA}$$

Figure 5.1 Inviscid Modelling Scheme of Phase 1

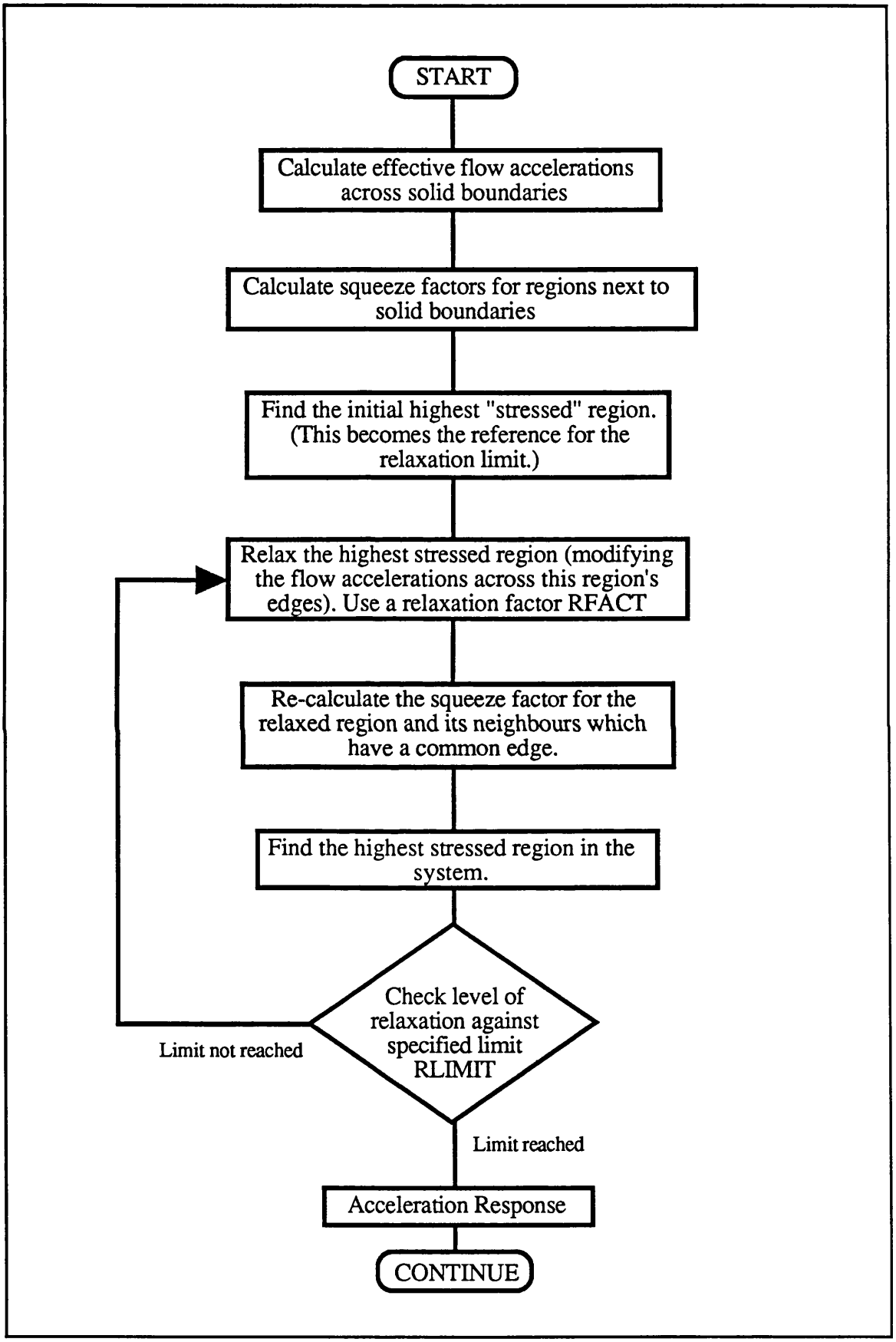

Figure 5.2 Flowchart of the Relaxation Technique of Phase 1

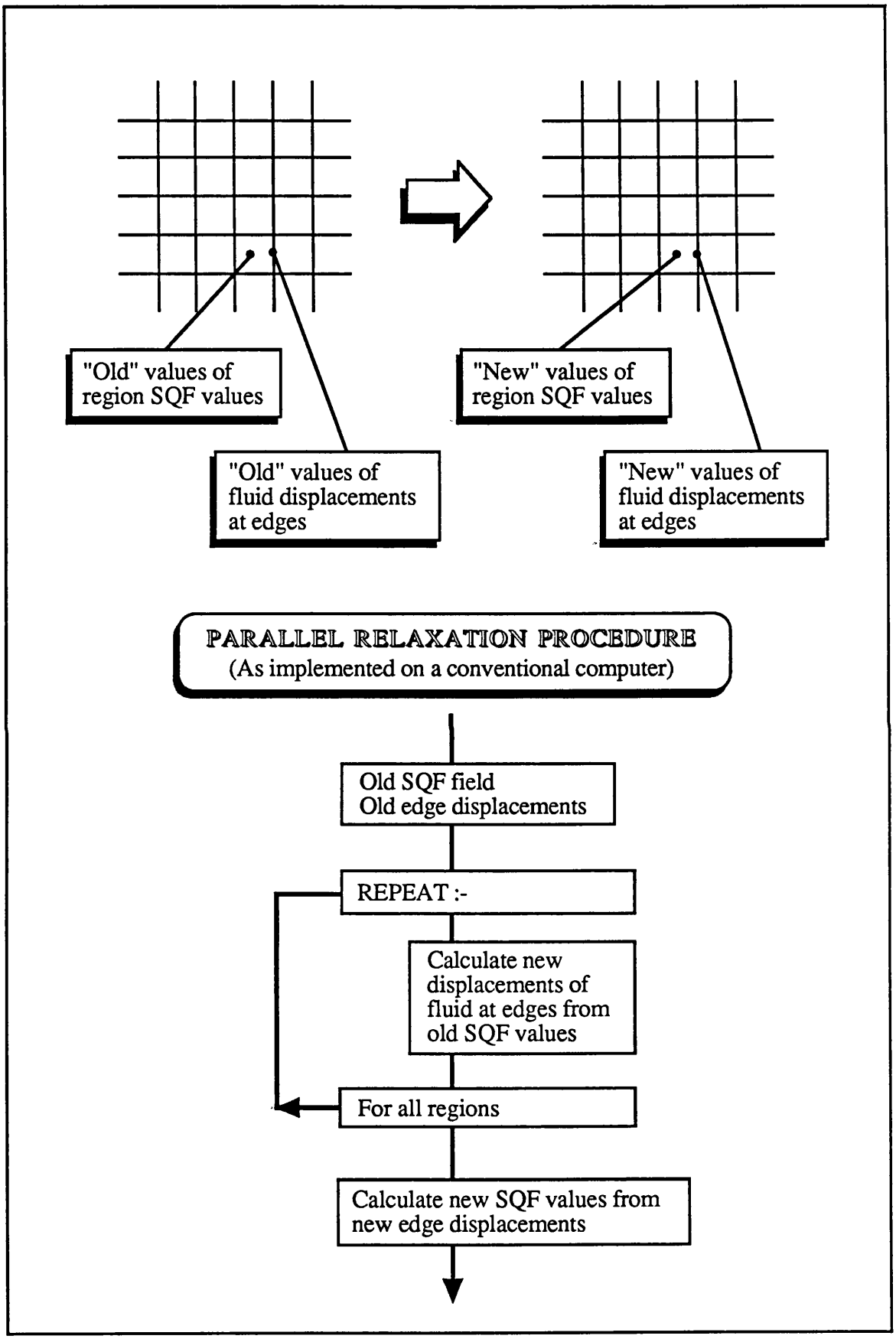

Figure 5.3 Parallel Relaxation

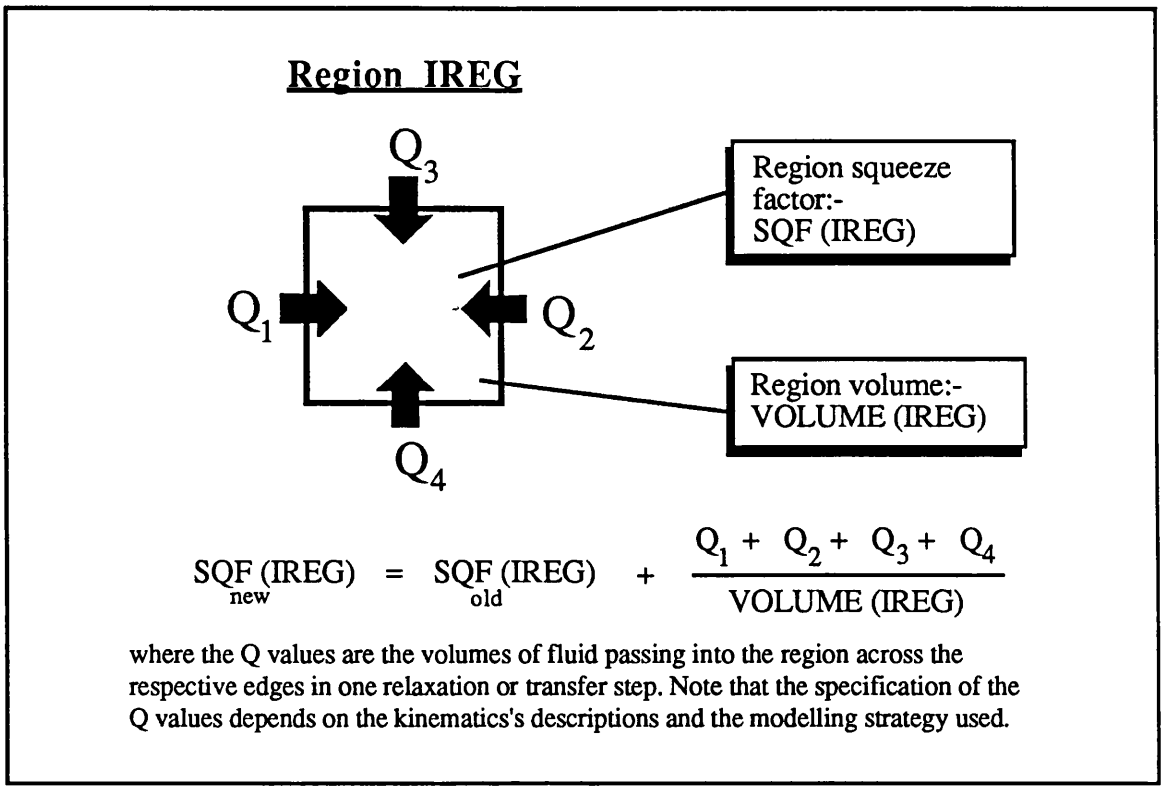

Figure 5.4 New Definition of Squeeze Factor

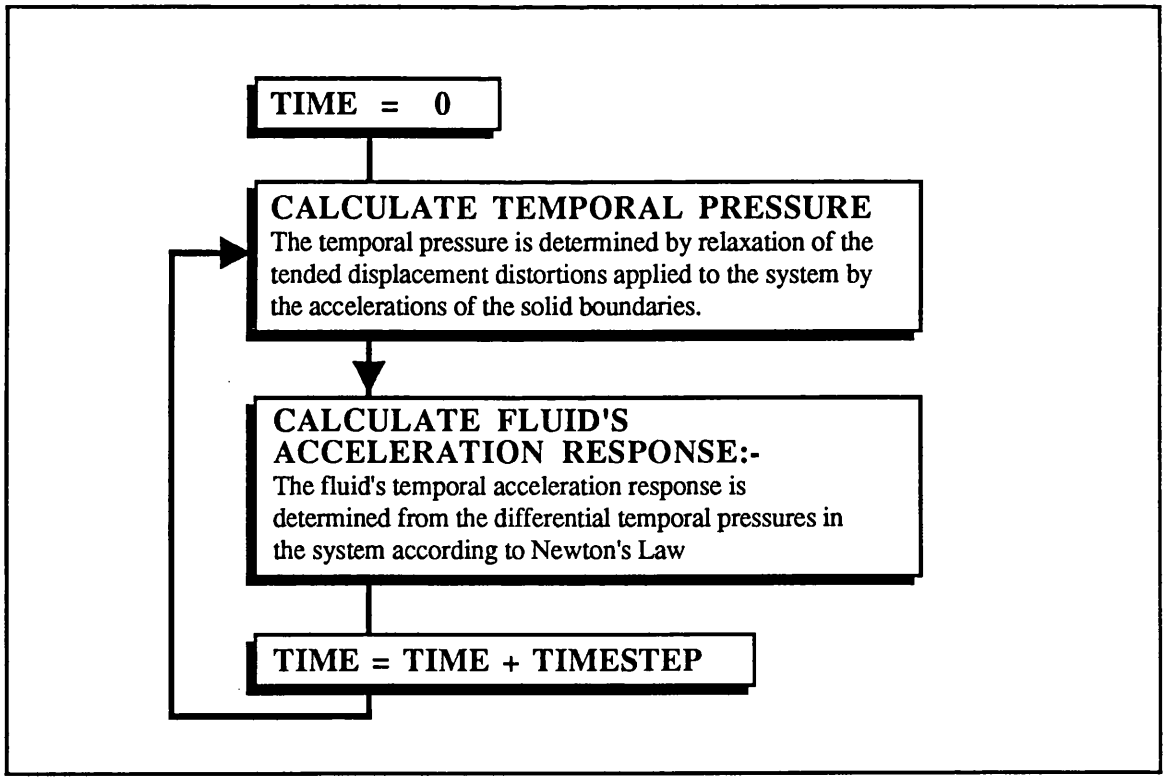

Figure 5.5 Pressure-FOR-Acceleration Strategy

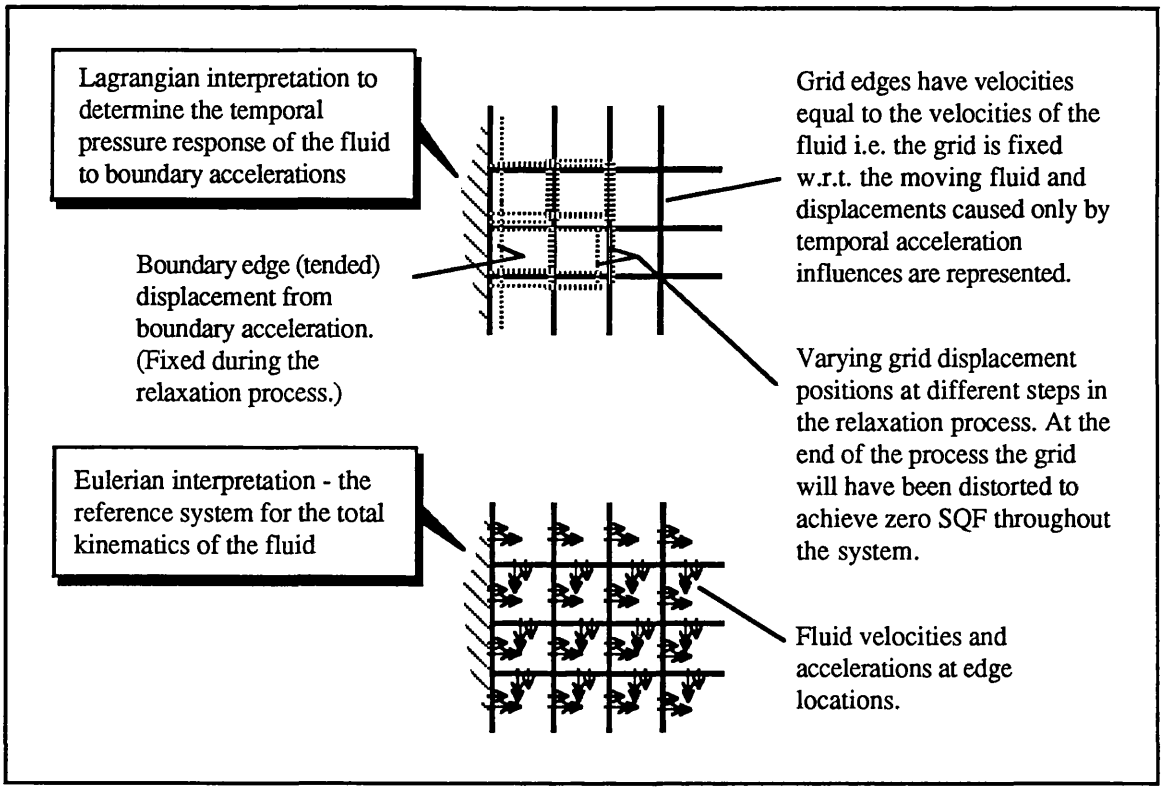

Figure 5.6 Two Interpretations of Grid Discretisation in the Pressure-FOR-Acceleration Strategy

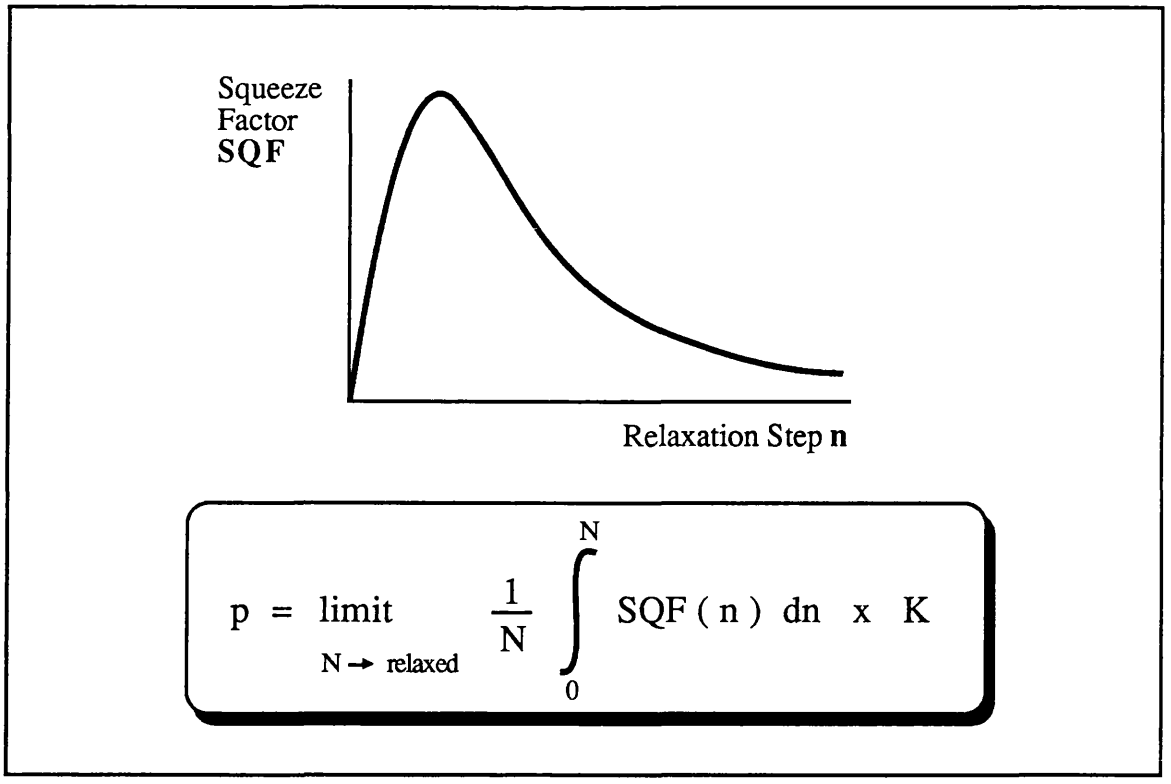

Figure 5.7 Interpretation of Pressure from the Relaxation Process (Pressure-FOR-Acceleration Approach)

Consider region IREG and its neighbours:-

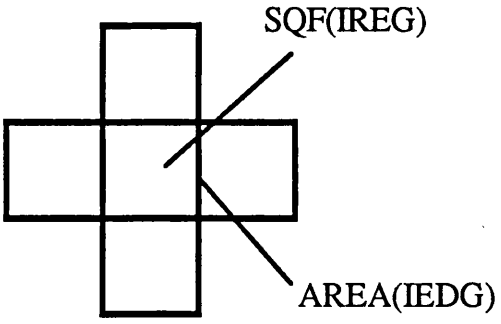

If region IREG has a squeeze factor of SQF(IREG) at a given step in the relaxation process, this corresponds to a build-up of fluid in the region which, for an incompressible fluid, cannot be sustained. The tendency, therefore, will be to exhaust this excess fluid and this is done equally across all fluid edges in the old relaxation technique. Increments to the edge displacements, then, are calculated as follows:-

$$DINC(IEDG) = -\,RFACT * \{\, SQF(IREG) * VOLUME(IREG) \,\} * \frac{AREA(IEDG)}{TAREA}$$

Minus sign because +ve DINCs are INTO region

A relaxation factor

Total build-up of fluid at given stage in relaxation process

Exhaust proportioned according to area of edge to the total area TAREA available for removal of fluid

-ve DINCs arising from a +ve SQF(IREG)

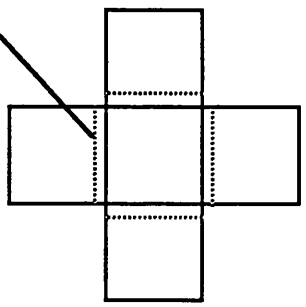

Note that with the parallel relaxation technique there will be another contribution to each DINC in a given relaxation step coming from relaxation of the neighbours

Figure 5.8 The Old Relaxation Approach

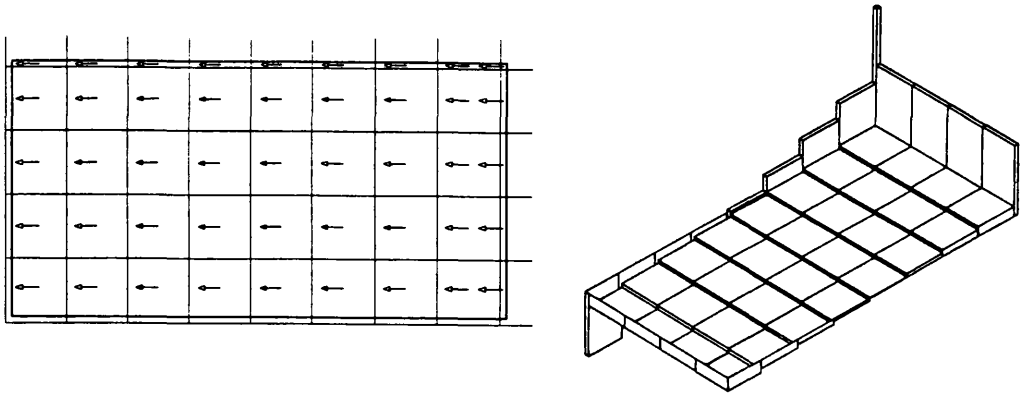

(a) Example of channel flow with non-uniform discretisation, showing "balanced" grid displacements after relaxation and a picture of the integrated SQF levels during the relaxation process.

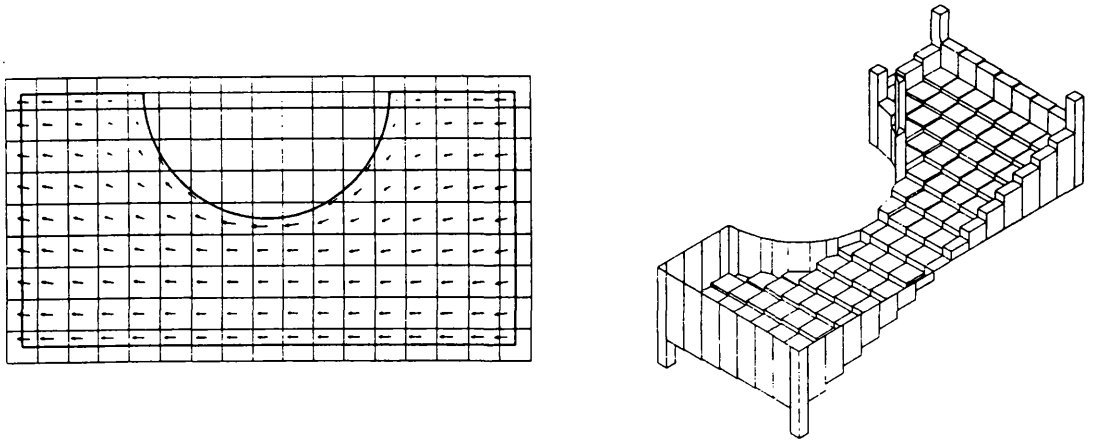

(b) Example of flow around a half cylinder.

Figure 5.9 Results Obtained for Integrated SQF Distribution with the Old Relaxation Technique

Consider a simple example of developing uniform channel flow, where variations in SQF are effectively one-dimensional:-

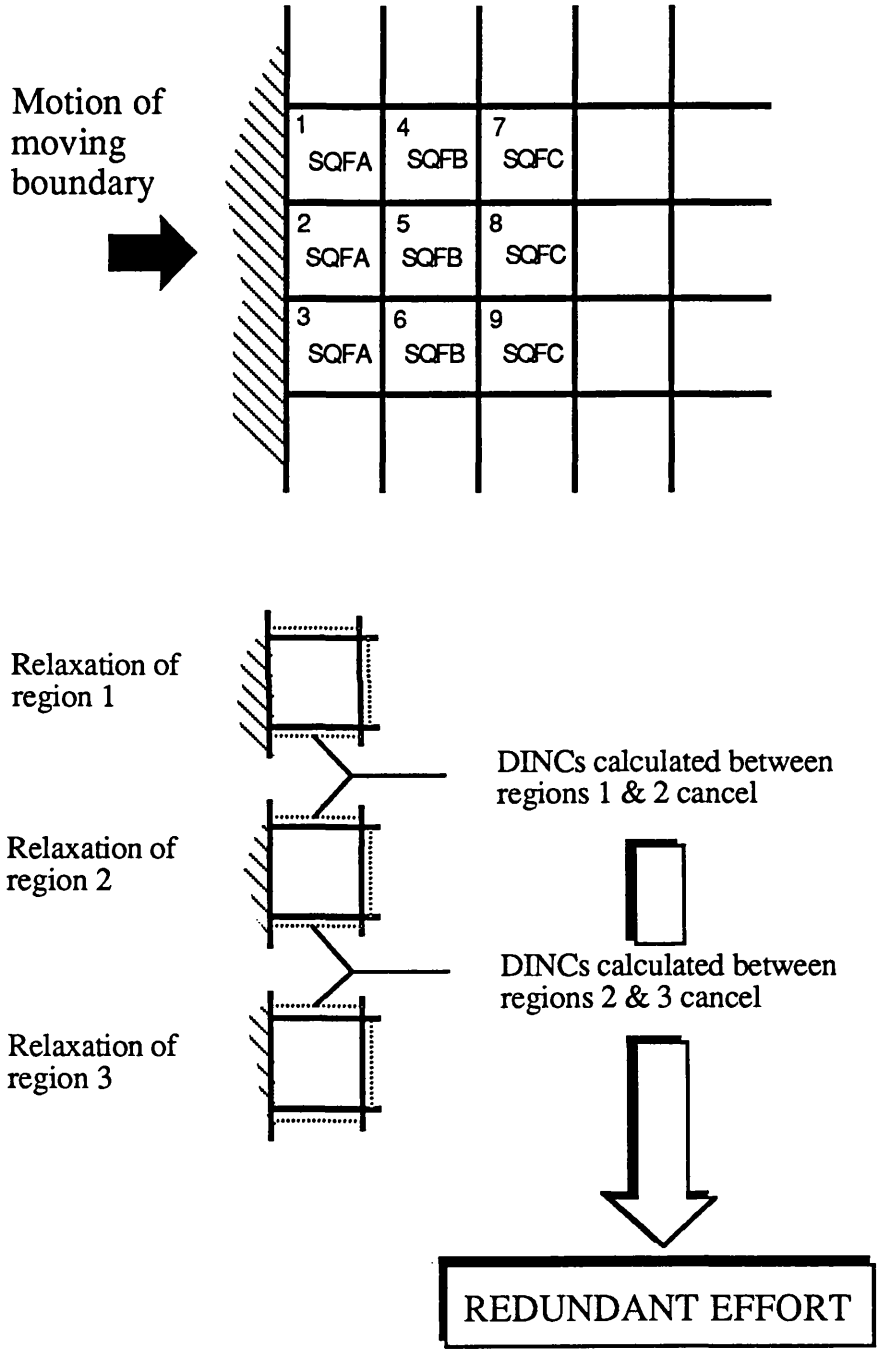

Figure 5.10 Redundancy of Effort in the Old Relaxation Process

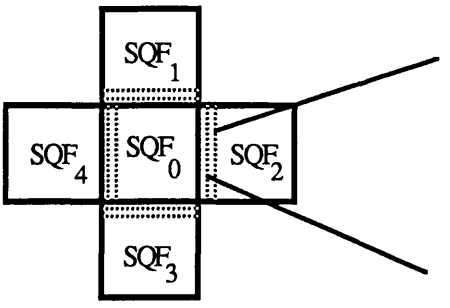

Edge displacement increment (DINC) tendency to equalise SQF between adjacent regions

Moderated DINC, based on other tended DINC values for other edges of the given region. The net effect is a reduction of SQF for the given region to an averaged value with the neighbouring regions.

Procedure:-

Step 1. Determine DINC for each region if it were to equalise SQF values between the associated regions on its own (i.e. not considering other edge displacements).

Step 2. Sum these tended outflows as

$$S\_DINC\_AREA = \sum_{\text{All edges}} DINC * AREA$$

for the region.

Step 3. Scale each of the tended DINC values by the proportion of its contribution to S_DINC_AREA

$$DINC = RFACT * DINC * \left| \frac{DINC * AREA}{S\_DINC\_AREA} \right|$$

Figure 5.11 Outline of the New Relaxation Technique

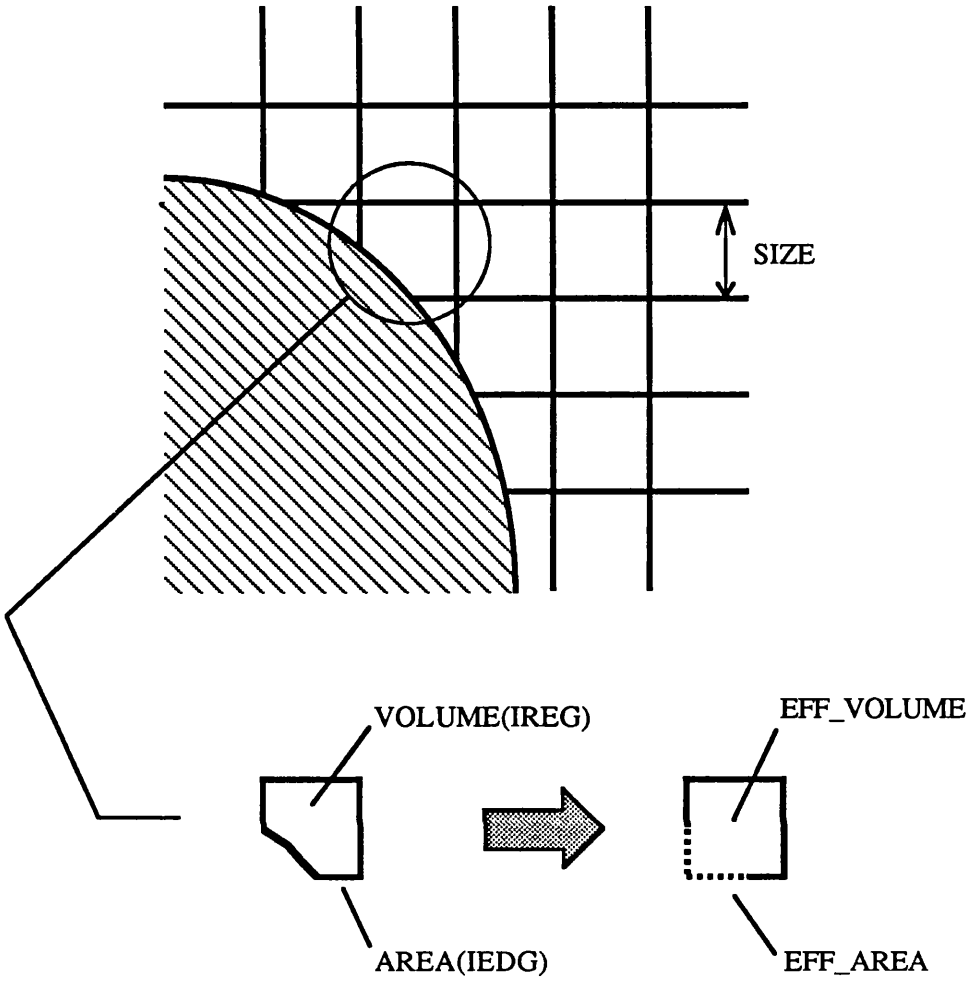

For partial regions, DINC values (see figure 5.11) are calculated using SQF values related to an effective volume EFF_VOLUME rather than the actual region volume VOLUME(IREG). Also, edge contributions are based on an effective area EFF_AREA rather than the actual area AREA(IEDG) of edges.

Note that if SIZE is the size of the discretisation grid at the given level of subdivision, then

$$\text{EFF\_VOLUME} = \text{SIZE} * \text{SIZE}$$
$$\text{EFF\_AREA} = \text{SIZE}$$

Figure 5.12 The Use of Effective Volumes/Areas for Relaxation of Partial Regions

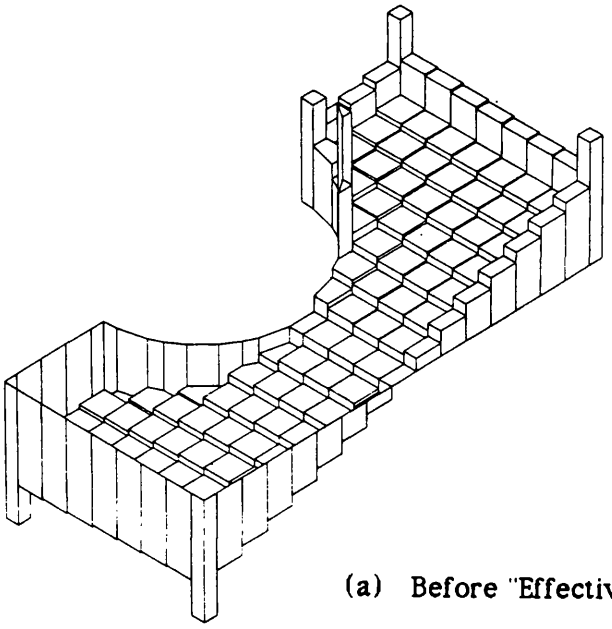

(a) Before "Effective Region" Modelling

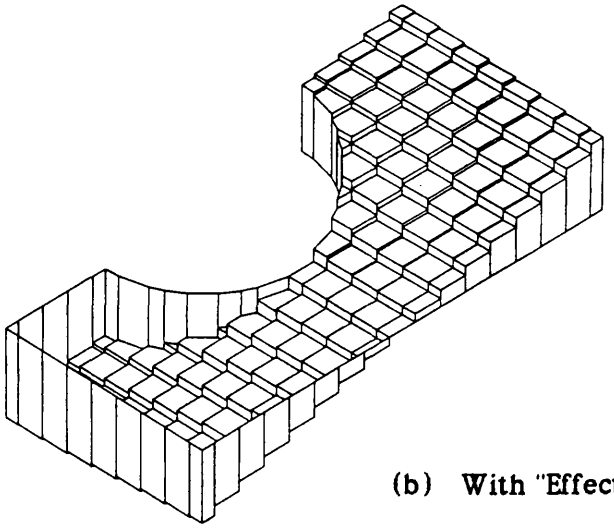

(b) With "Effective Region" Modelling

Figure 5.13 Improvements in the Form of the Pressure Field Using "Effective Region" Modelling of Partial Regions

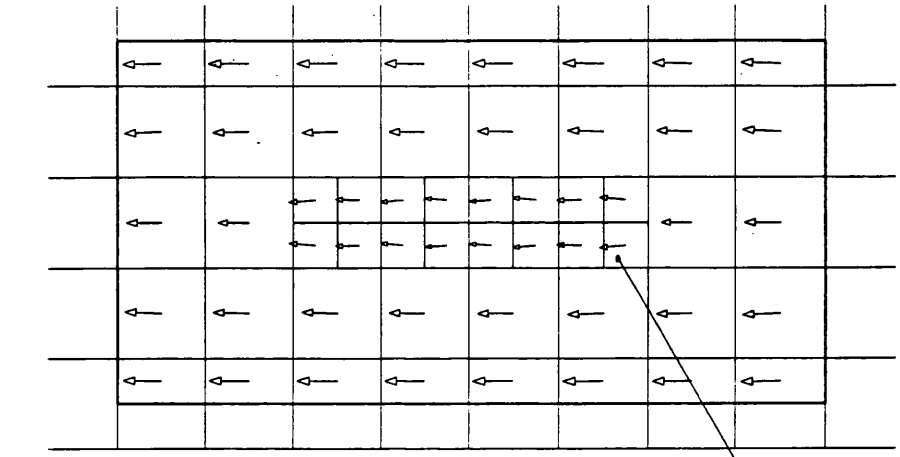

Flow "blockage" created in way of subdivision.

Accumulation of fluid in smaller regions.

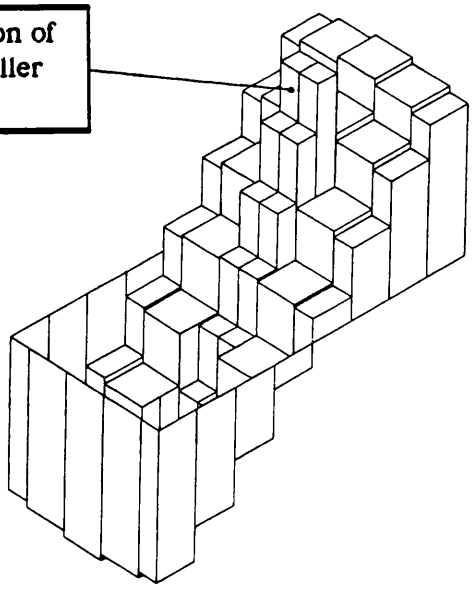

Figure 5.14 Problems Associated with Relaxing a System Using the Same Number of Steps for Each Discretisation Level

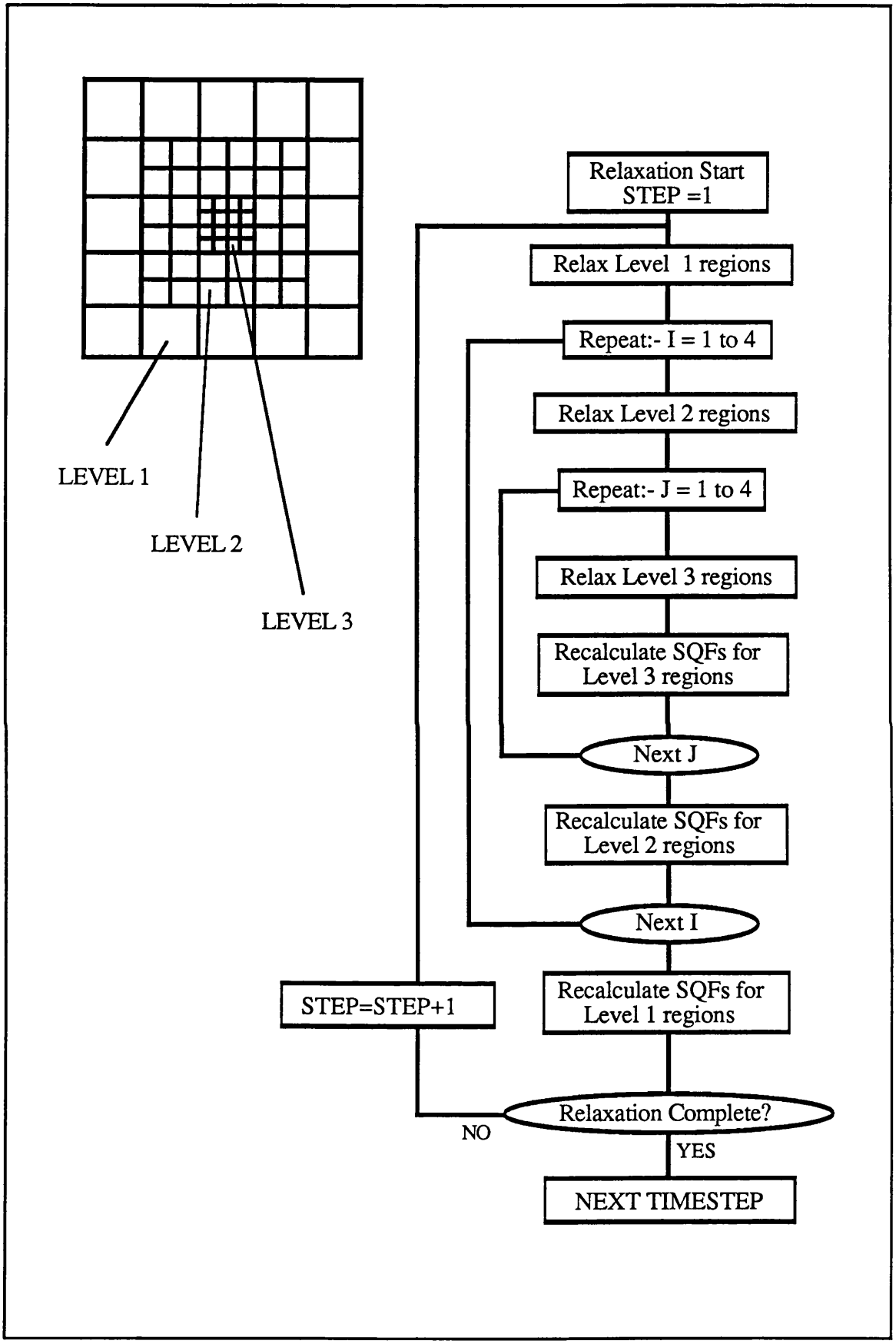

Figure 5.15 Relaxation Flowchart for a Sub-Divided System

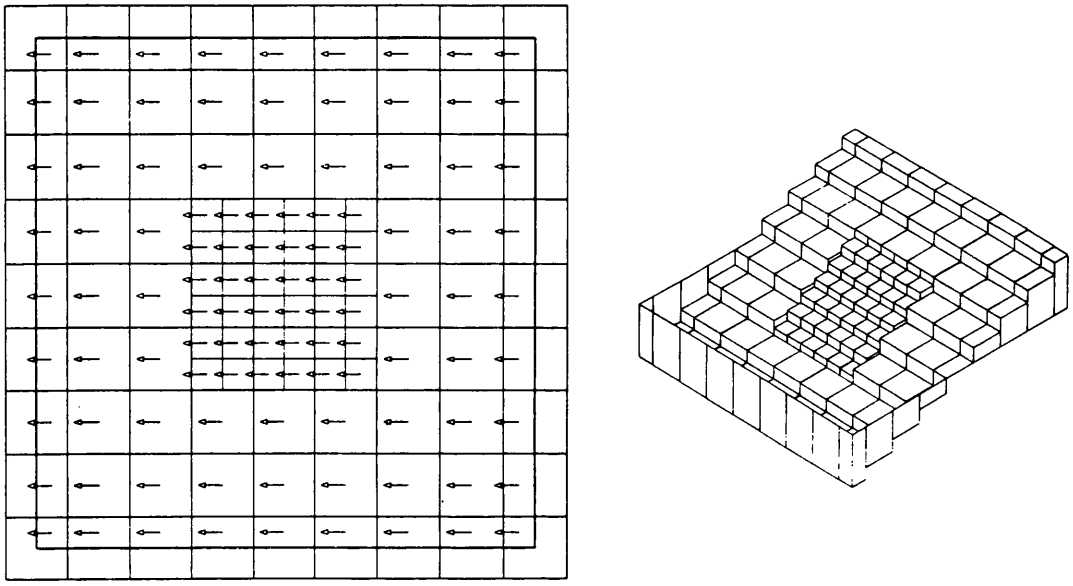

Example of channel flow

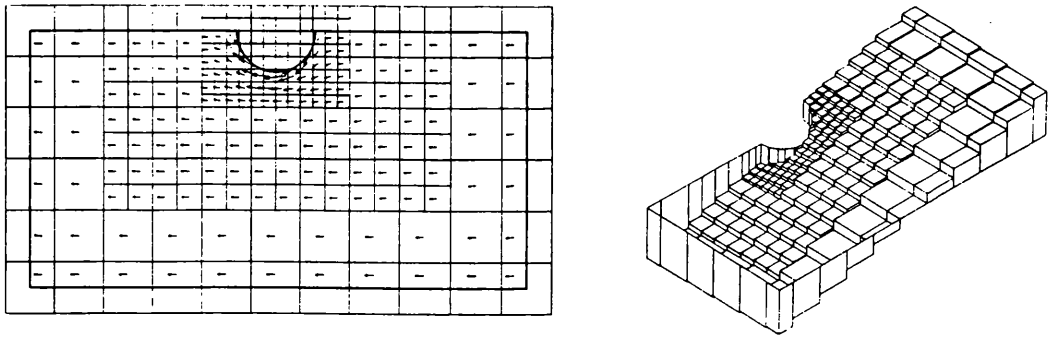

Example of flow past a circular cylinder

Figure 5.16 Improved Results for Sub-Divided Systems

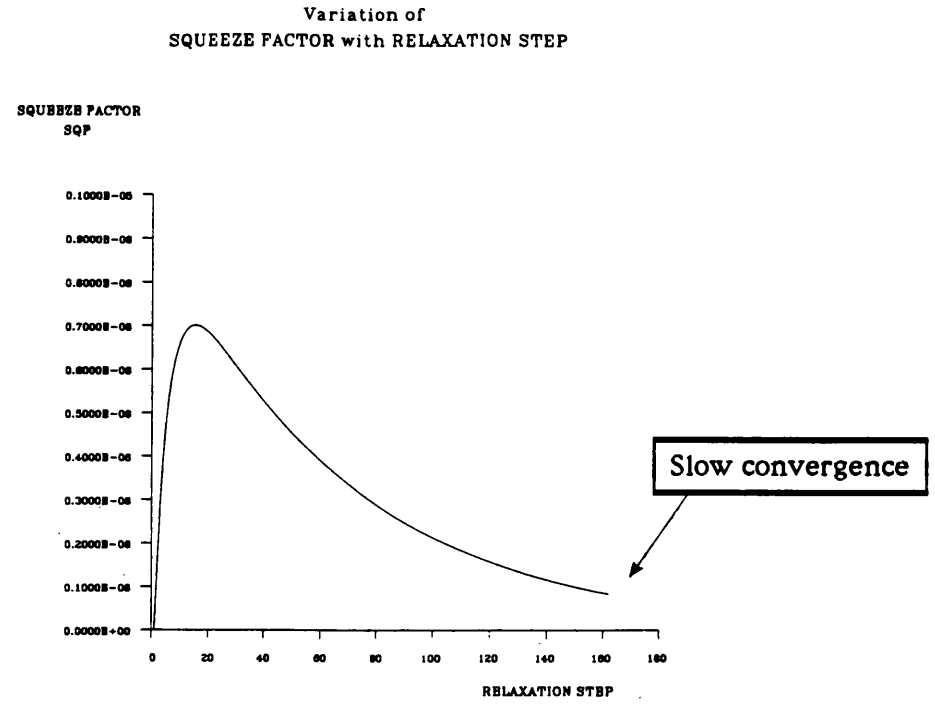

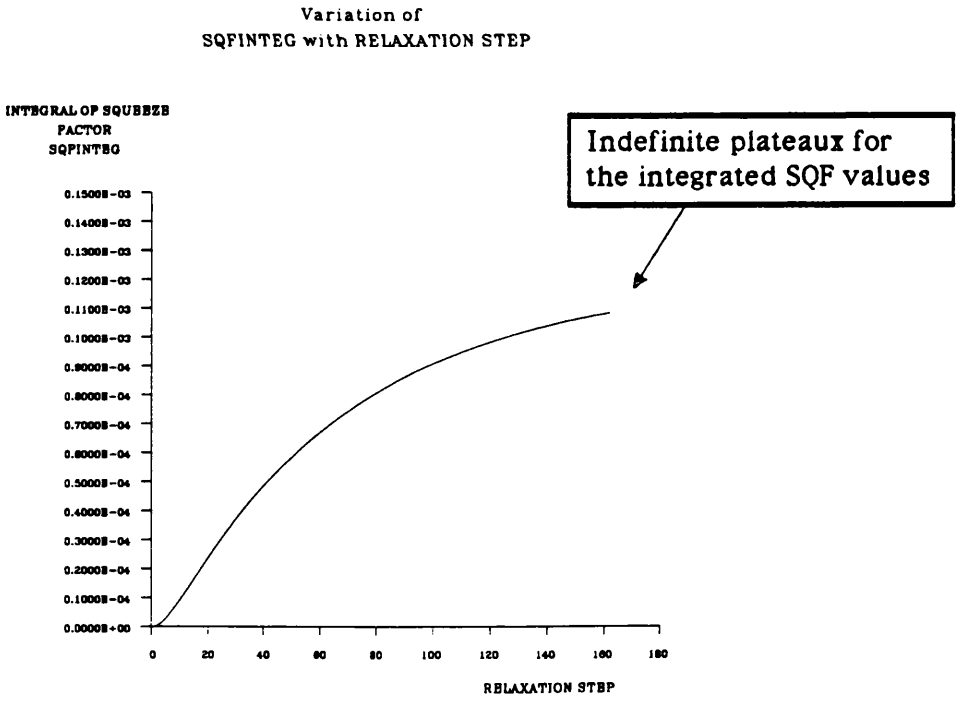

Figure 5.17 The Problems of Scaling from Integrated SQF (SQFINTEG) to Pressure

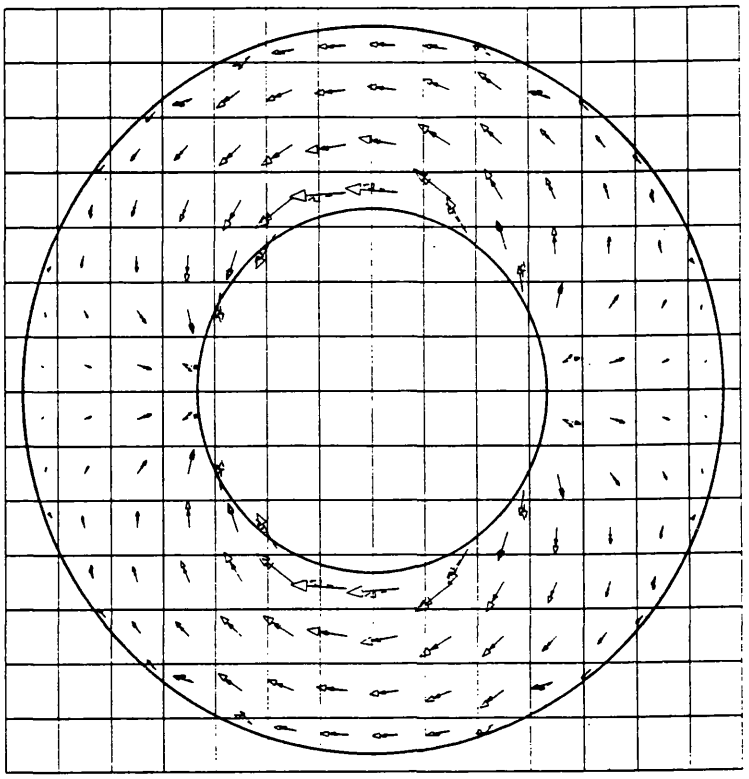

(a) Superposition of Acceleration Response from SQFINTEG/Pressure Distribution (Solid Vectors) and Acceleration deduced from Scaling of Relaxed Edge Displacements (Dashed Vectors)

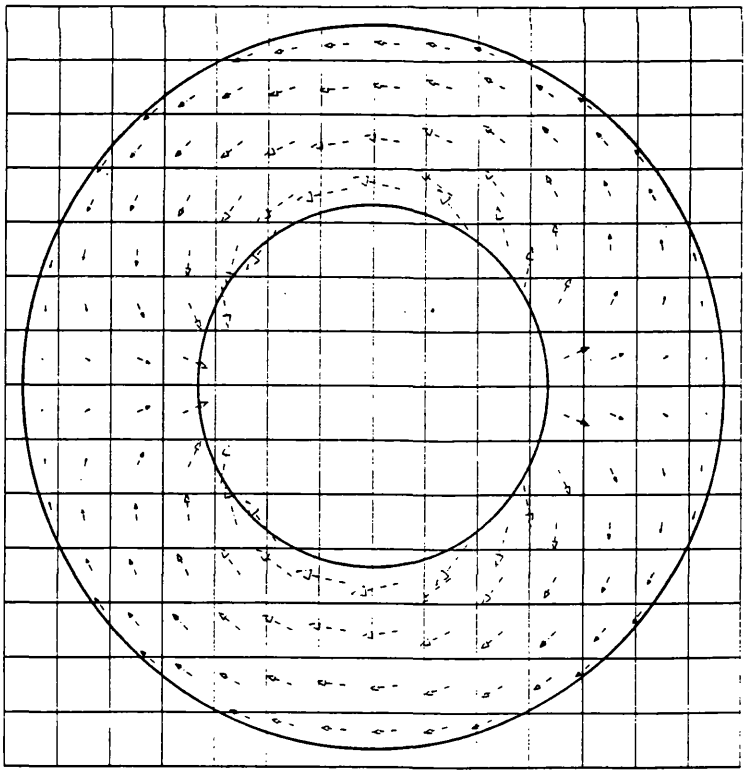

(b) Analytical Solution

Figure 5.18 Acceleration Response Predictions from Pressure-FOR-Acceleration Technique

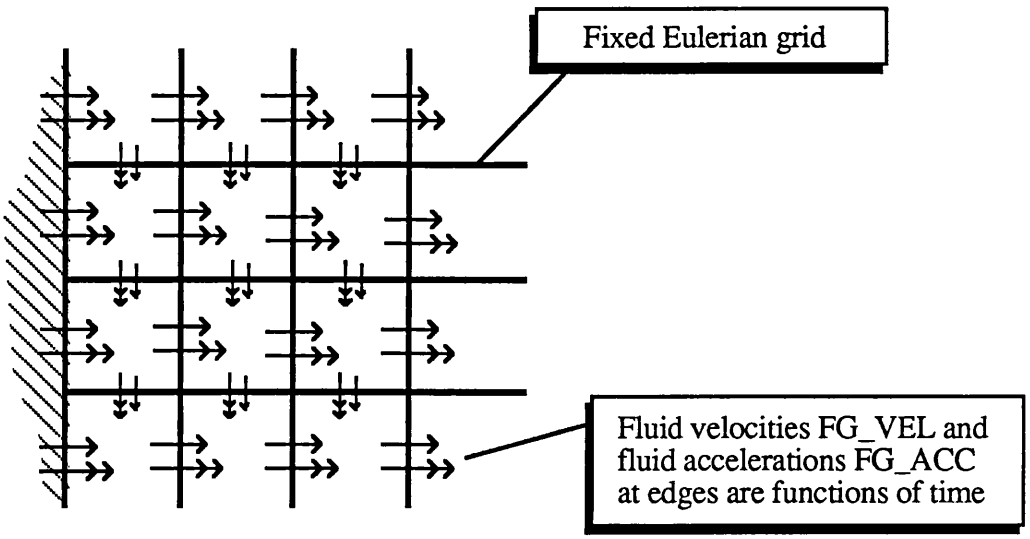

During a sub-timestep DT the volume of fluid passing across an edge IEDG into a region is given by:-

FG_DISP(IEDG) * AREA(IEDG)

where

$$FG\_DISP(IEDG) = FG\_VEL(IEDG) * DT + 0.5 * FG\_ACC(IEDG) * DT^2$$

The SQF values for each region will be altered according to figure 5.4 where the Q values are given by:-

$$Q = FG\_DISP(IEDG) * AREA(IEDG)$$

The resulting pressure in a region will then be given by:-

$$PRESS(IREG) = SQF(IREG) * BULKMOD$$

where BULKMOD is the bulk modulus of the fluid.

Between sub-timesteps the kinematics are altered by the driving influence of the pressure levels according to the "transfer model" used. (E.g. see figure 5.20.)

Figure 5.19 Pressure Synthesis in the Time Domain

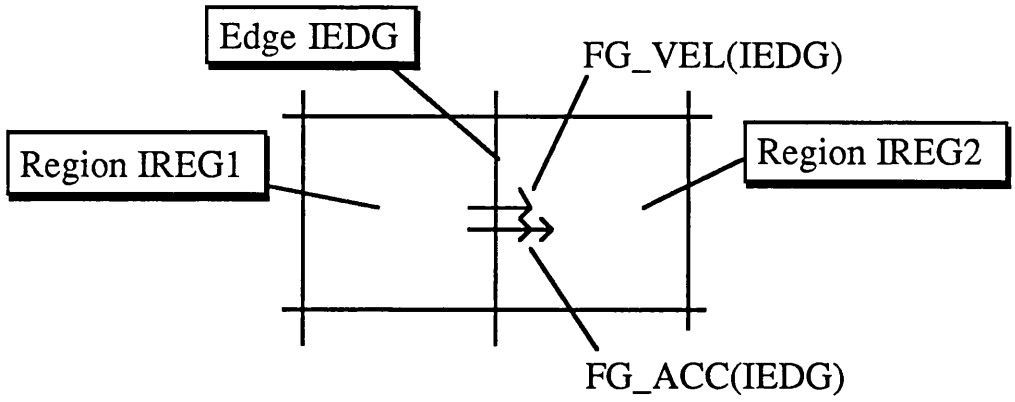

Effectively applying Euler's equation to the fluid local to the edge IEDG, where

$$\text{PRESS(IREG1)} = \text{SQF(IREG1)} * \text{BULKMOD}$$

$$\text{PRESS(IREG2)} = \text{SQF(IREG2)} * \text{BULKMOD}$$

DIST = distance between centres of regions

$$\text{PRESS\_GRAD} = \frac{\text{PRESS(IREG1)} - \text{PRESS(IREG2)}}{\text{DIST}}$$

V_DV_DS = convective acceleration

gives the temporal acceleration at the edge:-

$$\text{FG\_ACC(IEDG)} = \frac{\text{PRESS\_GRAD}}{\text{DENSITY}} - \text{V\_DV\_DS}$$

from which the new value of fluid velocity can be deduced as:-

$$\text{FG\_VEL(IEDG)} = \text{FG\_VEL(IEDG)} + \text{FG\_ACC(IEDG)} * \text{DT}$$

With the new values of FG_VEL and FG_ACC the pressure levels in the system can be updated as described in figure 5.19.

Figure 5.20 Explicit Edge Driver in the EDGE TRANSFER METHOD of Spreading the Pressure in the Pressure-AND-Acceleration Strategy

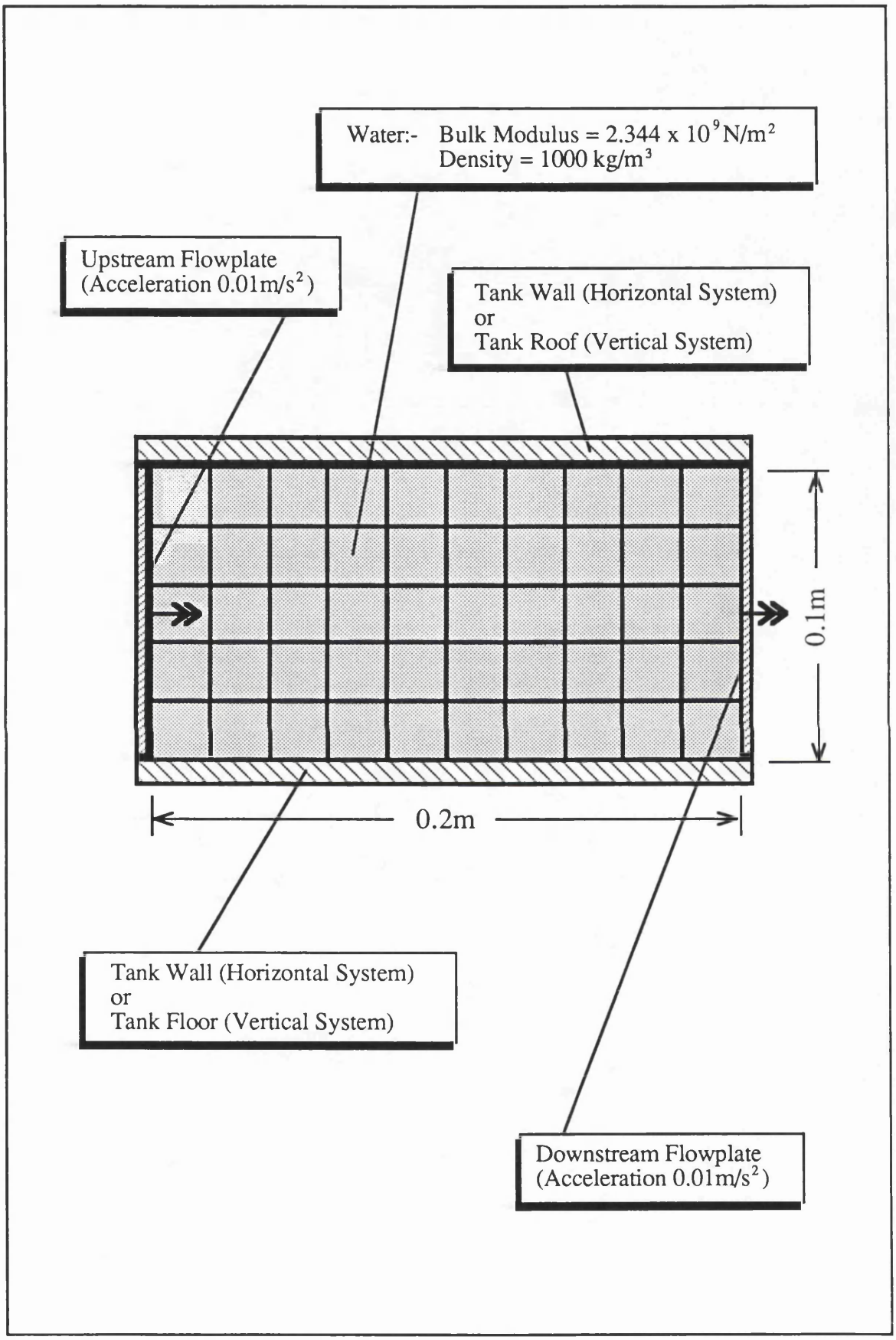

Figure 5.21 Computer "Test Tank" Set-Up

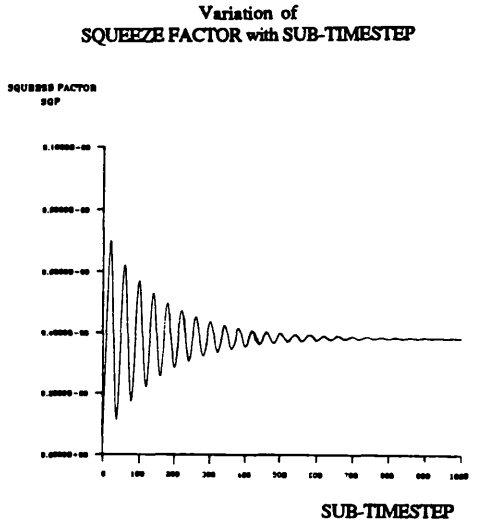

(a) SQF response in regions adjacent to the upstream flowplate

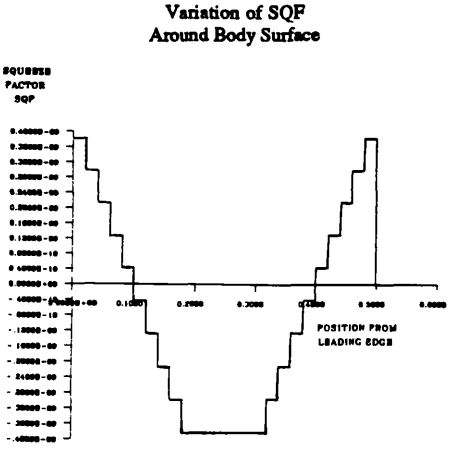

(b) SQF distribution around the walls of the tank after 1000 sub-timesteps. Equivalent pressure gradient along the tank = 9.6 Pa/m

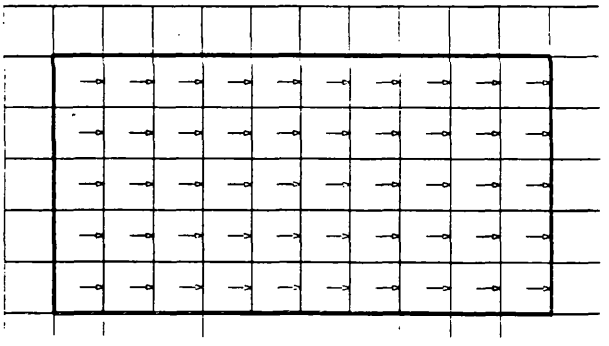

(c) Acceleration response after 1000 sub-timesteps (scale x1)

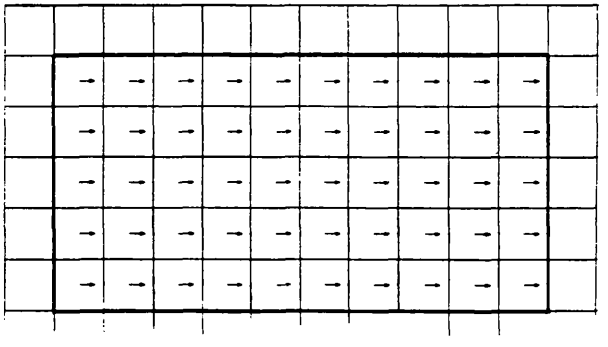

(d) Velocity response after 1000 sub-timesteps (scale x100)

Figure 5.22 Results for Developing Channel Flow in the Computer Test Tank

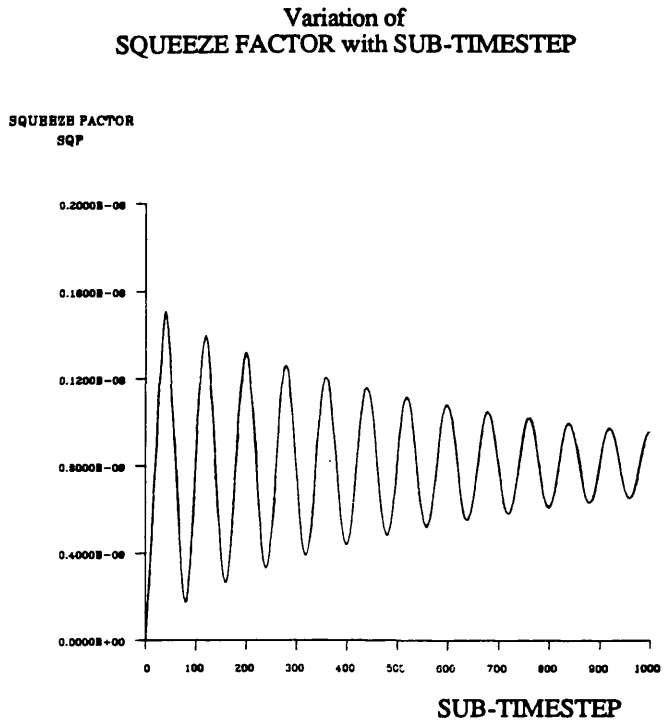

(a) Results for a test tank twice as long as that in figure 5.21.

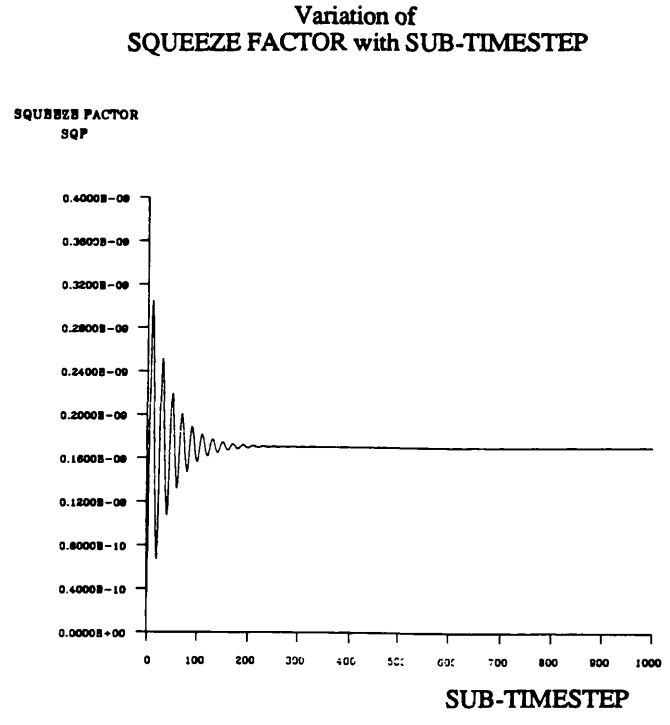

(b) Results for a test tank half as long as that in figure 5.21.

Figure 5.23 Effects of Tank Aspect Ratio on the Pressure Response

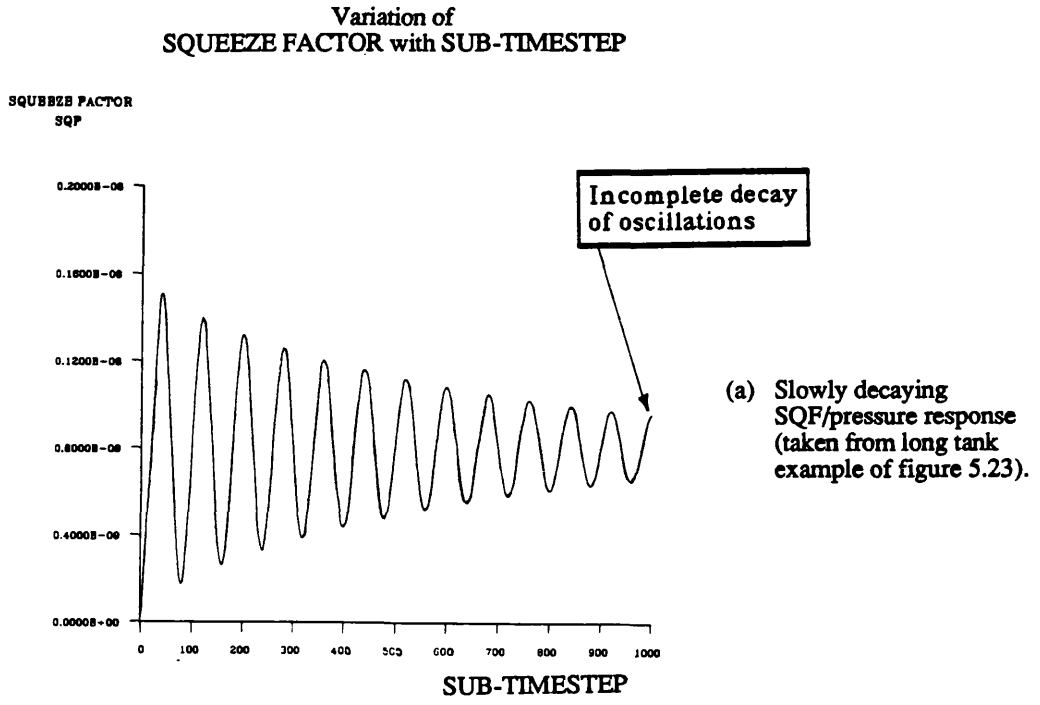

(a) Slowly decaying SQF/pressure response (taken from long tank example of figure 5.23).

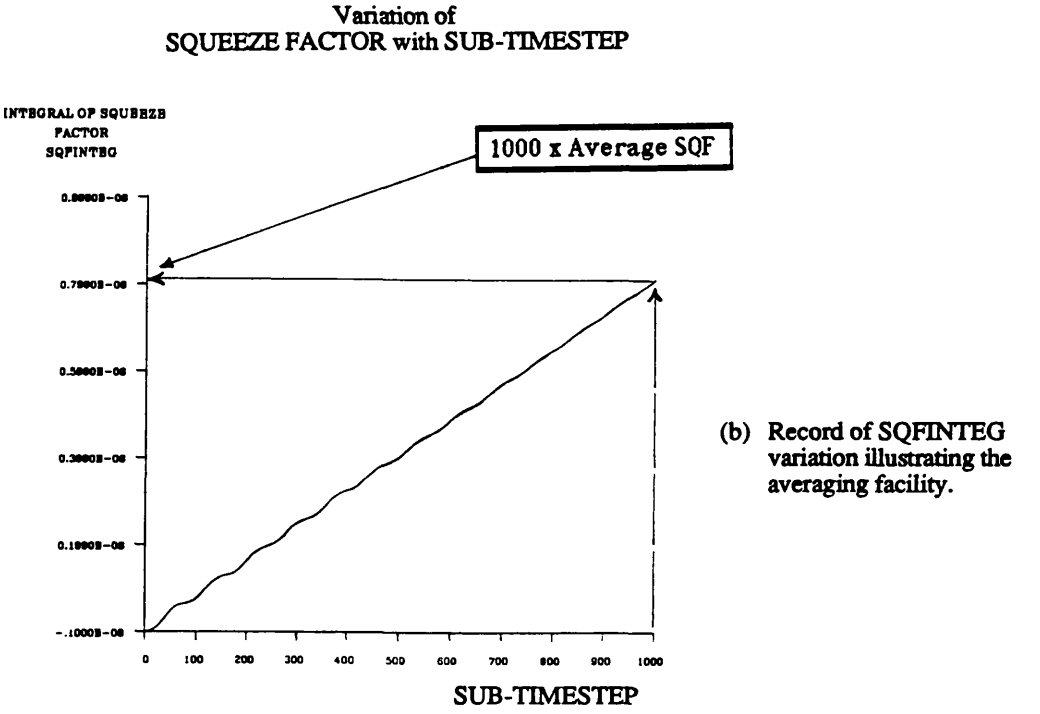

(b) Record of SQFINTEG variation illustrating the averaging facility.

Figure 5.24 The Smoothing Effects of SQFINTEG - Facilitating Early Pressure Estimation

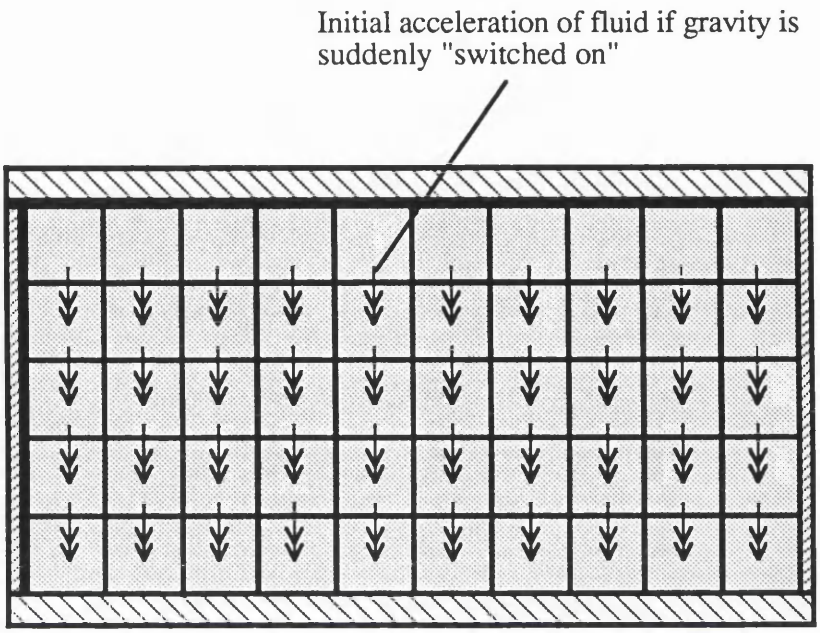

The model in words:-

Fluid at rest with no gravity acting.

Gravity is "switched on".
This causes an initial acceleration of fluid across all horizontal free edges. In turn, this causes a pressurization in regions adjacent to the floor (+ve) and the roof (-ve).

The pressurization will modify the edge accelerations accordingly and the process will continue until an equilibrium condition is reached.

The model is effected by including the gravitational acceleration in the expression for FG_ACC for horizontal edges (see figure 5.20):-

$$FG\_ACC(IEDG) = \frac{PRESS\_GRAD}{DENSITY} - GRAVITATION - V\_DV\_DS$$

Figure 5.25 Modelling Pressure with Depth

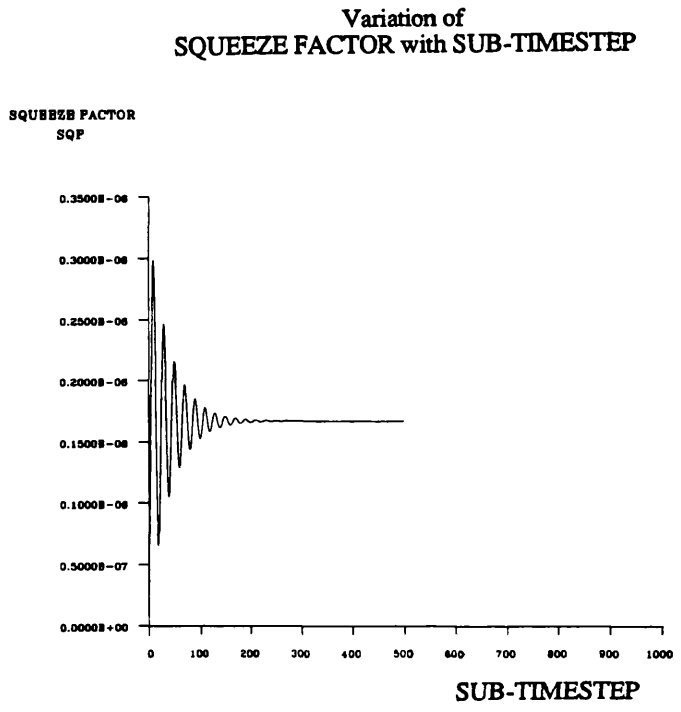

(a) Pressure response in the region adjacent to the floor of the tank (see figure 5.21).

SQF at lowest regions in tank = 1.67×10^{-7}
gives pressure = SQF x 2.344×10^{9} = 392Pa

(Check with $p = h\rho g \rightarrow 0.04m \times 1000kg/m^3 \times 9.81m/s^2 = 392Pa$)

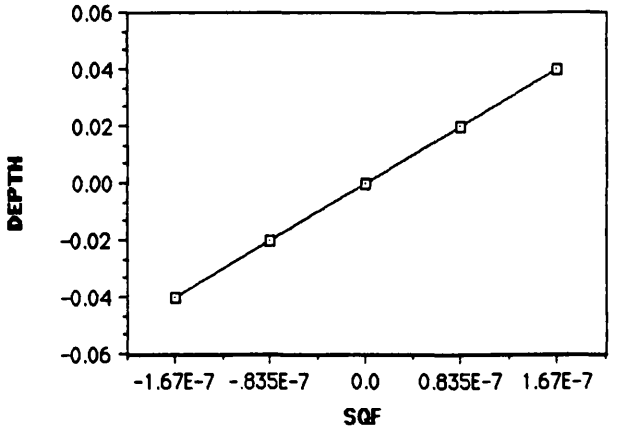

(b) Variation of pressure with depth in equilibrium.

Figure 5.26 Pressure Variation with Depth Using the Pressure-AND-Acceleration Method

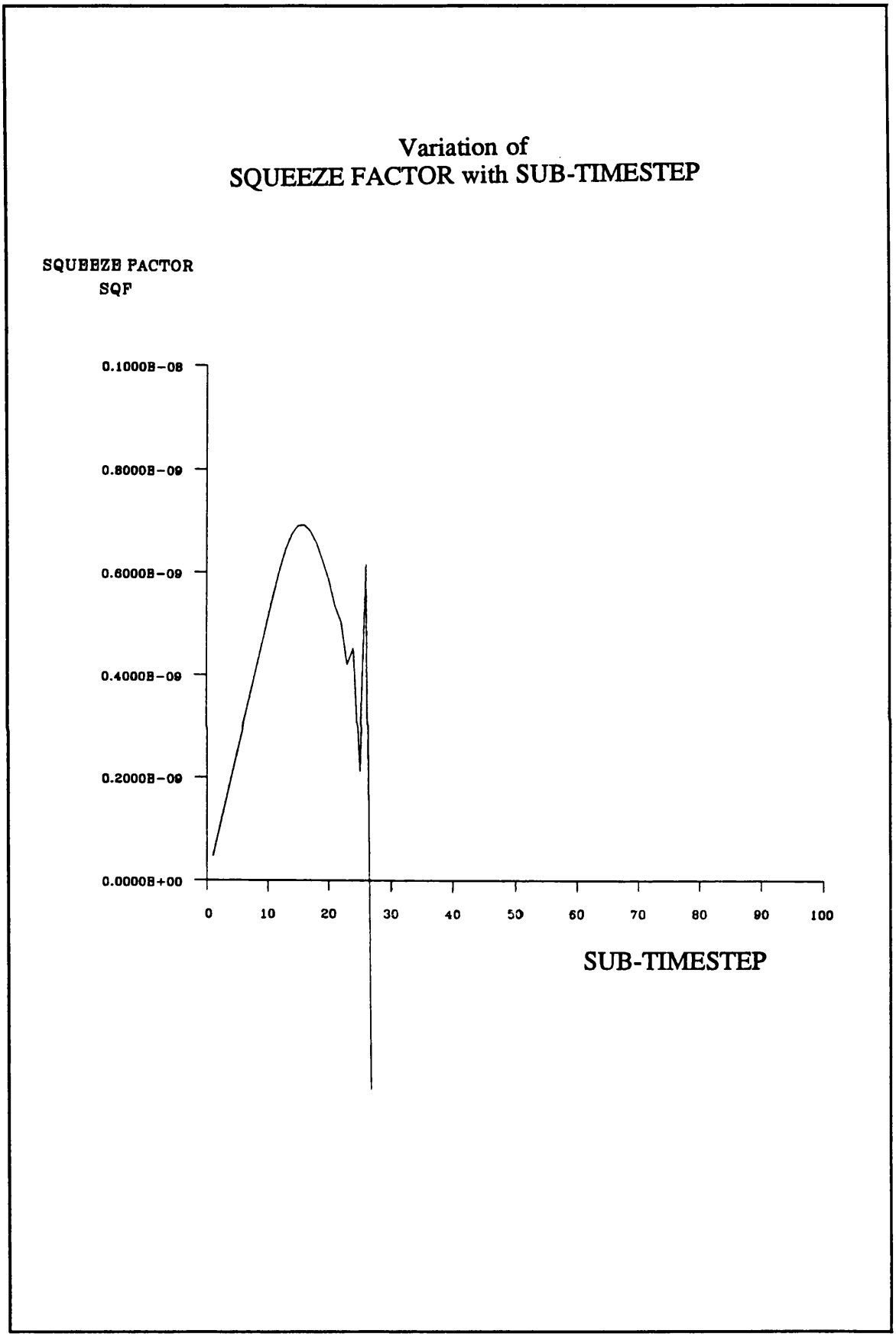

Figure 5.27 Manifestation of Instability with the Edge Transfer Method

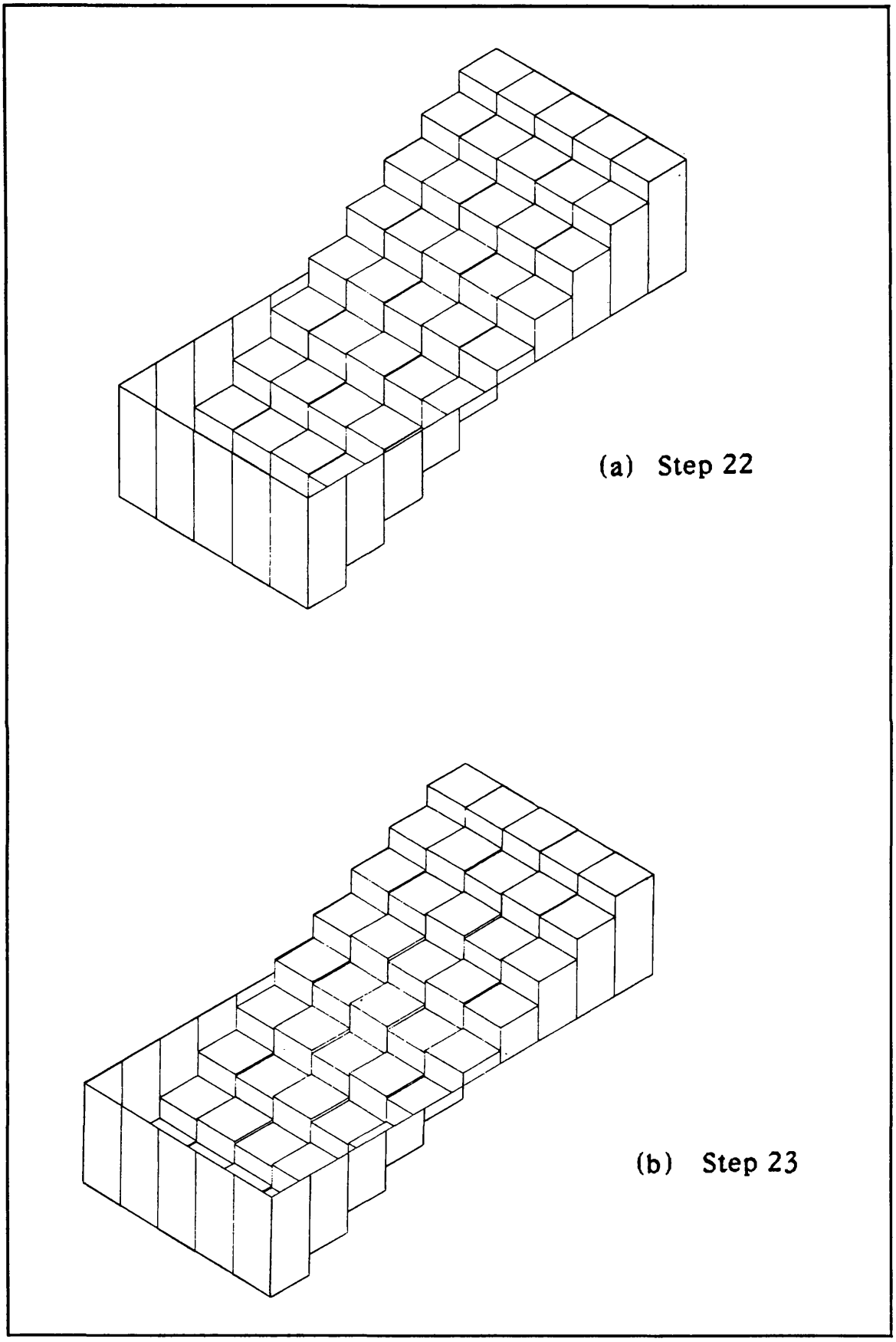

Figure 5.28 Nature and the Development of the Instability in the Pressure Field

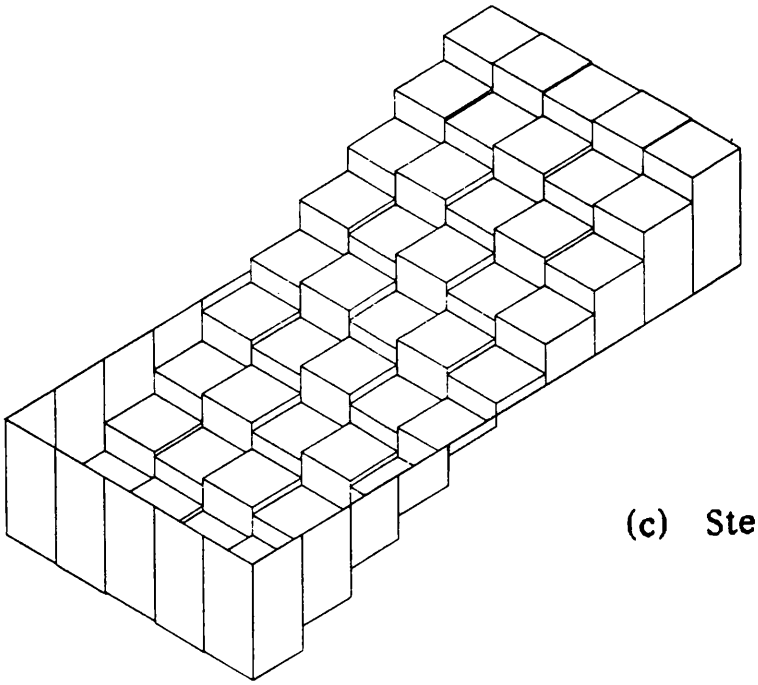

(c) Step 24

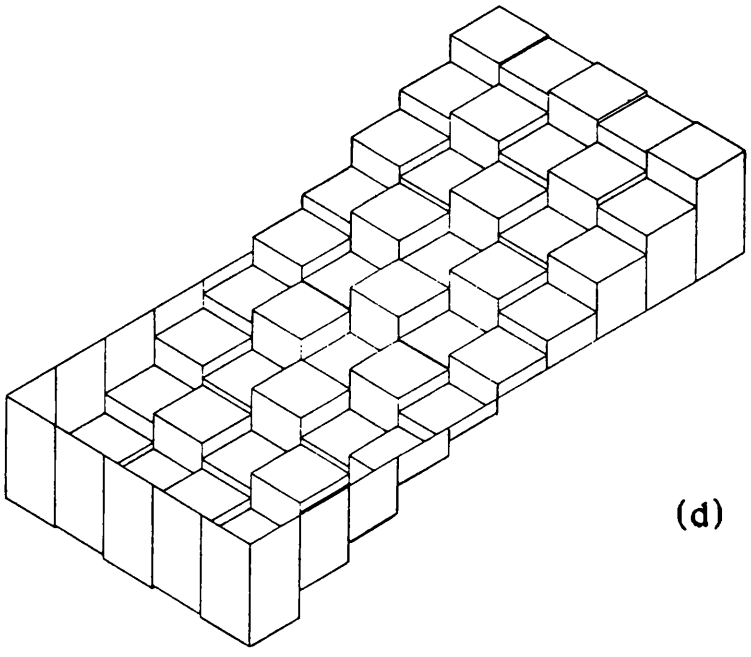

(d) Step 25

Figure 5.28 (Continued)

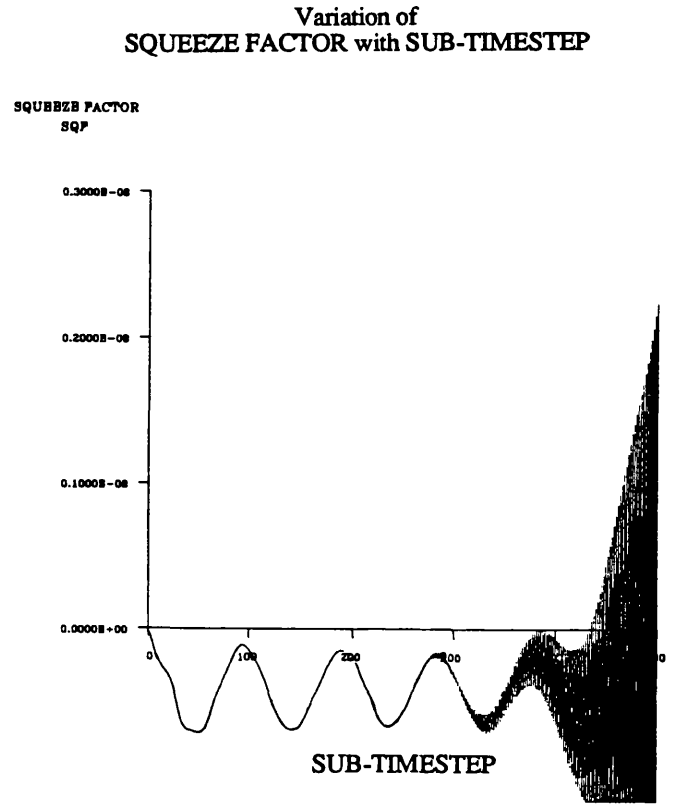

(a) **Pressure response of a region behind the cylinder.**

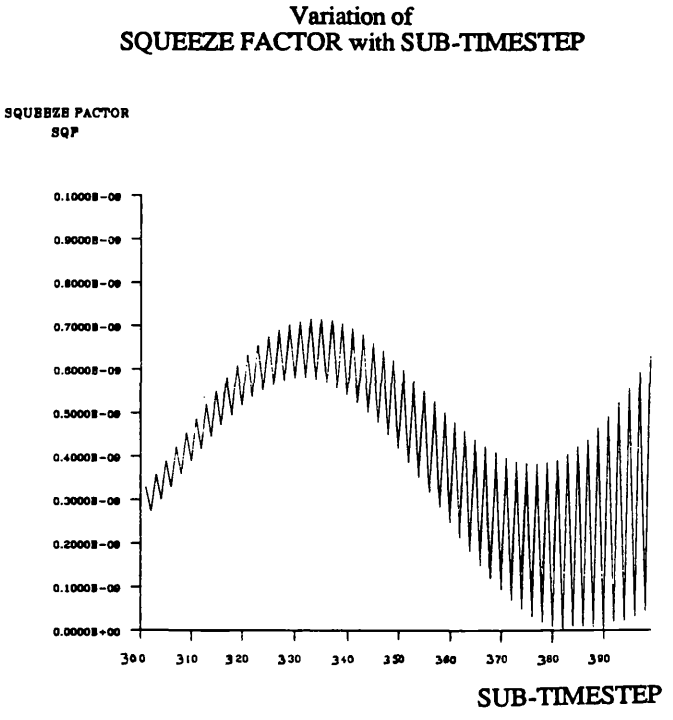

(b) **Detail of (a) but with sign of pressure changed.**

Figure 5.29 Breakdown of the Pressure Response for the Cylinder in Cylindrical Annulus Problem

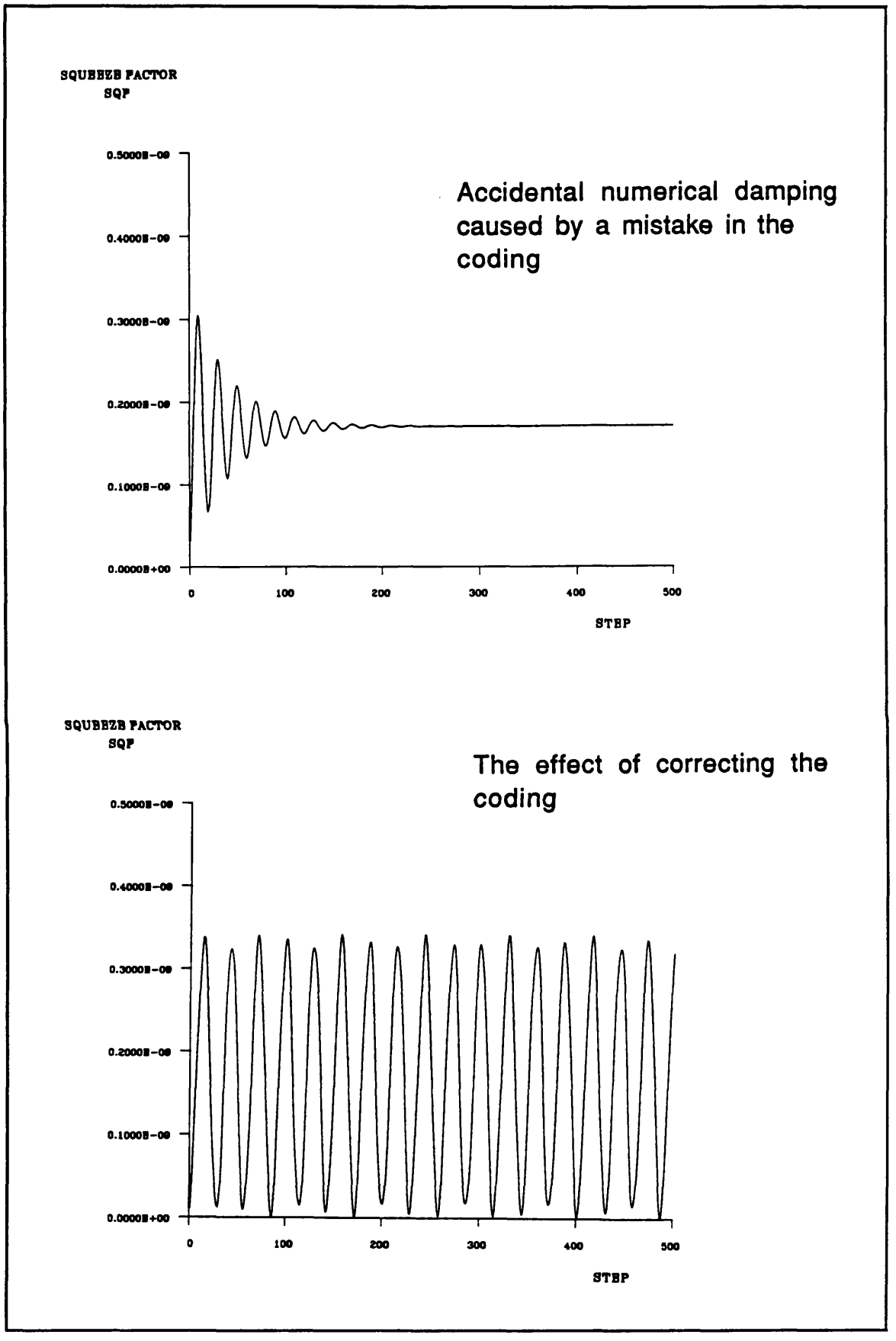

Figure 5.30 Inviscid Response with No Damping

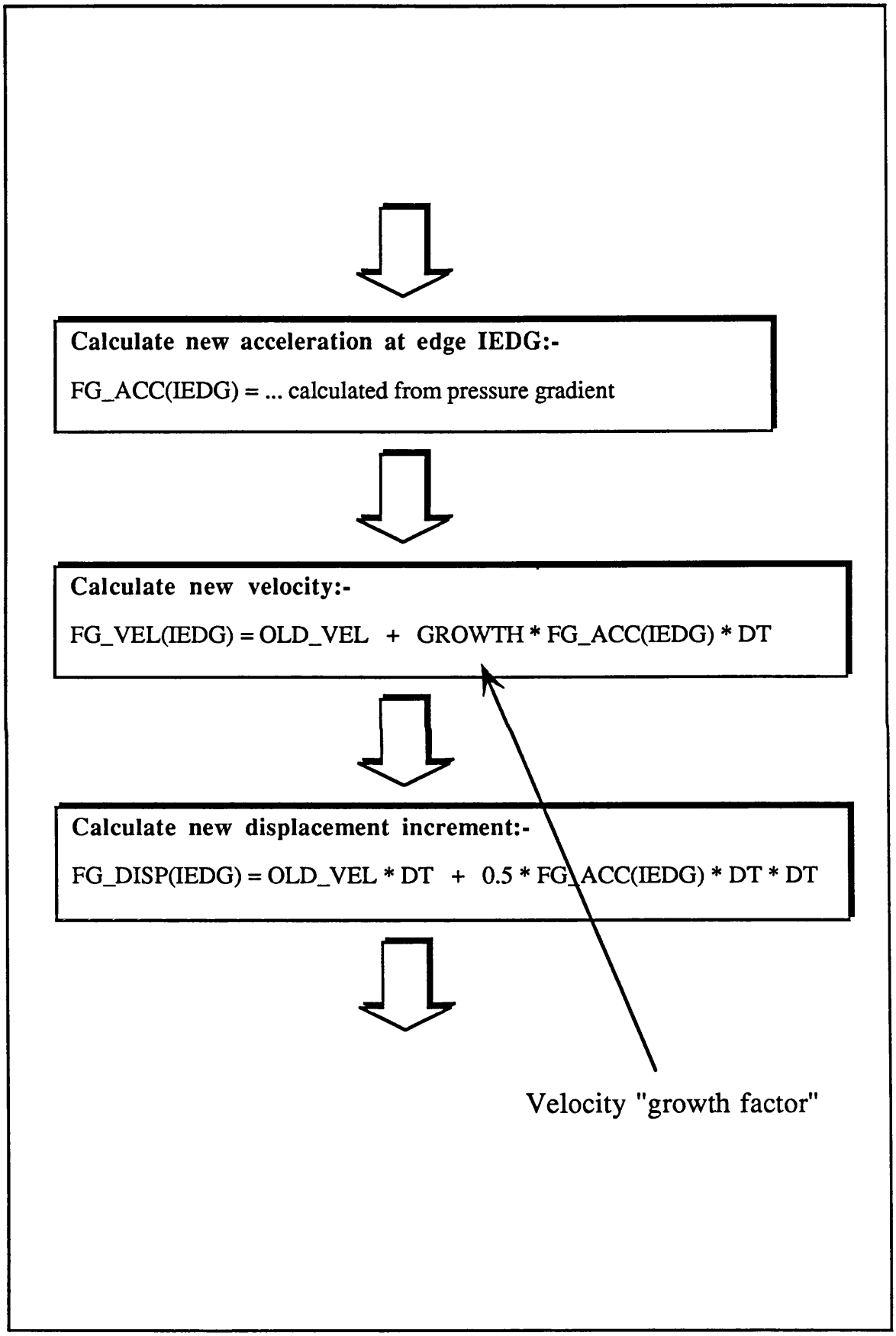

Figure 5.31 "Growth Factor" in Displacement Calculation

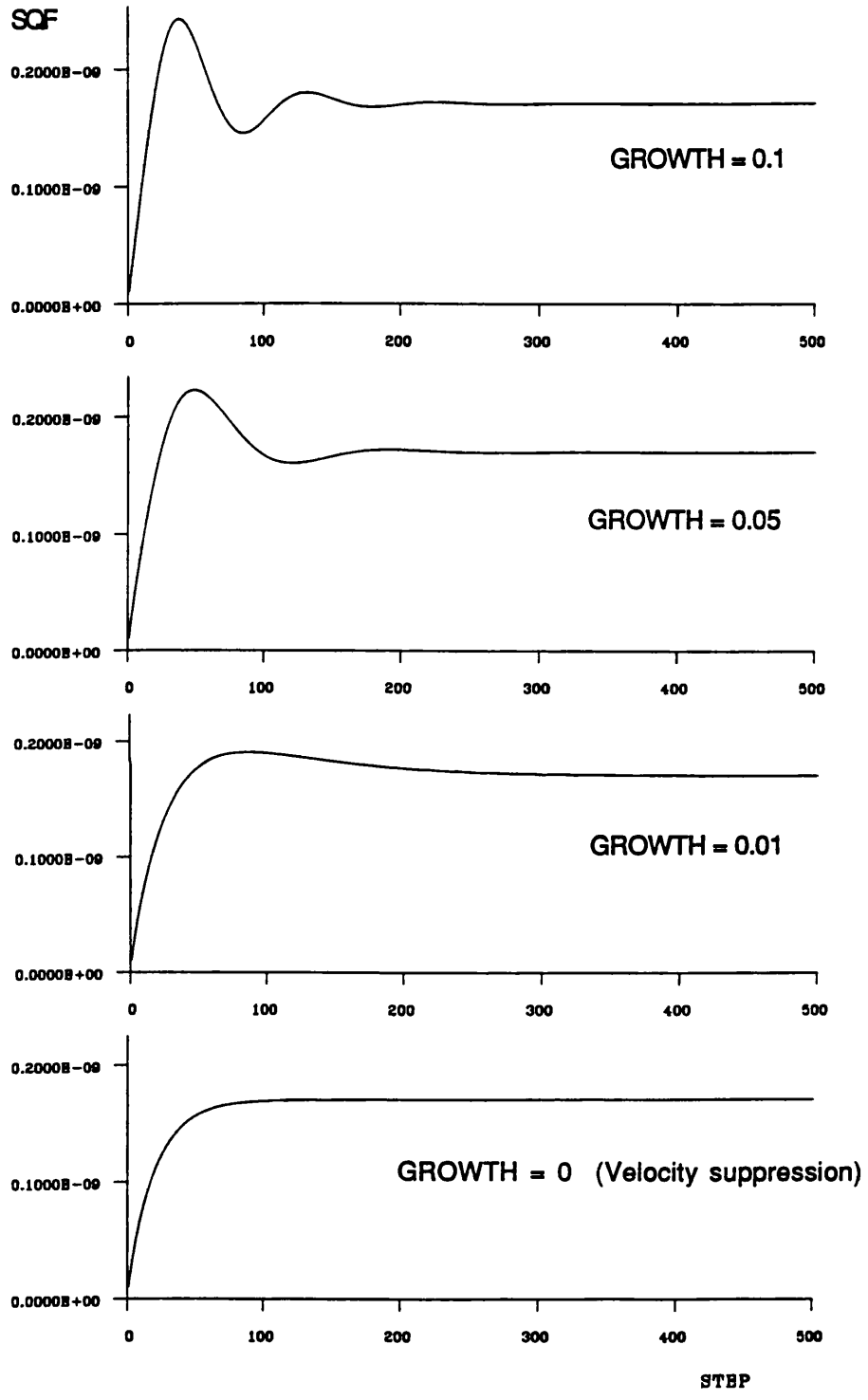

Figure 5.32 Variation with Growth Factor of Pressure Response in a Tank

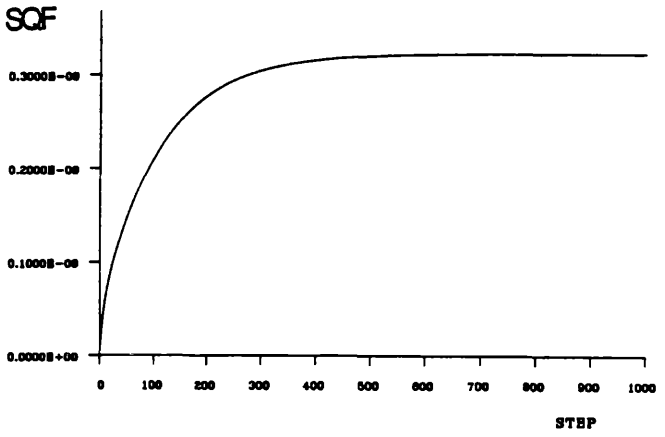

SQF/Temporal pressure synthesis for region A

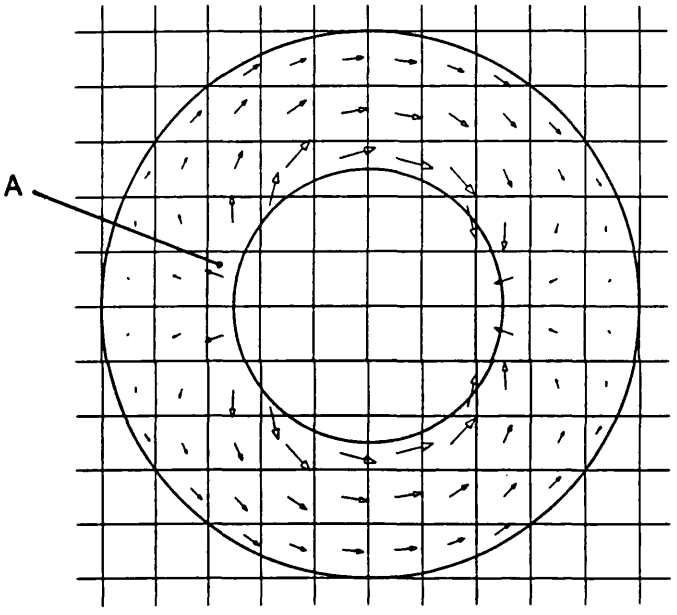

Temporal acceleration field

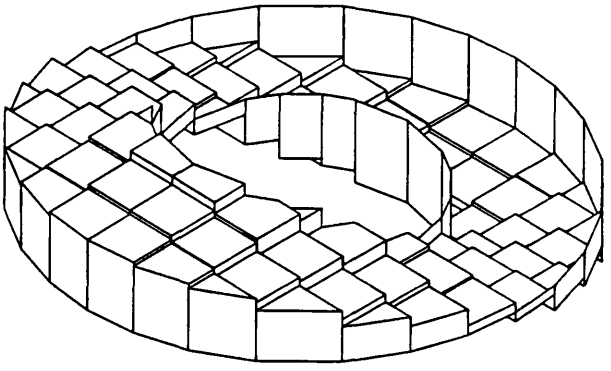

Temporal pressure levels

Figure 5.33 Pressure Synthesis with Velocity Suppression in Cylinder-in-Annulus Problem

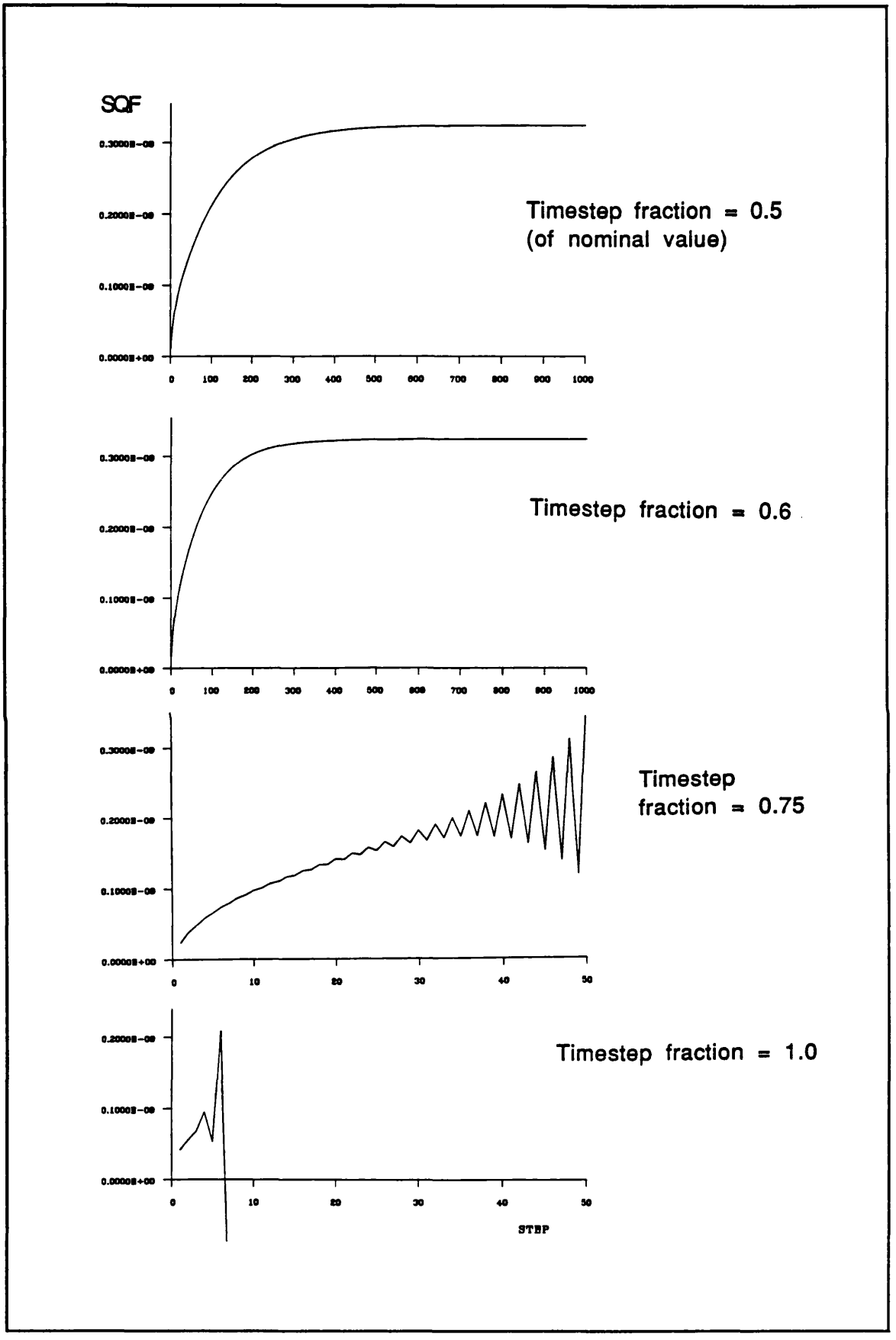

Figure 5.34 Increasing Timestep with Velocity Suppression

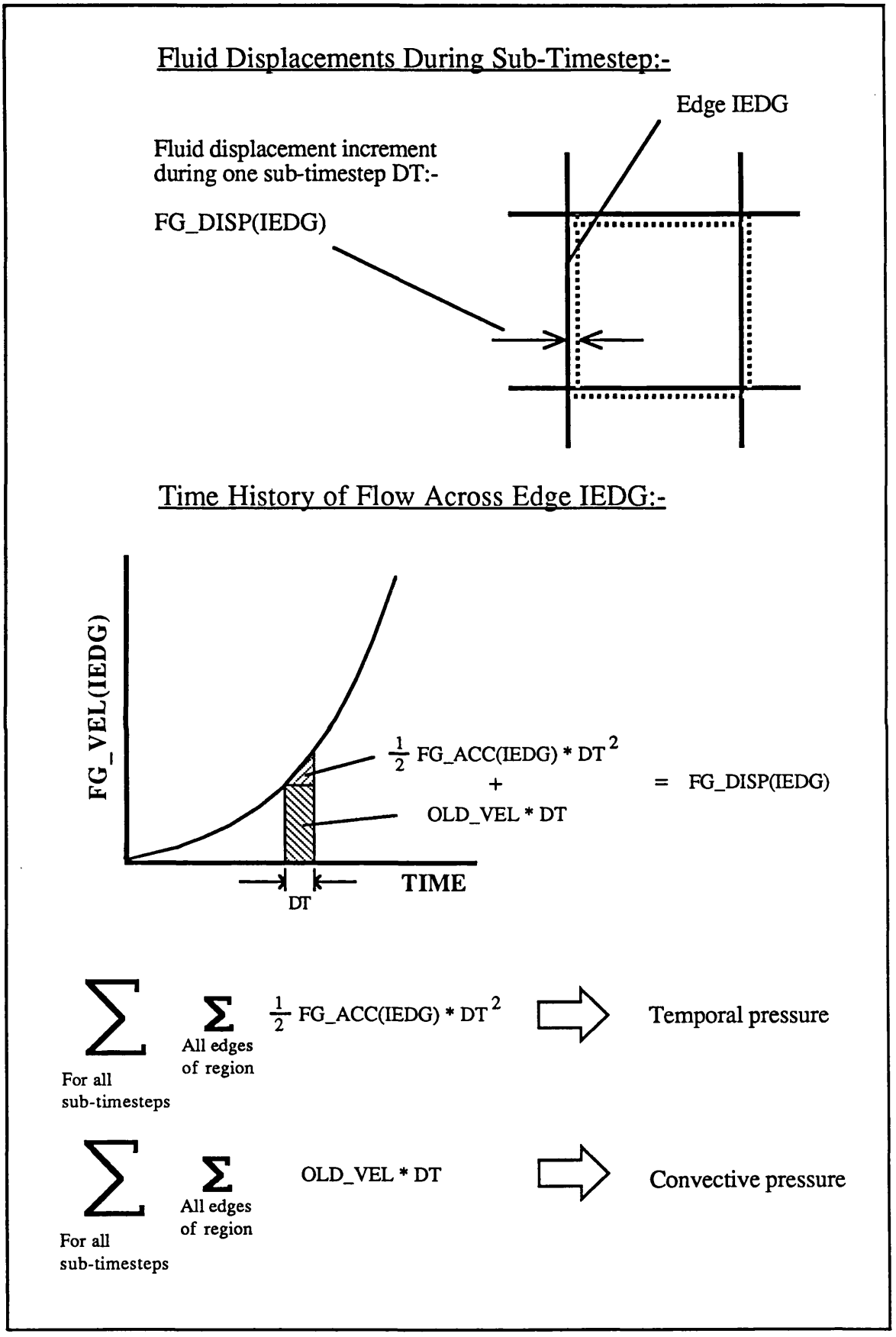

Figure 5.35 Suppression of Velocity - Physical Interpretation/Justification

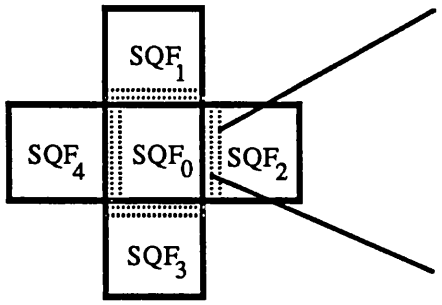

DINC tendency to equalise SQF between adjacent regions

Moderated DINC, based on other tended DINC values for other edges of the given region. The net effect is a reduction of SQF for the given region to an averaged value with the neighbouring regions.

Procedure for each region:-

Step 1. Determine DINC for each edge if it were to equalise SQF values between the associated regions on its own (i.e. not considering other edge displacements).

Step 2. Sum the tended inflows and outflows for the region as:-

$$S\_DINC\_A\_IN = \sum_{\text{All edges with inflow}} DINC * AREA$$

$$S\_DINC\_A\_OUT = \sum_{\text{All edges with outflow}} DINC * AREA$$

Step 3. Scale each of the tended DINC values by the proportion of its contribution to the inflow/ouflow sum as:-

$$DINC = DINC * \left| \frac{DINC * AREA}{S\_DINC\_A\_IN} \right|$$

or

$$DINC = DINC * \left| \frac{DINC * AREA}{S\_DINC\_A\_OUT} \right|$$

as appropriate.

Figure 5.36 The Region Transfer Method

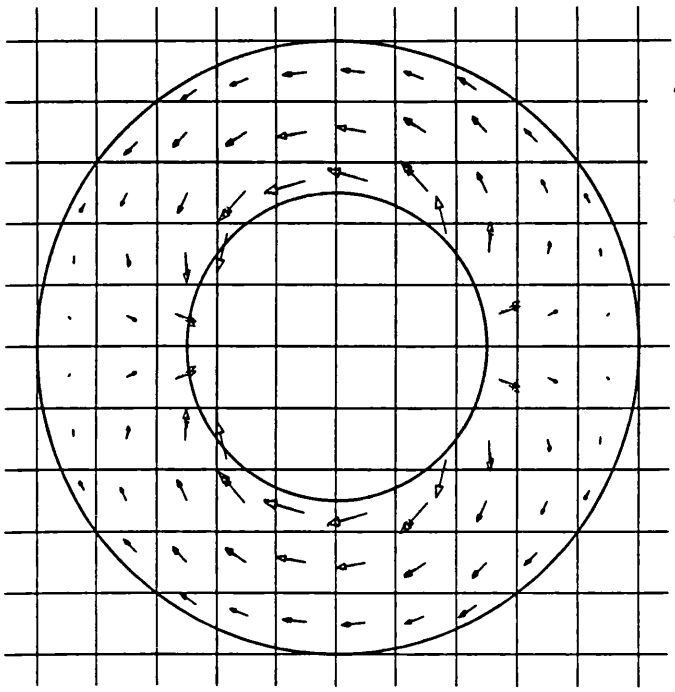

Acceleration field using EDGE TRANSFER approach (with analytical solution superimposed ---)

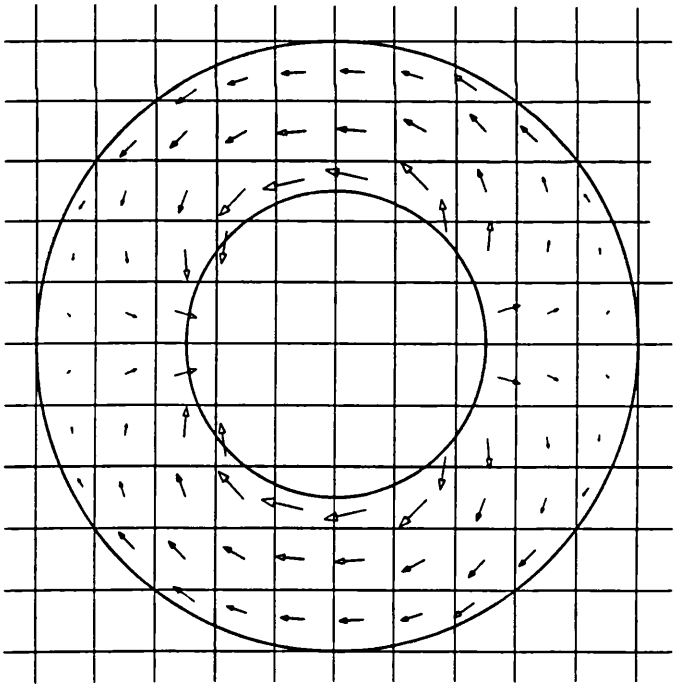

Acceleration field using REGION TRANSFER method

Figure 5.37 Example of the Acceleration Field Obtained Using the Region Transfer Method

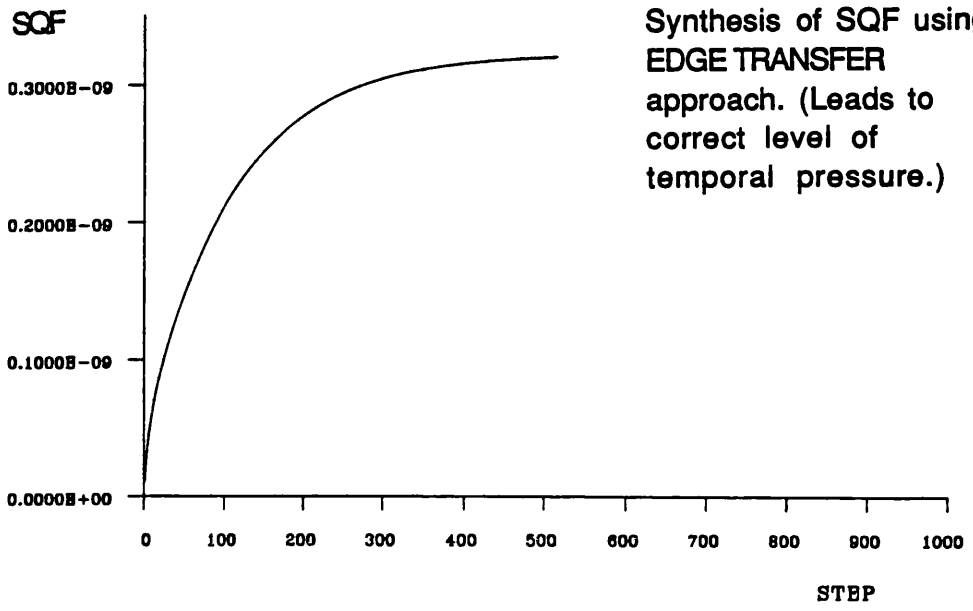

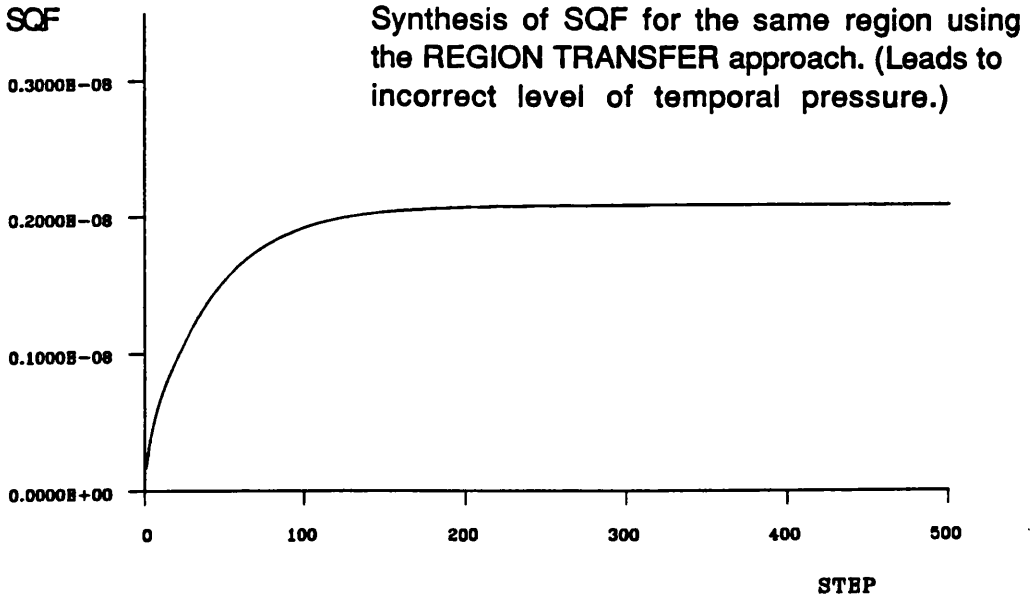

Figure 5.38 Comparison of SQF Response for the Edge and Region Transfer Methods

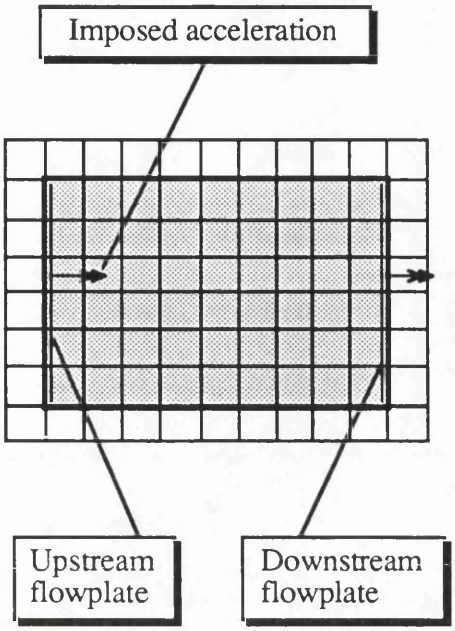

Flowplates are caused to have instantaneous accelerations equal to those required in "equilibrium" by the accelerating flow at the given planes in the fluid. The imposed accelerations, therefore, must satisfy continuity requirements. The flowplates are virtual boundaries which do not actually move within the discretised system. They cause the acceleration "input" to the flow and generate a unique pressure field. There is no independent control of the resulting pressure levels at the flowplate surfaces.

Figure 5.39 The Indirect Modelling of Pressure Boundary Conditions Using Accelerating Flowplates

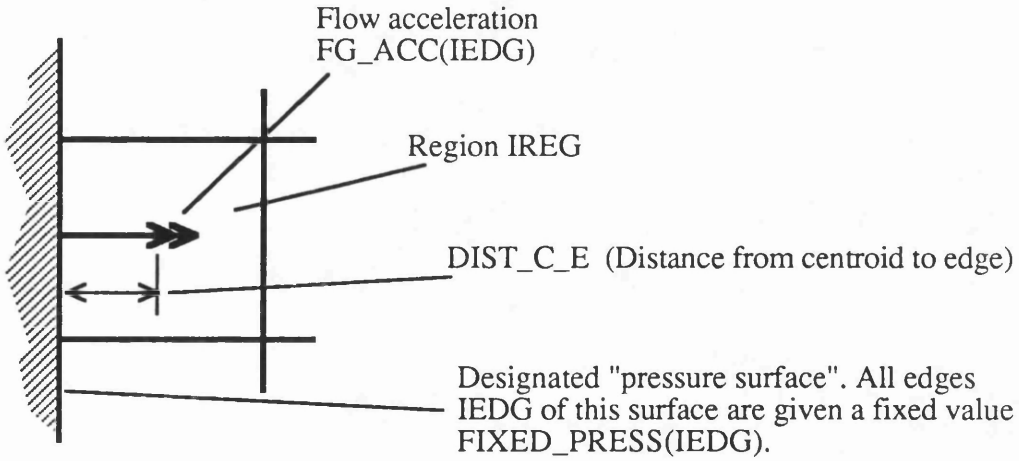

$$\text{PRESS\_GRAD} = \frac{(\text{FIXED\_PRESS(IEDG)} - \text{SQF(IREG)} * \text{BULKMOD})}{\text{DIST\_C\_E}}$$

$$\text{FG\_ACC(IEDG)} = \text{PRESS\_GRAD} / \text{DENSIT}$$

Figure 5.40 Accelerations Across Pressure Surfaces

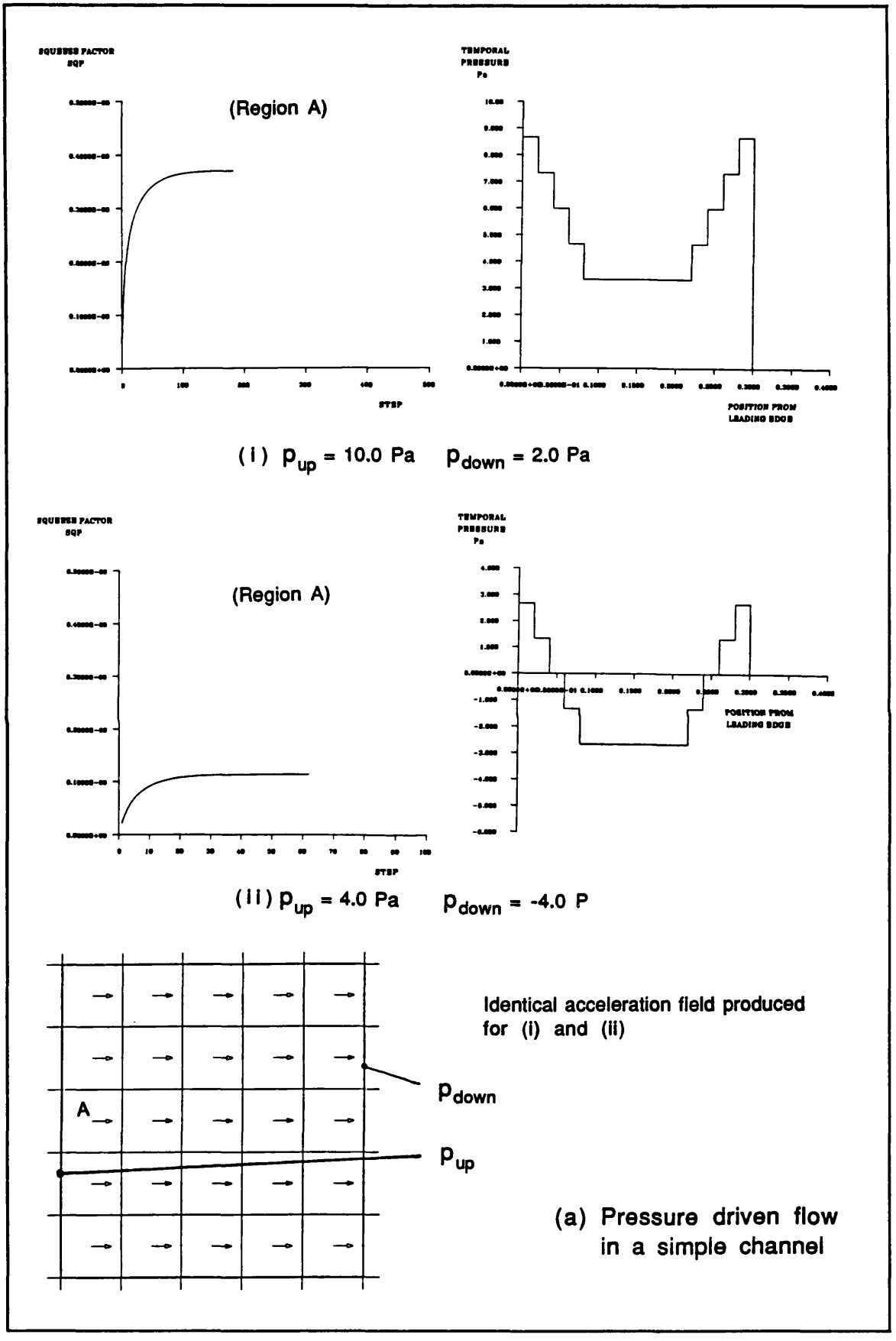

Figure 5.41 Examples of Pressure Driven Flow

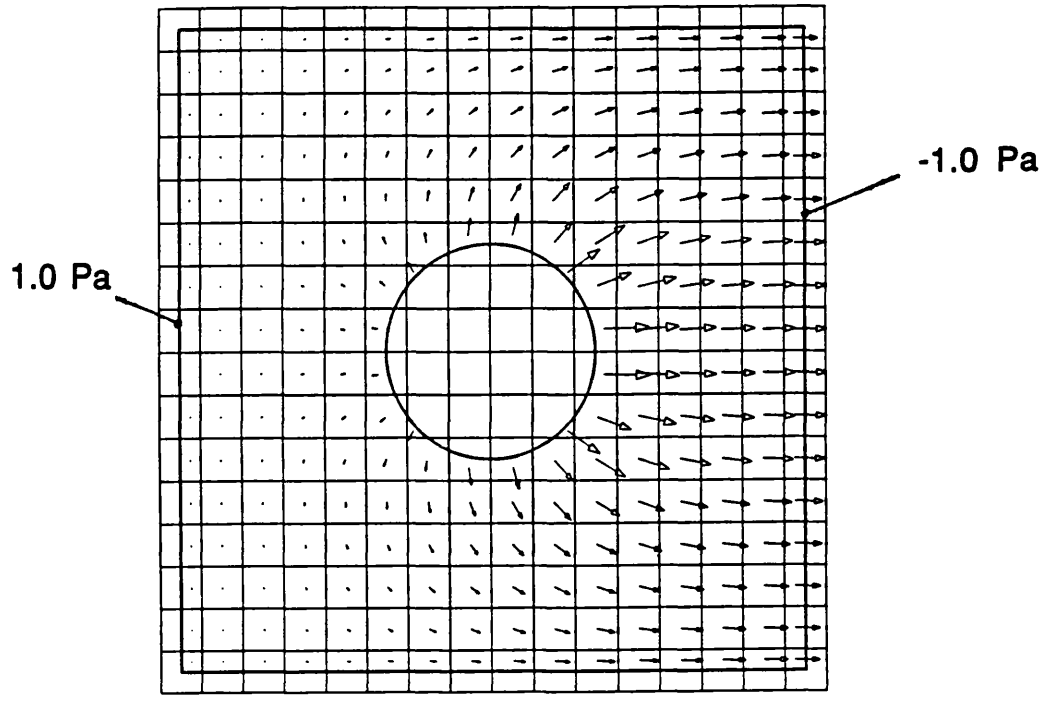

(b) Mistaken designation of upstream pressure surface for flow past a cylinder in a channel

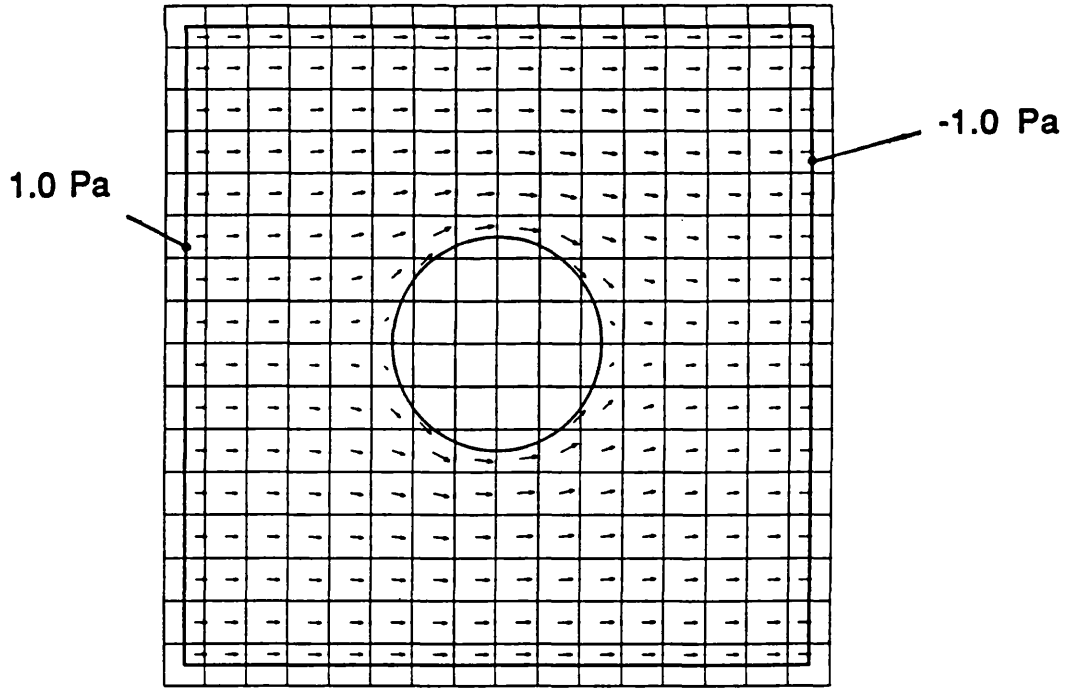

(c) Corrected version of (b)

Figure 5.41 (Continued)

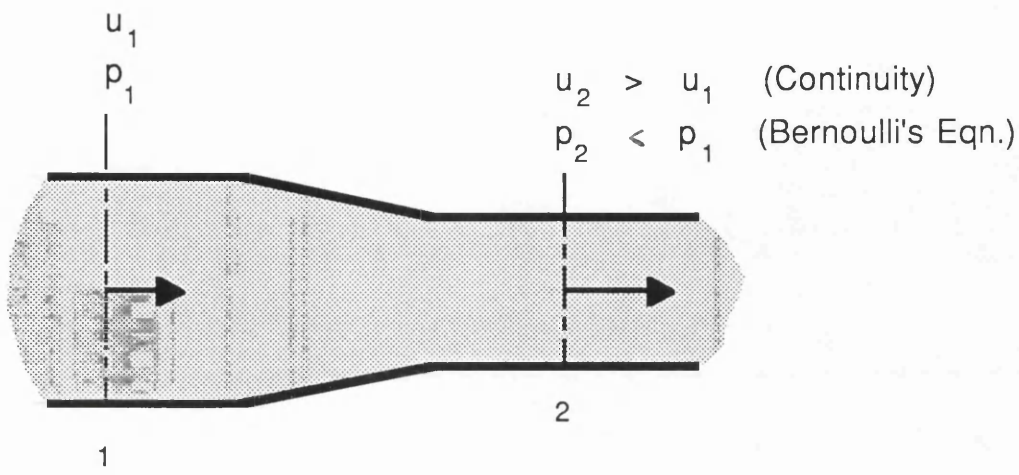

Bernoulli's Equation (for steady flow in the horizontal plane):-

$$p + \tfrac{1}{2}\rho u^2 = \text{constant}$$

Clearly (from this expression) pressure p reduces as the velocity u increases in the duct. Here p is the convective pressure, gradients of which must exist if the velocity is not uniform along streamlines. (The derivation of Bernoulli's equation is based on the recognition of the balance that must exist between the gradients of pressure and the convective accelerations known to exist from continuity considerations.)

Figure 5.42 Bernoulli's Equation Applied to Flow in a Duct

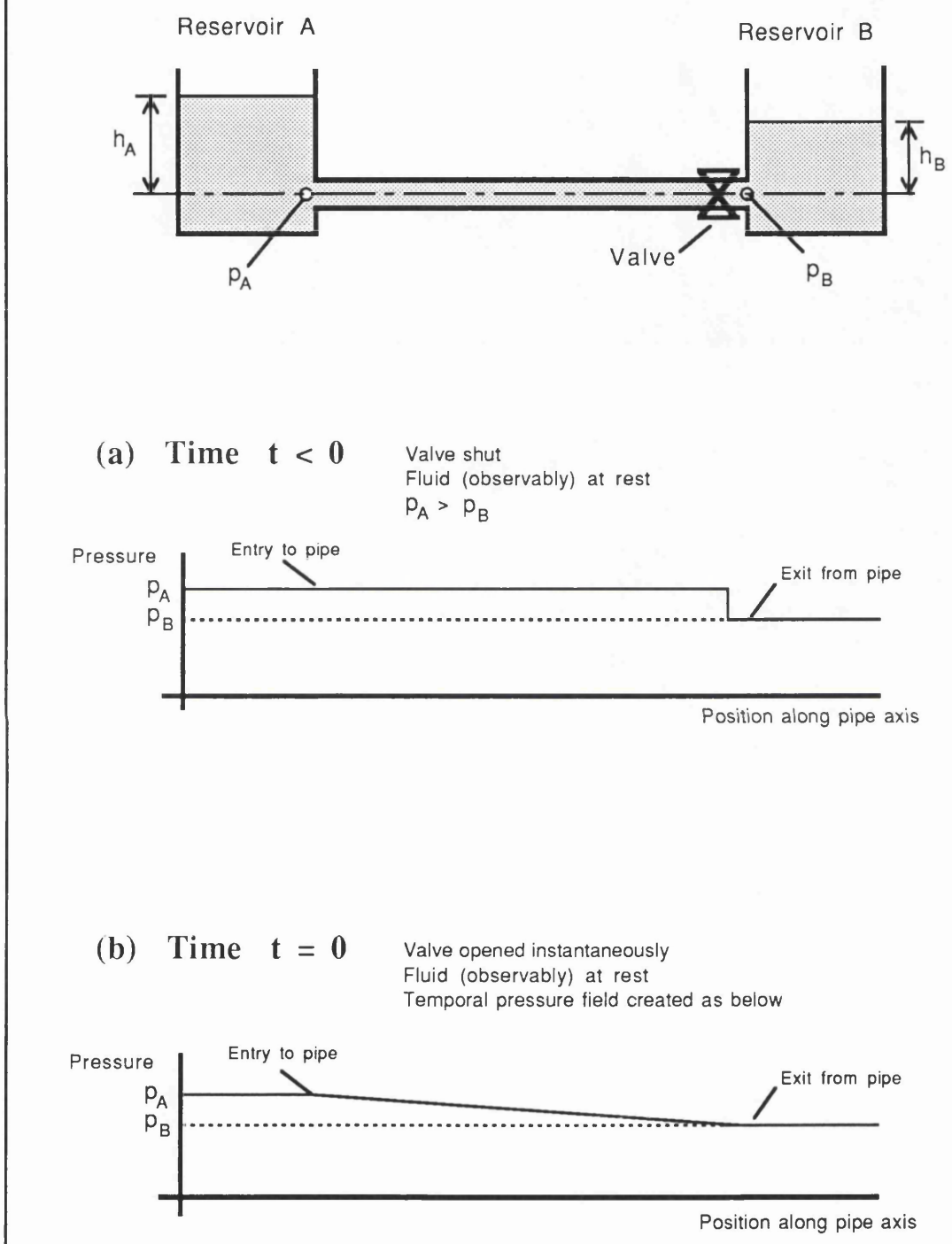

Figure 5.43 Pressure Synthesis in a Pipe Between Two Reservoirs

(c) Time $t = t_{steady}$ Level of fluid in B raised to h_A

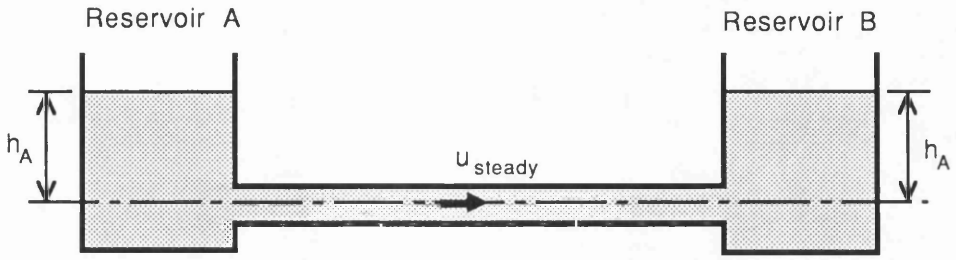

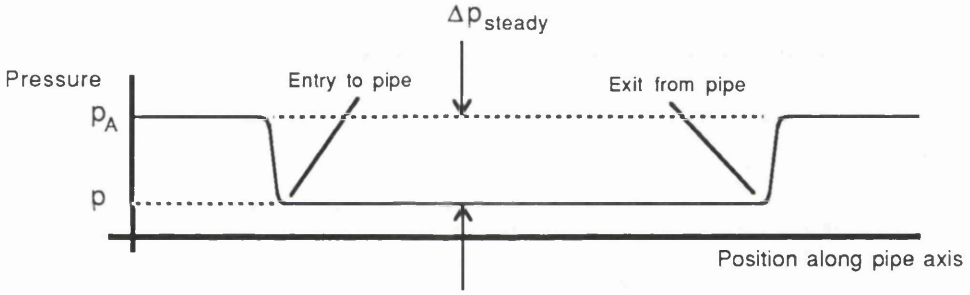

$$\left| \Delta p_{steady} \right| = \frac{1}{2} \rho u^2_{steady}$$

$$\longrightarrow \quad p = p_A - \frac{1}{2} \rho u^2_{steady} \qquad \text{(Bernoulli)}$$

Figure 5.43 (Continued)

(d) Time $0 < t < t_{steady}$

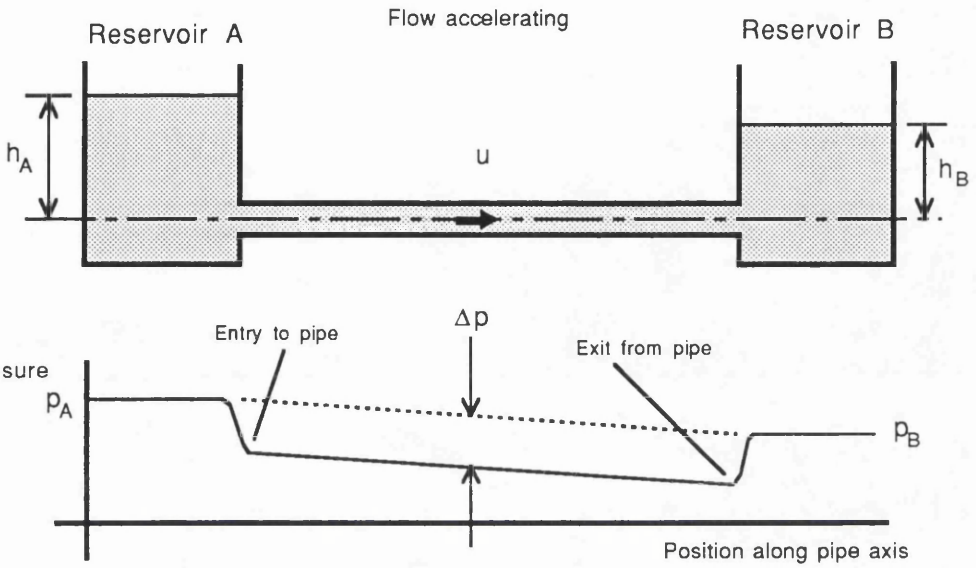

$$|\Delta p| = \tfrac{1}{2}\rho u^2$$

(e) Pressure Components

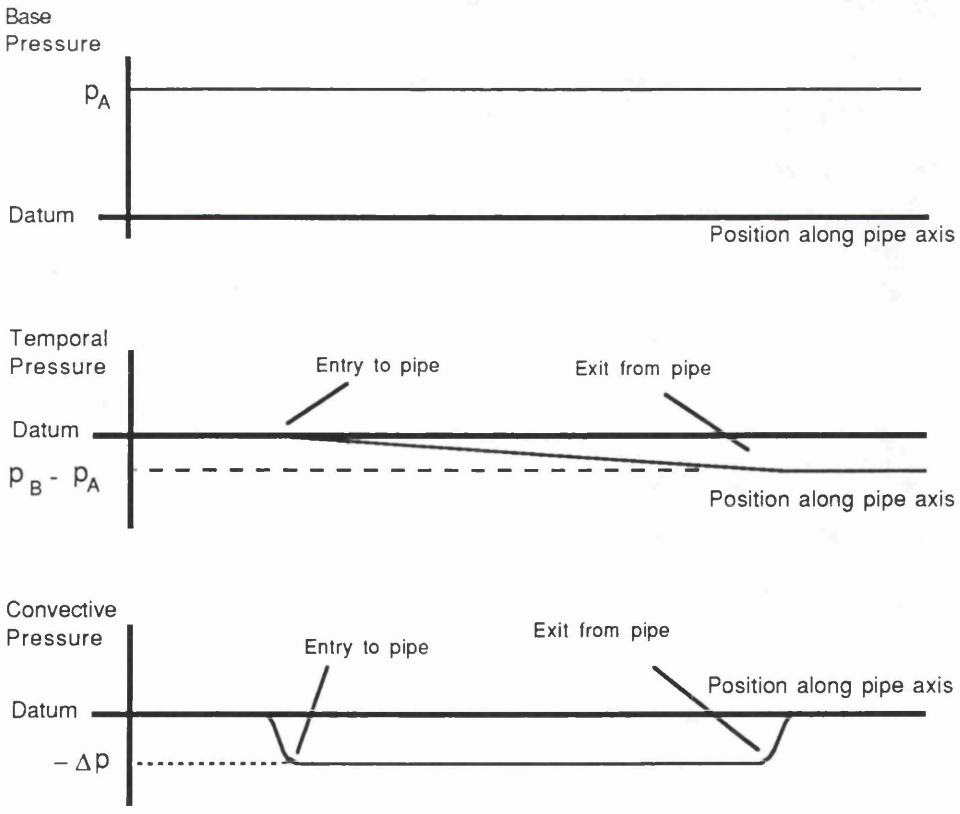

Figure 5.43 (Continued)

(f) Identifying the Origin of Convective Pressure

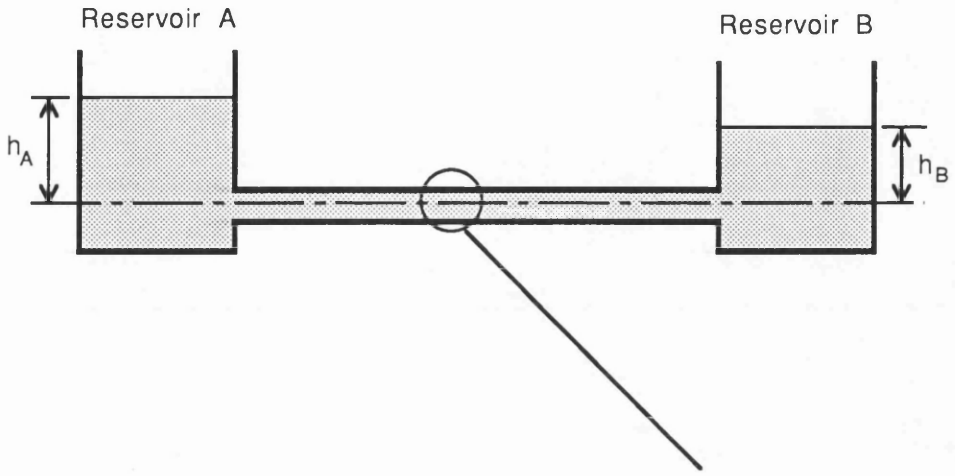

(i) Fluid at rest before opening of valve ($t < 0$)

$\rho_1 = \rho_2 = \rho_3 = \rho_4 = \rho_5 = \rho_6$

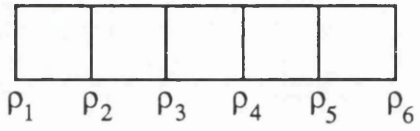

(ii) Temporal pressure influence applied ($t = 0$)

$\rho_1 > \rho_2 > \rho_3 > \rho_4 > \rho_5 > \rho_6$

$a_1 < a_2 < a_3 < a_4 < a_5 < a_6$

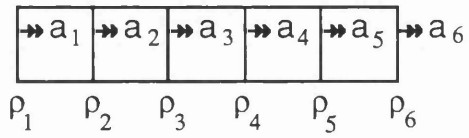

(iii) Flow developing ($0 < t < t_{steady}$)

$u_1 < u_2 < u_3 < u_4 < u_5 < u_6$

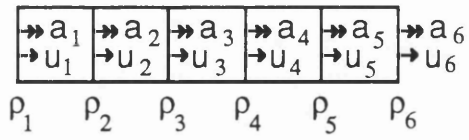

Figure 5.43 (Continued)

(g) Generation of Convective Pressure

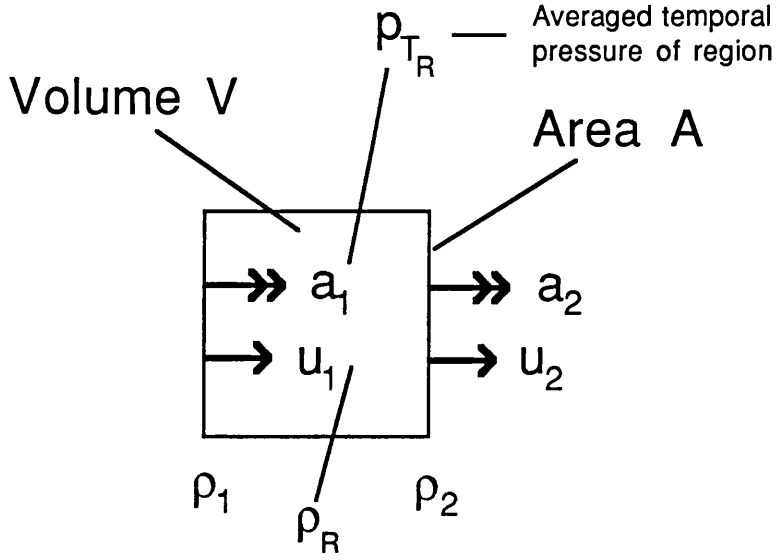

The convective pressure in a timestep δt can be calculated in two ways:-

1. By identifying a FIXED MASS of fluid

$$\delta p_c = -K\frac{\delta V}{V} = -K\frac{(u_2 - u_1)\,A\,\delta t}{V}$$

2. By identifying a FIXED VOLUME of fluid

$$\delta p_c = K\frac{\delta \rho}{\rho} = K\frac{-\delta\rho_1 u_1 A\,\delta t + \delta\rho_2 u_2 A\,\delta t}{\rho_R V}$$

$$= K\frac{-(\rho_1-\rho_R)u_1 A\,\delta t + (\rho_2-\rho_R)u_2 A\,\delta t}{\rho_R V}$$

$$= -(p_{T_1} - p_{T_R})\frac{u_1 A\,\delta t}{V} + (p_{T_2} - p_{T_R})\frac{u_2 A\,\delta t}{V}$$

Figure 5.43 (Continued)

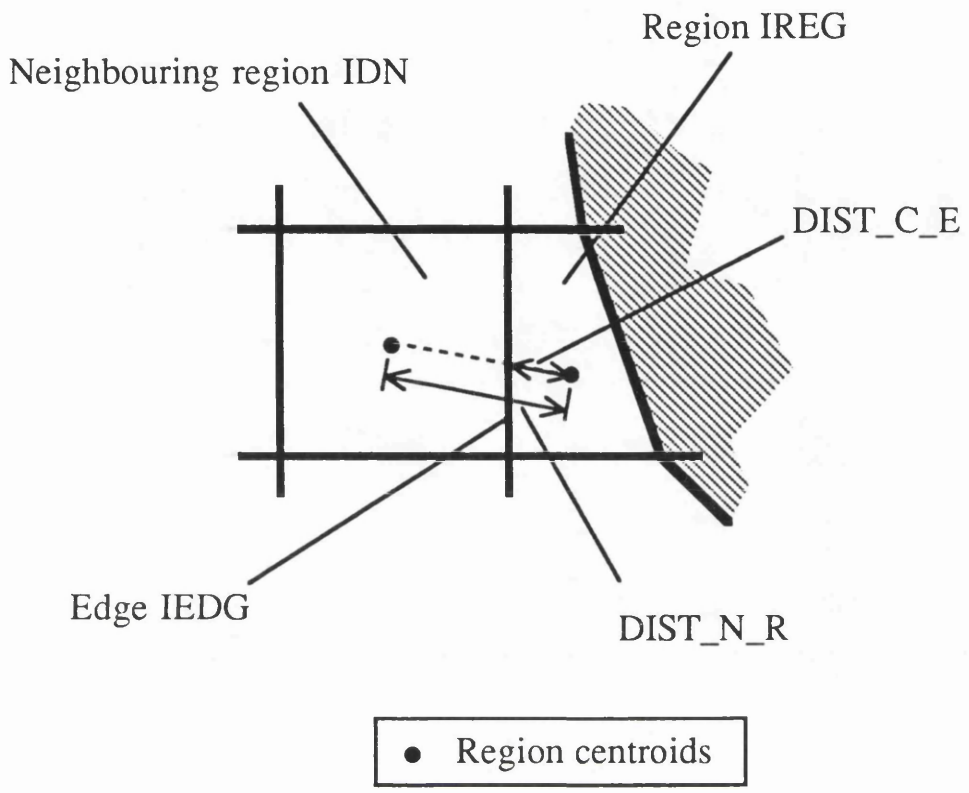

Calculation of pressure at edge IEDG:-

$$EDGE\_PRESS(IEDG) = PRESS(IREG) + \frac{DIST\_C\_E}{DIST\_N\_R} (PRESS(IDN) - PRESS(IREG))$$

Figure 5.44 Simple Interpolation of Pressure at an Internal Edge

CLASSIFICATION OF NODES:-

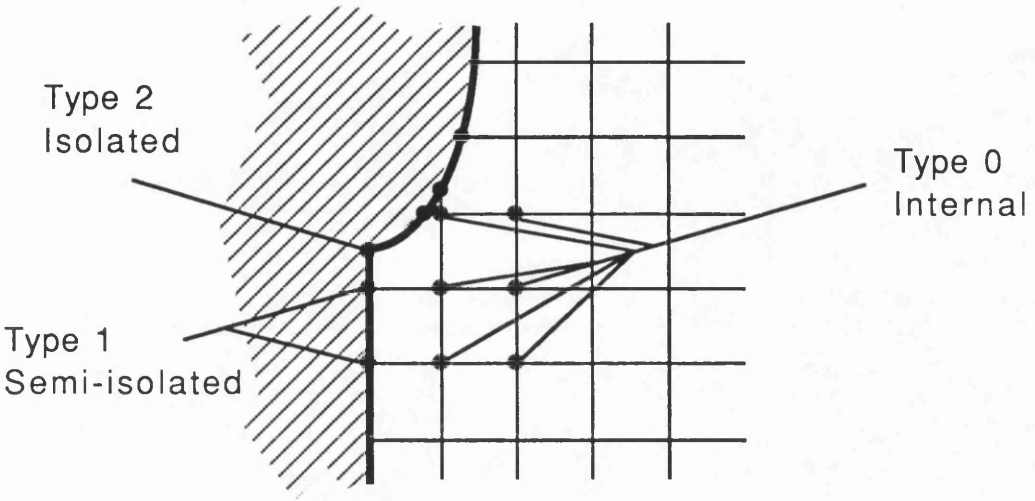

SMOOTHING PROCEDURE
(CALCULATION OF NODE PRESSURES):-

Step 1. Get edge pressures at internal edges.

Step 2. Get TYPE 0 node pressures from averaging of associated edge pressures.

Step 3. Get TYPE 1 node pressures from associated known edge pressure and known TYPE 0 node pressure.

Step 4. Get TYPE 3 node pressures from known average region pressure and known TYPE 1 and TYPE 2 node pressures.

Figure 5.45 Current Smoothing Algorithm for Pressure

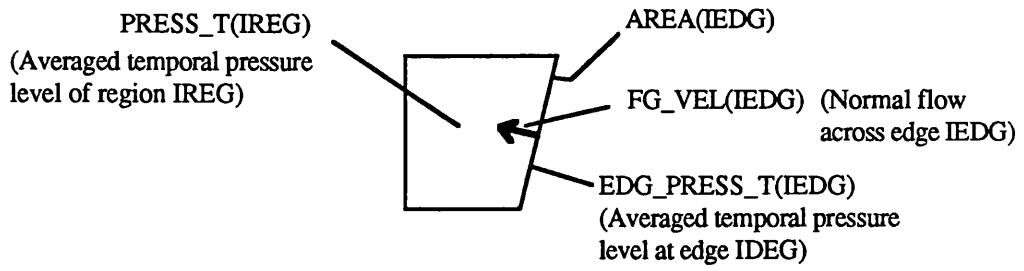

INCREMENTAL CALCULATION

Fractional volume exchange across edge IEDG in time interval DT:-

$$EXCHANGE = FG\_VEL(IEDG) * AREA(IEDG) * DT / VOLUME(IREG)$$

Convective pressure increase due to volume exchange of fluid of different density at edge IEDG:-

$$PRESSINC = -EXCHANGE * (EDG\_PRESS\_T(IEDG) - PRESS\_T(IEDG))$$

Total convective pressure increase for region IREG in time interval DT:-

$$PRESS\_C(IREG) = PRESS\_C(IREG) + \sum_{\text{All edges}} PRESSINC$$

CUMULATIVE CALCULATION

Constant temporal pressure acts from TIME = T1 to T2

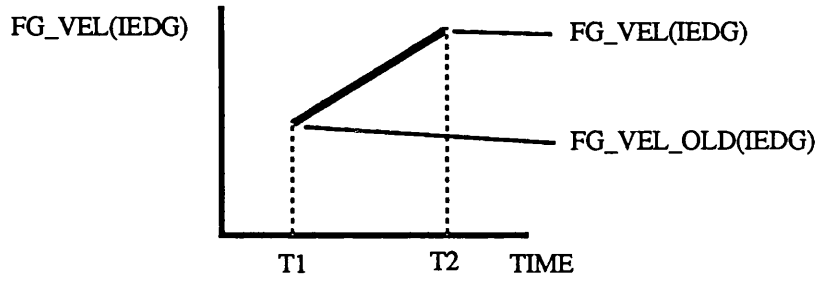

$$CUM\_EXCHANGE = \frac{0.5*(FG\_VEL\_OLD(IEDG)+FG\_VEL(IEDG))*AREA(IEDG)*(T2 - T1)}{VOLUME(IREG)}$$

$$PRESS\_C(IREG) = PRESS\_C(IREG) - \sum_{\text{All edges}} CUM\_EXCHANGE*(EDG\_PRESS\_T(IEDG)-PRESS\_T(IEDG))$$

Figure 5.46 Algorithm for Synthesis of Convective Pressure for Stream Flows

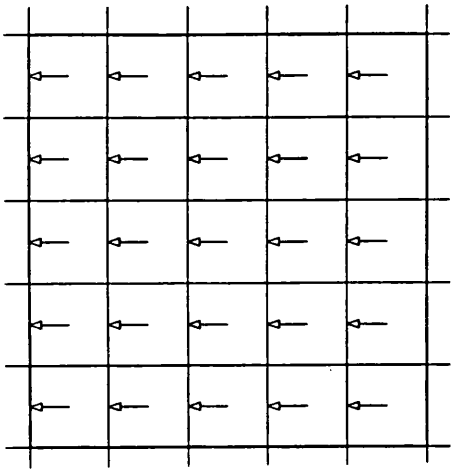

Uniform flow 0.01m/s
(Water density 1000 kg/m ^{3})

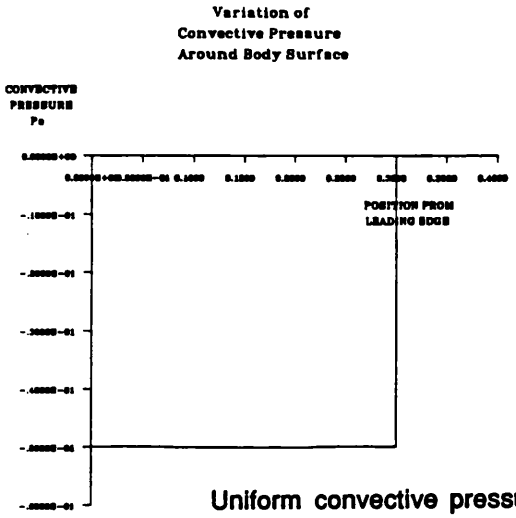

Uniform convective pressure generated along channel of 0.0502 Pa (Error = 0.4%)

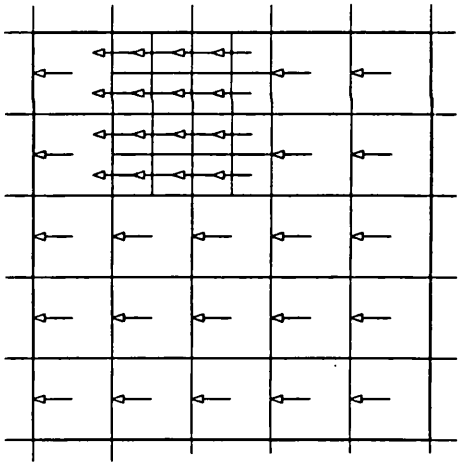

Velocity field
with subdivision

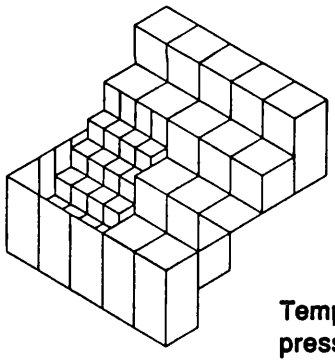

Temporal
pressure field

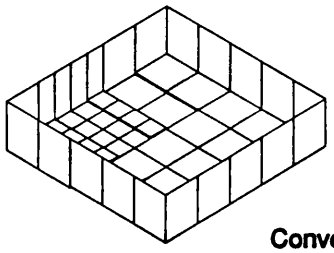

Convective
pressure field

(a) Convective pressure in simple channel flow

Figure 5.47 Results of Convective Pressure Algorithm for Stream Flows

Temporal pressure field
(Vertical scale x 1)

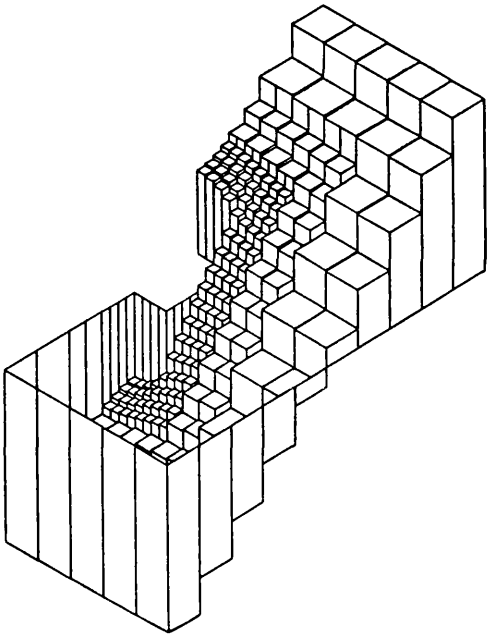

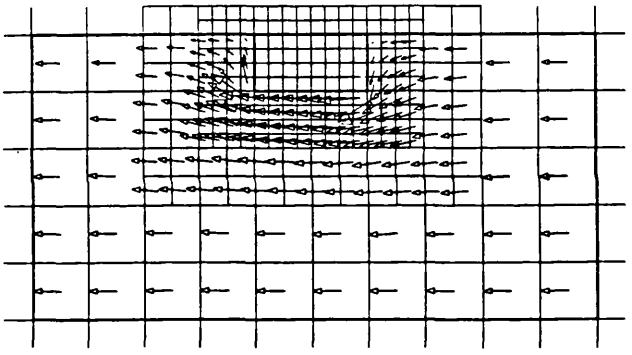

Temporal acceleration field (scale x10)

Upstream pressure 0.1Pa

Downstream pressure -0.1Pa

Convective pressure field after 1 second from rest (Vertical scale x 20)

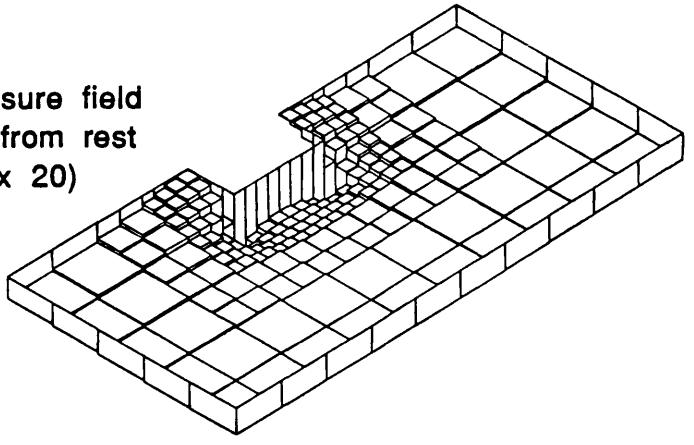

(b) Convective pressure generation around a half rectangular cylinder (0.02m x 0.04m)

Figure 5.47 (Continued)

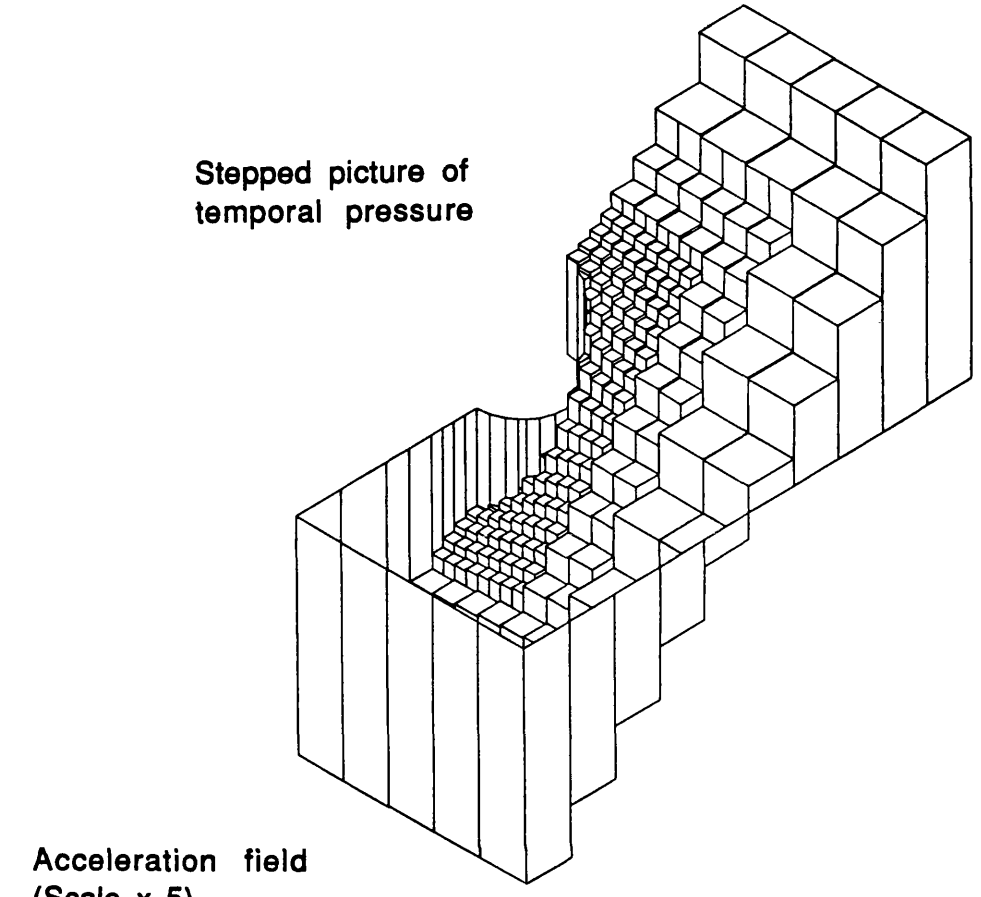

Acceleration field
(Scale x 5)

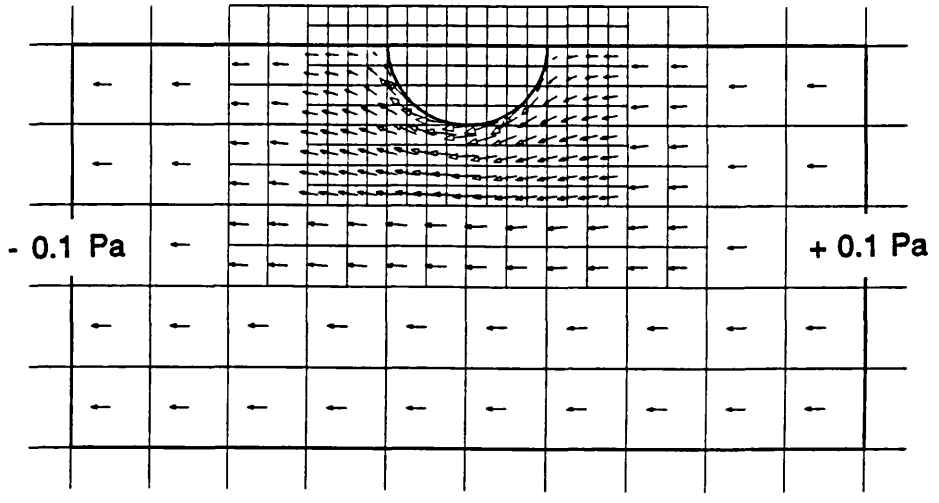

(a) Temporal pressure and acceleration fields for water flow developing around a circular cylinder of radius 0.02m

Figure 5.48 Analytical and Predicted Convective Pressure Around a Circular Cylinder in a Stream

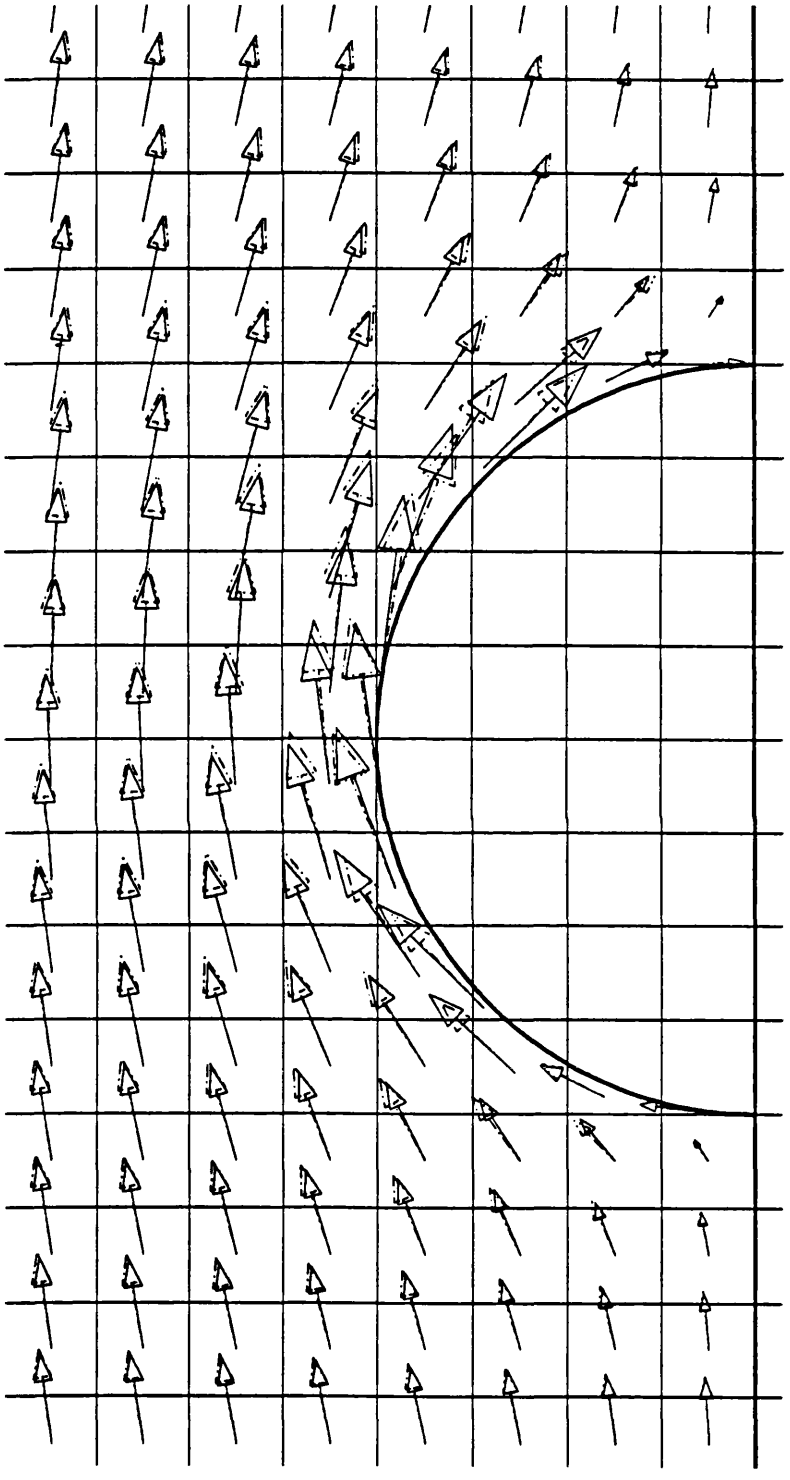

(b) Close-up of velocity/acceleration field showing analytical solution as —·—·—

Figure 5.48 (Continued)

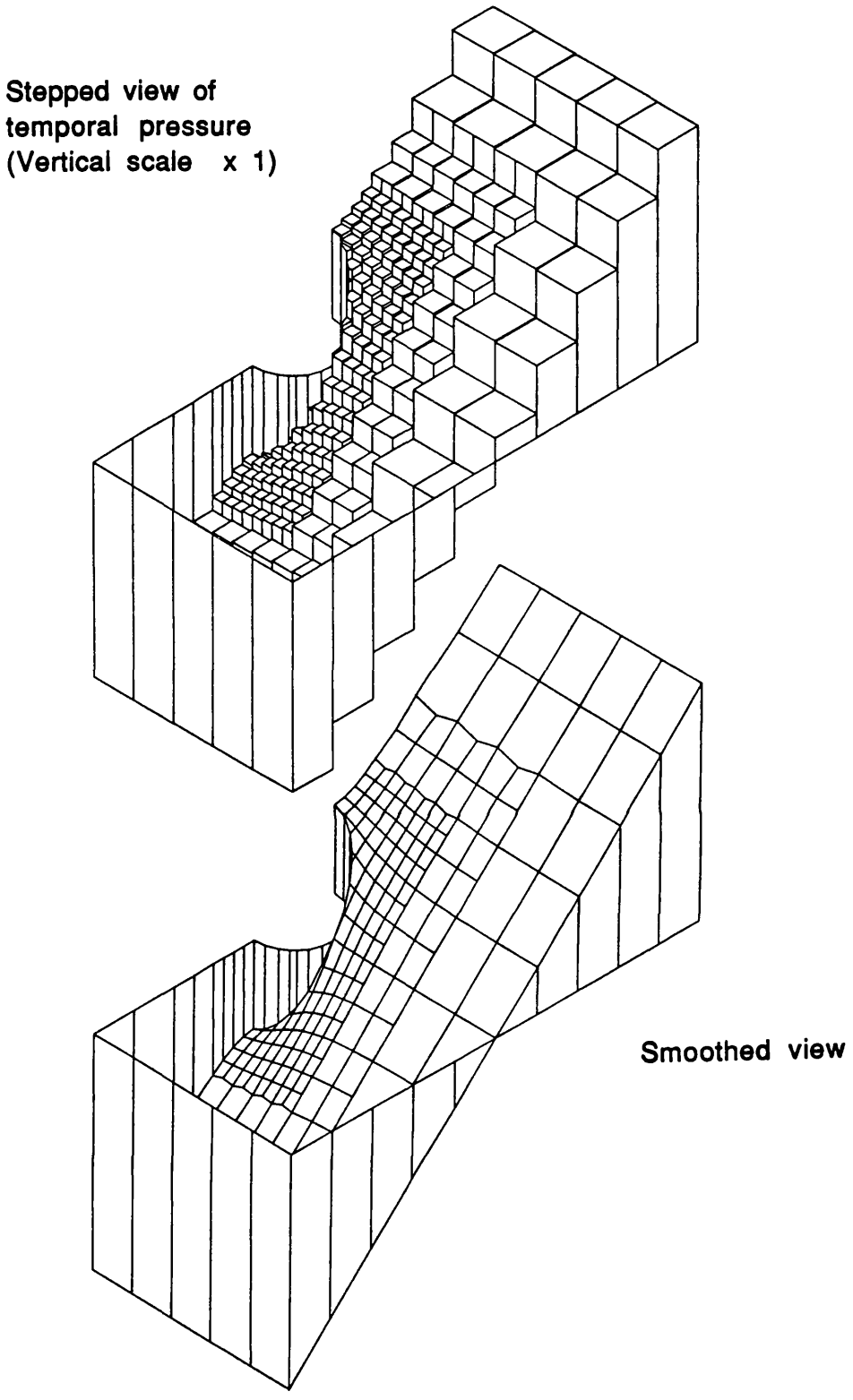

(c) Comparison of "stepped" and "smoothed" pictures of temporal pressure field

Figure 5.48 (Continued)

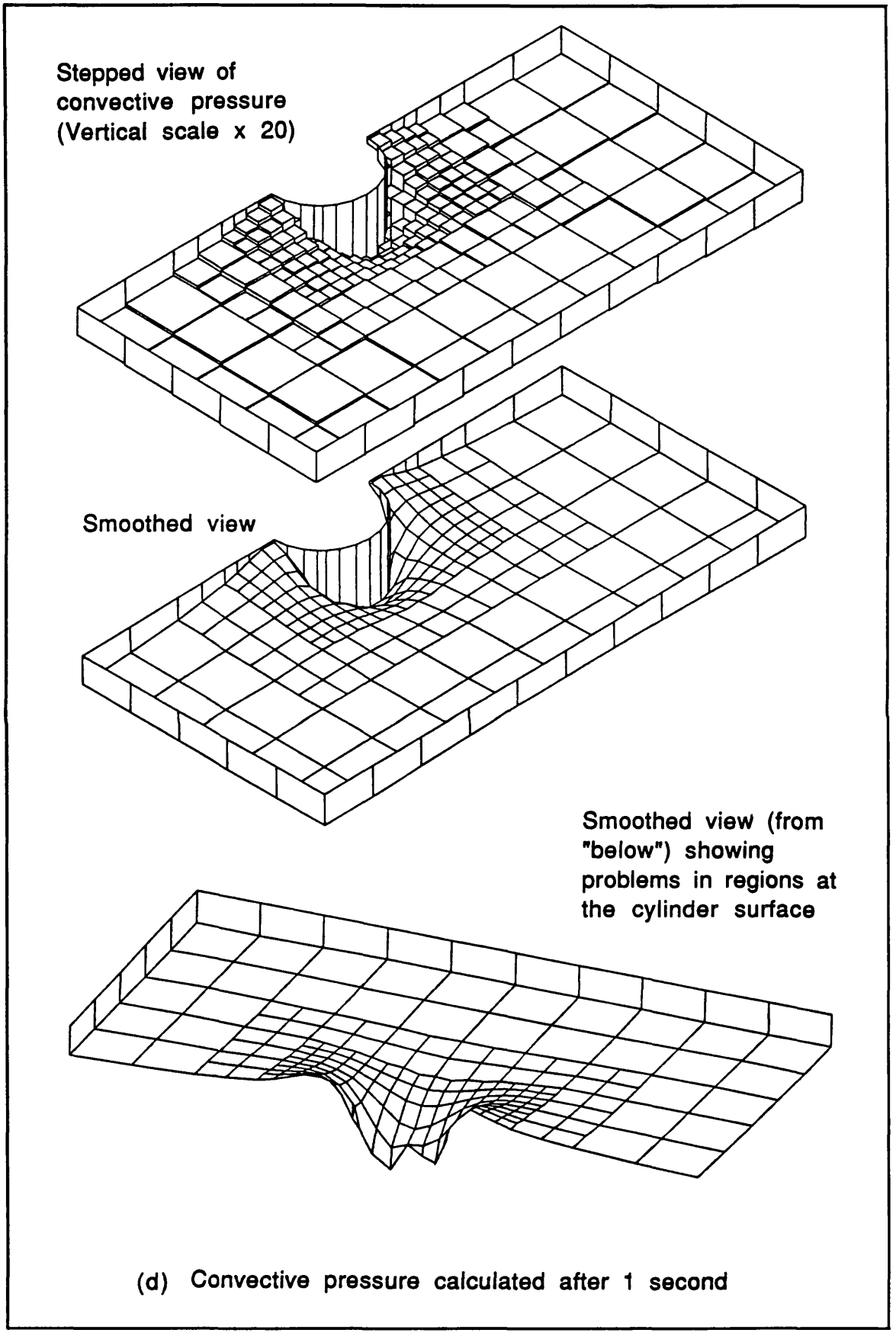

(d) Convective pressure calculated after 1 second

Figure 5.48 (Continued)

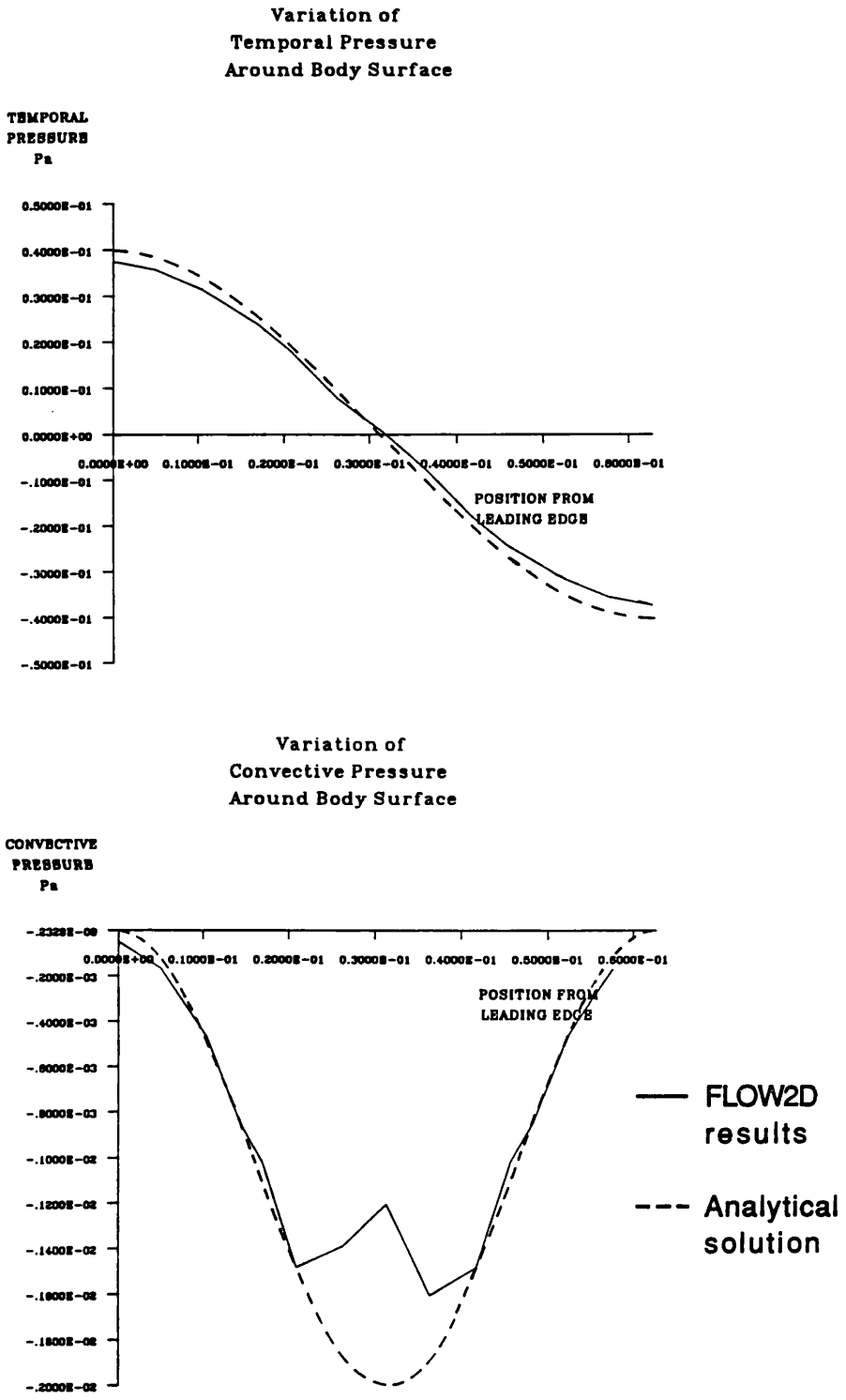

(e) Comparison of pressures on cylinder surface with analytical solution

Figure 5.48 (Continued)

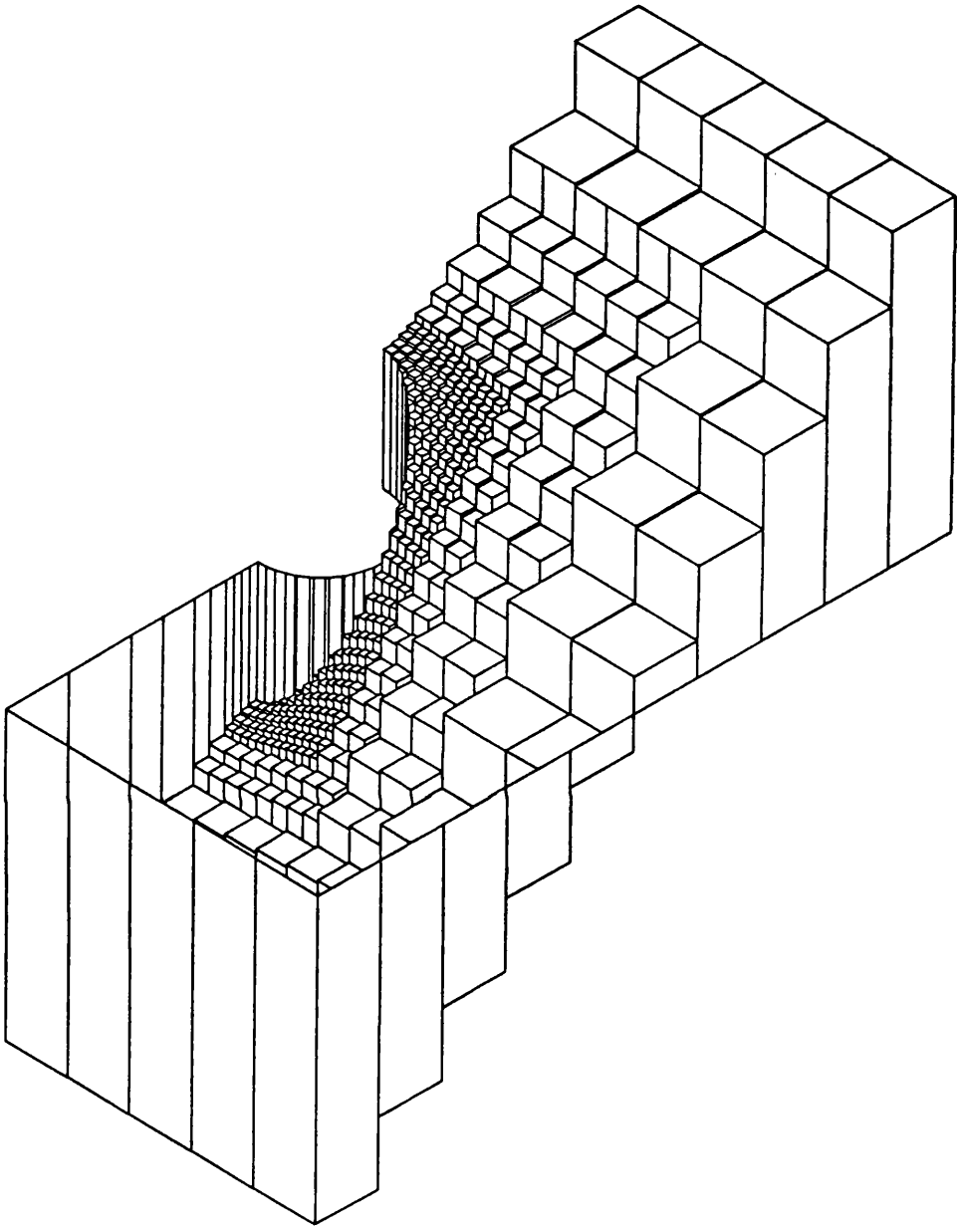

(f) Temporal pressure field (vertical scale x 1) for refined grid analysis

Figure 5.48 (Continued)

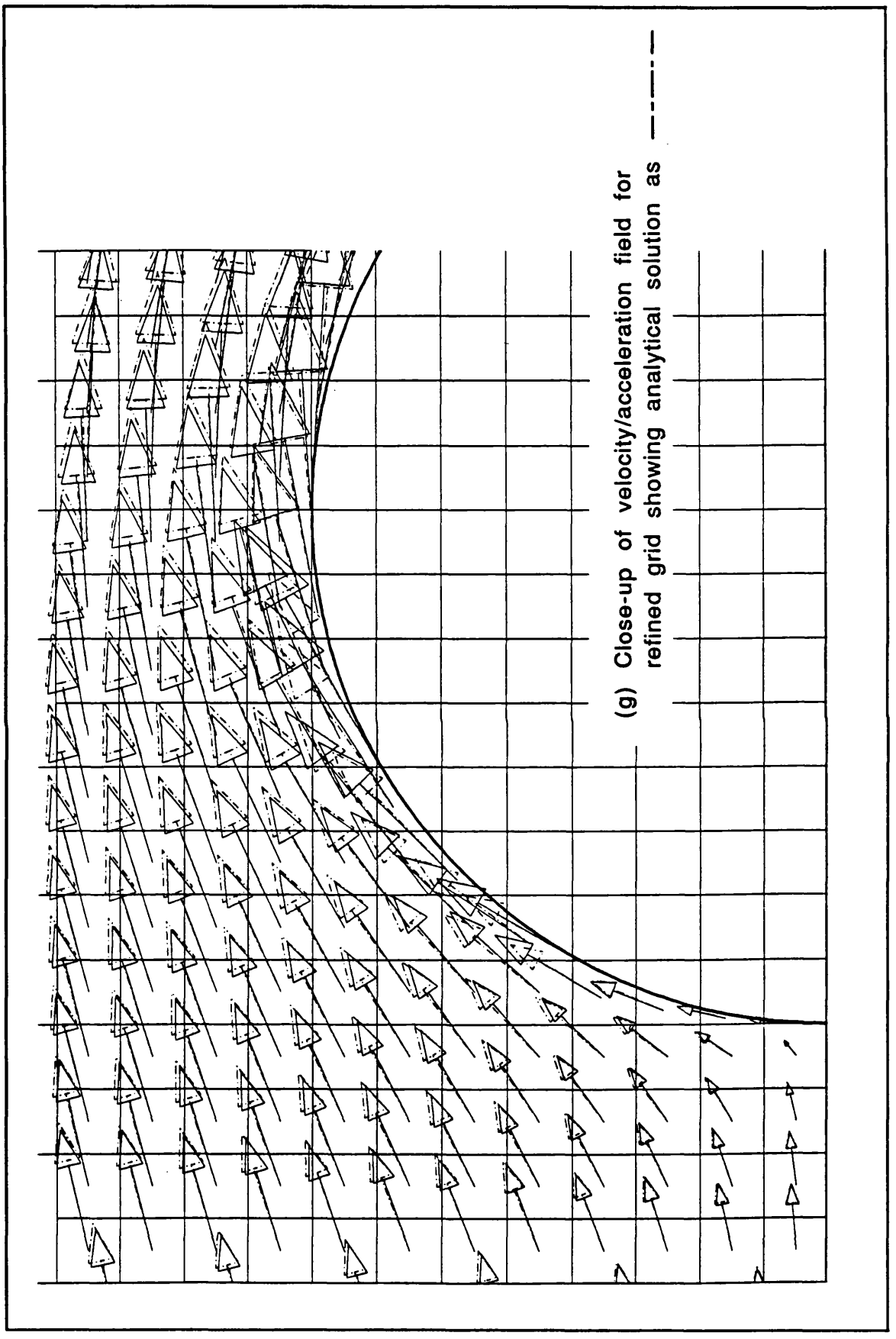

Figure 5.48 (Continued)

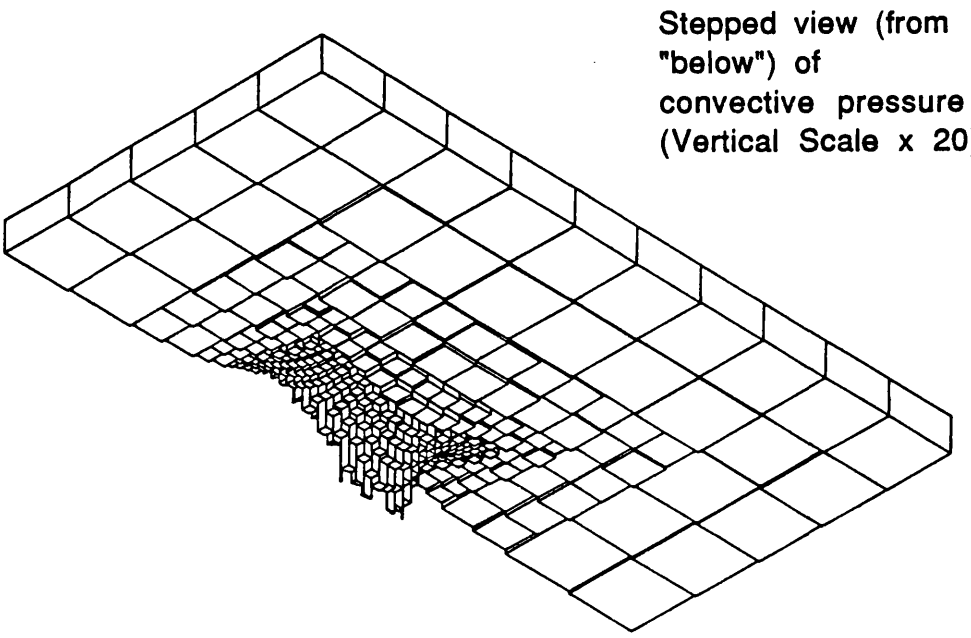

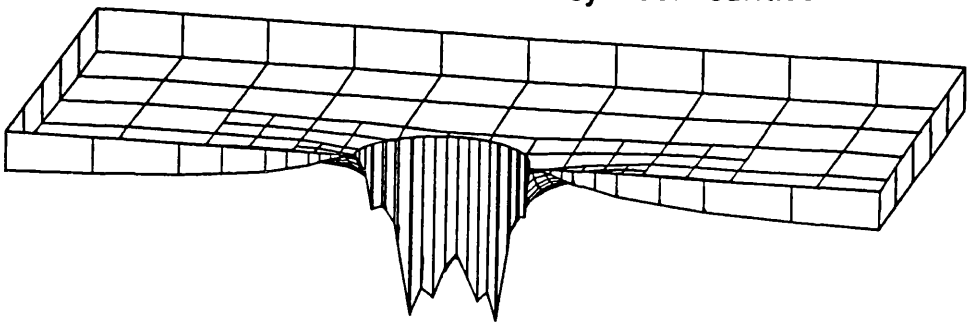

(h) Refined grid results for convective pressure

Figure 5.48 (Continued)

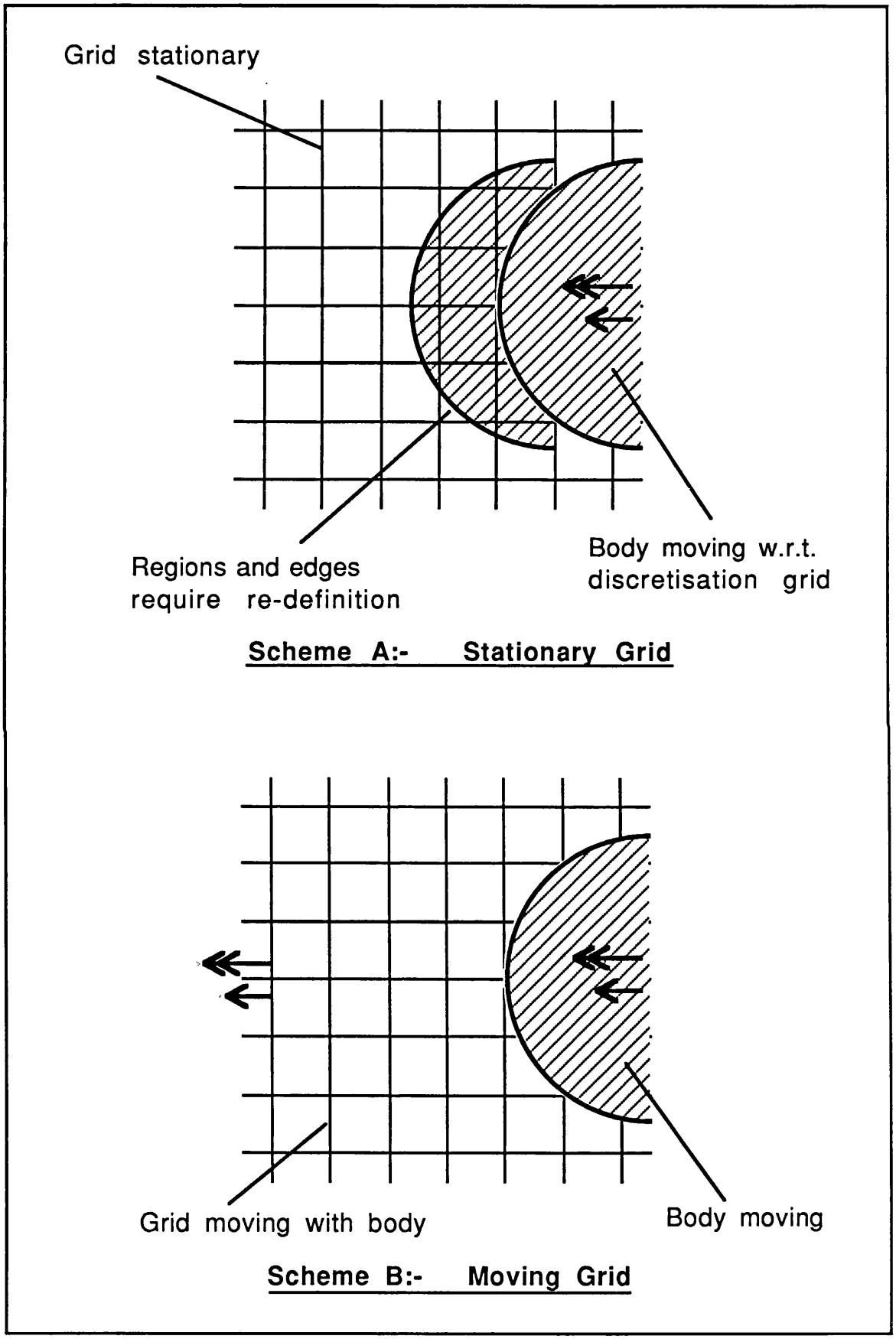

Figure 5.49 Alternative Schemes for Synthesising Convective Pressure from Accelerating Bodies

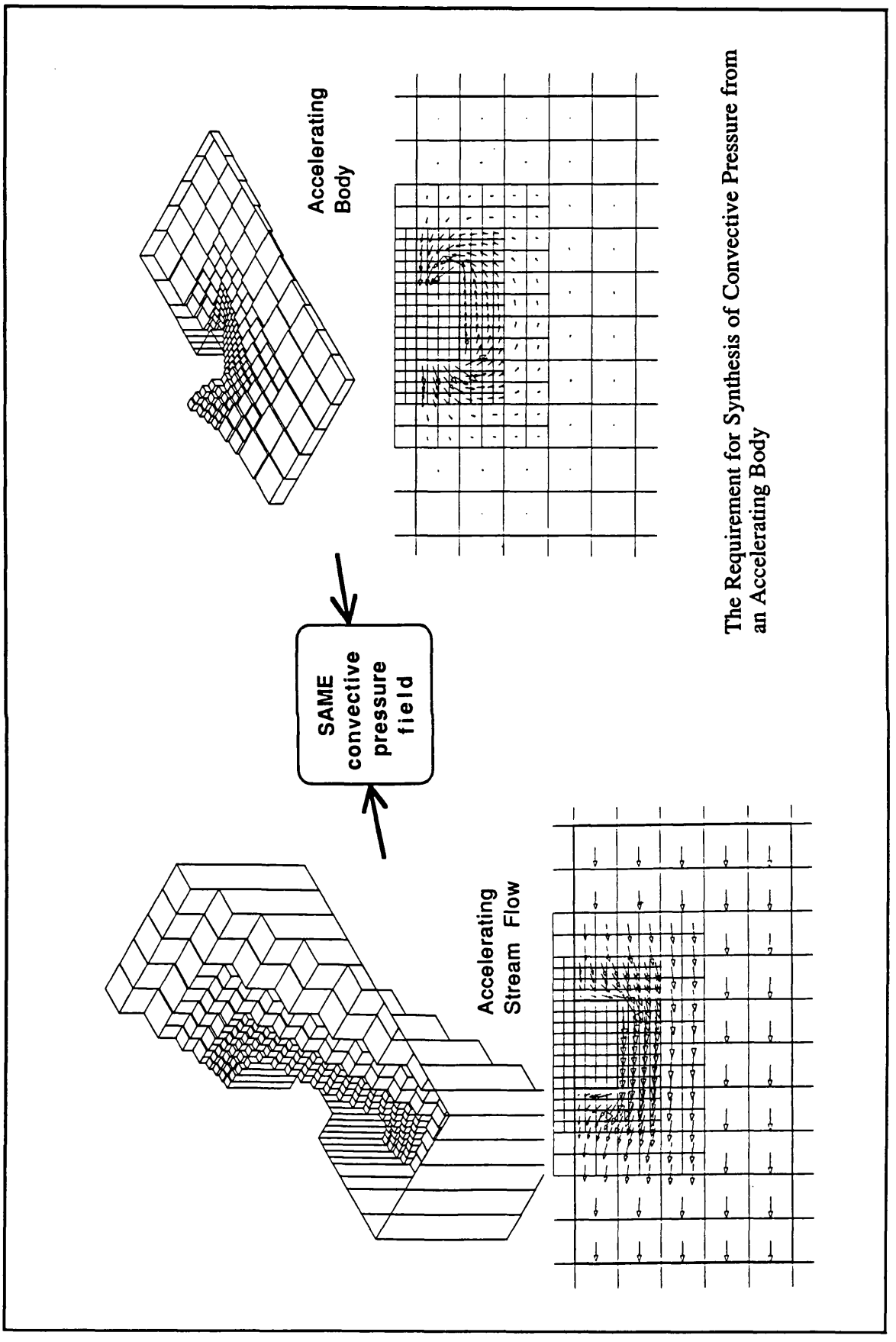

Figure 5.50 The Requirement for Synthesis of Convective Pressure from an Accelerating Body

(a) Description of Algorithm

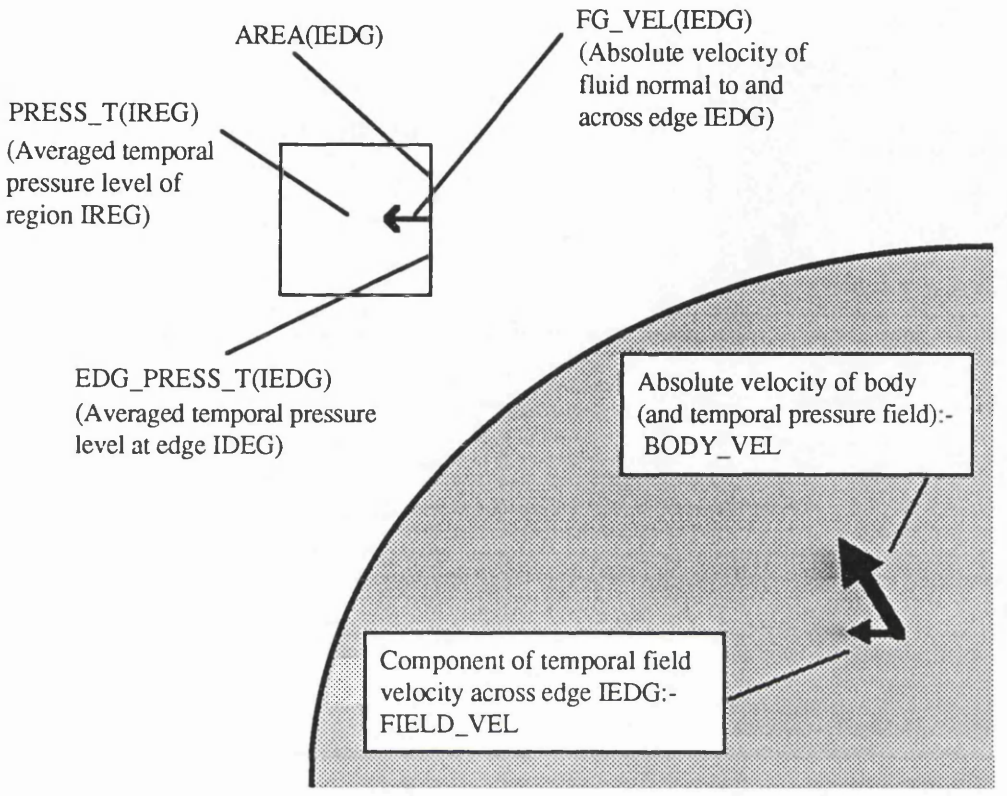

Velocity of fluid across edge IEDG relative to temporal pressure field:-

REL_VEL(IEDG) = FG_VEL(IEDG) - FIELD_VEL

Constant temporal pressure acts from time t = T1 to T2:-

$$CUM\_EXCHANGE = \frac{0.5*(REL\_VEL\_OLD(IEDG)+REL\_VEL(IEDG))*AREA(IEDG)*(T2 - T1)}{VOLUME(IREG)}$$

$$PRESS\_C(IREG) = PRESS\_C(IREG) - \sum_{\text{All edges}} CUM\_EXCHANGE*(EDG\_PRESS\_T(IEDG)-PRESS\_T(IREG))$$

Figure 5.51 First Attempt at Algorithm for Synthesis of Convective Pressure for Accelerating Bodies

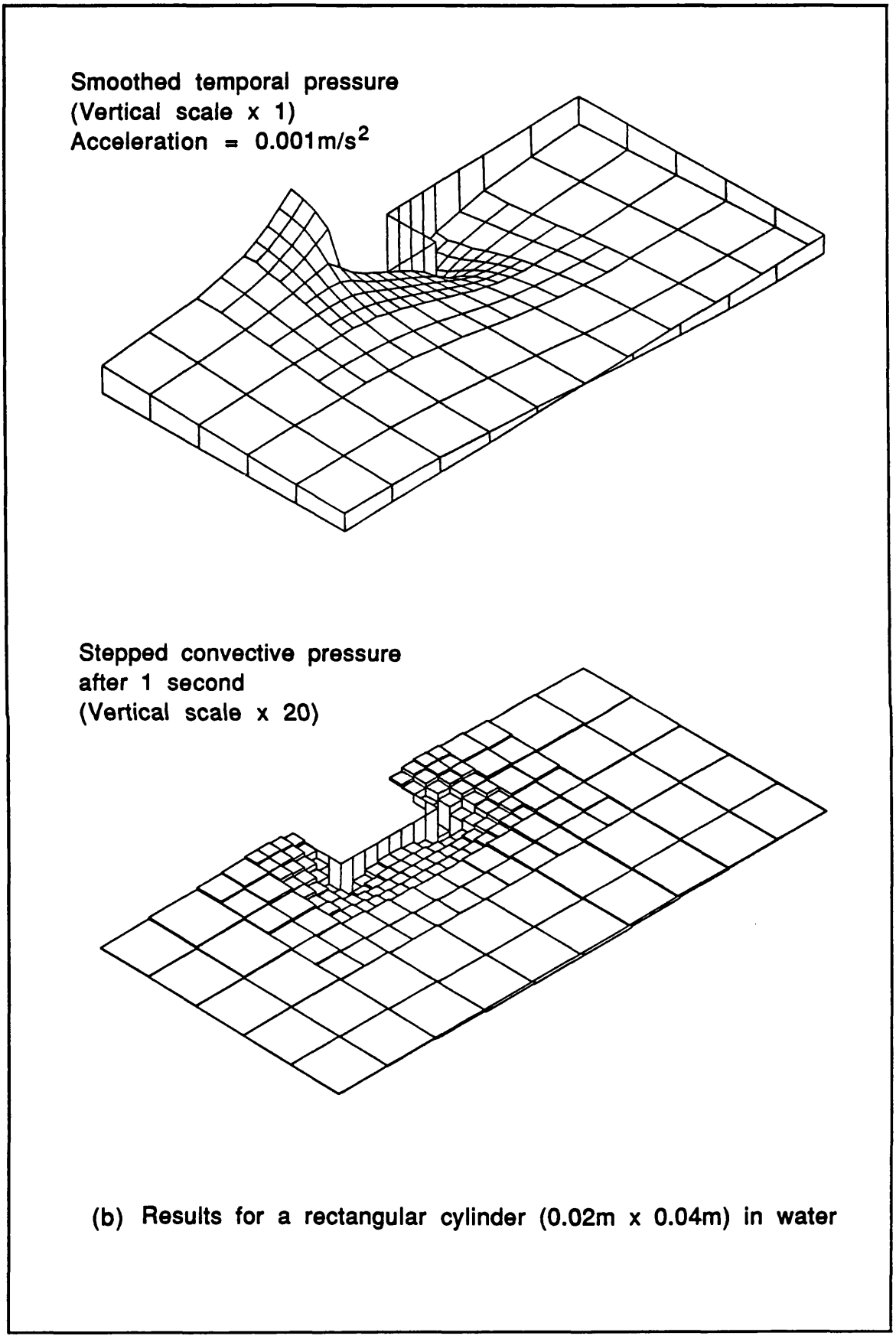

(b) Results for a rectangular cylinder (0.02m x 0.04m) in water

Figure 5.51 (Continued)

(a) Description of Algorithm

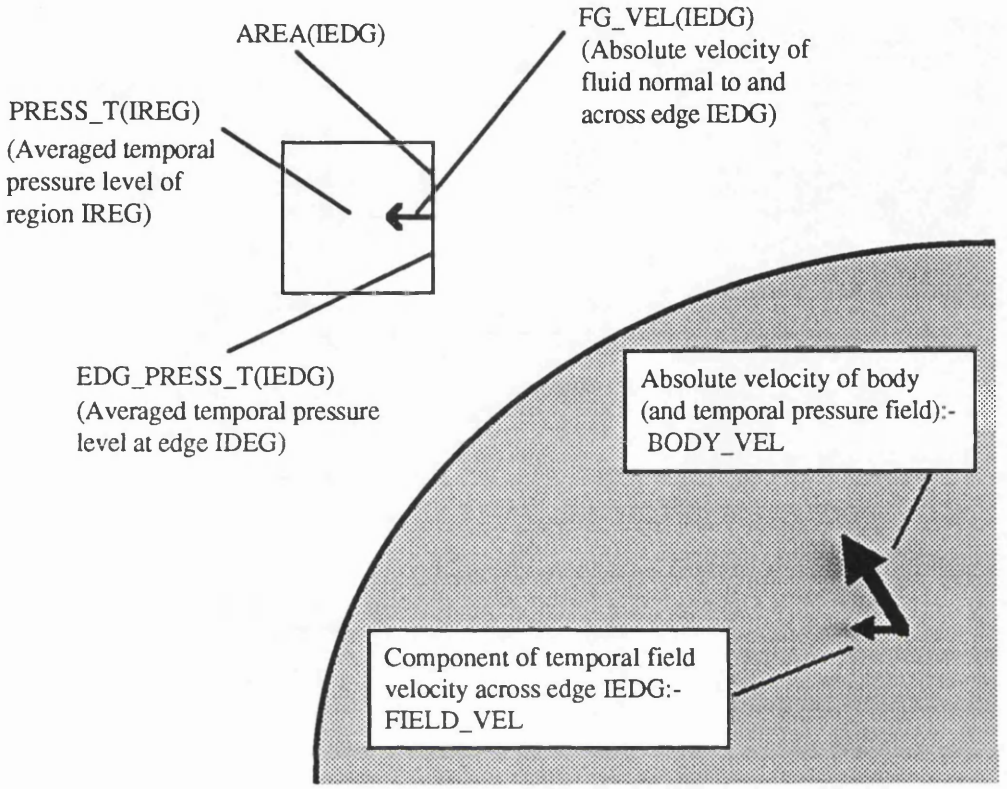

Velocity of fluid across edge IEDG relative to temporal pressure field:-

$$REL\_VEL(IEDG) = FG\_VEL(IEDG) - FIELD\_VEL - FIELD\_VEL$$

Additional term accounting for the rate of change of the temporal pressure at the instantaneous location of the edge IEDG.

Constant temporal pressure acts from time t = T1 to T2:-

$$CUM\_EXCHANGE = \frac{0.5*(REL\_VEL\_OLD(IEDG)+REL\_VEL(IEDG))*AREA(IEDG)*(T2 - T1)}{VOLUME(IREG)}$$

$$PRESS\_C(IREG) = PRESS\_C(IREG) - \sum_{\text{All edges}} CUM\_EXCHANGE*(EDG\_PRESS\_T(IEDG)-PRESS\_T(IREG))$$

Figure 5.52 Algorithm for Synthesis of Convective Pressure for Accelerating Bodies

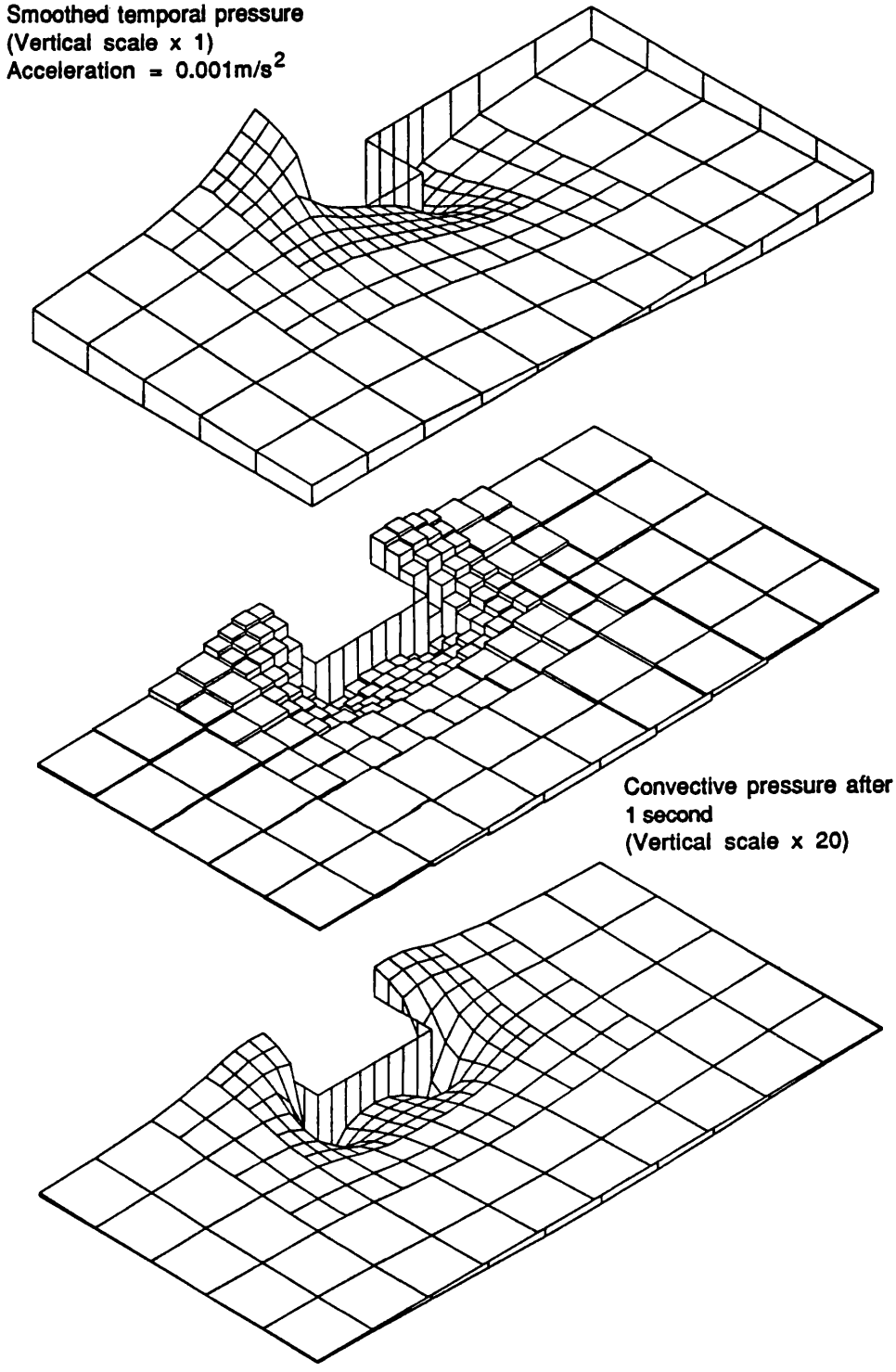

(b) Results for a rectangular cylinder (0.02m x 0.04m) in water

Figure 5.52 (Continued)

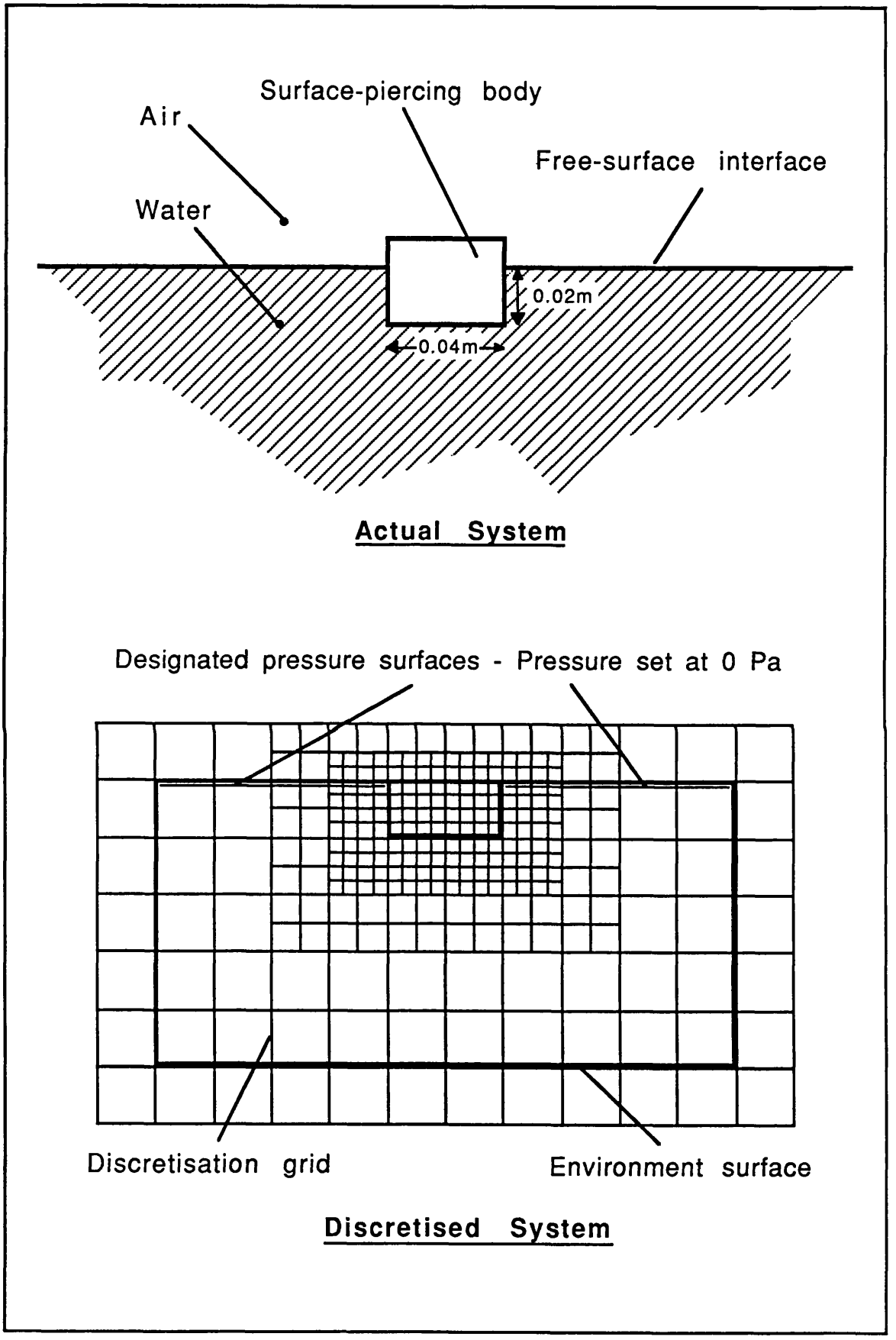

Figure 5.53 Rectangular Surface-Piercing Body

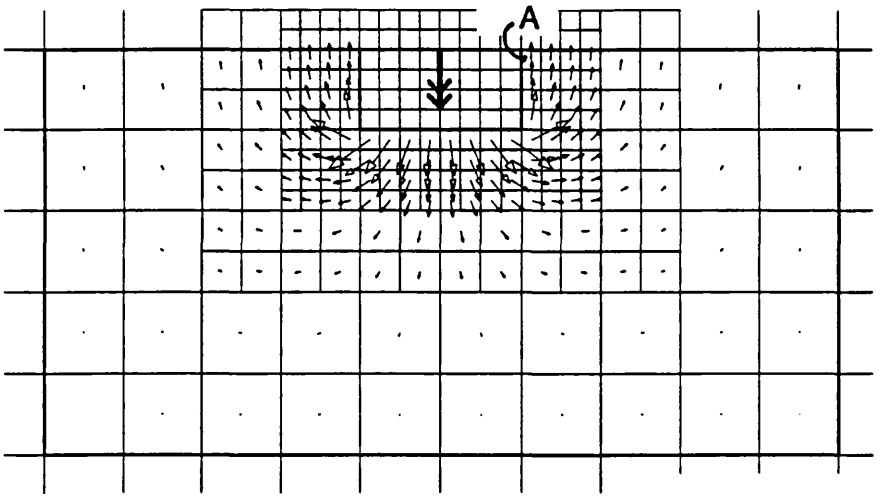

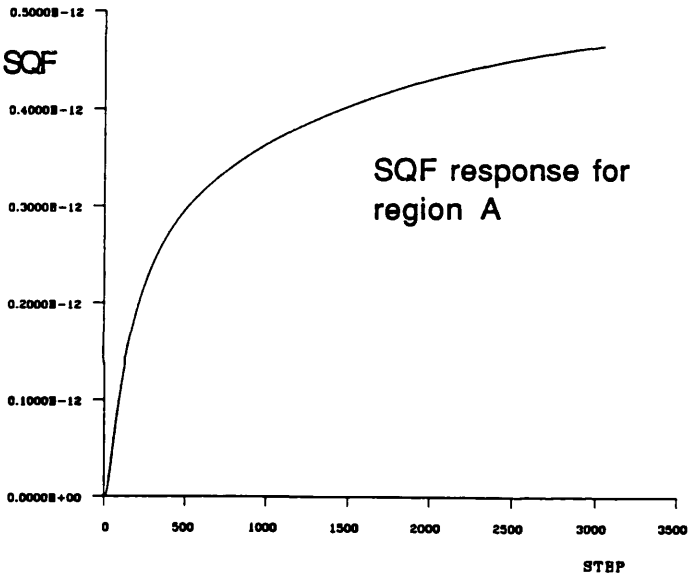

Acceleration response (scale x 10) for body acceleration of $0.001 m/s^2$

SQF response for region A

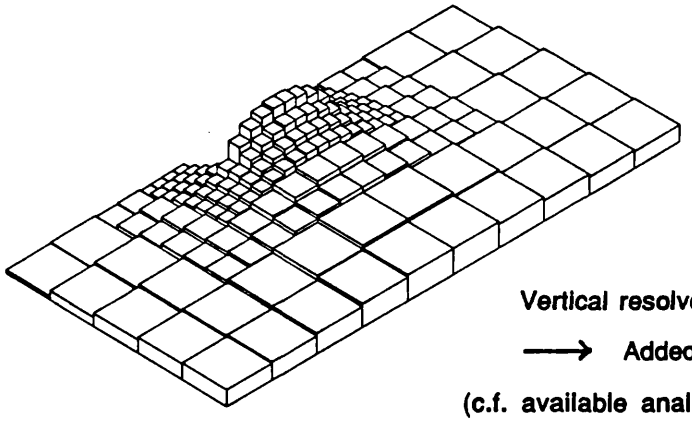

Temporal pressure (Vertical scale x 1)

Vertical resolved force = 0.9568×10^{-3} N

⟶ Added mass in heave = 0.9568 kg

(c.f. available analytical solution = 0.9508 kg)

(a) Neglecting gravity influences

Figure 5.54 Results for Vertical Acceleration of a Rectangular Surface-Piercing Body

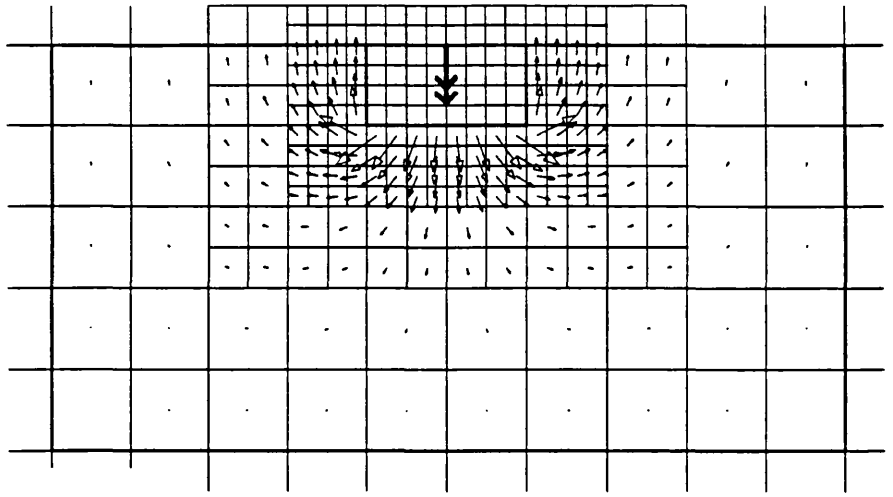

Acceleration response

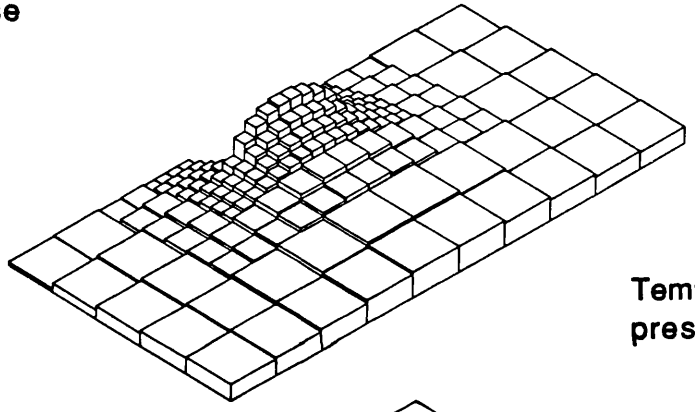

Temporal pressure

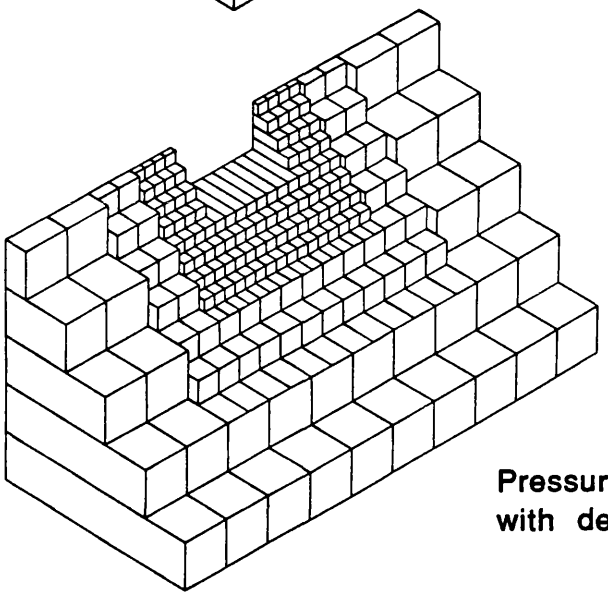

Pressure variation with depth activated

(b) Identical results when gravity is considered

Figure 5.54 (Continued)

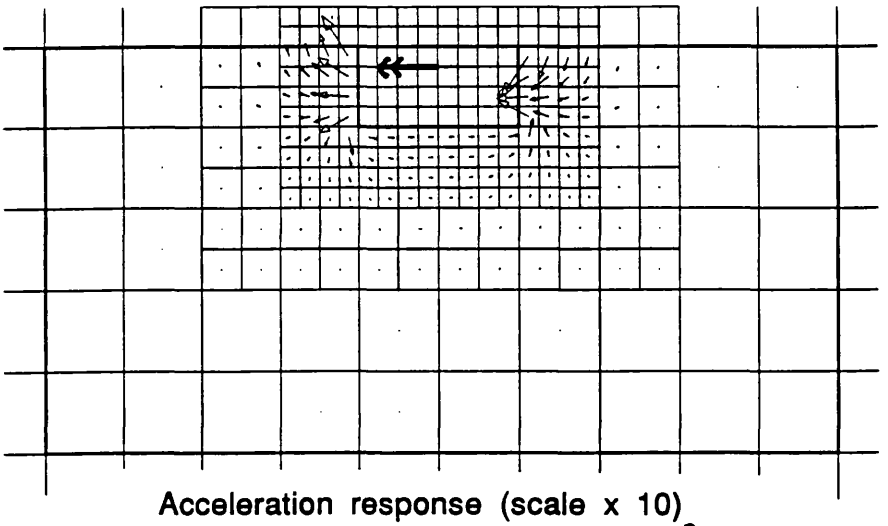

Acceleration response (scale x 10)
for body acceleration of 0.001m/s^2

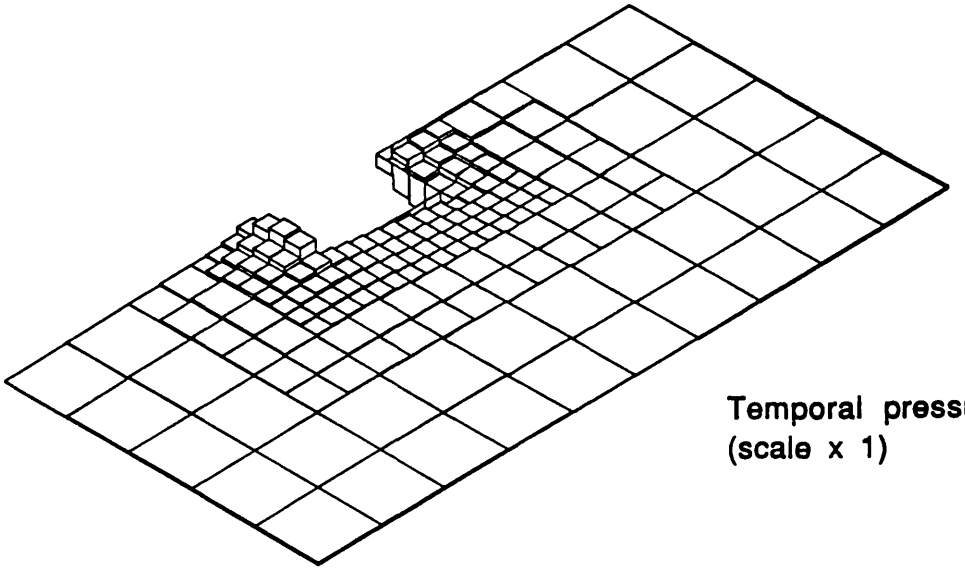

Temporal pressure
(scale x 1)

Horizontal resolved force = 0.2554 x 10^{-3}N

→ Added mass in sway = 0.2554 kg

Figure 5.55 Results for Horizontal Acceleration of a Rectangular Surface-Piercing Body

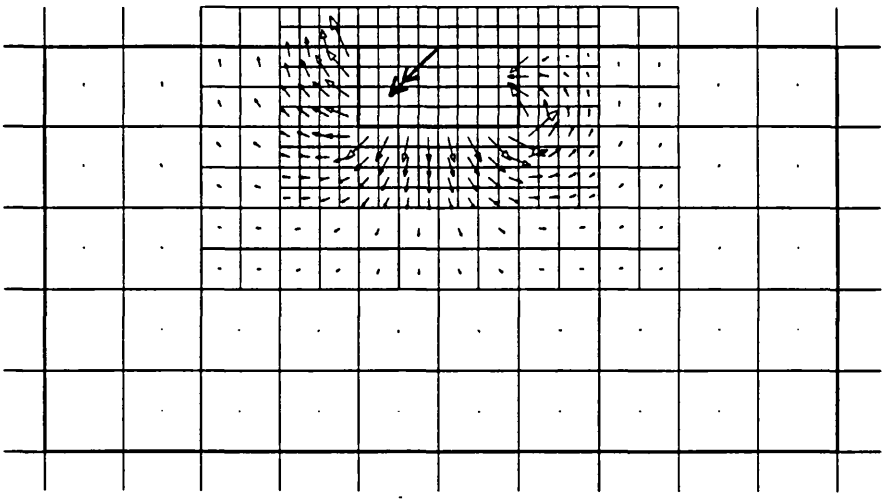

Acceleration response (scale x 10) for body acceleration of 0.001m/s ^{2} at 45 degrees to free-surface

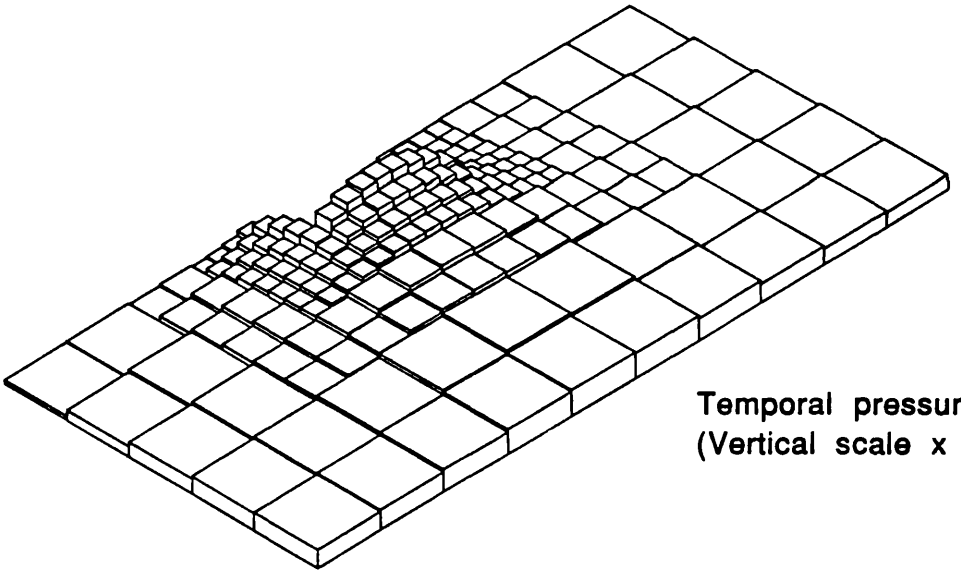

Temporal pressure
(Vertical scale x 1)

Vertical resolved force = 0.6760 x 10 $^{-3}$N

→ Added mass in heave = 0.9560 kg

Horizontal resolved force = 0.1807 x 10 $^{-3}$N

→ Added mass in sway = 0.2555 kg

Figure 5.56 Results of Combined Modes of Acceleration of Rectangular Surface-Piercing Body

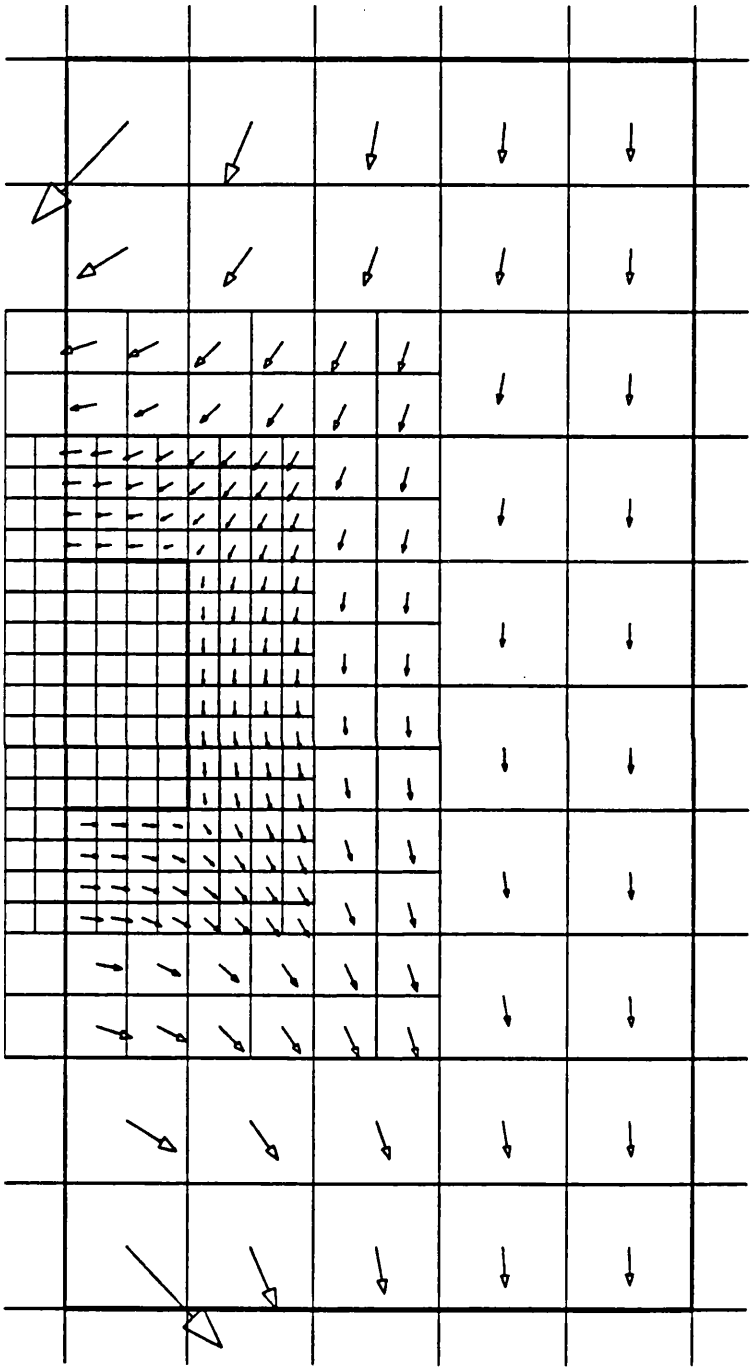

Figure 5.57 Accelerating Free-Stream Past Rectangular Surface-Piercing Body

CHAPTER 6

DISCUSSION

1. INTRODUCTION

The purpose of this chapter is to review the contribution of this thesis towards realising the concept of a "direct" computer model of fluids and to discuss the developments that still need to be made towards this goal. The discussion will be centred on the final state of the algorithms and modelling strategy as described in the latter part of chapter 5 since the various earlier approaches have already received sufficient attention during their presentation (and rejection) within chapters 3 to 5. Section 2 will review the objectives of the research and then compare these with the state of development of the flow modelling algorithms and the realisation of these in the test program FLOW2D. Section 3 will discuss the future directions for this research in terms of both the scope of study and the specifics of the necessary developments and additions to the flow modelling algorithms.

2. ACHIEVEMENTS VERSUS OBJECTIVES

2.1 Review of Objectives

The principal objective of this research was to demonstrate and realise the principles of a direct approach to computer modelling of fluids (chapter 3, section 4). A direct approach was defined as one where the algorithms were physically transparent throughout (i.e. avoided mathematical interpretations and manipulations) and additionally provided an insight into the understanding of fluid behaviour (chapter 1, section 6). This objective has remained consistent throughout the work. The scope of the investigations, on the other hand, had to be reviewed during the course of the research. In Phase 1 modelling considerations were "restricted" to 2-dimensional, viscous, incompressible flow in the absence of free-surface distortions. It was found that at the end of Phase 1, however, that this scope was too ambitious and that for Phase 2 it was feasible only to concentrate on 2-dimensional, *inviscid* flow modelling, although now allowing for the possibility of free-surface distortions. It is with respect to this latter scope that the achievements in terms of algorithm design and program implementation will be assessed. The scope of application to viscous flow will be discussed in section 3.

2.2 Algorithms

The high-level structure of the necessary algorithms for inviscid flow is shown in figure 6.1. Flowcharts for the temporal and convective pressure modules devised are shown in figures 6.2 and 6.3. The solid boxes in figure 6.1 represent those modules that have been successfully incorporated in the 2-dimensional flow modelling test program, FLOW2D, while the dashed boxes indicate the modules which have yet to be implemented. The remaining work can be seen to lie in the area of grid re-generation and associated developments in the free-surface distortion and influence algorithms. Without grid re-generation the test program is limited to considerations of stream flow past bodies in the absence of actual wave distortions, body motions in unrestricted environments, or certain instantaneous characteristics of the flow with or without free-surfaces. These capabilities (and limitations) will be discussed in more detail in section 2.3.

All of the rules for algorithm development given in chapter 3 (section 2) are believed to have been satisfied in the latest versions of the algorithms. A continuum model, which was considered most likely to lead to the most physically transparent model *on the observable level*, is used. In the interests of generality and an expectation of future developments in computing hardware, speed and efficiency considerations did not influence the choice of the flow modelling strategy in terms of either discretisation (spatial or temporal) or the subsequent "solution" procedure. Most important, of course, is that the "solution" is not sought from an equation of balance; rather, it is driven from a known state by interacting influence algorithms. These influence sub-models are based firmly on the physics of fluid behaviour and are structured to reflect causes-and-effects in flow development. It is the modularisation of the modelling of the fluid mechanisms and the consequent flow attributes (such as temporal and convective pressure) which is believed to contribute to the aim of understanding flow behaviour; for with modularisation the presentation of the influence sub-models and the overall flow model become uncomplicated.

In the following sub-sections the details of the algorithms developed will be reviewed and, where appropriate, contrasted with existing schemes in conventional CFD.

2.2.1 Spatial Discretisation

The choice of a rectangular grid system and sub-division (chapter 4, section 4.3) goes against the advice of most contemporary research in CFD (see chapter 2, section 4.3). This type of spatial discretisation was chosen because it was the simplest to conceive and apply to any general system geometry. (The author certainly finds a cartesian reference easiest to relate to.) If such a scheme does exhibit inefficiencies from poor spatial

resolution when sub-division is applied, it may reasonably be assumed that these inefficiencies will become less significant as advances in computer hardware continue.

The "regions" defined by the discretisation process might look very much like control volumes as defined in the finite volume technique. However, no "nodes" in the usual sense needed to be defined in the work, although this term was used to describe the region corners when the necessity to incorporate a smoothing algorithm arose in the pressure synthesis model (chapter 5, section 3.8.3). Nevertheless, an implicit node structure might be interpreted as being formed by the regions' centroids where the average flow conditions for the regions are assumed to apply. Furthermore, the use of a staggered grid system, which is common in finite volume techniques, could also be interpreted in the associated algorithms, even though this is not explicitly defined. This is shown in the use of both average region values and values calculated at the region edges.

Despite the apparent resemblance of the presented scheme to certain aspects of the finite volume discretisation method, it should be remembered that all of the discretisation schemes in conventional CFD refer to *the way in which the differential equations of motion are discretised with a view towards getting a set of soluble analytical equations*. In the "direct" model the region definition algorithms were developed to provide a reference for obvious flow information for whatever flow influence algorithms were devised. They were not designed with the aim of discretising the global equations of motion. This intention can be seen when examining the specifics of the sub-models for driving the flow. For example, whereas the pressure is determined by a finite volume like calculation, the inputs to this calculation of pressure - i.e. the kinematics of the flow at the region edges - are provided by a finite difference like calculation.

2.2.2 Time Discretisation

The temporal discretisation used in the direct model is based on a simple forward-differencing scheme common to conventional techniques where new velocities are simply calculated from the old velocities and the temporal accelerations of the fluid calculated from the flow influence algorithms.

2.2.3 Solution Procedure

The "solution procedure", when compared to conventional approaches (chapter 2, section 4.5), can be seen to be "fully explicit" in character. This, in the end, was not a

choice as such, but rather a *necessity* to keep to the ideals of physical transparency in the algorithms. In conventional CFD, because of the mathematical emphasis, the fully explicit approach is seen merely as an option which, particularly for moderately compressible flows, tends to be eliminated on the grounds of computational inefficiency. Furthermore, this option is only available for compressible flow since the formulation of the equations of motion for incompressible flows denies any pressure generation mechanism and demands that the pressure solution for the flow, at least, be obtained by an implicit scheme (i.e. a balancing exercise).

In the direct approach two levels of explicit treatment can be observed in the solution procedure (refer to figures 6.1 and 6.2). The lower level is the sub-timestep model used for spreading temporal pressure disturbances within a system and determining the temporal acceleration response of the fluid at any instant. The higher level comes into play in circumstances where system geometries are not changing significantly during the time-scale of the total transient required to get the "steady" temporal pressure/acceleration response. In these cases (which will be common for incompressible flows and most applications in Naval Architecture) the temporal pressure/acceleration response can be considered as constant over a much larger timestep than the pressure spreading algorithm uses. It should not be necessary, therefore, to model a complete flow process on the sub-timestep level required to ensure stability of the pressure spreading algorithm.

The solution procedure is not global-equation based. Rather, it is influence based and structured to represent the causes and effects of these influences as they occur. This more individual modelling and treatment of the fluid mechanisms is believed to have significant advantages for the presentation of flow modelling concepts, the understanding of flow behaviour, and consequently the selling of such software to design engineers. The need to identify individual influences and their causes lead to the separation of the treatments of temporal and convective pressure and this is probably the most significant contribution and sign of promise of this work. For it illustrates that it is possible to lift the lid off what can tend to be "black box" models in conventional approaches (that are formed once equation formulation and discretisation have been performed) and understand the mechanisms and behaviour of fluids a little better. The author felt this quite poignantly in a number of places in the work. First when developing the pressure spreading algorithm which *predicted* the sonic velocity of the fluid rather than using it, exhibited pressure wave phenomena, and allowed the static variation of pressure with depth in a fluid to be generated; second when at last understanding Bernoulli's equation and the actual mechanisms whereby variations of static pressure in both steady and unsteady flow of "incompressible" fluids are generated.

2.3 Capabilities of the Test Program FLOW2D

Section 2.2 has indicated that the test program FLOW2D is still limited quite considerably in application without any grid re-generation routines being written. For without these only flows where the system geometries do not change with time can be modelled. Such systems include stream flows (i.e. uniform flows past one or more stationary bodies), single bodies moving linearly in large expanses of fluid, or such systems where additional boundaries are present but the actual geometry does not vary with time (for example, a body moving parallel to the walls of a uniform straight channel). It should be remembered, also, that the current algorithm for the development of convective pressure is not yet "bug free" and requires further attention (see section 3.2.1).

The most significant limitation resulting from the absence of grid re-generation (particularly as far as Naval Architecture is concerned) is that flows where a free surface actually distorts cannot yet be modelled. This means that wave profiles and associated wave resistances cannot yet be determined. However, as will be discussed in section 3.2.3, this facility may not involve too much effort to implement.

In addition to the above limited flow motion problems that can be modelled, the program can provide information on certain instantaneous aspects of a fluid system's behaviour. In particular, instantaneous fluid reactions to body accelerations (i.e. added mass characteristics) can be determined, even if the boundary geometries are changing. This includes bodies accelerating at or near (calm) free-surfaces; for the algorithm that determines the fluid temporal pressure reaction to a body acceleration need not involve any finite movements in the system. It should be noted that instantaneous rotational accelerations, or combined linear plus rotational accelerations can also be considered.

The direct model has been shown to exhibit numerical instabilities which are similar to those encountered in conventional CFD for explicit schemes. Indeed a condition limiting the maximum sub-timestep to ensure pressure conditioning and stability of the pressure spreading model was deduced which is similar to the Courant-Friedrichs-Lewy condition recognised in conventional approaches (see appendix 2). As in conventional approaches the accuracy of the flow prediction tends to increase with greater resolution, at a cost of computational effort required and rate of convergence (see figure 6.4). The overall speed of the direct approach at present is limited by the sub-timestep pressure spreading model, which was to be expected in view of the poor efficiencies of explicit schemes generally (see chapter 2, section 5). A rough idea of the comparative slowness of this part of the explicit algorithm is that the calculation of the temporal pressure field in the example of figure 5.48(f) with 168 regions took 200 seconds of CPU time; this contrasts with a CPU

time of only 10 seconds on the same machine for a one timestep calculation of the 3-dimensional Navier-Stokes equations (using a fully implicit solution scheme on a finite volume formulation) for smoke clearance in a rectangular room using 1000 node points [10d]. The two problems, of course, are not directly equivalent and the comparison of speeds has been left deliberately vague for two reasons. The first is because no attempt has been made so far to optimise the algorithm itself, or the coding as written for the given computer. The second and more important reason is because such considerations of comparative efficiencies are inappropriate at this stage of the work; for there are still significant developments to be made in the direct modelling approach as a concept alone, and to introduce constraints on speed and efficiency performance of algorithms now would only compromise these advances.

2.4 Ease of Understanding

One principal motivation for developing a direct approach to computer modelling of fluids was to provide a technique that would be easier to understand than the conventional mathematical approaches. This was in the interests of attracting more users to the field of CFD which could only be beneficial for research and development. Yet the author cannot deny experiencing several conceptual difficulties himself while developing the algorithms described here and observing problems while describing these algorithms to colleagues. These conceptual difficulties, however, are believed to be associated with breaking away from conventional lines of thought which have been channelled not only from CFD experience but also, and perhaps more deeply, from early education in general fluid dynamics*. In view of these potential difficulties, the author hopes that the reader has been able to follow this work with an open mind.

3. FUTURE DIRECTIONS

The program FLOW2D, even with its limitations, is believed to have satisfied the project's aim which was to demonstrate and realise the principles of a direct approach to computer modelling of fluids. The success and state of the work reported here directs future development effort and these requirements will now be broken down and discussed.

---

* This latter observation suggests that the work of this thesis could have appreciable benefits for general fluid dynamics education, quite apart from any potential advantages for applications in CFD.

3.1 Scope for System Modelling and Implementation

The scope for flow modelling in this research was constrained to considerations of "incompressible" inviscid flow, although allowing for the possibility of free-surface distortions taking place. The implementation of the test program was constrained to sequential processing due to the availability of machines with only conventional architecture. With the promising results so far obtained with this limited scope and implementation it is now possible and reasonable to consider more advanced systems and more dedicated algorithm implementation.

3.1.1 Implementation

The nature of the algorithms devised lend themselves directly to spatial parallel processing. This stands to reason since the individual mechanisms of real flow behaviour/action act simultaneously (or in parallel) at every position within a fluid system. A parallel implementation of the existing software would certainly enhance the viability of the approach at present compared to conventional techniques, but of course considering the ideals of the research this type of justification is not of great concern in itself. Rather, a parallel implementation would be chosen simply because it is a more physically transparent representation of the real system.

Since parallel processing machines are still not widely available and are still limited in the degree of parallelism offered, the obvious alternative implementation would be to vectorise the algorithms and try them out on today's supercomputers. For the long term aims of the research, however, this could only be considered as an expedient rather than ideal implementation until highly parallel machines become first available and then eventually affordable.

3.1.2 Advanced Systems

There are two main advances that could be made in terms of system description. The first is to extend the model to three dimensions and the second is to incorporate viscous effects. The extension to three dimensions should not be too demanding with respect to development of the algorithms for these were designed with 3-dimensionality in mind. However, this extension will involve considerable, if somewhat mundane, re-development of the system set-up algorithms for defining and discretising system geometries (see

chapter 4, section 4)*. The extension to include viscous modelling on the other hand will require considerable development and "investigative research" effort (see chapter 1, section 1) and this will be discussed further in section 3.2.5.

The nature of the required development effort for these two advances would suggest that they be tackled separately, but ideally in parallel as two closely linked research projects. The viscous development should continue in two dimensions and when successful could be incorporated into a ready and working 3-dimensional program. A particular reason for continuing the development of inviscid flow modelling semi-independently is because this is especially relevant to Naval Architecture for wave resistance predictions and seakeeping analysis.

3.2 Specific Studies

Section 3.1 has outlined the broad directions for continuing the research on the "direct approach". Associated with these developments are certain specific studies that need to be performed. These will now be covered in sections 3.2.1 to 3.2.5, the order of discussion indicating the order of priority.

3.2.1 Pressure Smoothing

The algorithm for generation of convective pressure has been shown to work well providing that fluid regions are reasonably regular in shape and similar in overall size within any level of discretisation. Errors in the convective pressure modelling, however, occur in the vicinity of the very small or distorted regions that can be formed adjacent to the boundary surfaces in a system. The source of these discrepancies was traced to the accuracy of description of the temporal pressure field (from which the convective pressure is deduced) and some form of pressure smoothing had to be employed (chapter 5, section 3.8.3). The current state of the pressure smoothing algorithm (see figure 5.45) however is not yet general enough to ensure accurate and smooth variations of pressure for arbitrary sized and shaped regions in all situations. It is possible to identify cases where the pressure distribution calculated will be erroneous. The suggested route to improving the pressure smoothing routine will simply involve identifying these "problem cases" and revising/extending the algorithm to cover them. The earlier experience of trying to get

* The alternative route, of course, now that the required data is known, would be to utilise standard commercial software for this purpose.

consistent SQF levels in partial regions (see chapter 5, section 3.5) indicates that this should be soluble, but may not be straightforward.

3.2.2 Momentum Balancing

The algorithm for synthesising convective pressure in a flow has not involved an explicit momentum balance. The increments to the convective pressure field were determined directly from pressurising actions resulting from the very small variations in the fluid's density arising within a temporal pressure field (see chapter 5, section 3.8). The limited scope of application of the program FLOW2D without grid re-generation routines meant that the cumulative effects of convective pressure generation by this technique could not be studied. Nevertheless, it is envisaged that with discretisation errors (particularly where grid re-generation is involved) and numerical errors generally, the level of convective pressure produced by the algorithm will not satisfy an instantaneous momentum balance exactly. These discrepancies will have to be monitored and controlled during flow development, but exactly how this will be done is not yet clear. One option would be simply to "correct" the convective pressure field until the momentum balance is satisfied for all regions of the fluid. This, however, would go against the ideals of the work in that it would be a mathematical adjustment of the results. An alternative approach would be to treat the "errors" as proper forcing influences in the system, augmenting the temporal pressure influences in some way. The details of this option should become clearer when work on the viscous influence modelling continues (see section 3.2.5) since the forcing influence here is similarly flow generated.

3.2.3 Grid Re-Generation

Grid re-generation will be required for modelling systems where the relative geometries change with time. One example of this is where distortion of a free surface takes place and waves are generated; however, this is discussed more specifically in section 3.2.4. Here discussion is centred on situations where geometries change due to moving solid boundaries.

Figure 6.5 illustrates the alternative schemes for analysing, say, the fluid response to a body moving within a restricted environment. Either the discretisation grid may be made to move with the moving body or is kept fixed in space. In each case grid re-definition is required. To keep within the ideals of the direct approach the latter is recommended. For this makes the understanding of the modelling much simpler since the kinematics are

straightforward (see, for example the discussion of section 3.8.5 in chapter 5). Besides, in the general case there may be more than one body in the system and these will likely be moving with different velocities; in such cases there is no obvious choice to which body the moving grid should be connected.

The actual mechanism of re-generating a grid for new positions of a body or bodies in a system should utilise existing modules to a large extent. Re-generation should, if anything, be much quicker than the first generation since only regions in way of the moving bodies need to be re-defined. The details of how the new grid will be utilised and how discretised flow properties will be related to the old grid values, however, is subject to further research. At present two schemes can be envisaged. The first is where the main timesteps are limited to produce body movements which are a fraction of the nominal size of the lowest level of subdivision. In this way regions and flow values discretised for specific regions can be adapted together (see figure 6.6(a)). With this scheme there may be problems of suddenly disappearing or appearing partial regions which would have to be dealt with. The alternative scheme is where, during a timestep, the global flow picture is predicted for the next location of the body and "cut" from the discretisation grid. The grid is then re-generated for the next position of the body and the predicted picture of the flow is "pasted" into the new grid (see figure 6.6(b)). Although the latter scheme could well turn out to be the easier to implement, the concept is somewhat mathematical. At this stage, therefore, the author is inclined to favour the former approach for this development.

3.2.4 Free-Surface Distortion

In order to model finite distortions of a free-surface a grid re-generation facility is required (see section 3.2.3). In this case the free-surface profile will follow the flow movement predictions for the fluid at the location of the free-surface rather than following distinct kinematics of a solid boundary surface (see figure 6.7). When finite distortions take place the weight and the variation of pressure due to depth in the fluid will have to be represented in the computer model as accelerating influences.

As for the case of grid re-generation schemes for solid boundary motion problems, the *details* of how finite wave responses will be modelled is subject to further research. However, one question of academic and some practical interest is worth addressing here: that is, how far can you go without *actually* distorting the free-surface? When embarking on the limited free-surface modelling in this work it was hoped that some greater understanding of the observed variation of added mass with frequency for bodies oscillating at or near the free-surface would be gained. That the constant acceleration tests

performed showed no variation of added mass with magnitude of acceleration (see chapter 5, section 3.9.1) confirmed and illustrated that this distortion of loading with oscillatory motions is caused by the consequences of the free-surface being allowed to move. The question here is; is it necessary to consider finite movements of the free-surface (which will involve the grid re-generation algorithms) or will considerations of infinitesimal or tended motions suffice for the determination of added mass distortions and wave damping effects? For the latter would probably be easier to implement and of considerable interest, for example to linearised seakeeping applications. The scheme envisaged is where a tended free-surface distortion is obtained for a unit acceleration of the body and a secondary superimposed flow and pressure response is predicted for this tended wave distortion influence. The added mass distortion and damping characteristics could then be deduced from the secondary pressure loading on the body surface. If such a technique were to succeed it would certainly make a more physically tangible alternative to the linearised oscillatory potential flow calculations commonly performed [11b], even if it was not perfectly general in application.

3.2.5 Viscous Modelling

The modelling of viscous influences will undoubtedly be the most demanding of the specific studies in the development of the direct approach to computer modelling of fluids. Early attempts at such modelling were postponed after Phase 1 of the research in the interests of laying firm foundations for the overall modelling concept and getting the inviscid influence modelling right. With hindsight the revised scope for Phase 2 which concentrated on inviscid flow with free-surfaces was a much more rational first target for the modelling development than the original scope of viscous flow in the absence of free-surface distortion, particularly since this revised scope still covered areas of significant interest in Naval Architecture. However, now that the direct modelling of inviscid flow has been shown to be viable it is necessary to reconsider the directions for modelling the actions of viscosity.

Review

Reviewing the work of Phase 1 (chapter 4) it is now possible to be more constructively critical of the efforts made to model viscous influences as described in chapter 4, section 5.2. Scheme 1, although believed sound in respect of the *principles* of the method for calculating the initial viscous acceleration, was doomed to failure for two reasons. First, because the resolution of the grid was inadequate; and second, because the proposed scheme for satisfying the subsequent continuity clashes was not physically justifiable. The modifications put forward in schemes 2 and 3, then, clumsily and naively

attempted to get plausible viscous disturbances, but they sacrificed physical veracity even more. Scheme 4, however, which postulated a model for separating *inviscid* flows, is believed worthy of further exploration but is not discussed further here. Finally, scheme 5, which involved the "ROTATION" quantity, although considered promising at the time in some respects, clearly contradicted the ideals of physical transparency.

The scale on which the dominant viscous influences take place, and the highly localised nature of this, means that descriptions of viscous mechanisms using a conventional and relatively coarse grid system as used so far in the modelling are not appropriate if physical transparency is to be achieved. Using a conventional grid system makes it conceptually difficult to identify tangible "boundary condition" inputs for the viscous mechanisms equivalent to the fixed pressure boundaries or motions of solid boundaries that are used in the inviscid influence model to which there is an obvious reaction. This conceptual difficulty was manifested in the viscous schemes of chapter 4; for example, where the rather vague notion of "soft" inputs to the disturbance spreading model was proposed. Those ideas arose, however, in the context of a kinematic model of the flow which, with hindsight, was conceptually difficult in itself. In the work described in chapter 5 the modelling strategy was altered to a dynamic representation and although the initial viscous input is now clearly identified in terms of shear forces, the reaction of the fluid to such an influence would still be not at all obvious within the current scheme of discretisation. This is best visualised at boundaries in the flow where the no-slip condition applies and viscous influences are most significant. The problem is that most of the flow distortion and development takes place in the boundary layer which can be extremely thin and certainly initially much thinner than the size of conventional discretisation. The definition of the wall shear stress and the fluid's reaction to this, therefore, requires more information than the gross region flow descriptions that are currently sufficient for the inviscid model.

In conventional CFD it is necessary for turbulent flow predictions to use "wall function" descriptions between wall nodes and adjacent nodes away from the wall in order to connect the wall fluxes to the outer flow conditions. These provide log-law models of the velocity distortions and empirically based variations of the turbulent kinetic energy in the boundary layer. They obviate the need otherwise for up to about 40 mesh points within the boundary layer with the consequent mis-matching of discretisation requirements for the outer flow. In laminar flow calculations the velocity gradients at the wall (leading to the shear force values) are simply based on the velocity value at the first grid location from the wall. In both laminar and turbulent calculations it is conventional and clearly necessary to examine the convergence of the flow solution with finer grid definition. This tends to

underline the observation that the choice of the level of discretisation in CFD at present is rather a "hit or miss" affair.

Suggested Approaches for Discretisation

From the discussion above two features for the representation required to model the actions of viscosity in the direct modelling technique suggest themselves. The first is to provide fine discretisation in the vicinity of the solid boundaries in the system, without incurring wastage of discretisation in the outer flow. The second is to provide a facility where the levels of this discretisation at various locations in the flow, for viscous effects at least, are self adapting.

Two possibilities can be envisaged for effecting the finer discretisation. The first scheme is to provide a separate discretisation grid for the "boundary layer" flow* which does not have to be matched to the main discretisation grid, but which can be two-way blended with the main grid as required in calculations (see figure 6.8(a)). The second scheme to be explored is where finer discretisation is achieved by including two features on top of the existing discretisation for inviscid effects. The first is to be able to split regions into flow "zones" (sub-regions effectively) as appropriate in order to represent movable flow features (such as separation contours and eddy boundaries) more accurately. The second is to incorporate a means of representing and using velocity profiles for regions and sub-regions in the model. These features of the second scheme are illustrated in figure 6.8(b).

Approach to Influence Modelling

The key to being able to model viscous influences and effects physically is believed to lie in providing the appropriate level of discretisation which allows transparent *description* of the mechanisms involved. That key, therefore, may be provided by one of the schemes outlined above. The subsequent route for modelling the viscous actions then would be based on Newton's Laws of motion and should be straightforward in most respects, just as the explicit edge transfer method approach turned out to be very straightforward for inviscid influences (see chapter 5, section 3.6.2). However, during the course of the development certain specific elements of the overall strategy will be tested, particularly with regard to the viability of the envisaged modularity of the whole approach as described in chapter 3, section 5.

---

* Note that here the term "boundary layer" is being used in connection with the fluid adjacent to the body all over the body, whether separation had occurred or not. This should not be confused with the definition of boundary layer theory where certain conditions of definition for a boundary layer to satisfy the "boundary layer equations" must apply.

The modular influence structure presented in figure 3.2 was limited in terms of scope of application and was by no means comprehensive or entirely adequate in describing all of the causes and effects in real fluid flows. With the benefit of the development work carried out in chapters 4 and 5, it is now possible to introduce in figure 6.9 a more advanced version of that diagram. It can be seen that this new version of the influence structure now

- acknowledges (temporal) pressure influences as pre-cursors to the establishment of temporal accelerations;
- includes representations of the effects of gravity and geometry changes in the system (the latter of which includes solid boundary movements and free-surface distortions);
- describes what is believed to be a more plausible structuring of the effects of viscosity.

Whereas the modelling of the gravity and geometry change influences could turn out to be relatively straightforward, it is felt that the viscous modelling will require considerable effort. In figure 6.9 it is suggested that the temporal acceleration due to shear actions (described before as the "initial viscous acceleration") is kept separate from the consequent continuity clash problem which is now treated as a further influence for the temporal pressure field. Subsequent investigative research may well alter this perceived structure.

4. CLOSURE

This chapter has reviewed the achievements made in this research into the development of a "direct" computer model of fluid behaviour. The project objectives have been satisfied in that the viability of the direct approach has been confirmed and demonstrated in a test program FLOW2D. The revised scope of the work concentrated on inviscid flow, allowing for the possibility of free surface distortions. Only part of the free-surface modelling has been realised and completion of this could lead to a very usable tool for naval architecture calculations in seakeeping and wave resistance estimations. The most significant future development of the direct modelling concept for general engineering applications (including, of course, naval architecture) will lie in the modelling of viscous influences. The various specific studies required to achieve these longer term aims have been outlined.

No detailed comparative testing between the algorithms designed and those of conventional techniques has been performed: this must wait until the concepts of the direct modelling approach are fully worked out. Although at this stage it certainly looks as though the direct approach will be slower than the most efficient conventional methods, this deficiency should be weighed against any advantages that the technique may offer in

terms of versatility, ease of understanding, and development potential. With reference to speed, there should be some compensating gains when the algorithms are transported to a parallel processing environment to which they would be best suited.

Finally, whether or not the direct modelling technique will ever be able to compete in the CFD field, the concepts described in the approach should, at least, have a part to play in general fluid dynamics education since they are believed to promote a better understanding of fundamental aspects of fluid behaviour.

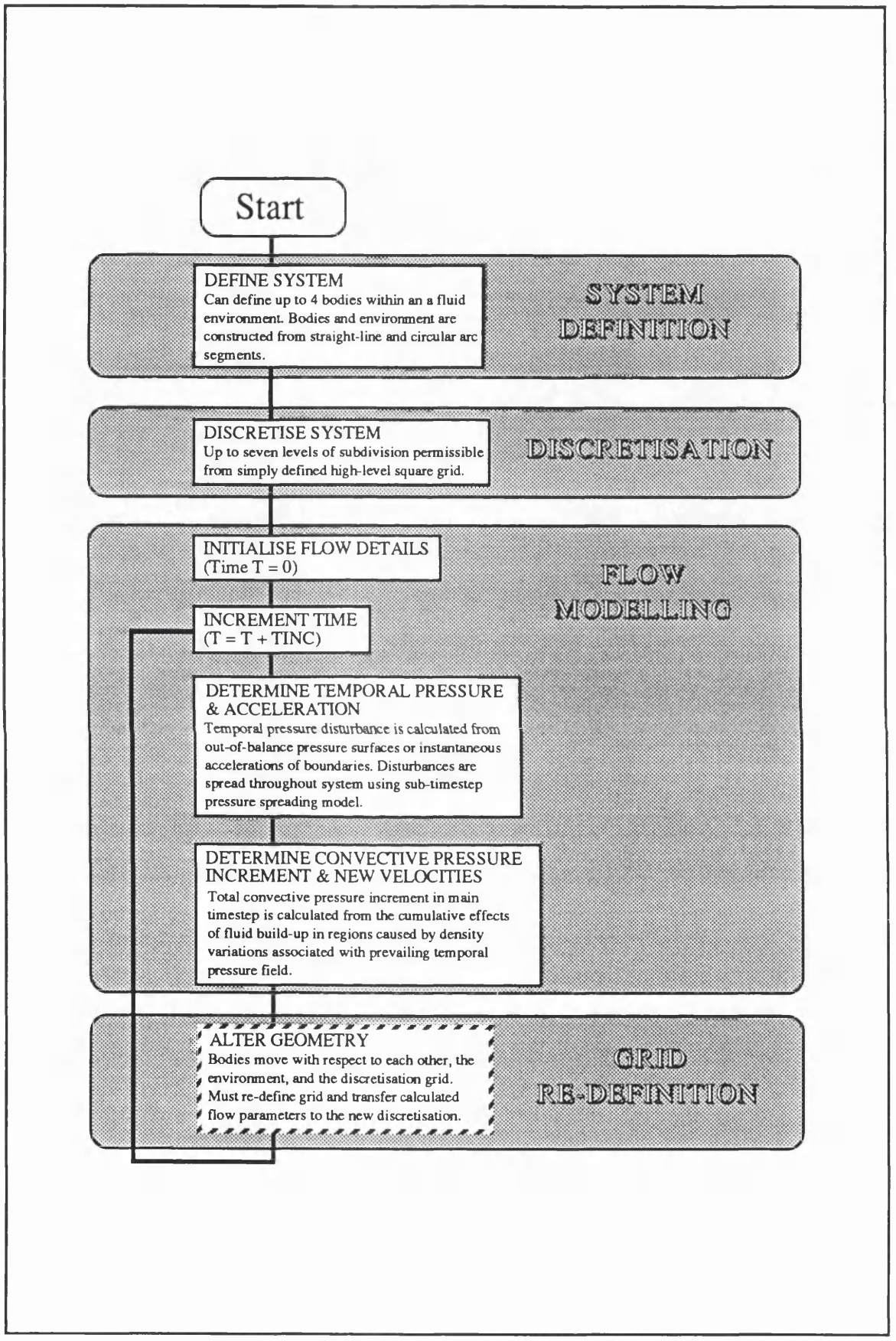

Figure 6.1 Review of the Direct Modelling Approach for Inviscid Flow

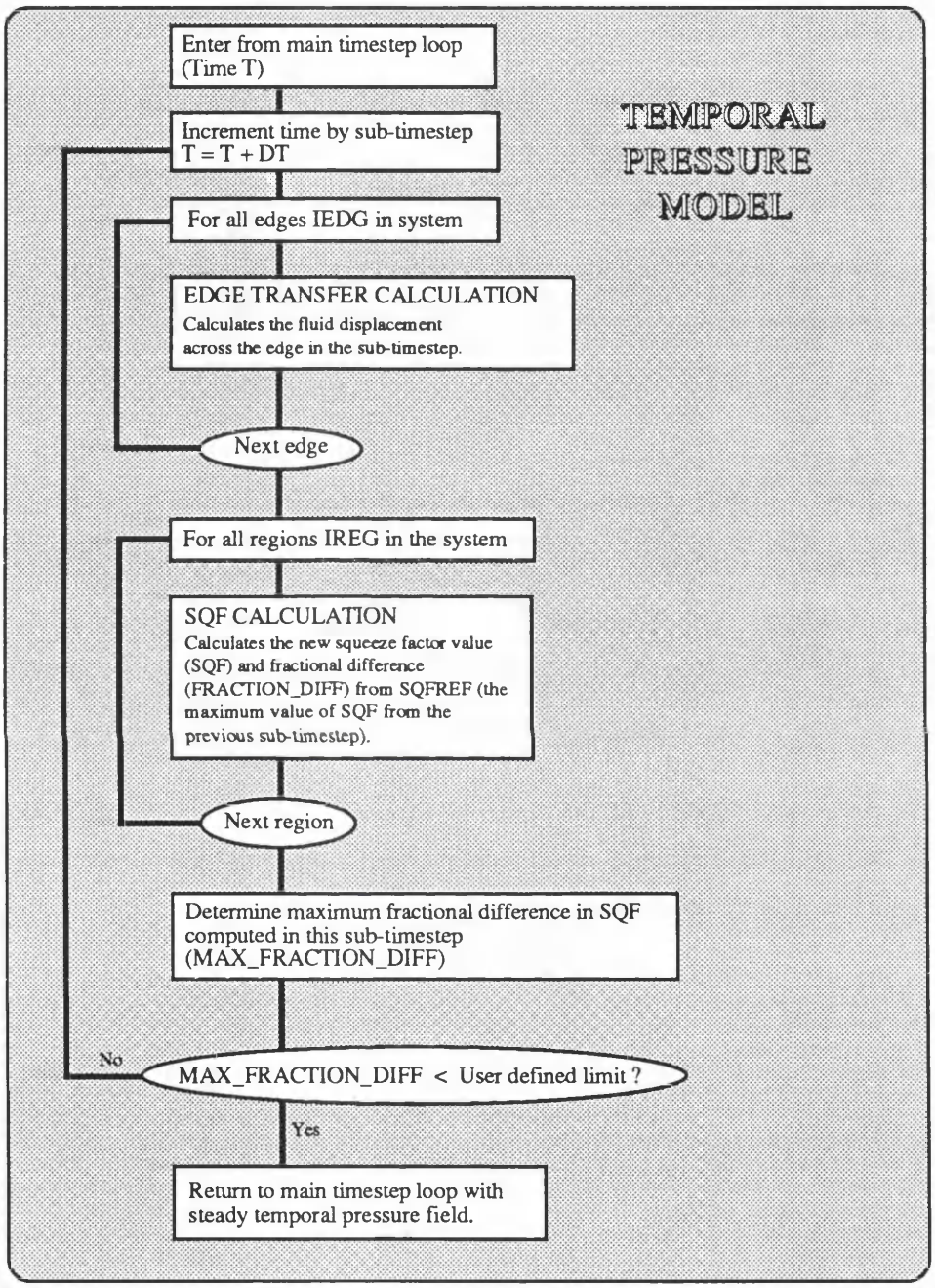

(a) Overall Scheme

continued →

Figure 6.2 Flowchart of Temporal Pressure Model

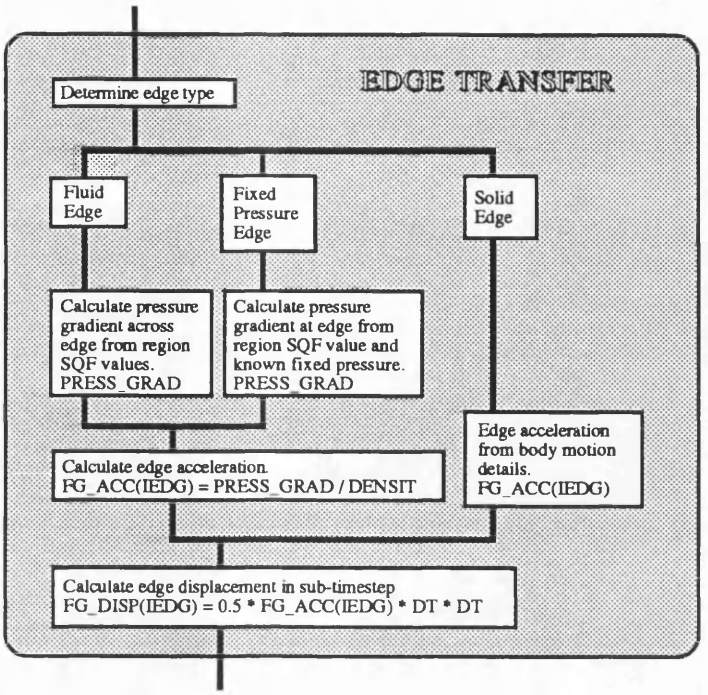

(b) Edge Transfer Routine

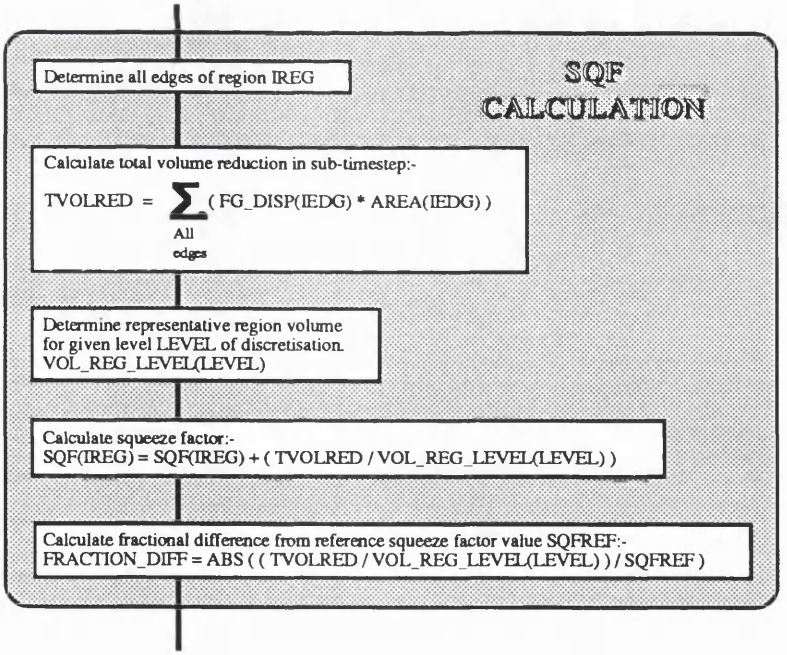

(c) SQF Calculation Routine

Figure 6.2 (Continued)

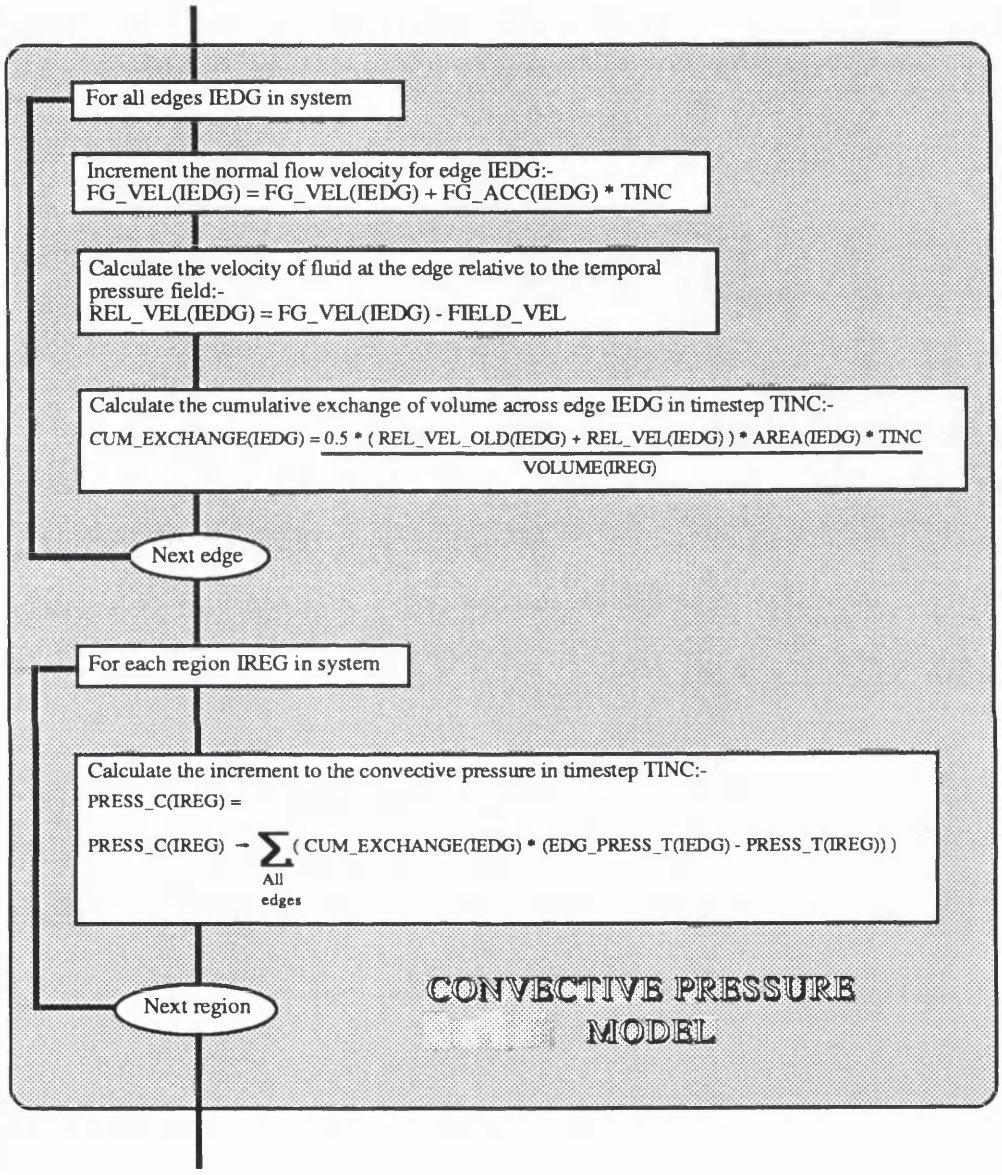

Figure 6.3 Flowchart of Convective Pressure Model

Test Case:- Accelerating (2-dimensional) Flat Plate

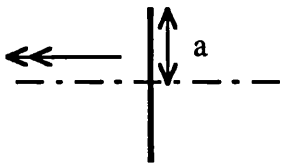

Expected added mass [12b] = $\pi \rho a^2$

Example of Discretisation:-

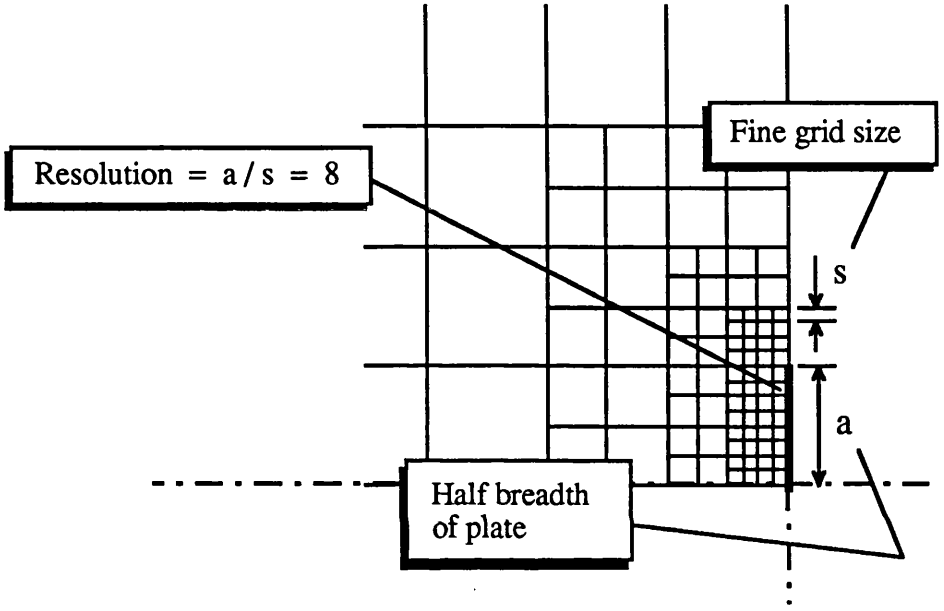

Variations of Accuracy and Computational Effort Versus Grid Resolution

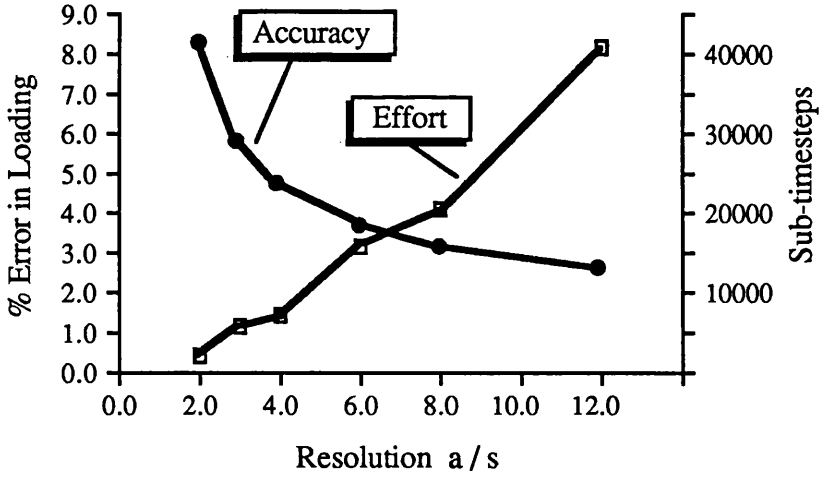

Figure 6.4 Accuracy and Convergence of Results

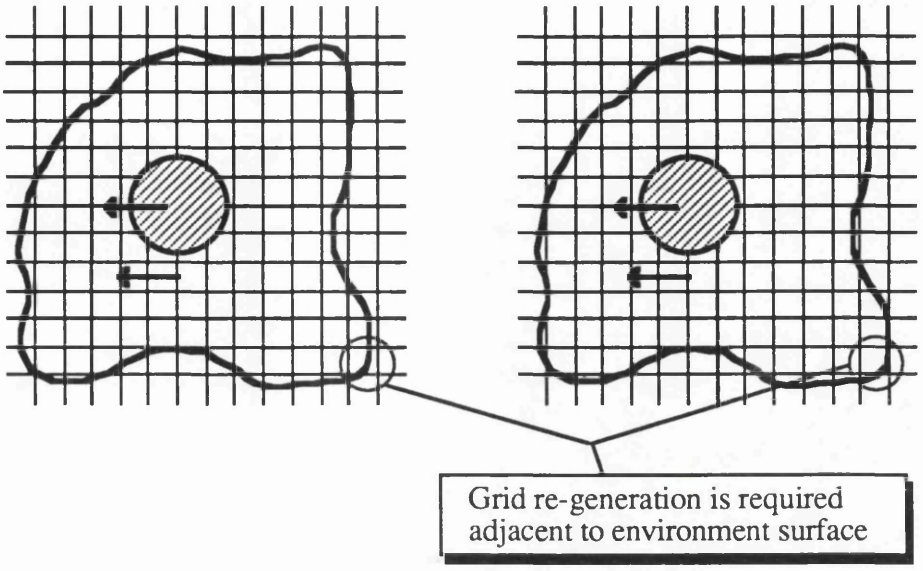

(a) Grid moving with body

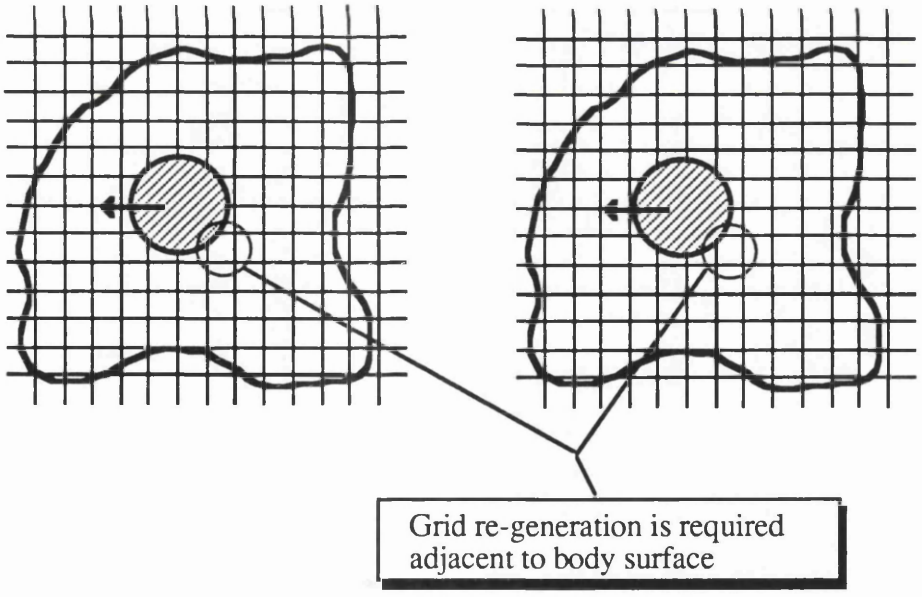

(b) Grid Fixed in space

Figure 6.5 Grid Re-Generation Alternatives

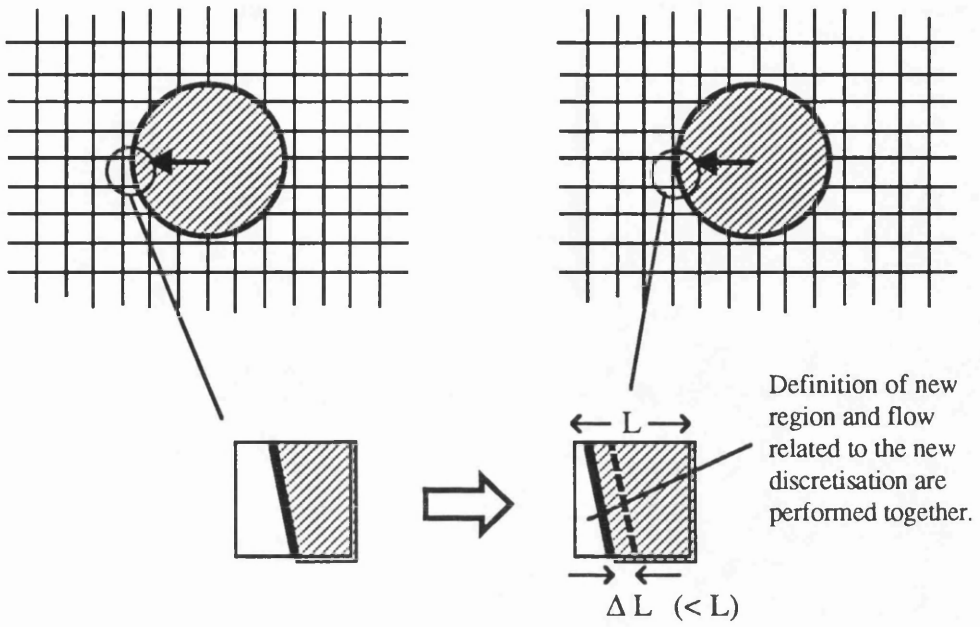

(a) Body movements restricted to a fraction of grid size

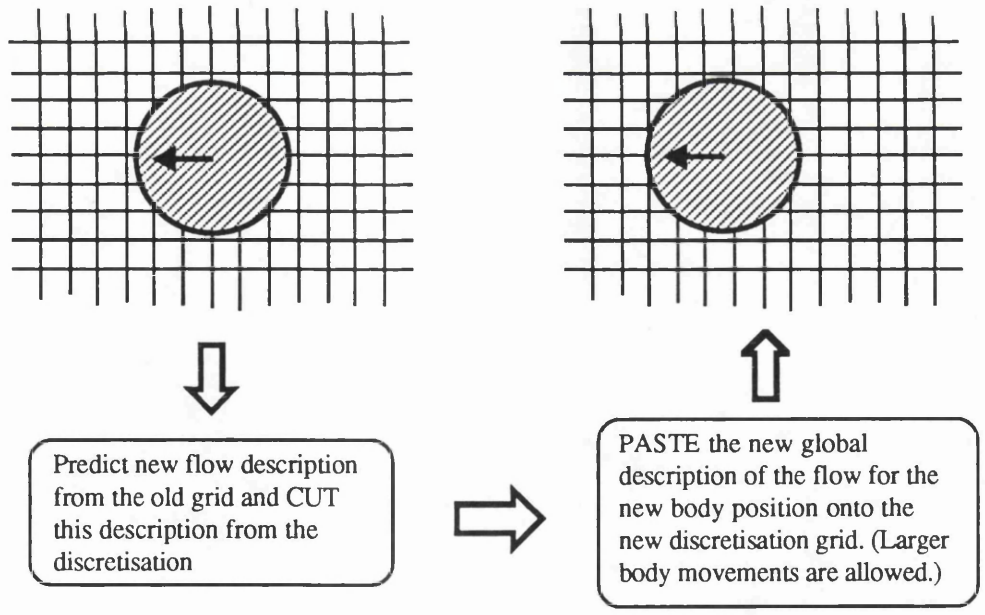

(b) Cut-and-Paste Procedure for Flow Description

Figure 6.6 Schemes for Flow Development Using Grid Re-Generation

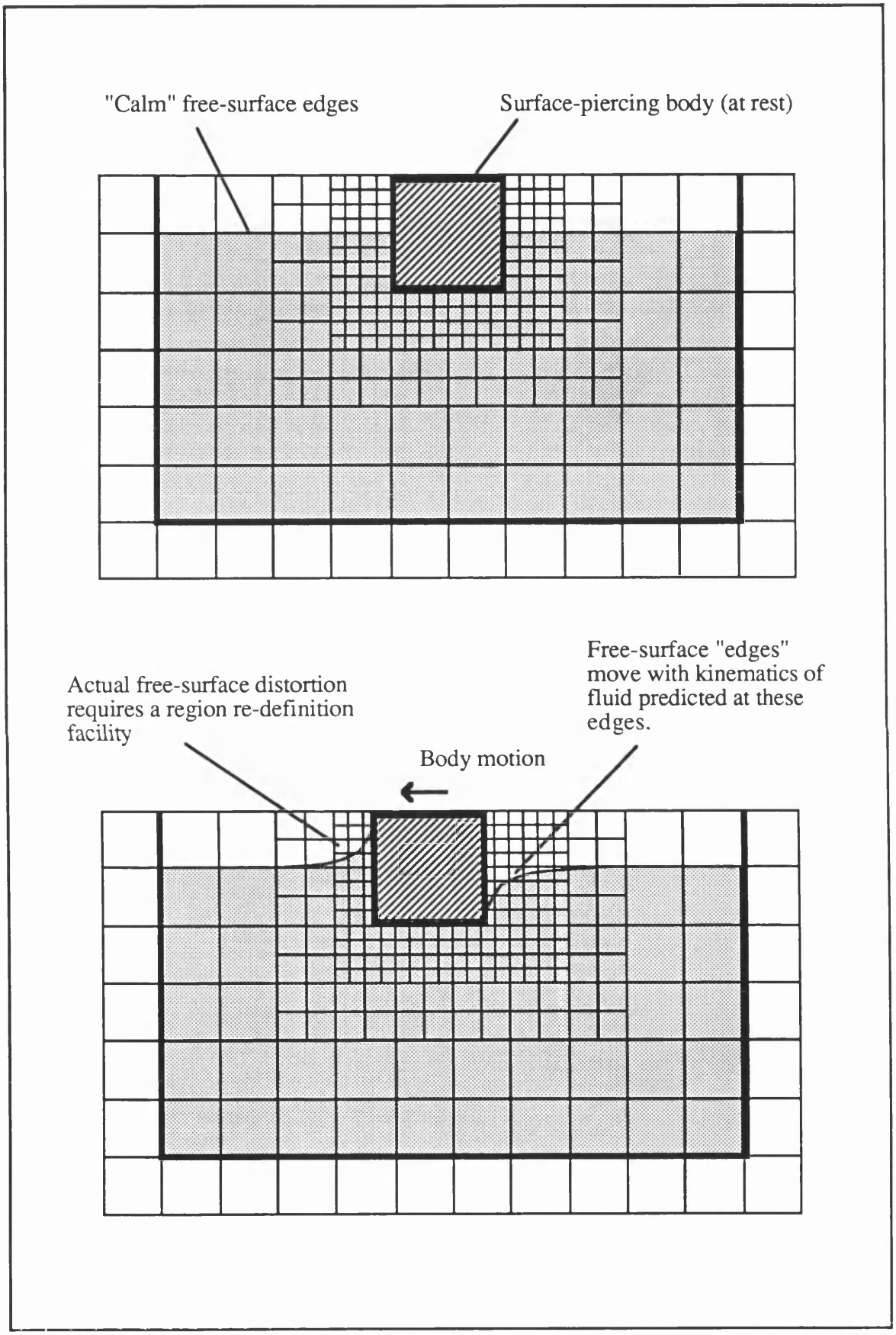

Figure 6.7 Finite Free-Surface Distortions

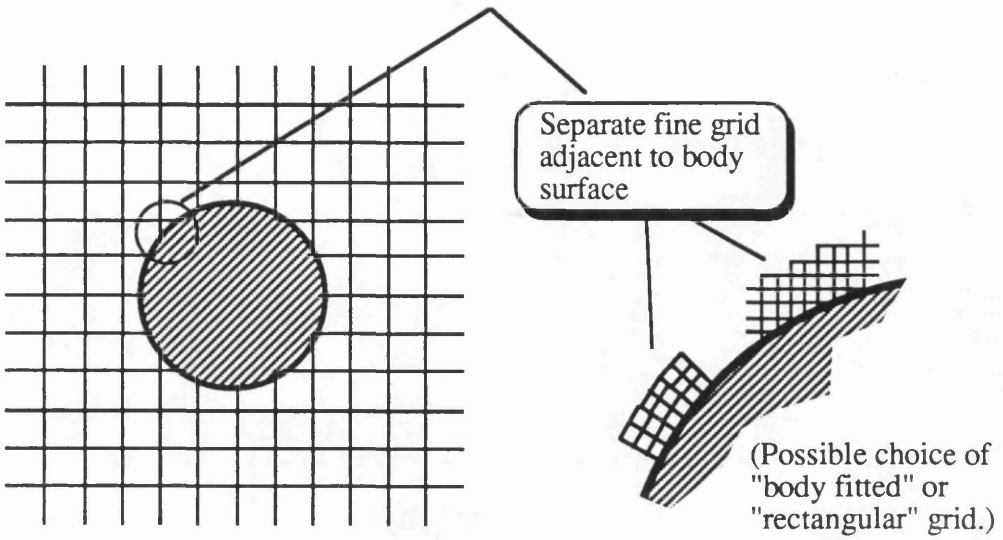

(a) Separate Grids for Bulk Flow and "Boundary Layer" Flow

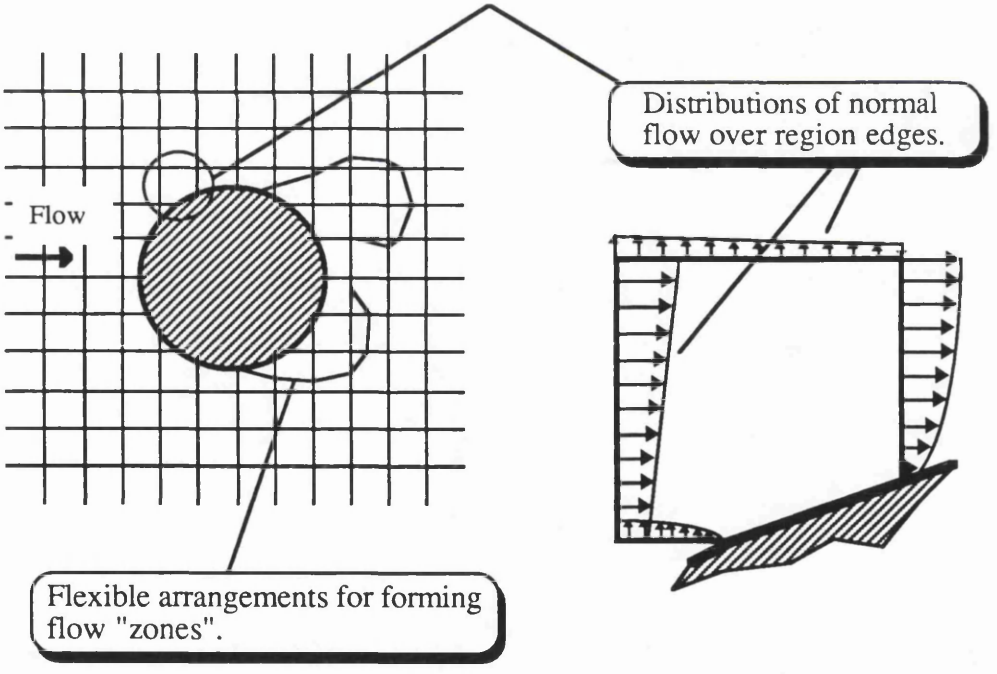

(b) Flow "Zoning" plus Distributions of Flow on Edges

Figure 6.8 Schemes for the Representation and Discretisation of the Dominant Effects of Viscosity

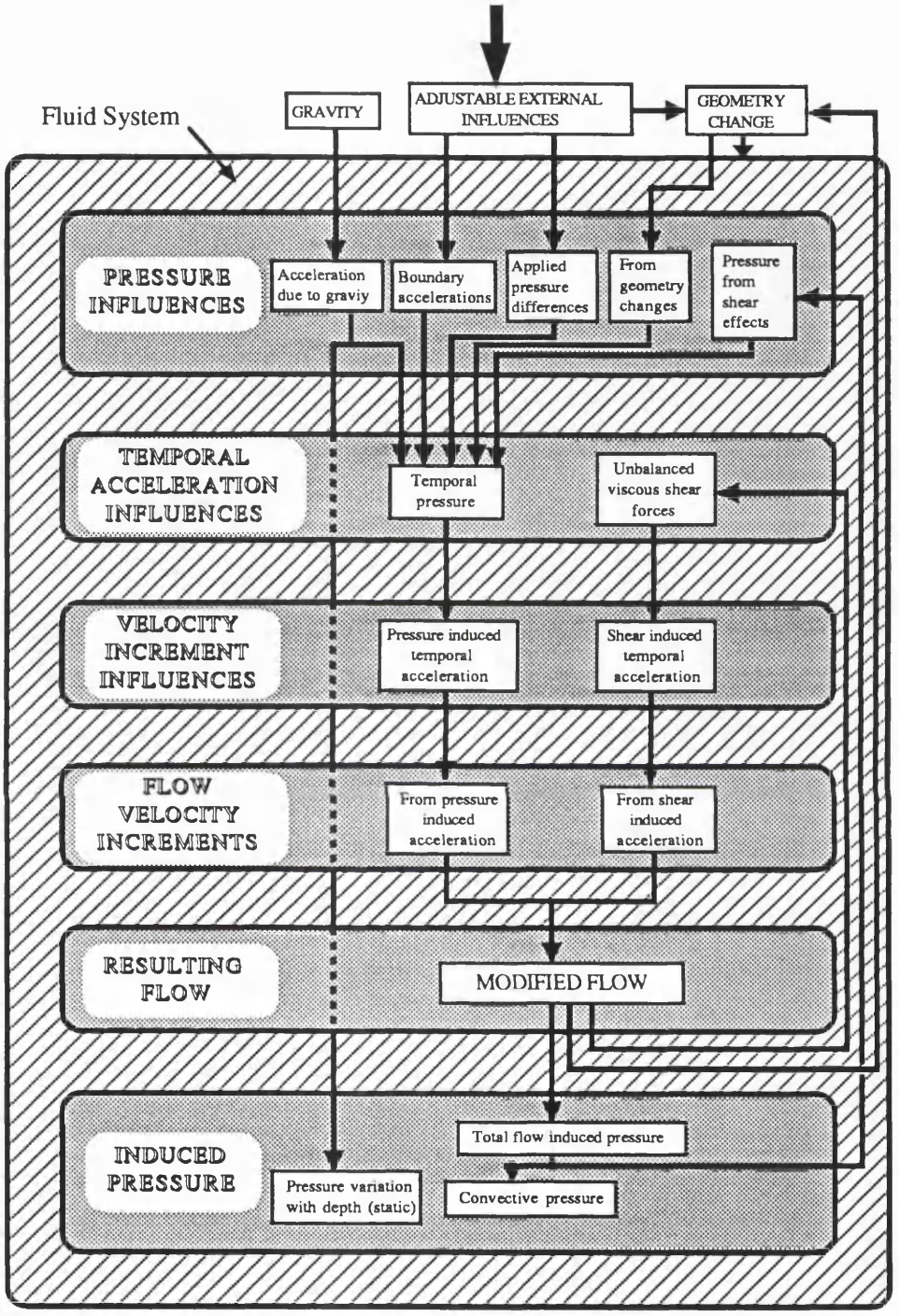

Figure 6.9 Revised Modular Influence Diagram for Flow Development

CHAPTER 7

CONCLUSION

The origins of this research lay in the recognition of an urgent need for advances in Computational Fluid Dynamics for the field of Naval Architecture. Current CFD capabilities still do not allow even the most basic ship performance characteristics of resistance and propulsion to be predicted reliably and, as a result of this, innovations in ship design are very slow to appear.

On examining conventional CFD techniques certain shortfalls in the approaches were identified as follows:-

(i) There is too much emphasis on solving the governing equations of motion throughout the system. This means that CFD techniques have become either wholly, or in part, *computer models of the mathematics* of the physics, rather than direct computer models of the physics *per se*.

(ii) The concepts involved in certain treatments of the equations of motion can be far removed from the reality of actual physical phenomena. This can inhibit progress in understanding fluid behavioural mechanisms, and thereby restricts research development.

(iii) There is a predominance of complex mathematics in the various CFD techniques. This arises from the range of discretisation strategies and differencing schemes that are possible, and from the favouring of "implicit" algorithms which demand iterative matrix solution methods with all the associated subtleties concerning stability and convergence. Such mathematics presents a severe obstacle to users of CFD codes who need to know the limitations of application of the software. Unfortunately, to understand these limitations it is necessary to be reasonably familiar with the mathematical treatments involved. To have to master CFD subtleties in order to use CFD software is very resource-wasteful and off-putting for design engineers.

(iv) Tradition in the presentation of most scientific research seems to demand "neatness" of all mathematical descriptions. This convention in both analytical fluid dynamics and CFD results in combined descriptions of different fluid behavioural mechanisms in one equation. With the process of discretisation then, the contributions from each mechanism to the resulting flow response can be lost

- thereby diminishing the effectiveness of the approaches for the purposes of really understanding flow behaviour.

(v) A particle of fluid knows nothing about the details of numerical schemes for solving the Navier-Stokes equations, potential flow, rotational flow, etc, and therefore it must be possible to develop a direct model of the physics of a fluid's behaviour without recourse to such concepts. (This is probably the most important observation since it underlies all the others.)

On the basis of the above criticisms of conventional CFD a "direct" approach to computer modelling of fluids was postulated. This was defined as an approach which was "physically transparent" throughout - that is, one which avoids intermediate mathematical interpretations and manipulations that so often obscure the physics of fluid behaviour. Rules were drawn up for developing a "direct model" of a fluid as follows:-

(i) A Continuum representation should be adopted.

(ii) Speed and "efficiency" considerations should not influence the algorithm design. (A conventional computer architecture may not be the most suitable for implementation.)

(iii) "Solution seeking" procedures for global relationships, couched as equations of balance, must not be involved.

(iv) Equations describing basic individual physical relationships may be used, but only to drive the computer model. Equations combining more than one physical mechanism should not be involved.

(v) Engineering approximations to describe certain physical influences within a fluid may be used. These, as the physical laws in (iv) above, must only be used to drive the computer model and could therefore be treated as replaceable modules within the driver algorithms of the program.

(vi) All driving influences used within the model must be physically justifiable, as opposed to mathematically justifiable.

(vii) The techniques employed should not be sensitive to the number, nature, or relative motions of the bodies/boundaries within the fluid.

Within the confines of this project it was necessary to limit the objective and scope of the work. The objective, then, was simply *to demonstrate and realise the principles of such a direct modelling approach.* Whereas this objective remained consistent throughout the course of the project work, the scope of the research (which essentially defined the specifics of the study) had to change quite radically.

For what has been referred to as Phase 1 of the research the scope of study was intended to describe the simplest realistic type of flow system which could demonstrate the viability of the direct approach to fluid modelling. The scope was, therefore, "restricted" to 2-dimensional, incompressible, viscous flow in the absence of free-surface distortions. With hindsight this scope was too advanced for the overall objective and it is unfortunate that the work for Phase 1 proceeded with a loophole in the *original* rules for development of a direct model which allowed "logical" (as well as physical) considerations to be used in the algorithms. As a result, the models devised in Phase 1 were kinematic in nature, rather than dynamic and properly physical. Although they gave some support to the *concept* of a direct approach to fluid modelling, they were far from the *realisation* of such a technique. The model for viscous flow influences, although showing some promise, was nowhere near giving realistic flow predictions; also, the model for inviscid influences, although successful in providing temporal acceleration responses of flow systems, failed to allow pressures to be determined in the flow. Without the pressure mechanism being properly modelled meant that the algorithms could not be extended to flows where free-surface distortion takes place.

For Phase 2 of the research it was necessary to revise the scope of study. It was clear at the end of Phase 1 that much effort was required to get the inviscid influence algorithms working properly on strictly physical lines and that development of the viscous algorithms could only continue once the inviscid model was sound. The scope of Phase 2, then, was to concentrate on 2-dimensional, *inviscid* flow, but now considering the possibility of free-surface distortions.

With this revised scope and the corrected rules for development, a test program was written which allows some simple inviscid flow systems to be represented using the direct approach to computer modelling of fluids. Systems involving actual *flow* that can be modelled are limited to (i) "stream flows" (i.e. uniform flows past one or more stationary bodies); (ii) single bodies moving linearly in large expanses of fluid; or (iii) such single body systems where additional boundaries are present but the actual geometry does not vary with time (for example, a body moving parallel to the walls of a uniform straight channel). In addition to these limited flow problems, the program can provide information on certain instantaneous aspects of a fluid system's behaviour. In particular, instantaneous

fluid reactions to body accelerations (linear, rotational, or both) yielding added mass characteristics can be determined, even if the boundary geometries are changing. This includes bodies accelerating at or near a (calm) free-surface.

Within the direct modelling algorithms devised elements which are similar to certain aspects of conventional CFD can be recognised. The important difference in the "direct" treatment, however, is that it approaches the modelling of the component fluid mechanisms in a modular fashion, and thereby retains the identity of the causes and effects within the development of a flow. This contrasts with conventional CFD techniques which effectively lump all the component mechanisms together once the Navier-Stokes (or Euler) equations are discretised. In conventional approaches, therefore, it is very difficult (in terms of both presentation of algorithms and analysing program performance) to keep track of the individual mechanisms influencing the flow in order to gain a real insight into the *understanding* of the behaviour of fluids.

In the inviscid model developed two principal mechanisms were identified. The first is the mechanism whereby temporal pressure is generated within the flow. (The temporal pressure is that component of the total pressure which is associated with the temporal variation of velocity at a point in the flow.) The second is the mechanism for synthesising convective pressure. (The convective pressure is that component of the total pressure which is associated with the convective acceleration of the fluid, i.e. the spatial variation of velocity in the flow.) The temporal pressure module is essentially a "fully-explicit" scheme for spreading temporal pressure disturbance inputs (for example, the influences of accelerating boundaries) throughout the flow system. It uses the bulk modulus model of the actual compressibility of fluids that are usually described as "incompressible". As an explicit scheme this part of the model is very computationally demanding because of the restrictions on the sub-timestep to ensure numerical stability. However, the question of speed of the algorithms (on today's machines) was not an issue in this work: the goal of physical transparency was not to be sacrificed for considerations of computational efficiency. The long term view was taken that computer hardware advances, and the very real suitability of the direct approach to parallel processing, will diminish such inefficiencies in time.

Work on the convective pressure generation model traced the origin of the synthesis of convective pressure to expansions of the fluid caused by its motion relative to a prevailing temporal pressure field. This is believed to be a new and much more understandable way of looking at convective pressure in flow systems and illustrates the benefits that the direct modelling approach offers general fluid dynamics education, quite apart from any potential benefits for CFD. The actual implementation of the convective

pressure algorithm in the test program exhibits some "bugs" for certain geometries, but these believed to be associated with the pressure smoothing algorithm required for the discretised model rather than the convective pressure algorithm itself, and should be relatively easily soluble.

The limitations of the realisation of the direct computer model for inviscid flows in the test program are caused because no grid re-generation routines were developed. Grid re-generation is a fairly mundane computational exercise, but is essential for the continuation of the work to more "interesting" flow situations, especially those involving surface wave generation which are of particular significance to Naval Architecture. Of great importance to general engineering applications (including Naval Architecture), of course, is the continued development of algorithms to model viscous influences in flows. Discussion of various aspects of the approach to viscous modelling using the direct technique is provided. It is believed that the inviscid influence models now provide firm enough foundations to commence the rebuilding of the models for viscous behaviour.

REFERENCES

Groupings:-

1. General Fluids Texts
2. Computational Methods in Fluids - Texts
3. Computational Fluid Dynamics - General Reviews
4. Grid Generation
5. Cellular Automata
6. Particle Models
7. Methods For Inviscid Flow
8. Viscous Flow - Zonal Approaches
9. Viscous Flow - Vortex Methods
10. Viscous Flow - Full Navier-Stokes Solvers
11. Free-Surface Modelling
12. Naval Architecture Texts
13. Miscellaneous

1. General Fluids Texts

(a) BATCHELOR, G.K. (1967). *An Introduction to Fluid Dynamics*. Cambridge University Press, UK. 615pp

(b) PANTON,.R.L. (1984). *Incompressible Flow*. John Wiley and Sons, New York. 780pp.

(c) RAUDKIVI, A.J. and CALLANDER, R.A. (1975). *Advanced Fluid Mechanics*. Edward Arnold, UK. 325pp

(d) MASSEY, B.S. (1975). *Mechanics of Fluids*. Van Nostrand Reinhold, London, UK. 528pp

2. Computational Methods in Fluids - Texts

(a) PEYRET, R. and TAYLOR, T.D. (1983). *Computational Methods for Fluid Flow*. Springer-Verlag, New York. 358pp.

(b) FLETCHER, C.A.J. (1988). *Computational Techniques for Fluid Dynamics* . Springer-Verlag, New York. 2 Volume set. 409pp, 484pp

(c) TELIONIS, D.P. (1981). *Unsteady Viscous Flow*. Springer-Verlag, New York. 408pp.

(d) THOMASSET, F. (1981). *Implementation of Finite Element Methods for Navier-Stokes Equations*. Springer-Verlag, New York. 160pp

3. Computational Fluid Dynamics - General Reviews

(a) AREF, H. (1986). The Numerical Experiment in Fluid Mechanics. *J. Fluid Mech.*, **173**, 15-41

(b) LEWIS, R.I. and PORTHOUSE, D.T.C. (1983). Recent Advances in the Theoretical Simulation of Real Fluid Flows. *North East Coast Inst of Engineers and Shipbuilders* **99**, 88-105

(c) JAMESON, A. (1983). The Evolution of Computational Methods in Aerodynamics. *Trans. ASME Journal of Applied Mechanics*. **50**, 1052-1070

(d) BORIS, J.P. (1989). New Directions in Computational Fluid Dynamics. *Ann. Rev. Fluid Mech.* **21**, 345-385

(e) EMMONS, H.W. (1970). Critique of Numerical Modelling of Fluid-Mechanics Phenomena. *Ann. Rev. Fluid Mech.*. **2**, 15-36

(f) MORGAN, W.B. and LIN, W-C. (1987). Computational Fluid Dynamics - Ship Design and Model Evaluation. *Int. Towing Tank Conf. Proc.* 329-337

(g) SPALDING, D.B. (1988). CFD Benefits, Goals, Stepping-Stones and Techniques. *Imperial College of Science and Technology* CFDU Report CFD/88/1, 31pp

4. Grid Generation

(a) HAUSER, J, PAAP, H-G, and SENGUPTA, S. (1986). Numerical Grid Generation in Applied Engineering Problems. *Chartered Mechanical Engineer*, March 1986, 50-51

(b) EISEMAN, P.R. (1985). Grid Generation For Fluid Mechanics Computations. *Ann. Rev. Fluid Mech.* **17**, 487-522

5. Cellular Automata

(a) TOFFOLI, T. and MARGOLUS, N. (1987). *Cellular Automata Machines*. MIT Press, Cambridge, Mass. 259pp

(b) MARGOLUS, N., TOFFOLI, T., and VICHNIAC, G. (1986). Cellular-Automata Supercomputers for Fluid-Dynamics Modelling. *Phys. Rev. Lett.* **56**, 1694-1696

(c) ORSZAG, S.A. and YAKHOT, V. (1986). Reynolds Number Scaling of Cellular-Automaton Hydrodynamics. *Phys. Rev. Lett.* **56**, 1691-1693

(d) FRISCH, U., HASSLACHER, B. and POMEAU, Y. (1986). Lattice Gas Automata for the Navier-Stokes Equation. *Phys. Rev. Lett.* **56**, 1505-1508

6. Particle Models

(a) HARLOW, F.H., (1959). Two dimensional Hydrodynamic Calculations. *Los Alamos Scientific Laboratory Report* LA-2301.

(b) HARLOW, F.H. and MEIXNER, B.D. (1961). The Particle-And-Force Computing Method For Fluid Dynamics. *Los Alamos Scientific Laboratory Report* LAMS-2567

(c) HARLOW, F.H. (1962). Theory of Correspondence Between Fluid Dynamics and Particle-And-Force Models. *Los Alamos Scientific Laboratory Report* LA-2806

(d) RAVIART,P.A. (1986). Particle Numerical Models in Fluid Dynamics. *Numerical Methods for Fluid Dynamics II*. Clarendon Press, Oxford, UK.

(e) GREENSPAN, D. (1985). Computer Studies in Particle Modelling of Fluid Phenomena. *Math. Modelling* **6**, 273-294

7. Methods for Inviscid Flow

(a) EATOCK TAYLOR, R. and WU, G.X. (1986). Wave Resistance and Lift on Cylinders by a Coupled Element Technique. *Int. Shipbuilding Progress*, **33**, 2-9

(b) MUSKER, A.J., LOADER, P.R. and BUTCHER, M.C. (1988). Simulation of a Submarine Under Waves. *Int. Shipbuilding Progress*, **35**, 389-410

(c) GADD, G.E. (1976). A Method of Computing the Flow and Surface Wave Pattern Around Full Forms. *Trans. Royal Instit. Naval Arch.*, **118**, 207-219

(d) INGLIS, R.B. and PRICE, W.G. (1981). A Three Dimensional Ship Motion Theory: Calculation of Wave Loading and Responses with Forward Speeds. *Trans. Royal Instit. Naval Arch.*, **124**, 183-192

(e) ABBOTT, I.H. and VON DOENHOFF, A.E. (1949). *Theory of Wing Sections*. Dover Publications, New York. 693pp

(f) LERBS, H.W. (1952). Moderately Loaded Propellers With a Finite Number of Blades and an Arbitrary Distribution of Circulation. *Trans. Society Naval Arch. Marine Eng.* **60**, 73-123

(g) HESS, J.L. and SMITH, A.M.O. (1962). Calculation of Non-Lifting Potential Flow About Arbitrary Three Dimensional Bodies. *Douglas Aircraft Report ES40622*.

(h) OGIWARA, S. and MASUKO, A. (1986). A Method for Computation of Steady Ship Waves by Means of Rankine Sources and Its Application to Hull Form Design. *CADMO 86, Washington D.C.,* 97-116

(i) RUBBERT, P.E. and SAARIS, G.R. (1968). A General Three Dimensional Potential Flow Method Applied to V/STOL Aerodynamics. *SAE Paper 680304*.

(j) HESS, J.L. (1990). Panel Methods in Computational Fluid Dynamics. *Ann. Rev. Fluid Mech.*, **22**, 255-274

8. Viscous Flow - Zonal Approaches

(a) SCHLICHTING, H. (1968). *Boundary Layer Theory, 7th Ed.* McGraw-Hill, New York. 817pp

(b) KELLER, H.B. (1978). Numerical Methods in Boundary Layer Theory. *Ann. Rev. Fluid Mech.* **10**, 417-433

9. Viscous Flow - Vortex Methods

(a) LEONARD, A. (1985). Computing Three-Dimensional Incompressible Flows With Vortex Elements. *Ann. Rev. Fluid Mech.* **17**, 523-559

(b) KUIPER, G. (1971). Some Remarks on Lifting Surface Theory. *Int. Shipbuilding Prog.* **18**, 131-143

(c) KERWIN, J.E. (1986). Marine Propellers. *Ann. Rev. Fluid Mech.* **18**, 367-403

(d) GREELY, D.S. and KERWIN, J.E. (1982). Numerical Methods for Propeller Design and Analysis in Steady Flow. *Soc. Nav. Archit. Mar. Eng. Trans.* **90**, 415-453

(e) TINKER, S.J. (1988). A Discrete Vortex Model of Separated Flows Over Manoeuvring Submersibles. *Advances in Underwater Technology, Ocean Science and Offshore Engineering*, **15**, 157-176

10. Viscous Flow - Full Navier-Stokes Solvers

(a) ROGALLO, R.S. and MOIN, P. (1984). Numerical Simulation of Turbulent Flows. *Ann. Rev. Fluid Mech.* **16**, 99-137.

(b) GOSMAN, A.D. and ISSA, R.I. (1987). Computational Fluid Mechanics and Heat Transfer (Lecture notes for Post-Experience Course). *Imperial College of Science and Technology*, UK

(c) LAUNDER, B.E. and SPALDING, D.B. (1974). The Numerical Computation of Turbulent Flows. *Comput. Methods Appl. Mech. Eng.* **3**, 269-289

(d) BARCLAY, W.H. and ASTON, J.G.L. (In press). Influence of Vent Positions on Smoke Clearance from a Room. *Int. Journal Heat and Fluid Flow.*

11. Free-Surface Modelling

(a) SHIELDS, J.J, and WEBSTER,W.C. (1988). On Direct Methods in Water-Wave Theory. *J. Fluid Mech.* **197**, 171-199

(b) YEUNG, R.W. 1982. Numerical Methods in Free-Surface Flows. *Ann. Rev. Fluid Mech.* **14**, 395-442

(c) HUERTA, A. and LIU, W.K. (1988). Viscous Flow with Large Free Surface Motion. *Comput. Methods App. Mech. Eng.* **69**, 277-324

(d) VUGTS, J.H. (1968). The Hydrodynamic Coefficients for Swaying, Heaving, and Rolling Cylinders in a Free Surface. *Int. Shipbuilding Progress* **15**, 251-276

(e). WEHAUSEN, J.V. (1971). The Motion of Floating Bodies. *Ann. Rev. Fluid Mech.* **3**, 237-268

(f) WEHAUSEN, J.V. and LAITONE, E.V. (1960). Surface Waves. *In Handbuch der Physik, Springer Berlin*, **9**, 446-778

12. Naval Architecture Texts

(a) SAUNDERS, H.E. (1957). *Hydrodynamics in Ship Design.* The Society of Naval Architects and Marine Engineers, New York. (3 Volume Set) 648pp, 980pp, 507pp

(b) NEWMAN, J.N. (1978). *Marine Hydrodynamics.* The MIT Press, Cambridge, Massachusetts. 402pp

(c) COMSTOCK, J.P. (Ed) (1967). *Principles of Naval Architecture.* The Society of Naval Architects and Marine Engineers, New York. 827pp

(d) CLAYTON, B.R. and BISHOP, R.E.D. (1982). *Mechanics of Marine Vehicles.* E. & F. Spon Ltd., London, UK. 597pp

(e) PRICE, W.G. and BISHOP, R.E.D. (1974). *Probabilistic Theory of Ship Dynamics.* Chapman & Hall Ltd., London, UK. 311pp

(f) LLOYD, A.R.J.M. (1989). *SEAKEEPING: Ship Behaviour in Rough Weather.* Ellis Horwood Ltd., Chichester, UK. 486pp

13. Miscellaneous

(a) ASTON, J.G.L., MARSHALL, A.J. and RYDILL, L.J. (1987). Assessing the Hydrostatic Stability of Marine Vehicle Designs. *Trans. Royal Institution of Naval Architects* **129**, 81-102

(b) WITZ, J.A. and PATEL, M.H. (1985). A Pressure Integration Technique for Hydrostatic Analysis. *Trans. Royal Institution of Naval Architects*, **127**, 285-294

(c) RUSLING, S.C. (In preparation). *Performance Related Initial Design of Marine Vehicles.* PhD Thesis, University College London.

(d) CONNOLLY, M.P., MICHAEL, D.H. and COLLINS, R. (1988). The Inversion of Surface Potential Measurements to Determine Crack Size and Shape. *J. Appl. Physics*, **64**, 2638-2647

(e) STONE, H.S. (1990). *High Performance Computer Architecture, 2nd Ed.* Addison-Wesley, U.K. 459pp

(f) CHEN, S.S, WANBSGAUSS, M.W. and JENDRZEJEZYK, J.A. (1976). Added Mass and Damping of a Vibrating Rod in Confined Viscous Fluid. *J. Appl. Mech*, **43**, 325-329

(g) International Conference on *The Safeship Project: Ship Stability and Safety*, London, 1986. Royal Institution of Naval Architects.

APPENDIX 1

ANALYTICAL SOLUTION FOR FLOW WITHIN A CYLINDRICAL ANNULUS

The complex potential for irrotational flow past a 2-dimensional cylinder of radius B in an infinite free-stream of velocity V is given by

$$w = V\left(z + \frac{B^2}{z}\right) \qquad \text{A1.1}$$

where

$$z = x + i\,y \quad \text{(in cartesian coordinates)}$$
$$= r\left(\cos\theta + i \sin\theta\right) = r\,e^{i\theta} \quad \text{(in radial coordinates)}$$

This leads to the cartesian velocity components u and v as

$$-u + i\,v = \frac{dw}{dz} = V\left(1 - \frac{B^2}{z^2}\right) \qquad \text{A1.2}$$

or, alternatively, the radial and tangential velocities q_r and q_θ as

$$-q_r + i\,q_\theta = e^{i\theta} \cdot \frac{dw}{dz} = V\left(e^{i\theta} - \frac{B^2}{r^2} e^{-i\theta}\right) \qquad \text{A1.3}$$

The stream pattern is illustrated in figure A1.1 below.

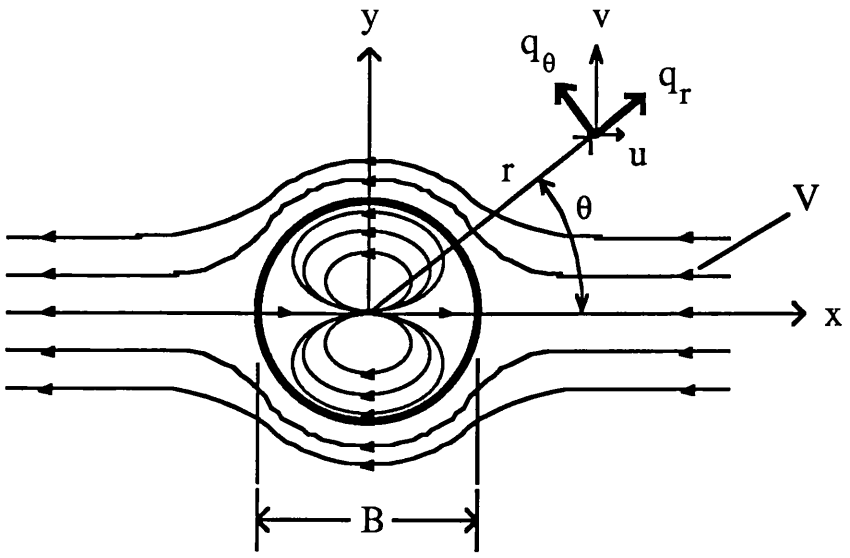

FIGURE A1.1

There are two regions of interest in the system above which may be interpreted to represent flow constrained between concentric cylindrical boundaries. It will be seen that the flow inside the radius B can be made to represent the instantaneous flow pattern created by an inner concentric cylinder of diameter d (<2B) executing small motions about the origin and constrained within a fixed tube of radius B. Similarly, the flow outside the radius B can be made to represent the instantaneous flow pattern of a concentric outer cylindrical tube of diameter D (>2B) executing small motions about the origin and a fixed cylinder of radius B.

MOTION OF AN INNER CYLINDER

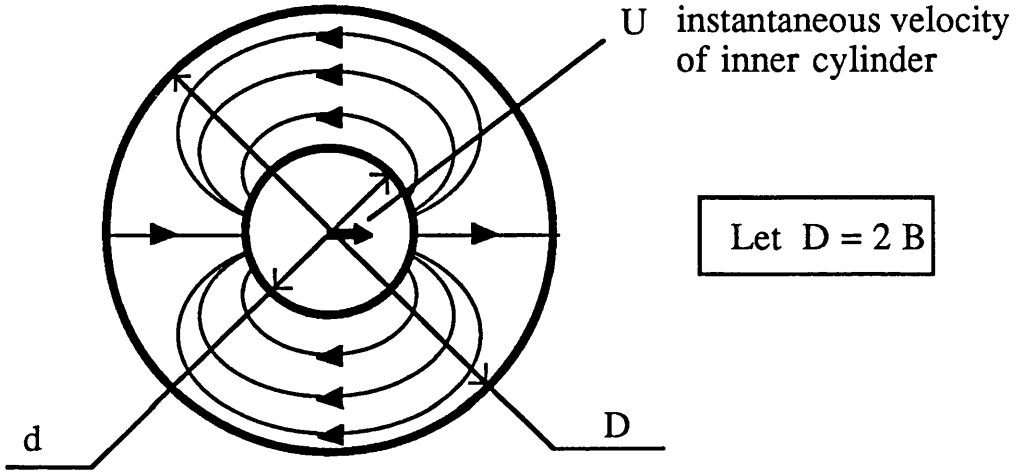

FIGURE A1.2

Velocity Transformation

Suppose the instantaneous velocity of the inner cylinder is U, then in order for A1.1 to A1.3 to describe the required flow it must be shown that the radial component of the velocity on the surface of the proposed inner cylinder can be made consistent with Ucosθ for all θ. From A1.3 it can be seen that the radial velocity at radius d/2 is given by

$$\begin{aligned} q_r &= \mathrm{Re}\left\{-V\left(e^{i\theta} - \frac{D^2}{d^2}e^{-i\theta}\right)\right\} \\ &= V\left(-1 + \frac{D^2}{d^2}\right)\cos\theta \\ &= V\left(\frac{D^2 - d^2}{d^2}\right)\cos\theta \end{aligned} \qquad \text{A1.4}$$

giving the required consistent variation according to cosθ. A1.4 then also provides the velocity transformation for calculations for the interpreted flow pattern where

$$V = U\left(\frac{d^2}{D^2 - d^2}\right) \qquad \text{A1.5}$$

Interpreted Flow Velocities

The absolute velocities of the flow within the cylindrical annulus of fluid may be obtained from A1.2 and A1.3 in terms of the virtual velocity V and then in terms of the actual reference speed U by using A1.5.

$$u = -V\left(1 - \frac{B^2}{r^2}\cos 2\theta\right) = -U\left(\frac{d^2}{D^2 - d^2}\right)\left(1 - \frac{D^2}{4r^2}\cos 2\theta\right) \qquad \text{A1.6}$$

$$v = V\left(\frac{B^2}{r^2}\sin 2\theta\right) = U\left(\frac{d^2}{D^2 - d^2}\right)\left(\frac{D^2}{4r^2}\sin 2\theta\right) \qquad \text{A1.7}$$

$$q_r = -V\left(1 - \frac{B^2}{r^2}\right)\cos\theta = -U\left(\frac{d^2}{D^2 - d^2}\right)\left(1 - \frac{D^2}{4r^2}\right)\cos\theta \qquad \text{A1.8}$$

$$q_\theta = V\left(1 + \frac{B^2}{r^2}\right)\sin\theta = U\left(\frac{d^2}{D^2 - d^2}\right)\left(1 + \frac{D^2}{4r^2}\right)\sin\theta \qquad \text{A1.9}$$

Added Mass of Accelerating Inner Cylinder

Using the kinetic energy approach [1d] the added mass m_L of the fluid per unit length of the cylinder may be determined from the the total kinetic energy of the fluid within the annulus $d/2 < r < D/2$ as follows:-

$$\text{K.E.} = \frac{1}{2} m_L U^2 = \frac{1}{2}\rho \int_{\frac{d}{2}}^{\frac{D}{2}} \int_0^{2\pi} (u^2 + v^2)\, r\, d\theta\, dr$$

$$= \frac{1}{2}\rho\pi V^2 \frac{1}{4}\left(\frac{D^4}{d^2} - d^2\right)$$

$$= \frac{1}{2}\rho\pi U^2 \left(\frac{d^4}{(D^2 - d^2)^2}\right)\frac{1}{4}\left(\frac{D^4}{d^2} - d^2\right) \qquad \text{A1.10}$$

$$= \frac{1}{2}\rho\pi\left(\frac{d}{2}\right)^2\left(\frac{D^2 + d^2}{D^2 - d^2}\right) U^2$$

$$= \frac{1}{2}\rho\pi\left(\frac{d}{2}\right)^2\left(\frac{1 + \gamma^2}{1 - \gamma^2}\right) U^2 \quad \text{where } \gamma = \frac{d}{D}$$

The added mass coefficient C_M (related to the mass of fluid displaced by the inner cylinder) is then given by

$$C_M = \left(\frac{1+\gamma^2}{1-\gamma^2}\right) \qquad \text{A1.11}$$

MOTION OF AN OUTER CYLINDER

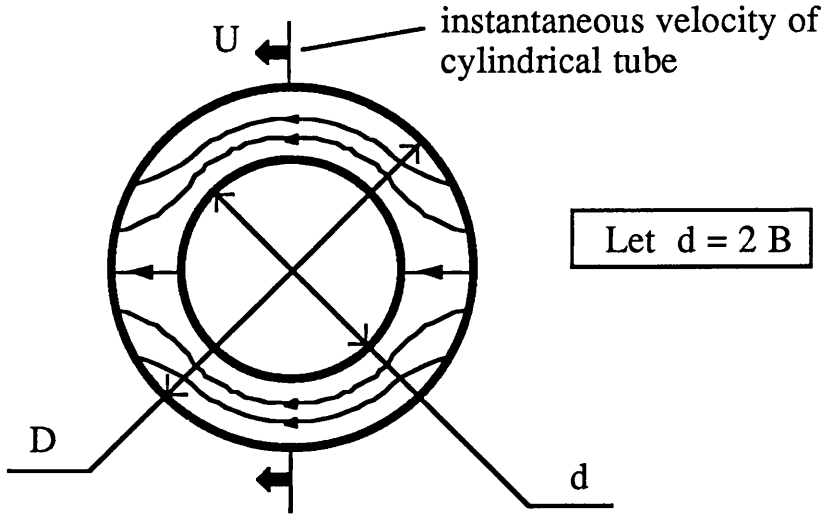

FIGURE A1.3

Velocity Transformation

Suppose the instantaneous velocity of the outer cylinder is U, then in order for A1.1 to A1.3 to describe the required flow it must be shown that the radial component of the velocity on the surface of the proposed inner cylinder can be made consistent with $-U\cos\theta$ for all θ. From A1.3 it can be seen that the radial velocity at radius D/2 is given by

$$\begin{aligned} q_r &= \mathrm{Re}\left\{-V\left(e^{i\theta} - \frac{d^2}{D^2}e^{-i\theta}\right)\right\} \\ &= V\left(-1+\frac{d^2}{D^2}\right)\cos\theta \\ &= -V\left(\frac{D^2-d^2}{D^2}\right)\cos\theta \end{aligned} \qquad \text{A1.12}$$

giving the required consistent variation according to $\cos\theta$. A1.12 then also provides the velocity transformation for calculations for the interpreted flow pattern where

$$V = U\left(\frac{D^2}{D^2-d^2}\right) \qquad \text{A1.13}$$

Interpreted Flow Velocities

The absolute velocities of the flow within the cylindrical annulus of fluid may be obtained from A1.2 and A1.3 in terms of the virtual velocity V and then in terms of the actual reference speed U by using A1.13.

$$u = -V\left(1 - \frac{B^2}{r^2}\cos 2\theta\right) = -U\left(\frac{D^2}{D^2 - d^2}\right)\left(1 - \frac{d^2}{4r^2}\cos 2\theta\right) \qquad \text{A1.14}$$

$$v = V\left(\frac{B^2}{r^2}\sin 2\theta\right) = U\left(\frac{D^2}{D^2 - d^2}\right)\left(\frac{d^2}{4r^2}\sin 2\theta\right) \qquad \text{A1.15}$$

$$q_r = -V\left(1 - \frac{B^2}{r^2}\right)\cos\theta = -U\left(\frac{D^2}{D^2 - d^2}\right)\left(1 - \frac{d^2}{4r^2}\right)\cos\theta \qquad \text{A1.16}$$

$$q_\theta = V\left(1 + \frac{B^2}{r^2}\right)\sin\theta = U\left(\frac{D^2}{D^2 - d^2}\right)\left(1 + \frac{d^2}{4r^2}\right)\sin\theta \qquad \text{A1.17}$$

Added Mass of Accelerating Outer Cylinder

Using the kinetic energy approach [1d] the added mass m_L of the fluid per unit length of the cylinder may be determined from the the total kinetic energy of the fluid within the annulus $d/2 < r < D/2$ as follows:-

$$\text{K.E.} = \frac{1}{2} m_L U^2 = \frac{1}{2}\rho \int_{\frac{d}{2}}^{\frac{D}{2}} \int_0^{2\pi} (u^2 + v^2)\, r\, d\theta\, dr$$

$$= \frac{1}{2}\rho\,\pi\, V^2 \frac{1}{4}\left(D^2 - \frac{d^4}{D^2}\right)$$

$$= \frac{1}{2}\rho\,\pi\, U^2 \left(\frac{D^4}{(D^2 - d^2)^2}\right)\frac{1}{4}\left(D^2 - \frac{d^4}{D^2}\right) \qquad \text{A1.18}$$

$$= \frac{1}{2}\rho\,\pi \left(\frac{d}{2}\right)^2 \left(\frac{D}{d}\right)^2 \left(\frac{D^2 + d^2}{D^2 - d^2}\right) U^2$$

$$= \frac{1}{2}\rho\,\pi \left(\frac{d}{2}\right)^2 \left(\frac{1}{\gamma^2}\right)\left(\frac{1 + \gamma^2}{1 - \gamma^2}\right) U^2 \quad \text{where } \gamma = \frac{d}{D}$$

The added mass coefficient C_M (related to the mass of fluid displaced by the inner cylinder) is then given by

$$C_M = \frac{1}{\gamma^2}\left(\frac{1 + \gamma^2}{1 - \gamma^2}\right) \qquad \text{A1.19}$$

APPENDIX 2

PRESSURE CONDITIONING REQUIREMENT ON SUB-TIMESTEP IN THE MODEL FOR TEMPORAL PRESSURE

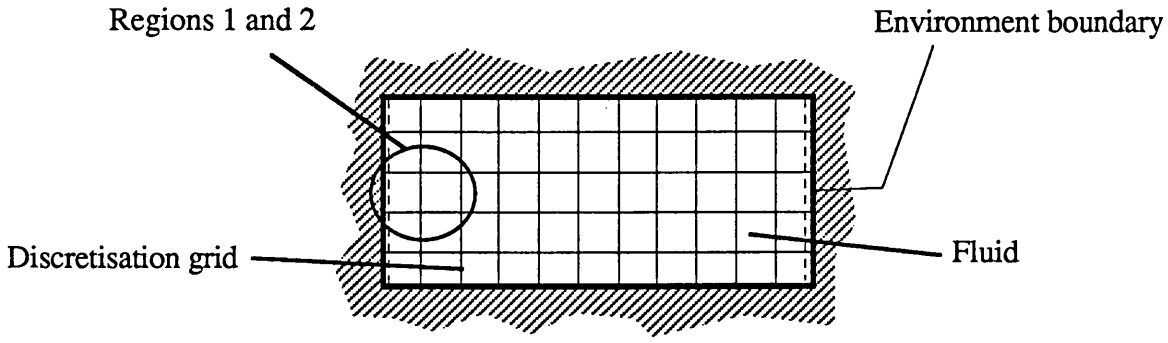

Figure A2.1

Consider, for convenience, a rectangular fluid system as shown in figure A2.1 experiencing some temporal disturbance. During the course of pressure spreading in the temporal pressure algorithm, pressure increments are experienced by each region in accordance with the displacements of the fluid at each edge of the region occurring during each sub-timestep. These displacements are determined from the acceleration arising from the pressure gradient across each edge as calculated from the pressure levels in the system at the previous sub-timestep. (See Chapter 5, section 3.6.) It is possible to deduce a restriction on the order of magnitude of the sub-timestep by considering the conditions required to ensure that pressure disturbances are propagated reasonably smoothly downstream in the discretised system.

Consider the simple case where the rectangular fluid system experiences an acceleration disturbance due to the acceleration from rest of two flowplates shown dotted in figure A2.1. The spread of pressure within the system will be conveniently simple since the rectangular environment ensures that the spreading is uni-directional. It is necessary only to determine what happens in the first two sub-timesteps to obtain a restriction on the magnitude of the sub-timestep.

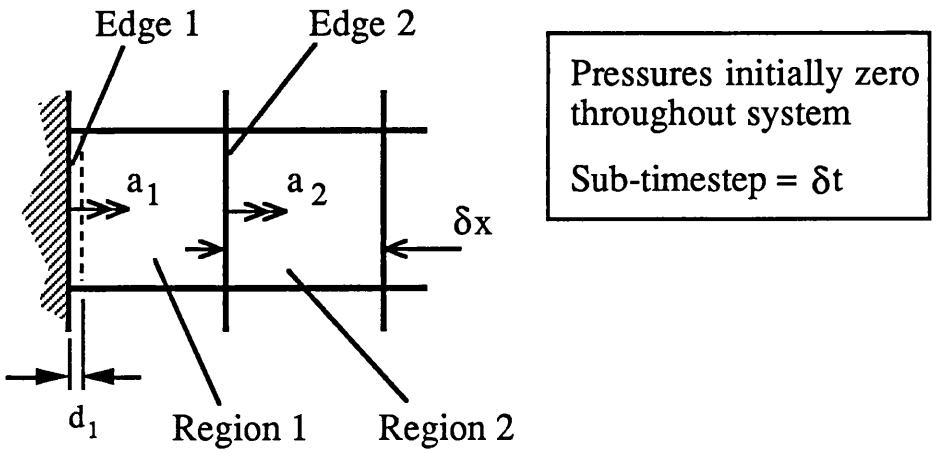

Figure A2.2

At the end of the first sub-timestep edge 1 has physically displaced a distance d_1 due to the acceleration a_1 of the flowplate, where

$$d_1 = \frac{1}{2} a_1 \delta t^2 \qquad \text{A2.1}$$

Thus the pressure synthesised in region 1 after the first sub-timestep is given by

$$p_1 = \frac{d_1}{\delta x} K = \frac{a_1 \delta t^2 K}{2 \delta x} \qquad \text{A2.2}$$

whereas the pressure in region 2 is unaffected as yet. The pressure gradient experienced across edge 2, then, as a result of the pressurisation occurring after the first sub-timestep, is $p_1/\delta x$; and so, the acceleration experienced by edge 2 during the second sub-timestep is given by

$$a_2 = \frac{p_1}{\rho \delta x} = \frac{a_1 \delta t^2 K}{2 \delta x^2 \rho} \qquad \text{A2.3}$$

In order for the transmission of pressure to be relatively smooth and well-behaved within the discretised system, the magnitude of the acceleration a_2 generated must be of the order of a_1 or less. This gives

$$\frac{\delta t^2 K}{\delta x^2 \rho} \leq O[1]$$

$$\rightarrow \quad \delta t \leq O\left[\frac{\delta x}{\sqrt{K/\rho}}\right] \qquad \text{A2.4}$$

$$\rightarrow \quad \delta t \leq O\left[\frac{\delta x}{c}\right]$$

In words, the sub-timestep chosen must be of the order of the time taken for a pressure wave to travel the length of the smallest spacing in the discretisation grid used to represent the continuous system.